Generation

and Phenotypic Analysis

of Coronin-1 Deficient Mice

Inauguraldissertation

zur

Erlangung der Würde eines Doktors der Philosophie

vorgelegt der

Philosophisch-Naturwissenschaftlichen Fakultät

der Universität Basel

von

Jan Christian Louis Massner

aus Heidelberg, Deutschland

Basel, 2006

Genehmigt von der Philosophisch-Naturwissenschaftlichen Fakultät auf Antrag von Prof. Dr. Jean Pieters und Prof. Dr. Martin Spiess.

Basel, den 19. September 2006

Prof. Dr. Hans-Peter Hauri

The work described in this thesis has been performed from January 2003 to April 2006 at the Biozentrum, Department of Biochemistry, University of Basel in the laboratory and under supervision of Prof. Dr. Jean Pieters.

The majority of the results described in this thesis is part of the following manuscript:

Philipp Mueller*, Jan Massner*, Imke Albrecht, Carmen Blum, Rod Ceredig, Désirée Griesemer, Ariel Quintana, Markus Hoth, Toru Miyazaki, Hans-Reimer Rodewald, Antonius J. Rolink and Jean Pieters (submitted).

Coronin 1 is Essential for T Cell Survival by Controlling Store Operated Ca^{2+} Entry

* equal contributors

ABSTRACT

Coronins represent an evolutionary conserved family of WD-repeat actin-binding proteins for which a role in regulating membrane and cytoskeleton related functions have been proposed. In mammalian organisms seven members of the coronin protein family have been described of which coronin-1 respresents the thus far best characterized molecule. Coronin-1 is specifically expressed in leukocytes and was originally identified as a key player in mediating the survival of pathogenic mycobacteria in infected murine macrophages by inhibiting the fusion of the mycobacterial phagosome with lysosomes. Further analyses demonstrated the capacity of coronin-1 to link the leukocyte plasma membrane with the underlying actin cytoskeleton suggesting a regulatory role of coronin-1 in leukocyte specific functions. However, a precise biological activity of coronin-1 in leukocytes and in mammalian organisms in general has not yet been defined. The aim of the work described in this thesis was to contribute to our understanding of the function of coronin-1 by generating and phenotypically characterizing coronin-1 knock-out mice.

Coronin-1 deficient mice were found to be viable and fertile. In-depth analysis of the immune system revealed that the lack of coronin-1 expression severly affected the homeostasis of the peripheral T-cell pool. Whereas T-cell development could be shown to be independent on coronin-1, peripheral T-cell numbers were found to be strongly reduced. The reduction of peripheral T-cell numbers in coronin-1 deficient mice was accompanied by changes in the composition and function of the peripheral T-cell pool. Coronin-1 deficient peripheral T-cells were prone to apoptosis, less efficient in homing to secondary lymphoid organs and unable to mount a proliferative response to allogeneic MHC stimuli. Cytoskeletal structures in coronin-1 deficient T-cells were found to be normally organized. Coronin-1 deficiency did not affect other leukocyte subsets, such as B-cells and macrophages. Macrophages isolated from coronin-1 deficient mice did neiter show any abnormalities in the organization of the actin cytoskeleton nor did the absence of coronin-1 expression affect their phagocytic properties. We therefore conclude that coronin-1 plays a crucial role in maintaining T-cell but not macrophage functions. Based on the results described in this thesis we propose a function of coronin-1 in regulating T-cell homeostasis by modulating T-cell specific functions such as T-cell activation.

TABLE OF CONTENTS

1 INTRODUCTION

1.1 The immune system

The vertebrate organism is constantly exposed to a variety of potentially pathogenic microorganisms, like bacteria, viruses or fungi. As an effective and protective defense mechanism against these infectious agents the immune system has evolved which ensures reliable recognition and subsequent elimination of the pathogens. Vertebrate immunity relies on two distinct but cooperating parts, the innate and the adaptive immunity. The mechanisms of innate immunity constitute the first line of defense against pathogens. Beside being based on a number of more unspecific barriers that are effective against a variety of pathogenic organisms, such as the skin, mucous membranes, the complement system and enzymatic mediators, innate immunity requires the involvement of phagocytic cells, namely macrophages and neutrophils. These phagocytes are able to detect pathogens by the presence of certain conserved, repetitive molecular structures the so-called PAMPs (pathogen-associated molecular patterns). PAMP recognition is achieved by the expression of pattern-recognition receptors (PRR) which represent a set of germline encoded cell bound as well as soluble molecules (for review see Janeway, 1989, Gordon, 1995, Silverstein, 1995, Janeway and Medzhitov, 2002). PRR mediated recognition of a pathogen by macrophages or neutrophils results in phagocytic uptake of the pathogenic organism and its subsequent degradation in the microbicidal lysosomal compartments.

Under circumstances where pathogens have managed to evade the mechanisms of innate host defense and an infection has been established, the adaptive immune response is induced. While the innate immune system relies on germline encoded invariant receptors recognizing common structural motifs on the surface of pathogens, the hallmark of the adaptive immune system is its ability to recognize practically all pathogens specifically through the generation of a diverse array of antigen-specific receptors expressed by lymphocytes. Furthermore, in the course of an adaptive immune response an immunological memory is established which ensures a more rapid and effective response upon a second encounter with a pathogen, thereby potentially providing lasting protective immunity.

1.2 The mechanisms of adaptive immunity: an overview

The central players in establishing adaptive immunity are the lymphocytes, consisting of B- and T-lymphocytes. Together, these are able to respond to virtually any kind of antigen by

clonotypically expressing antigen specific receptors of the immunoglobulin superfamily, the B-cell receptor (BCR) on B-cells and the T-cell receptor (TCR) on T-cells. The huge diversity in the specificity of these receptors is generated by somatic gene recombination of germline–encoded receptor gene segments, the so-called V, D and J genes (Tonegawa, 1988). The random process of V(D)J gene-segment rearrangements results in the production of B- and T-cells carrying a diverse set of antigen-specific receptors.

The B- and T-cells together with antigen presenting cells (APCs) such as macrophages and dendritic cells are the effector cells that ensure the efficient mounting of an adaptive immune response. B- and T-cells fulfill distinct functions which are reflected by the existence of the two types of adaptive immune response, the humoral and the cellular response (see Fig.1). The humoral response that is mediated by secreted antibodies is directed against pathogens present in the extracellular space. Upon encounter with an antigen, B-cells become activated and differentiate into effector B-cells (also referred to as plasma cells). Effector B-cells secrete their usually membrane-bound antigen receptor as a soluble version, which is then referred to as antibody. Secreted antibodies subsequently bind to the antigen and thereby facilitate its clearance from the body.

In contrast, the adaptive cellular immune response is directed against intracellularly residing pathogens. The adaptive cellular immune response relies on the action of the T-lymphocytes. T-lymphocytes occur in two flavors, the CD4 and CD8 positive T-lymphocytes. Unlike B-lymphocytes, T-lymphocytes are not able to recognize free antigens but instead require the presentation of antigens by antigen-presenting cells (APCs). APCs are specialized for the sampling and processing of antigens. Processing of antigens refers to the mechanims of converting either exogenous or endogenous antigenic proteins into peptide fragments that are then bound and presented on the cell surface by the major histocompatibility complex (MHC) molecules. Two subtypes of MHC molecules exist, MHC class I and class II molecules. MHC class I molecules bind peptides that are usually derived from pathogens residing in the cytosol. Recognition of MHC class I presented antigenic peptides is restricted to CD8 positive T-lymphocytes resulting in the activation of the CD8 positive T-cell. Activated CD8 positive T-lymphocytes, which are also called cytotoxic effector T-cells, are then able to kill the infected cell by secreting cytotoxic effector proteins (e.g. granzymes and perforin) or by inducing apoptosis in the target cell by the presence of apoptosis-inducing factors, such as Fas-ligand (for review see Berke, 1997). Death of the target cell can then either result in the simultaneous elimination of the infectious agent or its release into the extracellular space where it is subsequently cleared by macrophages or by the antibody-induced activity of the complement system (see Fig.1, reviewed in Liszewski et al., 1996).

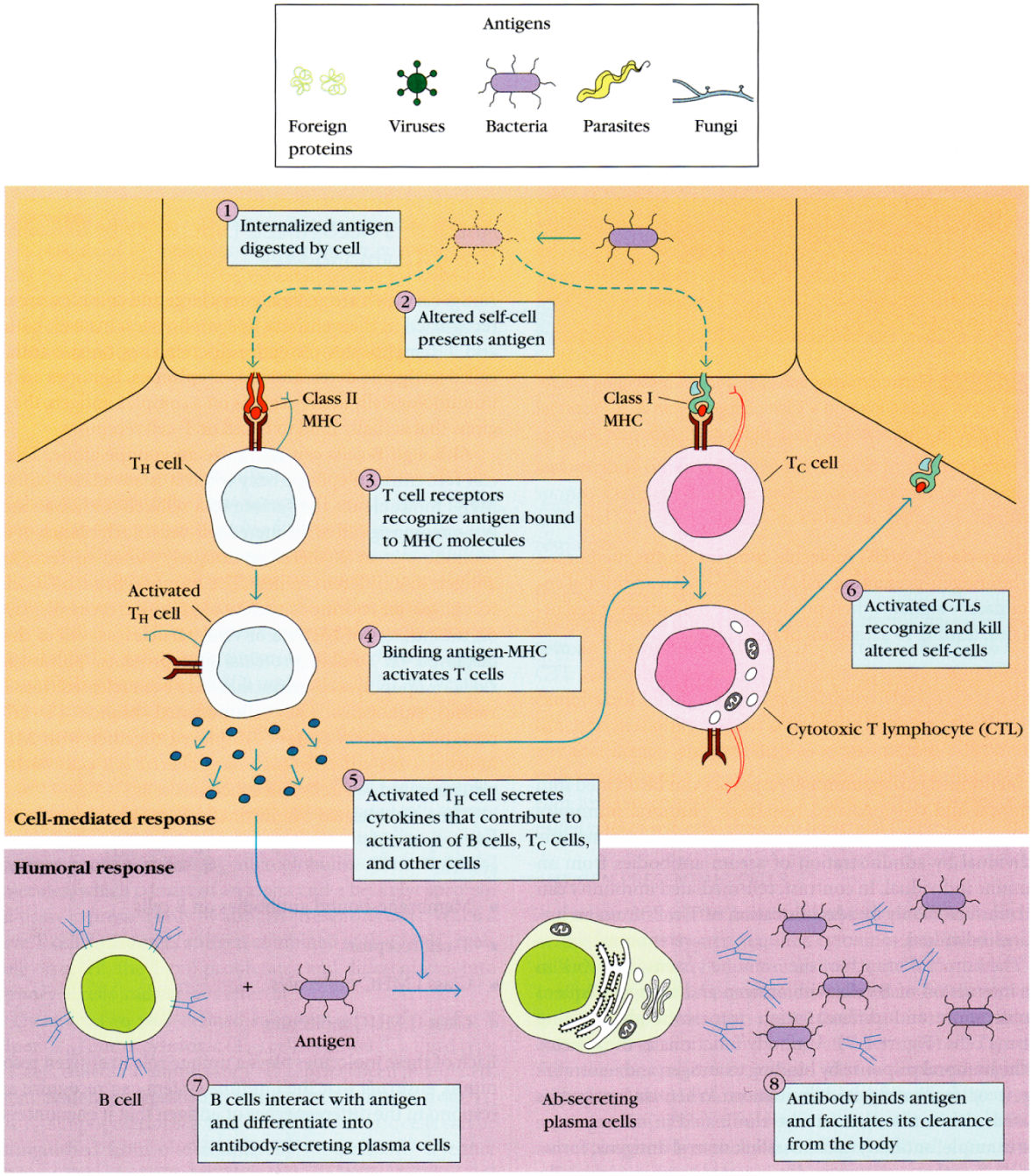

Fig. 1 Overview of the two types of adaptive immune response, the humoral and the cellular response. In the humoral response (lower panel), B-cells differentiate upon encounter with an antigen into antibody-secreting effector B-cells (also referred to as plasma cells). Subsequent binding of the secreted antibody to the antigen facilitates the clearance of the antigen from the body. In the cellular response, T-cells recognize antigens presented on the cell surface by major histocompatibility (MHC class I and class II) molecules. CD4 positive T-cells are specialized in recognizing MHC class II bound antigenic fragments. Activation of CD4 positive T-cells results in their differentiation into T-helper cells (T_H cells) which release cytokines required for the activation of B-cells, cytotoxic (CD8 positive) T-cells and macrophages. Recognition of MHC class I presented antigenic peptides is restricted to CD8 positive T-cells (here referred to as T_C cells) resulting in their activation. Activated CD8 positive T-cells differentiate into cytotoxic effector T-cells (CTL) which are able to kill the target cell by the secretion of cytotoxic effector proteins or by surface-expression of apoptosis-inducing factors. Taken from Goldsby et al., 2003.

MHC class II molecules, on the other hand, are responsible for the presentation of peptide ligands generated after internalization of extracellular material, e.g. bacteria and soluble antigens, and its subsequent processing in the endosomal/lysosomal pathway. CD4 positive T-lymphocytes are specialized in recognizing MHC class II bound antigenic fragments. Their activation results in the release of cytokines aiming at either the activation of macrophages to enhance their microbicidal activity or the induction of the differentiation of B-cells into antibody secreting plasma cells. Based on this ability to stimulate and activate other immune cells effector CD4 positive T-cells are also referred to as T-helper cells (for review see Abbas et al., 1996, Asnagli and Murphy, 2001).

1.3 Antigen presenting cells and antigen processing

The two classes of MHC molecules, MHC class I and class II, are the basis for antigen presentation to T-cells. They are expressed in a cell type specific manner; MHC class I molecules are expressed on all nucleated cells whereas MHC class II molecule expression is restricted to a set of specialized cells, the antigen-presenting cells (APCs). APCs comprise a subset of cells to which B-cells, macrophages and dendritic cells belong. Depending on the kind of antigen two different processing pathways can be employed by APCs to generate ligands for binding to either MHC class I or class II molecules.

1.3.1 Types of antigen presenting cells

B-cells, macrophages and dendritic cells are referred to as professional antigen-presenting cells due their ability to take up antigens, to process them for the loading on MHC molecules and to eventually activate naïve T-cells. The capacity of B-cells to present antigens relies on the surface expression of the antigen-specific BCR. Upon binding of an antigen, B-cells are able to internalize antigens and process them in the MHC class II pathway (Lanzavecchia, 1990, Watts, 1997).

Macrophages play a central role in innate immune responses against microbial pathogens but can also act as antigen-presenting cells due to their extraordinary capacity to internalize infectious agents. Uptake of virtually any kind of soluble or cell-associated antigen occurs either non-specifically or specifically through surface-expressed receptors. These receptors are either pattern-recognition receptors (PRRs) recognizing conserved structures of microbial origin (pathogen-associated patterns or PAMPs) or opsonic receptors mediating the binding of antibody- or complement-coated microbes (reviewed in Taylor et al., 2005). Infectious agents bind to their specific receptors which triggers the internalization of antigens via

receptor-mediated endocytosis or phagocytosis (Lanzavecchia, 1990, Aderem and Underhill, 1999). Whereas receptor-mediated endocytosis allows macrophages to efficiently internalize antigens that are present at low concentrations, phagocytosis enables the macrophage to take up particulate material, such as whole microbes or apoptotic cells (Lauber et al., 2004, Trombetta and Mellman, 2005). The endosomal and lysosomal compartments in macrophages are adapted for the digestion of internalized material. This specialization predominantly contributes to the function of macrophages in clearing invading microorganisms but also provides antigenic peptides for presentation on MHC molecules.

Both classes of MHC molecules as well as costimulatory molecules are expressed on macrophages but at significantly lower levels compared to B-cells and dendritic cells (Steinman et al., 1997). Even after activation of macrophages by inflammatory cytokines or microbial products the resulting upregulation of MHC class II and costimulatory molecule expression does not reach levels comparable to those found on B-cells and DCs. This may explain why macrophages were found both *in vitro* and *in vivo* to be less efficient than B-cells and dendritic cells in antigen presentation and subsequent T-cell activation (Inaba et al., 1990, Crowley et al., 1990, Banchereau and Steinman, 1998).

The primary function of dendritic cells (DCs) is, in contrast to B-cells and macrophages, to present antigens. This specialization relies on the unique surveilance and migratory properties of DCs (Randolph, 2001). DCs are present in almost all tissues in an immature state. Immature DCs are highly endocytic and can therefore sample a broad range of antigens non-specifically or via specific receptors. Upon receiving appropriate stimuli, like receptor-mediated antigen recognition and inflammatory cytokines, immature DCs undergo a dramatic reorganization in form and function to ultimately differentiate into mature DCs. Mature DCs are characterized by upregulation of surface-expressed MHC class II and costimulatory molecules and a markedly reduced endocytic capacity (Sallusto et al., 1994 and 1995, Cella et al., 1997, Engering et al., 1998, Garrett et al., 2000, Inaba et al, 2000). Furthermore, mature DCs migrate from the periphery into lymphoid tissues allowing them to transport antigens from the periphery to secondary lymphoid organs or to internalize antigens directly from the lymph (Itano et al., 2003). Here they accumulate in regions where macrophages and B-cells are generally excluded but which are instead enriched in T-cells. This unique distribution of DCs in the T-cell zones of lymphoid tissues allows them to efficiently activate naïve T-cells (von Andrian and Mempel, 2003, Catron et al., 2004, Mempel et al., 2004).

1.3.2 Antigen-processing and presentation of peptides on MHC molecules

Processing of antigens for their presentation by MHC molecules generally follows two distinct pathways (for review see Trombetta and Mellman, 2005). The MHC class I pathway generates 8-10 amino acid long antigenic peptides from proteins present in the cytosol. These proteins have to be ubiquitinated to be a substrate for the proteasome (reviewed in Baumeister et al., 1998) that degrades them and thereby provides peptide fragments for MHC class I presentation. The source of proteasomal substrates is quite varied and includes endogenous or viral proteins present in the cytosol, alternative translation products, defective proteins and proteins retrotranslocated from the endoplasmic reticulum (ER) to the cytosol (Boon and Van Pel, 1989, Bullock and Eisenlohr, 1996, Wang et al., 1996, Bacik, et al., 1997, Saeterdal et al., 2001, Yewdell et al., 2001, and reviewed in Shastri et al., 2002, Watts, 1997). The peptides generated by the proteasome are subsequently transported into the ER by the ATP-dependent transporter associated with antigen processing (TAP1/TAP2 heterodimer).

The heterodimer of the proteins TAP1 and TAP2 is an ATP-dependent transporter required for the transport of antigens into the ER lumen (Spies et al., 1990, Androlewicz et al., 1993, Neefjes et al., 1993). Once in the ER lumen the antigenic peptides are further proteolytically processed and then loaded onto newly synthesized MHC class I molecules. The binding of peptides to MHC class I molecules is mediated by chaperones such as calnexin, calreticulin, and ERp57. Only those MHC class I molecules stabilized by binding antigenic peptide are transported further to the cell surface (Grandea et al., 2000). The MHC class I pathway is constitutively active in all nucleated cells which allows CD8 positive, cytotoxic T-cells to survey protein expression for abnormalities caused by the presence of pathogens such as viruses.

The expression of MHC class II molecules is usually restricted to APCs but can be induced by interferon-γ stimulation of many other cell types (Steimle et al., 1994). The peptides (13 - 25 amino acids long) generated in the MHC class II pathway originate from exogenous proteins that have been internalized and processed along the endocytic route. Proteolytical processing of internalized exogenous proteins occurs in specialized, acidic endosomal and lysosomal compartments, which are also referred to as MHC class II compartments (Pieters et al., 1991, Amigorena et al., 1994, Tulp et al., 1994, West et al., 1994, Engering et al, 1998). Newly synthesized MHC class II molecules are transported from the ER to the MHC class II compartments. Targeting to MHC class II compartments relies on the binding of an invariant chain (Ii) to newly synthesized MHC class II molecules (Bakke and Dobberstein,

1990, Lotteau et al, 1990, Pieters et al., 1993, Brachet, 1997). As long as the invariant chain occupies the peptide binding site of MHC class II molecules with its class II associated invariant chain peptide (CLIP) unspecific binding of peptides is prevented (Roche and Creswell, 1990, Teyton et al., 1990, Eynon et al., 1999). Upon arrival in the MHC class II compartments the invariant chain is cleaved which results in the release of CLIP that is subsequently exchanged for an antigenic peptide. Exchange of CLIP for antigenic peptides in the binding sites of MHC class II molecules is assisted by HLA-DM, a chaperone related to MHC class II molecules (Kelly et al., 1991, Denzin and Cresswell, 1995, Ferrari et al., 1997, Kropshofer et al., 1997). Transport of loaded MHC class II molecules to the cell surface is only initiated when MHC class II molecules form a stable complex with antigenic peptides (Lanzavecchia et al., 1992). Recognition of MHC class II bound peptides is restricted to CD4 positive T-cells, which are also referred to as T-helper cells. Depending on the cytokines released by activated CD4 positive T-cells two subpopulations of T-helper cells can be distinguished, the T_H1 and T_H2 helper cells. Cytokines released by T_H1 cells activate professional phagocytes such as macrophages resulting in an enhancement of their microbicidal mechanisms. The cytokines released by T_H2 cells aim at initiating and regulating antibody based immune responses mediated by B-cells (for review see Abbas et al., 1996, Asnagli and Murphy, 2001).

Besides the above described mechanisms to generate ligands for MHC class I or class II molecules another route for the generation of MHC class I molecules exists which is referred to as cross-presentation (Bevan, 1976). Cross-presented antigenic proteins are of exogenous origin but can gain access to the MHC class I processing pathway which accounts for a variety of immune responses such as the tolerance against peripheral antigens, anti-tumour response and the activation CD8 positive, cytotoxic T-cells by professional antigen-presenting cells (reviewed in Trombetta and Mellman, 2005).

1.4 Development and functions of the major cell types of the immune system

The cells of the immune system are generated in the bone marrow. They subsequently migrate out of the bone marrow into the peripheral tissues, the blood circulation and the lymphatic system. Here they either mature further (as B-cells in the spleen or the progenitors of T-cells in the thymus) or fulfill their cell-type specific functions. The bone marrow is responsible for the generation of the cellular components of the blood which all are derived from the same precursors, the hematopoietic stem cells (HSC). Initially, HSCs differentiate into intermediate progenitors of limited potential that undergo further lineage commitment

and subsequently develop along a single pathway. Although the precise definition of the individual lineages is still a matter of debate, it is currently believed that the early steps of HSC differentiation result in progenitors of three independent lineages: the erythroid-megakaryocyte, the myeloid and the lymphoid lineages (see Fig.2, Katsura, 2002).

The progenitors of the erythroid-megakaryocyte lineage give rise to erythrocytes, platelets and megakaryocytes. Erythrocytes, also referred to as red blood cells, are responsible for the transport of oxygen through blood vessels, whereas the platelets derived from megakaryocytes fulfill important functions in maintaining the vascular system. Within the myeloid lineage dendritic cells, macrophages, monocytes, granulocytes and polymorpho-nuclear cells (neutrophils, baso-phils and eosinophils) develop. Macrophages, which mature from monocytes, dendritic cells and neutrophils are the three types of phagocytic cells in the immune system that play a crucial role in both innate immune (clearance of infectious agents by phagocytosis) and adaptive immune responses (antigen presentation). The function of granulocytes, basophils and eosinophils is less well understood but seems to be important at sites of inflammation (granulocytes) and in the defense against parasitic infections (eosinophils and basophils).

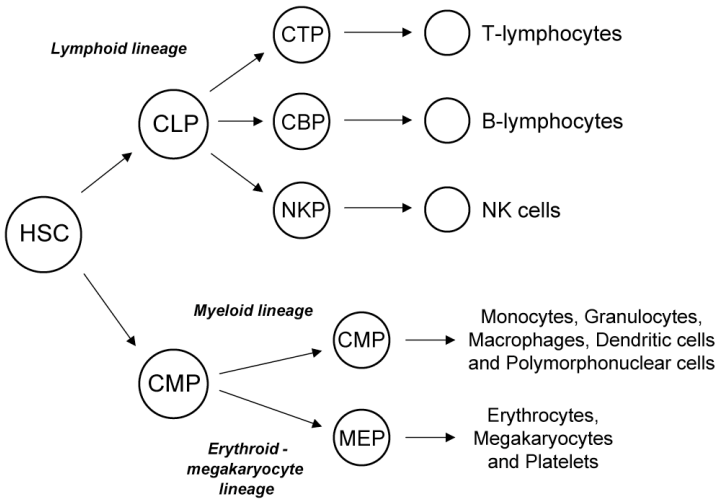

Fig. 2 Model for the development of the three main classes of blood cells from hematopoietic stem cells (HSCs). Although the precise definition of the individual lineages with their cognate precursors is still a matter of debate, it is currently believed that the early steps of HSC differentiation result in progenitors of three independent lineages: the erythroid-megakaryocyte, the myeloid and the lymphoid lineages. The first branch from hematopoietic stem cells (HSCs) is between the common lymphoid progenitor (CLP) and the common myeloid progenitor (CMP). Common lymphoid progenitors give rise to common T-cell progenitors (CTP), common B-cell progenitors (CBP) and natural killer cell progenitors (NKP) which ultimately develop into T- and B-lymphocytes and natural killer (NK) cells. The common myeloid progenitor is capable of generating monocytes, granulocytes, macrophages, dendritic cells and polymorphonuclear cells (neutrophils, basophils and eosinophils) along the myeloid lineage. The megakaryocyte-erythroid progenitor (MEP) derives from common myeloid progenitors and eventually differentiates into erythrocytes, megakaryocytes and platelets. Adapted from Katsura, 2002.

The lymphoid lineage gives rise to B- and T-lymphocytes and natural killer (NK) cells. The natural killer cells are thought to be the prototype of T-cells. They have important functions in innate immunity since they can detect and attack certain virus-infected cells despite their lack of antigen-specific receptors. In the following, the function and development of B- and T-cells will be discussed in more detail.

1.4.1 Development and functions of B-lymphocytes

B-cell development takes primarily place in the bone marrow. Immature B-cells travel via the blood to the spleen where they undergo further maturation. During B-cell development the genes for the B-cell receptor (BCR) are rearranged from germline encoded receptor gene segments. Depending on the rearrangement status of the heavy and light chains of the BCR, discrete stages of B-cell development have been described for which we will use the nomenclature suggested by Melchers and Rolink (1998).

1.4.1.1 The organization of the BCR complex

The BCR is a multiprotein protein complex that consists of clonally variable antigen-binding chains – the heavy and light immunoglobulin chains –, which are associated with invariant accessory proteins (see Fig.3). By disulfide bonds each light chain is covalently linked to one of the two heavy chains. The heavy chains itself are also covalently associated by disulfide bonds. The immunoglobulin complex constituting the BCR is normally membrane-bound but upon activation of B-cells and their differentiation into plasma cells it is secreted in the form of an antibody. Surface expression or secretion of the immunoglobulin complex is regulated by alternative splicing of the primary mRNA which either retains or excises the exons encoding the trans-membrane domain of the BCR (Early et al., 1980, Rogers et al., 1980). The two invariant accessory proteins associated with the immunoglobulin chains in the BCR complex are called Igα and Igβ (Fig.3 B). They are both required for the transport of the receptors to the cell surface (Hombach et al., 1990) and, more importantly, for signal transduction upon engagement of the BCR. Since the immunoglobulin complex of the BCR can itself not generate a signal, signal transduction relies on the presence of immunoreceptor tyrosine-based activation motifs (ITAMs, Reth, 1989) in the cytosolic tails of Igα and Igβ.

The huge diversity in the specificity of the BCR and antibodies is based on the variability of the amino-terminal regions of the light and heavy chains which form the antigen binding site. These domains of highly variable sequence are referred to as V regions. Beside the V regions the immunoglobulin chains are made up of domains with relatively constant sequence the so-called C-regions. The variety of the immunoglobulin chains of the BCR is generated by the somatic rearrangement of germline encoded gene segments (V(D)J recombination). Three different loci carry these gene segments: the immunoglobulin heavy chain (IgH) locus and the two loci containing the gene segments for two types (κ and λ) of light chains. Each of these loci is characterized by the presence of regions encoding various variable (V), diversity (D), joining (J) and constant (C) segments. In the stochastic process of

V(D)J recombination single variable regions are combined with joining (J) and, in the case of the heavy chain, diversity (D) gene segments (Tonegawa, 1983). The somatic recombination leads to the generation of a new exon encoding the variable region of a particular immunoglobulin chain that is joined to a constant region gene segment by splicing of the primary mRNA transcript. As we will see in the following, V(D)J recombination is tightly regulated according to the developmental stage of B-cell development. Due to the random specificities of the generated BCRs, B-cells are subjected to selection processes during development leading to the elimination of cells which are potentially non- as well as self-reactive. Only those B-cells that have been selected for their ability to recognize foreign antigens specifically are clonally expanded.

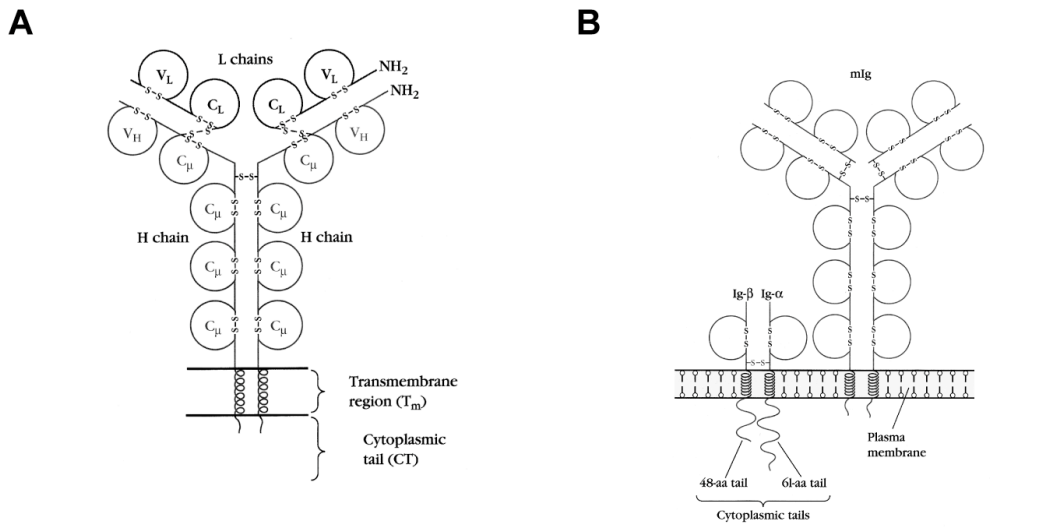

Fig. 3 Schematic representation of the B-cell receptor complexed with the two invariant accessory chains Igα and Igβ. (**A**) The BCR consists of clonally variable antigen binding chains: the heavy (H) and light (L) immunoglobulin chains. These chains are covalently linked by disulfide bonds (S-S) and are made up of the highly variable V regions and the relatively constant C regions. (**B**) Association of the BCR with the two invariant accessory chains Igα and Igβ is required for transport of the BCR to the cell surface and for signal transduction. Signal transduction relies on the presence of immunoreceptor tyrosine-based activation motifs (ITAMs) in the cytosolic tails of Igα and Igβ. Schemes taken and modified from Goldsby et al., 2003.

1.4.1.2 Development of B-cells in the bone marrow and the spleen

The development of B-cells in the bone marrow has been elucidated to proceed through discrete stages which are characterized by defined rearrangement intermediates of the immunoglobulin chains and by the expression of a series of surface- and cytoplasmatically expressed marker proteins (see Fig.4, for review refer to Melchers and Rolink, 1998).

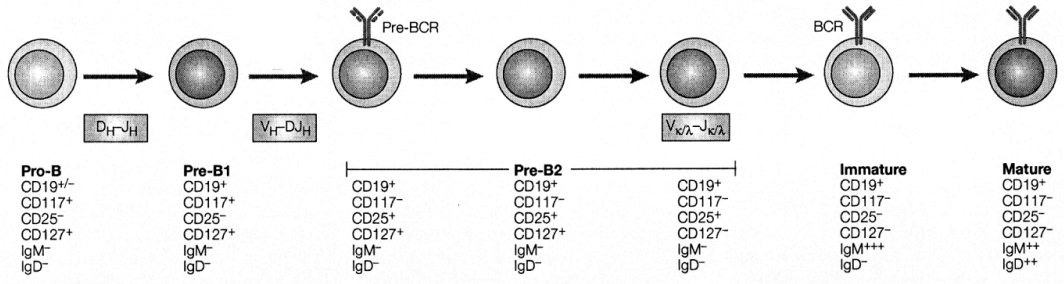

Fig. 4 Scheme of early B-cell development. The development of B-cells in the bone marrow proceeds through discrete stages which are characterized by defined rearrangement intermediates of the immunoglobulin chains (shown here in boxes) and by expression of a series of surface expressed markers proteins. In this scheme, cell development from less mature to more mature cells proceeds from the left to the right. Not shown is the earliest well-defined B-cell progenitor (pre/pro B-cell) which gives rise to pro-B cells. The cell-surface phenotype of each subpopulation is shown below it. BCR: B-cell receptor, D: diversity region, Ig: immunoglobulin, J: joining region, V:, variable region. Scheme taken from Ceredig and Rolink, 2002.

The earliest well-defined B-cell progenitors are the pre/pro-B cells. They are positive for the pan B-cell marker B220 and express the interleukin 7 receptor □-chain (CD127) and the receptor for stem cell factor CD117 (c-kit). The next stage, the pro-B cells, are phenotypically similar but started to express CD19 and are characterized by undergoing rearrangement of D and J regions on their IgH chain loci. Upon sucessful DJ rearrangement on both IgH alleles pro-B cells develop into pre-B1 cells. Pre-B1 cells are indistiguishable from pro-B cells in terms of surface expressed markers. In the following transition step from pre-B1 to large pre-B2 cells rearrangement of a V region to the existing, recombined DJ segment of the IgH locus is initiated. From the resulting V(D)J rearranged exon the so-called □H chain is expressed which associates with the surrogate light chain components □5 and VpreB and with the signal-transducing proteins Ig□ and Ig□ eventually constituting the pre-BCR complex on the cell surface. Successful expression of the pre-BCR represents a first selective checkpoint in B-cell development since surface deposition of the pre-BCR is required for the induction of proliferation and differentiation of the large pre-B2 cells into the small, resting pre-B2 cells (Nussenzweig et al., 1987, Grawunder et al, 1995, Rolink et al., 2000). The small pre-B2 cells start to rearrange their □ and □ light chain loci which is prerequisite for the differentiation into surface IgM (BCR) positive immature B-cells. Immature B-cells can furthermore be identified by the expression of intermediate levels of B220. These cells are subject to selection processes in the bone marrow which result in the removal of cells expressing a BCR with autoreactivity. Only immature B-cells expressing high levels of alloreactive IgM leave the bone to migrate into the spleen where they undergo further maturation (Rolink et al., 2004).

Immature B-cells originating from the bone marrow enter the spleen through the terminal branches of central arterioles to reach the inner region of the white pulp which is divided into a periarteriolar sheet (PALS), containing mainly T-cells, and a flanking B-cell corona (see Fig.5 A). Here, the immature B-cells pass through further developmental stages which require engagement of the BCR (Liu, 1997). The resulting mature B-cell types in the spleen are the follicular and marginal zone B-cells. They can be identified by differences in the expression of the surface markers CD21 and CD23. Follicular B-cells are highly positive for CD21 and CD23, are topolocially found inside follicles and play a role in thymus-dependent (also referred to as T-cell dependent) immune responses. In contrast, marginal zone B-cells are CD21 positive but express CD23 at low levels. Marginal zone B-cells are found at the outer rim of follicles which is adjacent to the marginal sinus. Here, these B-cells come into close contact with macrophages and dendritic cells of the marginal zone which allows them to participate in the early and therefore thymus-independent (also referred to as T-cell dependent) response to blood-borne antigens.

1.4.1.3 Functions of mature B-cells

Mature B-cells as the main effector cells of the humoral adaptive immune response recirculate among the lymphoid follicles of the spleen and lymph nodes (see Fig.5). The antibodies produced by activated B-cells provide a first line of defense by neutralizing and opsonizing free extracellular pathogens. Based on the recognition of epitopes formed by the native three-dimensional structure of the antigen (Amit et al., 1985 and 1986, Colman et al., 1987) antibodies are able to bind soluble or membrane-associated antigens. Binding of antigens by antibodies confers to neutralization of extracellular pathogens and their products and facilitates phagocytosis by opzonisation of antigenic structures. Furthermore, binding of antibodies to antigens is crucial for the activation of the complement system and for the induction of antibody-dependent cell-mediated cytotoxicity (ADCC; reviewed in Ward and Ghetie, 1995). Therefore, antibodies as the mediators of the adaptive humoral response ensure the clearance of extracellular pathogens.

Generally, activation of B-cells through their BCR can be initiated in two ways either by binding of so-called thymus-dependent (T-cell dependent) or thymus-independent (T-cell independent) antigens (reviewed in Parker, 1993, Mond et al., 1995a). Thymus-dependent antigens are mostly protein antigens which are - after binding to the BCR - internalized, processed and presented as peptides on MHC class II molecules by the B-cell. In order to be activated, the B-cell requires a second signal that is provided by CD4 positive T-helper cells. This second signal relies on the TCR-mediated recognition of the peptide/MHC complex by

the T-helper cell and the subsequent clustering of the BCR together with the B-cell co-receptor complex consisting of the proteins CD19, CD21 and CD81 (reviewed in O'Rourke et al., 1997).

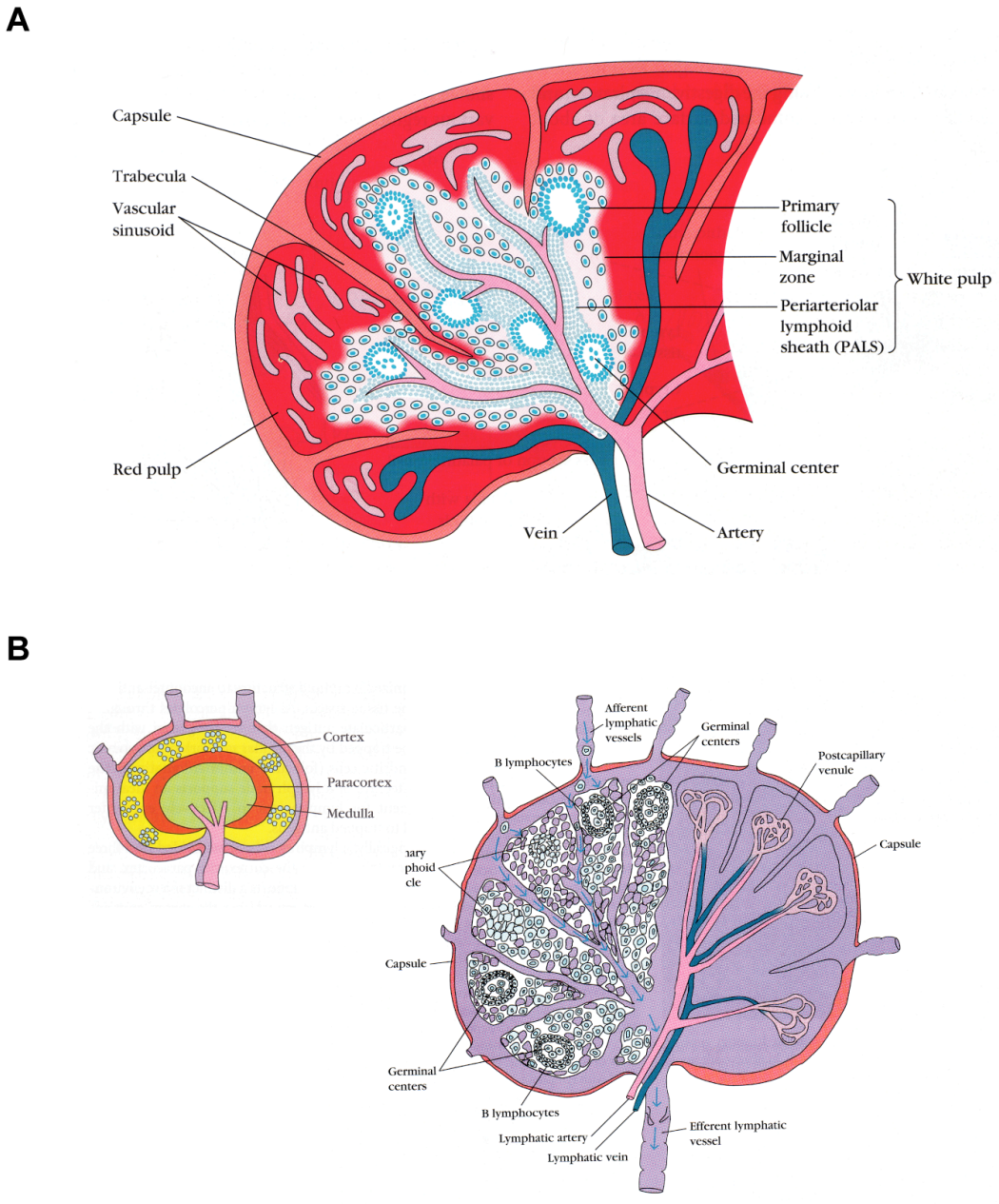

Fig. 5 Structure of the spleen (**A**) and a lymph node (**B**). (**A**) The spleen is the largest secondary lymphoid organ and specialized for trapping blood-borne antigens. The bulk of the spleen is composed of red pulp, where removal of red blood cells takes place. Lymphocytes surround the arterioles entering the spleen, forming areas of white pulp. The inner region of the white pulp is divided into the periarteriolar sheet (PALS), containing mainly T-cells and a flanking B-cell corona. Closely associated with the PALS is the marginal zone, an area rich in B-cells. The marginal zone furthermore contains primary follicles to which activated B-cells migrate. Upon antigenic challenge, these primary follicles develop into secondary follicles which are characterized by the germinal center. In the germinal center rapidly dividing B-cells and plasma cells are located. (**B**) The three layers (cortex, paracortex and medulla) of a lymph node are characterized by distinct cell types found in each layer. Macrophages and dendritic cells, which trap antigen from the lymph, are situated in the cortex and paracortex. T-cells are predominantly found in the paracortex (also referred to as T-cell zones). B-cells are located in the cortex, within primary/secondary lymphoid follicles and germinal centers. Taken and modified from Goldsby et al., 2003.

Furthermore, upon binding antigen presented by B-cells, the expression of CD40 ligand (CD40L) on T-helper cells is induced which binds to CD40 expressed on the surface of the antigen-presenting B-cell (Lane et al., 1992, Jaiswal and Croft, 1997). Together with cytokine release (Interleukin-4, Valle et al., 1989) by the T-cell, the T-cell mediated co-clustering of the BCR with accessory molecules leads to activation of the B-cell and its subsequent differentiation into long-lived antibody-producing plasma cells.

In contrast to protein antigens for which B-cells require T-cell help to be activated, many microbial components are able to induce antibody production in the absence of T-helper cells and are therefore referred to as thymus-independent antigens. The signals required to activate B-cells are provided by inducing massive crosslinking of the BCR due to the repetitive nature of microbial epitopes such as cell wall components (e.g. Lipopolysaccharide (LPS), for review see Mond et al., 1995b).

Typically, the development of the humoral adaptive immune response requires several days and results in the production of mono-specific, high-affinity antibodies, first of the immunoglobulin M (IgM) and later of immunoglobulin G type (reviewed in MacLennan et al., 1997). During the early phases of infection and before specific antibodies are produced, the so-called natural antibodies are present in the serum and aim at limiting the spread of the pathogens. Natural antibodies are mostly of IgM type and bind a variety of antigens with low affinity (Ochsenbein et al., 1999 and 2000). They are produced by another mature B-cell population, the B1 B-cells, in a thymus-independent manner. The developmental pathways leading to the generation of B1 B-cells are fundamentally different from the other mature B-cells (marginal zone and follicular B-cells). B1 B-cells originate from the fetal liver and require the spleen for their maturation and survival (Herzenberg et al., 1986). In summary, the function of B-cells lies in providing an initial as well as prolonged protection against free extracellular pathogens by producing antibodies as mediators of the humoral adaptive immune response.

1.4.2 Development of T-lymphocytes

Development of T-lymphocytes from progenitors originating from the bone marrow occurs in the thymus (Miller and Osoba, 1967). Developing T-cells in the thymus are referred to as thymocytes. Various thymocyte subsets representing particular developmental stages have been identified based on the expression of surface markers of which the most prominent ones are CD4 and CD8 (for review see Zuniga-Plücker, 2004). At each developmental stage discrete rearrangement of the genes encoding the T-cell receptor takes places. Their

successful completion together with the interaction of TCR expressing thymocytes with stroma and antigen-presenting cells leads via the processes of positive and negative selection to the generation of mature T-cells. Mature T-cells then leave the thymus to establish the peripheral T-cell pool.

1.4.2.1 Organization of the TCR complex

The T-cell receptor molecule is a disulfide linked heterodimer made up of clonally variable, membrane-bound polypeptide chains (see Fig.6 A). T-cells are grouped into □/□ and □/□ T-cells, depending on the expression of one of the two types of TCR heterodimers. Similarly to the immunoglobulin chains of the BCR, the T-cell receptor □ and □ chains are composed of a variable (V) amino-terminal region forming the antigen binding site and a constant (C) region. Generation of the diversity of TCR polypeptide chains relies, as for the immunoglobulin chains, on the somatic recombination of various V, J and additionally for the □ chain D gene segments (Tonegawa, 1988, for review see Jung and Alt, 2004). The genomic organization of the loci for the □ and □ chains resembles that for the □ and □ chains and somatic rearrangement of appropriate V, D and J gene segments provides the template for the expression of the □/□ TCR.

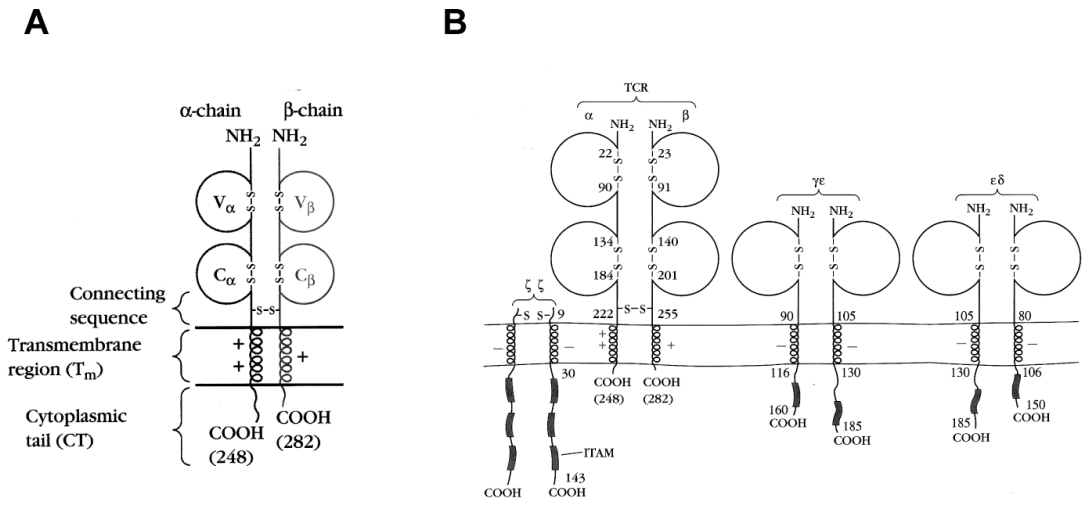

Fig. 6 Schematic representation of the T-cell receptor (TCR) complex. (**A**) The TCR is a disulfide-linked (S-S) heterodimer consisting of the two clonally variable, membrane-bound polypeptide chains α and β. Similar to the immunoglobulin chains of the B-cell receptor, the TCR α and β chains consist of variable (V) and constant (C) regions. Expression of and signal transduction by the TCR depend on the association of the TCR with the accessory proteins of the CD3 complex (**B**). The CD3 complex comprises four different chains (γ, δ, ε and ζ) which form the two non-covalently linked heterodimers CD3 γ/ε and CD3 ε/δ, and a disulfide-linked homodimer of ζ chains. Immunoreceptor tyrosine-based activations motifs (ITAMs) in the cytoplasmic tails of the CD3 chains ensure signal transduction upon TCR engagement. Schemes taken and modified from Goldsby et al., 2003.

The expression and appropriate signal transduction of the TCR depends, as in the case of the BCR, on the association of the TCR with accessory proteins, referred to as the CD3 complex (Samelson et al., 1985, Letourneur and Klausner, 1992). The CD3 complex comprises four different chains (□, □, □ and □) which form the two non-covalently linked heterodimers CD3 □/□ and CD3 □/□, and a disulfide linked homodimer made up of □ chains (see Fig.6 B). All the chains of the CD3 complex contain at least one ITAM which is important for signal transduction upon TCR engagement (reviewed in Garcia et al., 1999, Germain and Stefanova, 1999).

In contrast to the BCR and antibodies, the TCR is not able to recognize antigens in their native, three-dimensional conformation but instead requires the presentation of short antigenic peptides that have been processed and loaded onto MHC molecules by antigen presenting cells. Optimal recognition of peptide loaded MHC molecules relies on the association of the TCR complex with one of the two coreceptors, namely CD4 and CD8. T-cells express either CD4 or CD8 which restricts them in their capacity to recognize peptide/MHC complexes, CD4 positive T-cells recognize peptides bound to MHC class II molecules whereas CD8 positive T-cells interact with peptides loaded onto MHC class I molecules.

1.4.2.2 Development of T-lymphocytes in the thymus

T-lymphocytes are generated from hematopoietic stem cells that migrate to the thymus (Wallis et al., 1975). Their development is not driven cell autonomously but relies on signals from on the one hand non-hematopoietic stromal cells such as thymic epithelial cells and mesenchymal fibroblasts and on the other hand antigen-presenting cells like dendritic cells (reviewed in Anderson and Jenkinson, 2001). The intermediate stages of T-cell development, also referred to as thymocytes, reside in distinct anatomical locations in the thymus which provide exposure to appropriate differentiative signals. The anatomy of the thymus is characterized by the presence of an outer cortex and an inner medulla. During their development thymocytes migrate through these defined thymic regions (see Fig. 7). The hematopoietic progenitors of T-cell development enter the thymus at the cortico-medullary boundary, then migrate to the outer cortex, where most of the differentiation steps take place and eventually reach the medulla, where thymocytes undergo the final maturation steps before leaving the thymus as mature CD4 or CD8 positive T-cells (Lind et al., 2001, Prockop et al., 2002, Porritt et al., 2003).

Classically, thymocyte development can be tracked by the surface expression of CD4 and CD8 (Ceredig et al., 1983). Thymocyte development starts from a subpopulation of CD4/CD8 double-negative (DN) cells, which then differentiate into CD4/CD8 double-positive (DP) thymocytes and finally mature into T-cells being single-positive (SP) for either CD4 or CD8. The use of additional surface-expressed markers, namely CD3, CD25 and CD44, allowed to further subdivide the DN thymocytes into four subsets which appear sequentially on the way of differentiation into DP thymocytes (Godfrey et al., 1993, Ceredig and Rolink, 2002): DN1 ($CD3^-$, $CD25^-$, $CD44^{+++}$), DN2 ($CD3^-$, $CD25^{++}$, $CD44^{+++}$), DN3 ($CD3^{low}$, $CD25^{++}$, $CD44^+$) and DN4 ($CD3^{low}$, $CD25^-$, $CD44^{low}$). Along with thymocyte development through these distinct stages rearrangement of the TCR genes occurs (Fowlkes and Pardoll, 1989). During the DN1 to DN3 stages the loci encoding the γ, δ and β TCR chains are rearranged. DN3 thymocytes are characterized by the surface expression of a correctly assembled and CD3 complex associated TCR that is required for further survival and differentiation. While the γ/δTCR is expressed in the form typical for mature γ/δT-cells, the α/βTCR goes through an intermediate stage which is the assembly of a correctly rearranged β chain with the invariant pre-TCRα chain resulting in the so-called pre-TCR. Expression of the pre-TCR is the first crucial checkpoint in thymocyte development since without its expression there is no progession of thymocyte development beyond the DN3 stage (Groettrup et al., 1993, Groettrup and von Boehmer, 1993, Malissen et al., 1995, Fehling et al., 1995). Upon expression of a signaling-competent pre-TCR, thymocytes are committed to the α/βT-cell lineage and start to expand, to express the CD4 and CD8 coreceptors and to initiate rearrangement of the TCR α chain locus (reviewed in von Boehmer et al., 1998). In contrast, development of γ/δT-cells for which a function in their mature stage is presently not precisely defined, is unknown in its details.

At the DP stage of α/βT-cell development thymocytes have lost CD25 and CD44 expression and now express high levels of proteins of the CD3 complex. From the successfully rearranged TCRβ chain locus TCR α-chains are generated which replace the surrogate pre-TCRα chain. As soon as a functional α/βTCR is expressed, DP thymocytes are subjected to the processes of positive and negative selection resulting in the elimination of cells which are potentially non- as well as self-reactive (reviewed in Starr et al., 2003). The α/βTCR interacts with peptide loaded MHC molecules present on the surface of thymic epithelial and dendritic cells and initiates the corresponding downstream signaling cascades which respresent a critical factor in the decision whether a thymocyte survives or dies. If the interaction of the TCR with self-MHC/peptide complexes is too weak thymocytes die by `neglect`, if it is too strong thymocytes undergo apoptosis which ensures the removal of potentially self-reactive

cells (referred to as negative selection, Sprent and Webb, 1995). Only those thymocytes which show a weak but significant reactivity of their TCR with self-MHC/peptide complexes receive a survival signal and continue their development into self-restricted mature CD4 or CD8 single positive (SP) thymocytes (referred to as positive selection, Marrack and Kappler, 1997). In summary, the processes of positive and negative selection generate self-restricted and self-tolerant CD4 or CD8 T-cells which ultimately leave the thymus to establish the peripheral T-cell pool.

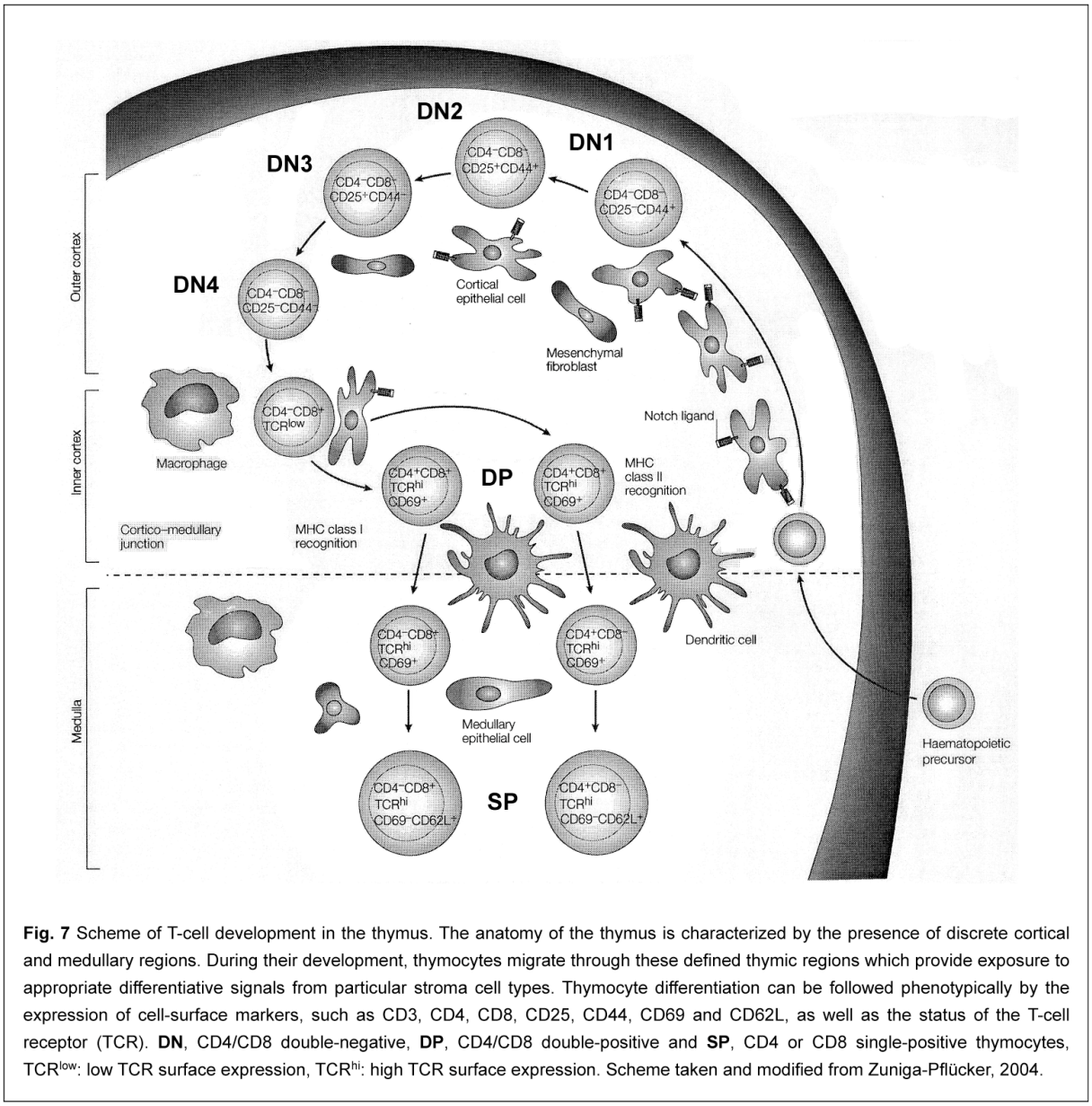

Fig. 7 Scheme of T-cell development in the thymus. The anatomy of the thymus is characterized by the presence of discrete cortical and medullary regions. During their development, thymocytes migrate through these defined thymic regions which provide exposure to appropriate differentiative signals from particular stroma cell types. Thymocyte differentiation can be followed phenotypically by the expression of cell-surface markers, such as CD3, CD4, CD8, CD25, CD44, CD69 and CD62L, as well as the status of the T-cell receptor (TCR). **DN**, CD4/CD8 double-negative, **DP**, CD4/CD8 double-positive and **SP**, CD4 or CD8 single-positive thymocytes, TCR^{low}: low TCR surface expression, TCR^{hi}: high TCR surface expression. Scheme taken and modified from Zuniga-Pflücker, 2004.

1.5 Activation and homeostasis of T-lymphocytes

Mature T-lymphocytes originating from the thymus seed the peripheral organs where they cycle for prolonged times between the secondary lymphoid organs and the blood in a naïve state. Following an infection, T-cells become activated by antigen-presenting cells within the peripheral lymph nodes, which results in proliferation and differentiation into so-called effector T-cells. Once an infection has been cleared successfully, effector cells are eliminated through apoptosis to maintain the homeostasis of the peripheral T-cell pool. Besides this, memory T-cells are generated which ensure a more rapid response upon a second encounter with a particular antigen (reviewed in Sprent and Tough, 2001, Jameson, 2002). The signals that are responsible for selection, proliferation, survival and differentiation of T-cells rely on the stimulation of the TCR by antigenic peptides bound to MHC molecules on the surface of antigen-presenting cells (for review see Starr et al., 2003, Lanzavecchia and Sallusto, 2000). In the following, the mechanisms of T-cell activation with a special emphasis on the architecture and function of the immunological synapse will be discussed in more detail.

1.5.1 Formation of the immunological synapse and T-cell activation

1.5.1.1 Architecture of the immunological synapse

Recognition of antigens by T-cells requires the engagement of their TCR with peptide/MHC complexes displayed on the surface of APCs. Once a T-cell has encountered an APC presenting their cognate peptide/MHC complex a tight, specialized contact is formed between the two cells also referred to as immunological synapse (IS; Wülfing et al., 1998, Grakoui et al., 1999). Formation of the immunological synapse is required for the specificity of the immune response by stabilizing and favoring continous TCR-antigen interaction and consequent activation of T-cells (reviewed in Dustin et al., 2000; Krummel et al., 2002; van den Merwe, 2002).

Activation of T-cells by triggering of TCRs results in their proliferation and differentiation in a variety of T-cell subtypes that determine the type of immune response. CD4 positive T-cells diffferentiate into either T_H1 and T_H2 cells which release a distinct set of cytokines aiming at the stimulation of professional phagocytes or B-cells as outlined previously (paragraph 1.3.2). CD8 positive T-cells develop into cytotoxic T-cells capable of killing the target cell presenting a viral, bacterial or an otherwise foreign peptide via MHC class I molecules. Furthermore, T-cells can differentiate into T-cells with regulatory function such as suppressor

T-cells capable of downregulating immune responses through the secretion of inhibitory cytokines. Most of these effector T-cells die after the antigen is cleared but some of the T-cells generated during the primary response persist for years as memory T-cells which ensure immediate protection and a rapid response upon reencountering a particular antigen.

Crucial for the decision of a T-cell's fate - differentiation, survival or death upon activation - is the duration of TCR stimulation (Lanzavecchia et al., 1999). The TCR as expressed on the surface of T-cells is associated with a variety of costimulatory molecules, such as the CD3 complex proteins, the coreceptors CD4 and CD8 and the costimulator CD28. During formation of the immunological synapse these costimulatory molecules are clustered together with the TCR leading to serial triggering of the TCR and sustained downstream signaling as long as the contact with the APC is maintained (reviewed in Germain and Stefanova, 1999). TCR signaling is downregulated as soon as the antigen is removed (Valitutti et al., 1995b, Valitutti and Lanzavecchia, 1997).

Whereas initiation of TCR signaling does not require formation of the immunological synapse (Valitutti et al., 1995a), continuous and sustained TCR signaling activity is only achieved by formation of the so-called mature immunological synapse as a stable and prolonged contact between the T-cell and the APC (Valitutti et al, 1995b, Hudrisier et al., 1998, Itoh et al., 1999). The mature immunological synapse is characterized by a distinct clustering pattern of the TCR and costimulatory molecules (Monks et al., 1998 and reviewed in Bromley et al., 2001). In the center of the synapse a structure referred to as central supramolecular activation cluster (cSMAC) is formed which is enriched with TCR/CD3 complexes interacting with the peptide/MHC complex. To the cSMAC a variety of costimulatory molecules and intracellular signaling molecules do localize of which the most important ones are CD4 or CD8, CD28, protein kinase C isoform □ (PKC□) and CD2. The cSMAC is surrounded by the peripheral SMAC (pSMAC) which stabilizes the contact site and is composed of adhesion molecules such as leukocyte function-associated antigen 1 (LFA-1) and cytoskeletal proteins like talin.

1.5.1.2 The role of lipid rafts and cytoskeletal structures in the formation of the immunological synapse

Crucial for the assembly of the immunological synapse are the lateral compartmentalization of the plasma membrane into lipid micro-domains (rafts) and pronouced rearrangements of the F-actin as well as microtubule cytoskeleton (reviewed in Harder, 2001, Acuto and Cantrell, 2000, Das et al., 2002). Lipid rafts have been described as sphingolipid/cholesterol-

enriched microdomains (Simons and Ikonen, 1997) which are located in the two-dimensional lipid bilayer of the plasma membrane and allow the recruitment and organization of distinct signaling components upon TCR engagement (Montixi et al., 1998, Xavier et al., 1998, Leitenberg et al., 2001). Many constituents of the immunological synapse are either constitutively associated with rafts like CD4, CD28 and CTLA-4 or are recruited to rafts upon TCR triggering such as the TCR/CD3 complex or the intracellular signaling molecules PKC and ZAP-70 (for review see Harder, 2001). T-cell activation is perturbed if protein localization to rafts is inhibited (Webb et al, 2000).

During formation of the immunological synapse both F-actin and microtubule cytoskeletal structures undergo profound changes which provide an essential structural support for T-cell activation (Cerottini and Brunner, 1972, Kupfer and Singer, 1989, Serrador et al., 1999). In a T-cell interacting with an APC the cytoskeleton undergoes polarization towards the contact site, actin accumulates at and the microtubule organizing center is localizes close to the immunological synapse (Geiger et al., 1982, Ryser et al., 1982). Whereas the molecular mechanisms governing the reorganization of the microtubule cytoskeleton are presently not well understood the actin cytoskeleton rearrangements where shown to require the activity of members of the Rho family of small GTPases, namely Rac1 and Cdc42 (Stowers et al., 1995). Especially Cdc42 was found to be required for the APC-mediated polarization of the actin cytoskeleton by activating the Wiskott-Aldrich syndrome protein (WASP; Snapper and Rosen, 1999, Rohagti et al., 1999). Activated WASP in turn regulates the temporal and spatial activation of the Arp2/3 complex that mediates actin nucleation and ultimately polymerization (reviewed in Millard et al., 2004). Besides a general structural role by stabilizing the immunological synapse, the precise function of cytoskeletal structures in T-cell activation remains to be further characterized. Current experimental evidence suggests the functional involvement of cytoskeletal structures in providing scaffolds for the recruitment of signaling complexes (Valitutti et al., 1995b, Kaga et al., 1998) and for polarized vesicle trafficking (Kupfer et al., 1991, Stinchcombe et al., 2001, Reichert et al, 2001, Das et al., 2004) or in supporting the recruitment of rafts and associated proteins to the immunological synapse (Harder and Simons, 1999).

1.5.1.3 Signaling events at the immunological synapse

Due to the lack of appropriate cytosolic tails the TCR itself is not able to generate intracellular signals. Signaling downstream of the TCR therefore requires the clustering of the TCR with the CD3 complex and other accessory proteins in the immunological synapse (see Fig.8). During the early phase of IS formation when the TCR recognizes its cognate peptide/MHC

complex membrane proximal protein tyrosine kinases (PTKs), like Lck and Fyn, are brought into close contact with the TCR/CD3 complex mediated by the clustering of lipid rafts (Chu et al., 1998, Clements et al., 1999). Subsequent activation of these PTKs leads to rapid phosphorylation at tyrosine residues of numerous proteins (Korade-Mirnics and Corey, 2000). Of special importantance is tyrosine phosphorylation at the ITAM of the CD3 ζ chain by Lck and Fyn since this leads to the recruitment of another PTK called ZAP70 (Kersh et al., 1998). ZAP70 associated with the CD3 ζ chain is phosphorylated by Lck and thereby activated. Activated ZAP70 is then able to phosphorylate and activate its substrates, namely the linker of activation of T-cells (LAT) and the adaptor molecule SLP76 (Gong et al., 2001, Magnan et al., 2001). Phosphorylated LAT and SLP76 are adaptor molecules which are capable of recruiting and thereby activating other kinases and adaptor molecules for signal transduction downstream of ZAP70 (reviewed in Rudd, 1999, Tomlinson et al., 2000). Especially for LAT which contains nine tyrosine residues the contribution of tyrosine phosphorylation to signal tranduction downstream of the TCR has been well described. Depending on which of the LAT tyrosine residue are phosphorylated distinct sets of cytosolic adaptor proteins (namely those bearing

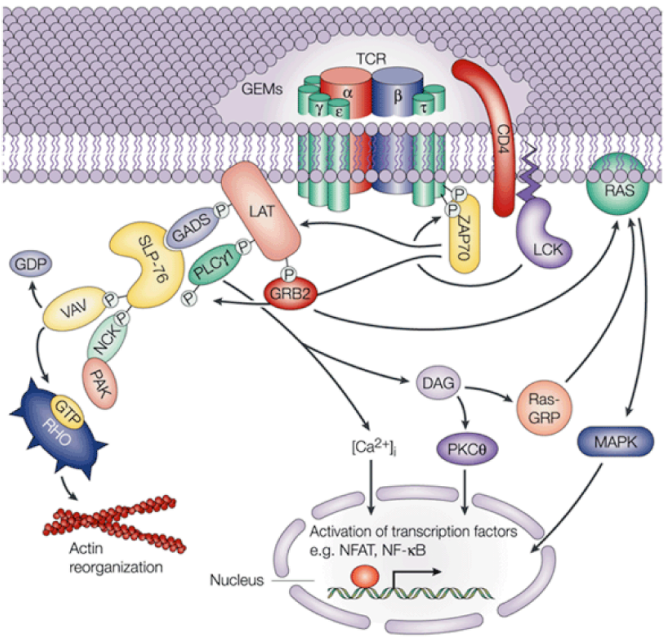

Fig. 8 Schematic overview of signaling pathways downstream of the T-cell receptor (TCR). Following engagement of the TCR formation of the immunological synapse leads to the clustering of the TCR with signaling components. Concomitant binding of CD4 or CD8 to the MHC (not shown here) amplifies the clustering of lipid rafts (lipid rafts are here referred to as GEM: glycolipid-enriched microdomains) and brings membrane proximal protein kinases, such as Lck (LCK) and Fyn (not shown here), into close contact with the TCR/CD3 complex. Activation of Lck (LCK) leads to tyrosine phosphorylation at the immunoreceptor tyrosine-based activation motifs of the CD3 ζ chains. Subsequently, the protein tyrosine kinase ZAP70 associates with the phosphorylated CD3 ζ chains and is activated by phosphorylation through Lck (LCK). Activated ZAP70 is then able to phosphorylate and activate its substrates, namely the linker of activation of T-cells (LAT) and the adaptor molecule SLP76 (SLP-76). Tyrosine-phosphorylated LAT recruits several Src-homology domain 2 (SH2)-containing proteins, including Grb2 (GRP2), Gads (GADS) and phospholipase C γ1 (PLCγ1), to lipid rafts. Activation of PLCγ1 results in the production of the second messengers inositol 3,4,5-triphosphate (IP_3) and diacylglycerol (DAG). IP_3 production leads to increases of free cytosolic $Ca2^+$ $[Ca^{2+}]_i$, whereas DAG can activate both protein kinase C θ (PKCθ) and MAP kinase (MAPK) pathways via the Ras guanyl nucleotide-releasing protein (RasGRP) and the GTPase Ras (RAS). Recruitment of Grb2 by LAT provides another means of activating Ras (RAS). Ultimately, this leads to activation of transcription factors, such as NF-κB and nuclear factor of activated T-cells (NFAT). Regulation of actin cytoskeleton rearrangements via Rho-family GTPases (RHO) has been proposed to be regulated by a trimolecular complex of SLP-76, the Rho-family guanine-nucleotide exhange factor Vav (VAV) and the NCK-associated p21-activated kinase 1 (PAK1). Scheme taken and modified from Koretzky and Myung, 2001.

Src-homology 2 (SH2) motifs: Grb2, Gads and phospholipase C γ (PLC γ)) are recruited which in turn mediate the activation of small GTPases (Paz et al., 2001, Lin and Weiss, 2001, Sommers, 2001). These small GTPases are responsible of regulating the activity of Erk, Jnk and MAP kinase which eventually control the activity of a variety of transcription factors, such as NF-κB, Jun and Fos (reviewed in Henning and Cantrell, 1998). The LAT mediated activation of PLCγ induces calcium and protein kinase C (PKC) dependent signaling pathways which eventually feed into MAP kinase pathways and lead to activation of nuclear factor of activated T-cells (NFAT, for review see Crabtree, 1999, Rao et al., 1997).

Although the diversity of components involved in signaling downstream of the TCR has been elucidated, it still remains to be established what precisely allows the TCR to generate signals governing opposing outcomes such as positive and negative selection during T-cell development in the thymus or survival or death of peripheral T-cells. Currently it is believed that the kinetics and quality of signal transduction is decisive as reflected by the duration and intensity of the activity of distinct signal transducing molecules depending on the affinity of a given peptide/MHC ligand (reviewed in Werlen et al., 2003).

Another important contribution to the type of cellular response mediated by the TCR is provided by coreceptors. CD4 and CD8 are coclustered with the TCR/CD3 complex upon peptide/MHC ligand binding. Concomitant binding of these molecules to either MHC class I (CD8) and MHC class II molecules (CD4) enhances clustering of raft-associated proteins and brings Lck and other coreceptor-interacting molecules into close vicinity to the TCR/CD3 signaling complex (Bosselut et al., 2000, Harder and Kuhn, 2000, Arcaro et al., 2001, Doucey et al., 2001, Dornan et al., 2002). Recruitment of the costimulatory molecules CD28 and cytotoxic T lymphocyte antigen 4 (CTLA-4) to the immunological synapse and subsequent PKCθ mediated downstream signaling was shown to be differentially regulated depending on the expression of their ligands, B7-1 (for CTLA-4) and B7-2 (for CD28), by the APC (Pentcheva-Hoang et al., 2004, Tseng et al., 2005).

1.5.2 T-cell activation and homeostasis

Upon generation in the thymus, naïve T-cells reside in the peripheral recirculating lymphocyte pool as long-lived resting cells. They constantly migrate between the blood and the lymph through specialized T-cell zones in secondary lymphoid tissues such as the spleen and the lymph nodes (see Fig.5). T-cell responses upon infection are initiated in these T-cell zones by mature dendritic cells. Recognition of the antigenic peptides presented on MHC molecules by the APC leads to selective accumulation and subsequent activation of antigen-

specific recirculating T-cells entering the lymphoid tissue from the blood. Activation of T-cells results in differentiation and proliferation of effector T-cells. Once an infection has been cleared most of the effector cells are eliminated while memory T-cells persist. These mechanisms ensure a relatively constant size of the lymphocyte pool in both the resting and the actively responding adaptive immune system (reviewed in Jameson, 2002). In the following the main factors regulating the homeostasis of the peripheral T-cell pool will be discussed.

The survival of naïve T-cells requires the constant TCR mediated recognition of self-peptides bound to MHC molecules and the exposure to the cytokine interleukin-7 (Takeda et al., 1996, Tanchot et al., 1997, Rathmell et al., 2001, Vivien et al., 2001). These two ligands are proposed to initiate moderate levels of downstream signaling activity which is sufficient to allow the naïve T-cell to survive but to not enter the cell cycle (Boise et al., 1995, Ernst et al., 1999, Sprent and Surh, 2001). In contrast, naïve T-cells recognizing a foreign MHC-bound peptide undergo pronounced proliferation along with their differentiation into effector T-cells. Crucial for the proliferation and differentiation into effector T-cells is sustained downstream signaling via the TCR which relies on the contribution of costimulatory molecules like CD4, CD8 and CD28 to the formation of a mature immunological synapse (Kundig et al., 1996, reviewed in Lanzavecchia and Sallusto, 2000a and 2000b). Prolonged TCR stimulation in the mature immunological synapse maintains transcription factors such as NFAT in the nucleus which regulate gene expression depending on the differentiation program of the activated T-cell (Weiss et al., 1987, Timmerman et al., 1996). Differentiation of T-cells into distinct effector subsets also requires the presence of cytokines. Exposure to interleukin-2 (IL-2) is required right after TCR engagement for the survival of activated T-cells keeping them susceptible for subsequent differentiation steps (for review see Ma et al., 2006). The polarization of CD4 positive T-cells into T_H1 and T_H2 helper cells relies on the presence of interleukin-4 and -12 (Iezzi et al., 1999, O'Garra and Arai, 2000). T_H1 differentiation is promoted rapidly by interleukin-12 whereas T_H2 cells need prolonged signaling from both the TCR and IL-4 receptor to develop. Mature CD4 T helper cell subsets as well as differentiated cytotoxic CD8 T-cells are dependent on IL-2, IL-4, IL-7 and IL-15 to survive and further proliferate (Vella et al., 1998).

After an infection has been cleared, most of the effector cells are eliminated by mechanisms which are not yet clearly understood (for review see Sprent and Surh, 2001). Rather than being short-lived cells which die by a default pathway, effector cells seem to require instructive signals to undergo apoptosis. Mutant mouse strains for a variety of molecules which are involved in regulating signaling pathways resulting in the survival or apoptosis of

effector T-cells - including Fas and Fas-ligand (FasL), PD-1, CTLA-4, NFAT, CD25, CD122 and CD45 - show massive accumulation of effector T-cells. These molecules are part of a tightly regulated network required to provide several death signals for effector cells (Nagata, 1997, Rathmell and Thompson, 1999, Sprent and Surh, 2001). Although the precise molecular mechanisms are not yet well defined, death of effector cells seems to be induced by prolonged TCR stimulation and stimulatory cytokines and then to involve negative signaling through CTLA-4 and PD-1 (Chambers and Allison, 1997, Freeman et al., 2000). Furthermore, activation of Fas-mediated apoptosis pathways as well as an increased sensitivity to inhibition by otherwise stimulatory cytokines like IL-2 are crucial steps in the clearance of effector T-cells (Irmler et al., 1997, Inaba et al., 1999). A tightly regulated proportion of effector T-cells are not eliminated but differentiate into memory T-cells by yet ill-defined mechanisms (reviewed in Sprent and Surh, 2001, Kalia et al., 2006). Proliferation and survival of CD4 and CD8 positive memory cells is independent of TCR stimulation and requires, at least in the case of CD8 positive memory cells, in addition IL-15 (Murali-Krishna et al., 1999, Swain et al., 1999, Becker et al., 2002, Goldrath et al., 2002, Schluns et al., 2002). Memory cells can be distinguished from naïve T-cells by the surface expression of cell-type specific markers. Both naïve as well as memory T-cells do not express markers of activated T-cells, namely CD69 and CD25, but they differ in the expression of CD44 which is upregulated during memory cell development. Naive CD4 T-cells are $CD45RB^{hi}CD44^{lo}$ and CD8 T-cells express $CD44^{lo}Ly\text{-}6C^{lo}IL\text{-}2R\beta^{lo}$ in their naïve state. In contrast, CD4 positive memory T-cells are $CD45RB^{lo}CD44^{hi}$ and CD8 positive memory cells express $CD44^{hi}Ly6C^{hi}IL\text{-}2R\beta^{hi}$ (reviewed by Jameson, 2002).

The homeostatic regulation of the peripheral T-lymphocyte pool not only relies on the duration and quality of TCR stimulation and cytokines but is also dependent on the action of regulatory CD4 positive T-cells also referred to as T_{reg} cells (reviewed in Stockinger et al., 2004). Of the several T_{reg} populations identified, the so-called naturally arising $CD4^+CD25^+$ T_{reg} population is most studied (Shevach, 2000, Sakaguchi, 2004). This population develops in the thymus along a specific lineage and makes up 5 – 10% of the peripheral CD4 positive T-cell pool. The key factor for the T_{reg} lineage decision is expression of the transcription factor scurfin, encoded by the *foxp3* gene (Fontenot et al., 2003, Hori et al., 2003, Khattri et al., 2003). The regulatory properties of T_{reg} cells were first identified through their capacity to prevent the development of auto-immune diseases that arise upon transfer of naïve CD4 positive peripheral T-cells into lymphopenic mice (Sakaguchi et al., 1995). Isolated T_{reg} cells are able to suppress the proliferation of conventional CD4 and CD8 positive T-cells *in vitro*. *In vivo* T_{reg} cells can prevent effector functions by inhibiting IL-2 transcription a process which is dependent on cell-cell contacts (Read et al., 1998, Takahashi et al., 1998, Thornton and

Shevach, 1998). The molecules involved in the formation of these contacts with their inhibitory effect on the target cell have not yet been defined.

As outlined above, by mechanisms regulating the quality and duration of TCR stimulation, by differential cytokine requirements and by the activity of regulatory T-cells, the size and the diversity of the T-lymphocyte pool after an adaptive immune response is re-established to its characteristic resting state. However, under circumstances of extreme disturbance of the peripheral T-cell pool, the balance cannot be kept. A partial or complete lack of T-cells, also referred to as T-lymphopenia, as induced by irradation usually results in pronouced changes of the composition of the T-cell pool despite the return of total lymphocyte number to normal levels (La Gruta et al., 2000). Under lymphopenic conditions, naïve T-cells were shown to start to proliferate a process called homeostatic or lymphopenia-driven proliferation. Lymphopenia-driven proliferation of naïve T-cells requires IL-7, TCR interaction with self-antigen and is enhanced by the availability of space, i.e. the lack of competition for limiting resources such as stimulatory cytokines due to the reduction in overall lymphocyte numbers (Goldrath and Bevan, 1999, Dummer et al., 2001, Seddon and Zamoyska, 2002, Troy and Shen, 2003). During lymphopenia-driven proliferation, expanding naïve T-cells adopt a memory-like phenotype as characterized by the upregulation of CD44 expression (Kieper and Jameson, 1999, Goldrath et al., 2000).

The mechanisms regulating lymphopenia-driven proliferation have been studied intensively in the context of autoimmune diseases. Several studies suggested a causal link between lymphopenia and autoimmune diseases based on the lymphopenia-driven proliferation of potentially autoreactive T-cells (Gleeson et al., 1996, King et al., 2004, Khoruts and Fraser, 2005). However, the full impact of mechanisms regulating T-cell homeostasis on the diversity and functionality of the naïve and memory T-cell pools is still unclear. In particular, appropriate model systems in which only specific peripheral T-cell subsets are defective are thus far rare. In these models, an analysis of the requirements for survival and proliferation of the remaining T-cell subsets would provide valuable insight into how T-cell homeostasis is differentially regulated.

1.6 The coronin family of proteins

The prototype coronin has been described in the slime mold *Dictyostelium discoideum* as an actin-binding protein containing five WD domains and being involved in a variety of actin-based processes such as phagocytosis, cell motility and cytokinesis (de Hostos, 1991 and 1993, Maniak, 1995, Hacker, 1997, Fukui, 1999). Subsequently, coronin-like proteins have

been found in many species, from yeast to mammals. Based on their structural features, coronins constitute an evolutionary conserved family of WD-repeat containing proteins which are collectively defined as actin-binding molecules. In mammalian organisms, the coronin family of proteins consists of seven members (coronin 1 – 7, see table 1) for which the degree of homology exceeds 60% amino acid identity depending on the region (reviewed in de Hostos, 1999; Rybakin and Clemen, 2005). In the following an overview is given on what is known about the mammalian coronins with a special emphasis on coronin-1 and its functions in leukocytes.

Coronin	Synonyms	Size (aa)	Accession no.	Species [a]	Main tissue expression [b]	References [c]
1	Coronin 1A, clabp, clipinA, TACO, p57	461	NM_009898	B, H, M	Thymus, spleen, bone marrow, lymph nodes, peripheral leukocytes	(1 - 3)
2	Coronin 1B, coroninse, p66	484	AK149639	M, R, RB, H-EST	Gastrointestinal mucosa, liver, spleen, kidney, lung	(4 - 7)
3	Coronin 1C	474	NM_011779	M, H-EST	Brain, lung, intestine, kidney	(8 - 10)
4	Coronin2A, clipinB, IR10	524	NM_178893	M-EST, H	Colon, prostate, testis, brain, lung, epidermis	(2)
5	Coronin2B, clipinC	475	NM_175484	H	brain	(11)
6	ClipinE (three splice variants)	471 (isoform A)	NM_139128	M-EST	brain	NM_139128
7	crn7	925	NM_030205	M, R, H	Thymus, spleen, brain	(12,13)

Table 1 Summary of the coronin proteins identified in mammalian species (adapted from de Hostos, 1999; Rybakin and Clemen, 2005). The size of the different coronin proteins is given in amino acids (aa) based on the sequence of murine coronin proteins. The accession number refers to the mRNA sequence of the coronins found in mouse. [a] given are the species for which expression of a particular coronin protein has been described: B, bovine; H, human; EST, expressed sequence tag; M, mouse; R, rat; RB, rabbit. [b] main tissue expression as described in the indicated references. [c] references are as follows: (1) Suzuki et al., 1995; (2) Okumura et al., 1998; (3) Ferrari et al., 1999; (4) Brown and Chew, 1989; (5) Chew et al., 1997; (6) Parente et al., 1999; (7) Morrissette et al., 1999; (8) Iizaka et al., 2000; (9) Spoerl et al., 2002; (10) Hasse et al., 2005; (11) Nakamura et al., 1999; (12) Muralikrishna et al., 1998; (13) Rybakin et al., 2004. For coronin-6 which has not yet been described in the literature the accession number of the murine coronin-6 mRNA sequence is indicated.

1.6.1 The mammalian coronin family: structure, expression and function

1.6.1.1 Structure of the mammalian coronin proteins

Alignment of the complete protein sequences of the seven mammalian coronin protein family members revealed that all coronins are characterized by the presence of WD40 repeats. With the exception of coronin-7, the most C-terminally located 25-40 amino acids of the coronin proteins are predicted to have a high tendency to fold into a coiled coil structure. According to a recent sequence analysis the WD repeat containing region is flanked by so-called highly conserved N- and C-terminal extensions (Uetrecht and Bear, 2006). In each coronin the C-terminal extension is preceeded by a stretch of variable length (50 - 200 amino acids) which is highly divergent and unique for each individual coronin family member. It is thought that this unique region contributes to functional diversity among the different coronins

(de Hostos, 1999; Rybakin and Clemen, 2005). Structural data as obtained for coronin-1 revealed that the WD repeat regions fold into a seven bladed β-propeller with the N- and C-terminal extensions forming the first and the last blade respectively (Gatfield et al., 2005, Appleton et al., 2006). This structure is reminiscent of the β-propeller fold of the β-subunit of trimeric G proteins and mediates protein-protein interactions of G proteins suggesting a similar function in coronin proteins (Neer et al., 1994, Sondek et al., 1996).
The most C-terminal sequences predicted to fold into a coiled-coil domain were shown to mediate homo-oligomerization of coronin proteins, namely homotrimerization of coronin-1 and homo-oligomers of not yet defined stochiometry for the coronin homologue in *Xenopus* and for mammalian coronin-3 (Asano et al., 2001, Spoerl et al., 2002). For coronin-1, homotrimerization was shown to be indispensable for association with the actin cytoskeleton (Gatfield et al., 2005).

Structurally, coronin-7 substantially differs from the other mammalian coronins. Coronin-7 is much longer and contains two complete copies of the basic coronin domain organization into the WD-repeat regions with flanking N- and C-terminal extensions. In addition, coronin-7 possesses a highly conserved acidic domain with a characteristic tryptophan residue at its very C-terminus. This domain is homologous to acidic domains found in the SCAR/WASP family of proteins regulating the activity of the actin nucleating complex Arp2/3 (Rybakin et al., 2004, Uetrecht and Bear, 2006).

1.6.1.2 Expression and function of mammalian coronin-2 – 7

Based on their homology to coronin-1 the members of the coronin protein family are presumed to play an important role in the regulation of cytoskeletal dynamics. Whereas for coronin-2, -3 and -7 functional data and biochemical properties are partially known, similar data for coronin-4, -5 and -6 are currently not available. Coronin-1 expression and function will be discussed in the following paragraphs.

Coronin-2 (originally termed coronin$_{se}$) has first been identified in rabbit as a phosphoprotein in hydrochloric acid secreting gastric parietal cells (Brown and Chew, 1989, Chew et al., 1999). Expression of coronin-2 in mouse tissue was found to be ubiquitous with highest levels in kidney, liver, lung and spleen (Okumura et al., 1998, Parente et al., 1999). On a subcellular level, coronin-2 was found to colocalize with the Arp2/3 complex at the leading edge and on vesicular structures in fibroblasts (Cai et al., 2005). This distribution was dependent on the phosphorylation of coronin-2 on serine residues by protein kinase C (Parente et al., 1999). Furthermore, coronin-2 was identified as a component of macrophage

phagosomes (Morrissette et al., 1999). Downregulation of coronin-2 expression by RNAi led to a reduction of neurite outgrowth in the neuroblastoma cell line PC-12 (Di Giovanni et al., 2005).

Coronin-3 expression in human and mouse tissue appeared to be ubiquitous and most prominent in brain, lung, intestine and kidney (Okumura et al., 1998, Iizaka et al., 2000, Spoerl et al., 2002, Hasse et al., 2005). In human embryonic kidney cells (HEK293) and mouse fibroblasts (3T3) coronin-3 was shown to localize to both the cytosol as well as the cortical cytoskeleton with pronouced accumulation in lamellipodia and membrane ruffles. Biochemical analysis of coronin-3 revealed a high degree of phosphorylation on so far unidentified residues. Using truncated versions of coronin-3 established a role for the C-terminus in mediating oligomerization, membrane association and actin binding of coronin-3. However, removal of the very C-terminal coiled coil sequence abolished membrane association presumably due to disturbance of the oligomerization state of coronin-3 (Spoerl et al., 2002).

Coronin-4 was shown to be exclusively expressed in colon, brain, prostate and testis at a low level (Okumura et al., 1998). Coronin-5 has been originally described to be expressed in neuronal tissue but presence in other tissue cannot be excluded (Nakamura et al., 1999). Coronin-6 is present in the genome but its expression as well as the protein have not yet been described (Uetrecht and Bear, 2006). Functional or biochemical data for the latter three coronins are currently not available.

Coronin-7 was identified as the mammalian homologue of POD-1 in *Drosophila* (Dpod-1) and *C. elegans* (Rybakin et al., 2004). The protein is expressed throughout mouse embryogenesis with pronouced upregulation in developing brain and hemato-/lymphopoietic tissues. In adult animals, coronin-7 appears to be ubiquitously expressed with highest levels in thymus, spleen and brain. Analysis of its subcellular localization revealed recruitment to Golgi membranes in a tyrosine-phosphorylation dependent manner. In contrast to other coronins, coronin-7 does not colocalize with actin and disturbance of actin cytoskeletal structures by the actin depolymerizing drug latrunculin B does not influence its distribution (Rybakin et al., 2004). Functional data for the mammalian coronin-7 are not available but results obtained for *Drosophila* and *C. elegans* suggest a role in regulating vesicle trafficking dependent on cytoskeletal structures. Depletion of POD-1 by RNAi severly affects early development of *C.elegans* due to defects in polarized vesicle transport (Aroian et al., 1997, Rappleye et al., 1999). *Drosophila* POD-1 was shown to be required for the development of the nervous system since flies mutant for *dpod1* displayed aberrant axonal guidance and

subsequent failure in innervation (Rothenberg et al., 2003). However, in contrast to their mammalian homologue both *C.elegans* and *Drosophila* POD-1 interact with actin. For *Drosophila* POD-1 a role in crosslinking the actin and microtubule cytoskeleton could be established. Further experimental work is required to analyse to which extent coronin-7 and its POD-1 counterparts are involved in regulating cytoskeleton dynamics as well as vesicle trafficking dependent on the actin or microtubule cytoskeleton.

1.6.2 Coronin-1 and its homologues in other eukaryotic organisms

Since its original discovery in *Dictyostelium* substantial biochemical, functional and structural data have been obtained for mammalian coronin-1 and its homologues in various other eukaryotic organisms. In the following an overview is given for what has been established for coronin-1 homologues in *Dictyostelium*, yeast and *Drosophila* before discussing available data on mammalian coronin-1.

1.6.2.1 Coronin-1 homologues in *Dictyostelium*, yeast and *Drosophila*

In *Dictyostelium*, coronin was shown to be associated with F-actin structures at crown-shaped phagocytic cups and macropinosomes. In mutants for coronin a variety of actin-based processes such as cytokinesis, cell locomotion, phagocytosis and macropinocytosis are impaired, although none of them is completely abolished (de Hostos, 1991 and 1993, Maniak, 1995, Hacker, 1997). Further analysis using a coronin fusion to GFP revealed that coronin is accumulated at all sites where the actin cytoskeleton is actively remodeled including the leading edge of pseudopods as formed during movement of cells, the cleavage furrow during cytokinesis and the sites of active macropinocytosis and phagocytosis (Fukui, 1997 and 1999).

In contrast to *Dictyostelium*, mutants for the coronin homologue in the yeast *Saccharomyces cerevisiae* (Crn1p) showed no obvious phenotype (Heil-Chapdelaine et al., 1998). Crn1p represents the only coronin protein in yeast and was originally identified by homology cloning and microtubule affinity chromatography (Heil-Chapdelaine et al., 1998, Goode et al., 1999). Crn1p colocalizes with cortical actin patches in a latrunculin A sensitive manner suggesting that its subcellular localization is dependent on F-actin. *In vitro* Crn1p was shown to bind to actin as well as microtubules implying a function of Crn1p in crosslinking these two cytoskeletal structures (Goode et al., 1999). Further *in vitro* analysis of the capacity of Crn1p to regulate the actin cytoskeleton revealed that Crn1p can bundle actin filaments. The direct interaction of Crn1p with the Arp2/3 complex could be demonstrated *in vivo* and *in vitro*

leading to inhibition of the ability of the Arp2/3 complex to nucleate and thereby promote actin polymerization (Goode et al., 1999, Humphries et al., 2002). It was therefore suggested that the interaction of Crn1p with the Arp2/3 complex regulates actin polymerization and branching as it is important for the formation of actin filament network supporting cell motility and vesicle transport.

A role for coronin-1 in cytoskeleton-based intracellular membrane and protein trafficking is further corroborated by the analysis of the coronin-1 homologue in *Drosophila* (Dcoro, Bharathi et al., 2004). Dcoro is highly and ubiquitously expressed in all cell types with exception of the larval central nervous system. Mutation of Dcoro resulted in a lethal phenotype at the early to late pupal stages concomitant with severe defects in the morphogenesis of appendages. These defects were on one hand correlated with the disruption of the actin cytoskeleton in embryonic imaginal disks and on the other hand with the impairment of the intracellular transport of the morphogen Dpp resulting in a failure to generate a Dpp morphogen gradient as required for proper appendage development (Bharathi et al., 2004). Interestingly, genetic evidence has been provided that Dcoro interacts with syx1A a gene encoding a Drosophila SNARE protein involved in exocytosis and calcium channel function (Schulze et al., 1995, Wu et al., 1999).

1.6.2.2 Mammalian coronin-1 and its potential function in leukocytes

Coronin-1 as identified in human and mouse is a 57 kDa protein that is highly and specifically expressed in leukocytes (Okumura et al., 1998, Ferrari et al., 1999, Nal et al., 2004). The subcellular localization of coronin-1 is characterized by the accumulation of coronin-1 at sites of actin cytoskeleton remodeling such as the cortical region, sites of phagocytosis and the immunological synapse (Ferrari et al., 1999, Nal et al., 2004). In human neutrophils, coronin-1 was shown to colocalize with F-actin around early phagocytic vacuoles (Itoh et al., 2002). Downregulation of coronin-1 expression or function by RNAi or expression of dominant-negative coronin-1 constructs resulted in the partial impairment of internalization of red blood cells by murine macrophage cell lines (Yan et al., 2005). Coronin-1 localization to the phagosome appears to be dependent on phosphorylation mediated by protein kinase C (Itoh et al., 2002). The phosphorylated residues have not yet been identified but coronin-1 seems to be differentially phosphorylated at multiple sites *in vivo* (Gatfield et al., 2005). In murine macrophages, coronin-1 was shown to be actively recruited and retained at the phagosome by pathogenic mycobacteria thereby allowing them to inhibit lysosomal delivery and to subsequently survive within the host cell in a specialized compartment, the mycobacterial phagosome (Ferrari et al., 1999).

As an interaction partner for coronin-1 besides F-actin, $p40^{phox}$ was identified. $p40^{phox}$ represents a cytosolic subunit of the NADPH oxidase complex which is responsible for the generation of the microbicidal superoxide burst in neutrophils (Grogan et al., 1997). Based on the results obtained for Crn1p in yeast an interaction of coronin-1 with the Arp2/3 complex in mammalian cells has been proposed. The only available data substantiating this hypothesis came from a study examining the composition of the Arp2/3 complex, in which coronin-1 co-purified as a main protein with Arp2/3 isolated from neutrophil lysates (Machesky et al., 1997). Furthermore, coronin-1 is recruited to F-actin tails by ActA-positive *Listeria monocytogenes* in infected host cells. F-actin based intracellular motility of *Listeria* relies on similar mechanisms as conventional actin polymerization (David et al., 1998).

In summary, the biochemical and functional data obtained for coronin-1 so far suggest that coronin-1 plays a role in membrane- and cytoskeleton-based leukocyte-specific processes.

1.7 Aim of this thesis

The mammalian coronin-1 is the closest homologue of coronin in *Dictyostelium*. Although subject of extensive functional and biochemical studies in various eukaryotic organisms such as *Dictyostelium* and yeast no precise biological activity has been assigned to coronin and other members of the coronin family of proteins. Especially for mammalian organisms, coronin-1 lacks detailed functional description. In mammalian organisms coronin-1 was found to be restricted in its expression to leukocytes. Experimental work from *Dictyostelium* and yeast suggests a role of coronin proteins in regulating cytoskeletal dynamics. Careful biochemical characterization of mammalian coronin-1 established this protein as a linker of the leukocyte plasma membrane with the actin cytoskeleton. Furthermore, coronin-1 was found to be recruited to and retained at the mycobacterial phagosome in murine macrophages thereby allowing pathogenic mycobacteria to persist within host cells presumably due to the coronin-1 mediated inhibition of phagosome-lysosome fusion. Taken together, these data led to the hypothesis that coronin-1 plays a role in regulating leukocyte-specific membrane- and cytoskeleton-based functions.

The aim of this thesis was to gain insight into the cell biological function of coronin-1 in leukocytes. For this purpose the coronin-1 gene was targeted by homologous recombination in murine embryonic stem cells which subsequently where used to generate coronin-1 deficient mices. Coronin-1 deficient mice where subjected to an extensive phenotypic analysis focusing on the following questions:

Can coronin-1 deficient mice be generated and do they display an obvious phenotype ?

The narrow expression pattern of coronin-1 together with its appearance only late during embryogenesis made coronin-1 a successful candidate for the generation of viable knock-out mice. However, due to the yet incomplete description of its expression and function it could not be excluded that the absence of coronin-1 causes severe deficiencies such as embryonic lethality, behavioural abnormalities and immunodeficiency.

If coronin-1 K.O. mice are viable, which cell types are affected by the lack of coronin-1 expression ?

The specific expression of coronin-1 in leukocytes suggested a phenotype of coronin-1 deficient mice within leukocyte subsets. Of special interest for our phenotypical analysis was the T-lymphocyte population. Coronin-1 has been described to be differentially expressed

during T-cell development and was suggested to play a role in regulating T-cell activation by being recruited to the immunological synapse. Both developing as well as peripheral leukocyte populations were therefore carefully studied for their cellularity and composition in coronin-1 K.O. mice.

In which cell types is coronin-1 expressed ?

The targeting construct for the coronin-1 locus was designed to replace coronin-1 exons by the coding region of the green fluorescent protein (GFP). Fusion of GFP in frame with the original start codon of the coronin-1 locus should allow analysis of coronin-1 expression by the means of GFP as a reporter gene. Heterozygous coronin-1 K.O. mice were used to study the reliability of GFP as a reporter for coronin-1 expression and to therefore draw detailed conclusion on coronin-1 expression in the various leukocyte subsets.

Given a cell type specific defect caused by the absence of coronin-1, what can be deduced on the precise cell biological function of coronin-1 in leukocytes ?

Cell types affected by coronin-1 deficiency were subjected to a functional analysis to understand the question at which point coronin-1 could play a regulatory role. Based on the proposed role of coronin-1 in regulating leukocyte-specific membrane and cytoskeleton-based functions a potential disturbance of cytoskeletal structures as well as defects caused in receptor-mediated processes, such as activation of T-cells and phagocytosis, were studied.

In summary, the generation and phenotypic analysis of coronin-1 deficient mice should provide a versatile model system to study the precise role of coronin-1 in regulating leukocyte-specific functions. Of special importance for immune cell function is the contribution of potentially disturbed cytoskeletal structures or receptor-mediated processes to the phenotype of coronin-1 deficient mice. The analysis of coronin-1 deficient mice could be valuable in demonstrating an involvement of coronin-1 in regulating cytoskeletal rearrangements or signaling downstream of immune receptor in a discrete and cell-type specific manner.

2 MATERIALS AND METHODS

2.1 Chemicals, reagents and kits

2.1.1 Chemicals

Acetic acid	Merck
Acetone	Merck
Acrylamide	Biorad
Agarose	Eurobio
Albumine, bovine, 96% pure	Equitech-Bio Inc.
Ammonium citrate	Sigma
Ammonium persulfate (APS)	Biorad
Ammonium sulfate [$(NH_4)_2SO_4$]	Merck
Ampicillin	Sigma
Antipain	Fluka
Aprotinin	Merck
Bacto-Tryptone	Difco
Bacto-Yeast Extract	Difco
Bisacrylamide (N',N-methylenbisacrylamide)	Biorad
Blocking reagent (for Southern blotting)	Roche
Boric acid	Merck
Bradford reagent	Biorad
Bromophenol blue	Merck
Calcium chloride [$CaCl_2$ x H_2O]	Sigma
Chloroform	Merck
Chymostatin	Merck
Coomassie brilliant blue R-250	Merck
Deoxynucleotides (dNTPs, PCR nucleotide mix)	Roche
Dimethylsulfoxide (DMSO)	Fluka
Dithiothreitol (DTT)	Sigma
DNA molecular weight standards	Roche
T4 DNA ligase	New England Biolabs
EBSS (10x)	Gibco BRL
Erythromycin	Sigma
Ethanol	Merck
Ethidium bromide	Sigma
Ethylendiamine tetraacetate (EDTA), sodium salt	Fluka
Ficoll-Paque	Pharmacia
FluoroGard Antifade reagent	Biorad
Formamide	Merck
Hi-Di™ Formamide	Applied Biosystems
D(+)-glucose	Fluka
Gelatine	Sigma
Glycine	Fluka
Glycerol	Fluka
Hydroxymethylpiperidine-ethanesulfonic acid (HEPES)	AppliChem
Hydrochloric acid (HCl)	Merck
Interferon-γ, murine, recombinant	BD Pharmingen
Isopropanol (2-propanol)	Merck
Ketalar	Parke-Davis
L-cysteine	Fluka
Leupeptin	Fluka

Lipopolysaccharide (LPS)	Sigma
Liquemine® (Heparin solution at 5'000 U/ml)	Roche
Magnesium chloride [$MgCl_2$]	Sigma
Magnesium sulfate [$MgSO_4$]	Sigma
Maleic acid	Sigma
Manganese chloride [$MnCl_2$]	Sigma
Manganese sulfate [$MnSO_4$]	Sigma
Methanol	Merck
Microscint® 40	Packard
Mitomycin C	Sigma
Paraformaldehyde, powder, 95 % pure	Sigma
PCR primer	Microsynth
Pepstatin	Fluka
Phalloidin, fluorescently labeled with Alexa® dyes	Molecular Probes
Phenylmethylsulfonylfluoride (PMSF)	Sigma
Phorbol-12-myristate-13-acetate (PMA)	Sigma
Piperazine-1,4-bis(2-ethanesulfonic)acid (PIPES)	Sigma
Poly-L-lysine	Sigma
Ponceau S	Sigma
Potassium chloride [KCl]	Sigma
Potassium dihydrogen phosphate [KH_2PO_4]	Merck
Potassium hydroxide [KOH]	Sigma
Propidium iodide	Sigma
Proteinase K	Roche
Random hexanucleotide primers	Promega
Restriction enzymes	New England Biolabs
Rompun	Bayer Healthcare
rRNAsin (recombinant RNAse inhibitor)	Promega
Saponin (from Quillaja bark)	Sigma
Sarcosyl	Sigma
SDS-PAGE molecular weight standards	Biorad
Shrimp alkaline phosphatase (SAP)	Roche
Sodium acetate	Fluka
Sodium chloride [NaCl]	Merck
Sodium citrate	Sigma
Sodium dihydrogen phosphate [NaH_2PO_4]	Fluka
Sodium dodecylsulfate (SDS)	Biorad
Sodium hydroxide [NaOH]	Merck
Di-sodium hydrogenphosphate [Na_2HPO_4]	Fluka
Sucrose	BDH
Sulfuric acid [H_2SO_4]	Fluka
N,N,N',N'-tetramethylenethylendiamine (TEMED)	Biorad
[methyl-^{3}H]-thymidine	Amersham
Trichloroacetic acid (TCA)	Merck
Tris(hydroxymethyl)aminomethane (Tris/TRIZMA base)	Sigma
Triton X-100	Boehringer Mannheim
TriZOL reagent	Invitrogen
Trypan blue	Sigma
Trypsin-EDTA in HBSS	Gibco BRL
Trypticase peptone	Becton Dickinson
Tryptose	Difco
Tween 20	Merck
Tween 80	Merck
Water, molecular biology grade	Eppendorf
Xylene cyanol FF	Sigma

Zymosan	Sigma

2.1.2 Kits and FPLC columns

AlexaFluor® 633 Protein Labeling Kit	Molecular Probes
BCA protein detection kit	Pierce
BigDye1.1® Terminator v1.1 Cycle Sequencing Kit	Applied Biosystems
DNA-free kit (for DNAse I treatment of RNA)	Ambion
Enhanced Chemiluminescence (ECL) kit	Amersham
Expand Long Template PCR System	Roche
Hi-Trap® Protein A HP 1 ml	Amersham
Lysing Matrix D	Qbiogen
Plasmid DNA Mini/Maxi-prep kit	Qiagen
QIAquick Gel Extraction Kit	Qiagen
QIAquick PCR Purification Kit	Qiagen
pGEM®-T-Easy Vector Kit	Promega
SuperScript III (reverse transcriptase + buffer)	Invitrogen
Taq polymerase + PCR buffer	Pharmacia

2.2 General buffers and solutions

Ammoniumchloride/Potassium (ACK)-erythrocyte lysis buffer	0.15 M NH_4Cl 10 mM $KHCO_3$ 0.1 mM EDTA pH 7.2 filter sterilized through 0.2 µm filter
DNA loading buffer (6x)	0.25% bromophenol blue 0.25% xylene cyanol 1 mM EDTA pH 8.0 30 % glycerol
Lysis buffer (10x)	200 mM HEPES pH 7.4 1 M NaCl 50 mM $MgCl_2$ 10 % Triton X-100
PBS	137 mM NaCl 2.7 mM KCl 8 mM Na_2HPO_4 1.5 mM KH_2PO_4
PBST	PBS + 0.2 % (v/v) Tween 20
SDS-PAGE electrophoresis buffer (10x)	1.9 M glycine 250 mM Tris SDS added to the 1x buffer at a final concentration of 0.1 % (w/v) just before use

SDS-PAGE reducing sample buffer (5x)	10% (w/v) SDS 20% (v/v) glycerol 500 mM DTT 300 mM Tris-HCl pH 6.8 0.015% (w/v) bromophenol blue
Semi-dry transfer buffer (10x)	480 mM Tris 390 mM glycine 0.375% (w/v) SDS Methanol added to a final concentration of 20% (v/v) to the 1x buffer just before use
TBE (5x)	54 g Tris 27.5 g Boric acid 20 ml 0.5 M EDTA (pH 8.0) dissolved in destilled water to a total volume of 1 l
TE buffer	10 mM Tris-HCl pH 8.0 1 mM EDTA
SSC (20x)	3 M NaCl 300 mM sodium citrate pH 7.0
CLAAP (100x)	100 µg/ml chymostatin 100 µg/ml leupeptin 100 µg/ml antipain 100 µg/ml aprotinin 100 µg/ml pepstatin
PMSF (100x)	87.1 mg PMSF dissolved in 5 ml 100% ethanol (corresponds to 1 mM PMSF) storage: -20°C
3% paraformaldehyde in PBS	100 ml 3% paraformaldehyde solution in PBS was prepared by dissolving 3 g paraformaldehyde in 90 ml destilled water containing 300 µl 0.1 M NaOH. Complete dissolution of paraformaldehyde was achieved by heating the solution to 60°C while stirring. The solution was then cooled down to 37°C, 10 ml 10x PBS were added and the pH was adjusted to 7.2.

2.3 Cell culture media and supplements

2.3.1 Bacterial media and supplements

Luria-Bertani (LB medium+glucose+$MgSO_4$)	10 g Bacto-tryptone (Difco) 5 g Bacto-yeast extract (Difco) 10 g NaCl dissolved in 1 l destilled H_2O sterilized by autoclaving (prior to use added: glucose (final concentration 0.1%) and $MgSO_4$ (final conc. 10 mM))
Lactobacillus medium	12.5 g trypticase peptone (Becton Dickinson) 6.25 g Bacto-yeast extract (Difco) 3.75 g tryptose (Difco) 2.5 g ammonium citrate (Sigma) 1.25 ml Tween-80 (Sigma) 1.25 g sodium acetate x 3 H_2O 0.25 g L-cysteine (Fluka) 0.6 g $MgSO_4$ x 7 H_2O 0.05 g $MnSO_4$ dissolved in 800 ml destilled water, autoclaved and supplemented with 200 ml 0.5 M potassium phosphate buffer pH 6.9 and glucose (final conc. 1%)
Ampicillin	Sigma, stock in destilled water at 100 mg/ml, used for cultures at 100 □g/ml
Erythromycin	Sigma, stock in ethanol 20 mg/ml, used for cultures at 5 □g/ml

2.3.2 Mammalian cell culture media and supplements

DMEM	Sigma
DMEM (for ES cell medium)	PAN Biotech
RPMI-1640	Gibco BRL
IMDM	Sigma
Fetal calf serum (FCS)	Gibco BRL
ES cell qualified FCS	HyClone
Human serum	Blutspendezentrum Basel, Switzerland
100x L-glutamine (200 mM)	Gibco BRL
50 mM □-mercaptoethanol	Gibco BRL
100x sodium pyruvate (100 mM)	Gibco BRL

100x MEM non-essential amino acids	Gibco BRL
1M HEPES	Gibco BRL
G418, powder	Sigma
Penicillin (10'000 U/ml) / Streptomycin (10 mg/ml)	Sigma
Murine recombinant LIF (ESGRO)	Gibco BRL
Trypsin-EDTA in HBSS	Gibco BRL

2.4 Vectors

Name (size in kb)	Vector	Insert	Constructor	Application
pGEM-T Easy (3 kb)	pGEM-T-Easy, ampicillin resistance	---	Promega	subcloning of PCR products
pBSK(+) (2.9kb)	pBluescript SK (+), ampicillin resistance	---	Stratagene	cloning of flanking homology regions of coronin-1 targeting constructs
pBSK(+) modified (2.9kb)	pBluescript SK (+), ampicillin resistance, XhoI site in MCS deleted	---	J.Massner, this thesis	vector backbone of coronin-1 targeting constructs
pEGFP-N2 (4.7 kb)	pEGFP-N2, ampicillin resistance	EGFP coding region	Clontech	source of the EGFP coding region for coronin-1 targeting constructs
pGEM7-SV40-floxed-Neo (7.2 kb)	pGEM7, ampicillin resistance	SV40 polyA signal-loxP-TK-Neo-Hygro-loxP via XhoI	S.Arber, Biozentrum, University of Basel	source of neomycin resistance cassette for coronin-1 targeting constructs
pBKS K.O. II (10.2kb)	pBluescript KS, ampicillin resistance	7.2 kb targeting construct for the coronin-1 locus	J.Gatfield, PhD-thesis (2001)	template for the PCR amplification of digoxigenin labeled Southern blot probes
No.15 (4.7 kb)	pBluescript SK (+), ampicillin resistance	1.8 kb flanking homology region (left arm) for coronin-1 targeting constructs No.154, No.206 and No.215 via NotI/EcoRI	J.Massner, this thesis	subcloning of flanking homology regions for coronin-1 targeting constructs
No.35 (5.6 kb)	pBluescript SK (+), ampicillin resistance	2.7 kb flanking homology region (right arm) for coronin-1 targeting constructs No.206 and No.215 via XhoI and EcoRI	J.Massner, this thesis	subcloning of flanking homology regions for coronin-1 targeting constructs
No.49 (6.4 kb)	pBluescript SK (+), ampicillin resistance	3.5 kb flanking homology region (right arm) for coronin-1 targeting constructs No.154 via XhoI and EcoRI	J.Massner, this thesis	subcloning of flanking homology regions for coronin-1 targeting constructs
No.67 (7.6 kb)	pBluescript SK (+), ampicillin resistance	4.7 kb flanking homology region as extension of the right arm of coronin-1 targeting construct No.215 via EcoRI/ClaI	J.Massner, this thesis	subcloning of flanking homology regions for coronin-1 targeting constructs
No.154 (12.4 kb)	pBluescript SK (+) modified, ampicillin resistance	9.5 kb targeting construct for the replacement of exon2 of coronin-1 by the coding region of EGFP	J.Massner, this thesis	Coronin-1 targeting construct for electroporation and selection of murine embryonic stem cells
No.206 (11.6 kb)	pBluescript SK (+) modified, ampicillin resistance	8.7 kb targeting construct for the replacement of exon2 - 11 of coronin-1 by the coding region of EGFP	J.Massner, this thesis	Coronin-1 targeting construct for electroporation and selection of murine embryonic stem cells
No.215 (16.3 kb)	pBluescript SK (+) modified, ampicillin resistance	13.4 kb targeting construct for the replacement of exon2 - 11 of coronin-1 by the coding region of EGFP	J.Massner, this thesis	Coronin-1 targeting construct for electroporation and selection of murine embryonic stem cells

Table 2 *Vectors used in this study.*

2.5 Primers

Name	Sequence (5' -> 3')	Source of sequence	Application
TCP2860	**GCT TAG CGG CC**G CGT CAG CAT CTG TTC GGG GG	murine coronin-1 locus: bp(-1728) -> bp(-1708)	Forward primer for the amplification of the left arm flanking homology region of coronin-1 targeting constructs; includes NotI site
TCP4675	**CGC AGA ATT CCG CCC ATG G**GG CTC ATC CTG AAG GAT ACA G	murine coronin-1 locus: bp(-14) <- bp(+5)	Reverse primer for the amplification of the left arm flanking homology region of coronin-1 targeting constructs; includes NcoI and EcoRI sites
TCP4862	**GTA TAC TCG A**GT GCT ACC CCT AGG CAA GGT	murine coronin-1 locus: bp(+180) -> bp(+199)	Forward primer for the amplification of the right arm flanking homology region of coronin-1 targeting construct No.154; includes XhoI site
TCP8373	**CAC GTG AAT TC**G GCT TTG GTC CAG CAC TAT C	murine coronin-1 locus: bp(+3672) <- bp(+3691)	Reverse primer for the amplification of the right arm flanking homology region of coronin-1 targeting construct No.154; includes EcoRI site
TCP11670	AAC GGT TCA GAG TCG TGT CC	murine coronin-1 locus: bp(+6988) -> bp(+7007)	Forward primer for the amplification of the right arm flanking homology region extension of coronin-1 targeting construct No.215
TCP16642	**C GTT ATA TCG** ATG AAG CAC CAG CCA GAG AG	murine coronin-1 locus: bp(+11941) <- bp(+11960)	Reverse primer for the amplification of the right arm flanking homology region extension of coronin-1 targeting construct No.215; includes ClaI site
ONP9150	GTG GCA CAC GCC TTT AAT CT	murine coronin-1 locus: bp(+4468) -> bp(+4487)	Forward primer for the amplification of the right arm flanking homology region of coronin-1 targeting constructs No.206 and No.215
ONP12651	GCC ATC GCA GAG TGT TGA TA	murine coronin-1 locus: bp(+7950) <- bp(+7969)	Reverse primer for the amplification of the right arm flanking homology region of coronin-1 targeting constructs No.206 and No.215
GFP605	CGA ATT CTG CAG TCG ACG GTA CCG	pEGFP-N2: bp628 -> bp651	Forward primer for the amplification of the EGFP coding region for coronin-1 targeting constructs
GFP1400	**CGC AGA ATT CGC CTC GAG** TTT ACT TGT ACA GCT CGT CC	pEGFP-N2: bp1384 <- bp1403	Reverse primer for the amplification of the EGFP coding region for coronin-1 targeting constructs; includes XhoI and EcoRI sites
WTCor1	CTG TTG TAG GGG CTG ATG GT	murine coronin-1 locus: bp(-229) -> bp(-210)	PCR genotyping of coronin-1 K.O. mice
WTCor2	CAC TGG CCT CAC AGA TCA GA	murine Coronin-1 locus: bp(+143) <- bp(+162)	PCR genotyping of coronin-1 K.O. mice
KOCor1	CTT CAT GTG GTC GGG GTA G	pEGFP-N2: bp904 <- bp922	PCR genotyping of coronin-1 K.O. mice
19712	GGA AAC AGC TAT GAC CAT G	pBluescript SK forward	Sequencing primer for PCR products cloned into pBSK(+)
19713	GTA AAA CGA CGG CCA GTG A	pBluescript SK reverse	Sequencing primer for PCR products cloned into pBSK(+)
M13 forward	GTT TTC CCA GTC ACG AC	pBluescript SK forward	Sequencing of PCR products cloned into pBSK(+) or pGEM-T Easy
M13 reverse	CAG GAA ACA GCT ATG ACC	pBluescript SK reverse	Sequencing of PCR products cloned into pBSK(+) or pGEM-T Easy
SLA1	CAG GAC TGT GGG ACT GTG G	murine coronin-1 locus: bp(-1391) -> bp(-1373)	All three SLA primers are forward primers used to sequence the left arm flanking homology region of coronin-1 targeting constructs
SLA2	GCT TTC CTT CTC CCA AAT CC	murine coronin-1 locus: bp(-987) -> bp(-969)	
SLA3	GGA AGC AGA AAT GGC TCA GA	murine coronin-1 locus: bp(-587) -> bp(-568)	
SRA1	TAG GAG GTG GAG GAC ACG AC	murine coronin-1 locus: bp(+6999) <- bp(+7018)	All six SRA primers are reverse primers used to sequence the right arm flanking homology region of coronin-1 targeting constructs No.206 and No.215
SRA2	ACT CTG ACC CCA GAG CAG TG	murine coronin-1 locus: bp(+6566) <- bp(+6585)	
SRA3	CAC AGG CGT ACA CAC TCA GG	murine coronin-1 locus: bp(+6149) <- bp(+6168)	
SRA4	TCA CAA GGA CCC CAA AAG AG	murine coronin-1 locus: bp(+5642) <- bp(+5761)	
SRA5	CCC CAG GTT CAG TCC TCA T	murine coronin-1 locus: bp(+5300) <- bp(+5318)	
SRA6	CTG CCA ACC ACT ACC CTG TT	murine coronin-1 locus: bp(+5014) <- bp(+5034)	

Table 3 *Primers used in this study. Primers were obtained from Microsynth GmbH, Balgach, Switzerland. As a source of the sequence for primers annealing to the murine coronin-1 locus, the position is given relative to the start codon of coronin-1 (position of the start codon arbitrarily set to +1). Negative position values indicate position of the primer 5' of the coronin-1 start codon, positive position values indicated location of the primer 3' of the coronin-1 start codon.*

Name	Sequence (5' -> 3')	Source of sequence	Application
EXK1	TTC ACC GGA GTC TGA GAG GT	murine coronin-1 locus: bp(+3399) <- bp(+3418)	
EXK2	GAC ATT GAG CAC ATC CAT GC	murine coronin-1 locus: bp(+2948) <- bp(+2967)	
EXK3	CTG GGA GGA GCA TAA GAG CA	murine coronin-1 locus: bp(+2593) <- bp(+2612)	All eight EXK primers are reverse primers used to
EXK4	TGA GTC ACC TTG CCA CAG AG	murine coronin-1 locus: bp(+2170) <- bp(+2189)	sequence the right arm flanking homology region
EXK5	GCC TCT CAC AGT CTC ACC AA	murine coronin-1 locus: bp(+1721) <- bp(+1740)	of coronin-1 targeting construct No.154
EXK6	AGA AGC ACA TTC TGG GCT GT	murine coronin-1 locus: bp(+1356) <- bp(+1375)	
EXK7	TCT GAA CCC AAT CCA ACC TC	murine coronin-1 locus: bp(+985) <- bp(+1004)	
EXK8	CTT CAA CCC GAC AAC CAC TT	murine coronin-1 locus: bp(+615) <- bp(+634)	
RAE1	GCG CTT CTT CGG TGT CTA CT	murine coronin-1 locus: bp(+7618) -> bp(+7637)	
RAE2	AGG GTA TCA GAC GCC CTC TT	murine coronin-1 locus: bp(+8042) -> bp(+8061)	
RAE3	CTC CTC AGA TGA AGG GGT GA	murine coronin-1 locus: bp(+8496) -> bp(+8515)	
RAE4	CCC TCC CTT CTC TCT GCT TT	murine coronin-1 locus: bp(+8842) -> bp(+8861)	All eleven RAE primers are forward primers used
RAE5	TTA CCA GAG CAG CCA TGT TG	murine coronin-1 locus: bp(+9281) -> bp(+9300)	to sequence the extension of the right arm flanking
RAE6	TCG ATT GAG GTT CCC TCT TG	murine coronin-1 locus: bp(+9566) -> bp(+9585)	homolopgy region of coronin-1 targeting construct No. 215
RAE7	GAA GGG GGA GGG GTG ATT AT	murine coronin-1 locus: bp(+10005) -> bp(+10024)	
RAE8	GGC GGG CTA GAC TGG TTT AT	murine coronin-1 locus: bp(+10462) -> bp(+10481)	
RAE9	GTA CCA AGG CCA GAT GCA GT	murine coronin-1 locus: bp(+10837) -> bp(+10856)	
RAE10	CTG CCA TGT TTG ACA GGA TG	murine coronin-1 locus: bp(+11127) -> bp(+11146)	
RAE11	CAC TGG ACA GAC TTG CTG GA	murine coronin-1 locus: bp(+11546) -> bp(+11565)	
PSC1	AAC AAT GGT TCC AGC AAA GG	murine coronin-1 locus: bp(-2275) -> bp(-2256)	Forward primer used for PCR screening of ES cell pools
PSC2	GCT CCT GGA CGT AGC CTT C	pEGFP-N2: bp953 <- bp971	Reverse primer used for PCR screening of ES cell pools
GFPF2	GTT CAC CTT GAT GCC GTT CT	pEGFP-N2: bp1158 <- bp1177	Forward primer used for the amplification of the digoxigenin labeled DNA probe DIGGFP
GFPR2	TCG TGA CCA CCC TGA CCT AC	pEGFP-N2: bp864 -> bp883	Reverse primer used for the amplification of the digoxigenin labeled DNA probe DIGGFP
5DP5	GCT CTC TAG AGG GGG AGC AC	murine coronin-1 locus: bp(-2095) -> bp(-2076)	Forward primer used for the amplification of the digoxigenin labeled DNA probe DIG2
5DP6	CAA CCA GCT TGA GAG CCT TC	murine coronin-1 locus: bp(-1869) <- bp(-1850)	Reverse primer used for the amplification of the digoxigenin labeled DNA probe DIG2
3DP1	AAC AGT CGG ACC CTG AGC TA	murine coronin-1 locus: bp(+4989) -> bp(+5008)	Forward primer used for the amplification of the digoxigenin labeled DNA probe DIG3
3DP2	GTG TGA AAC GGT CAC AGT GC	murine coronin-1 locus: bp(+5196) <- bp(+5215)	Reverse primer used for the amplification of the digoxigenin labeled DNA probe DIG3
3DP5	TTT CCA GGA GTT TGC AGG AC	murine coronin-1 locus: bp(+7457) -> bp(+7476)	Forward primer used for the amplification of the digoxigenin labeled DNA probe DIG5
3DP6	GAC GAG CAG GAT TGA CAG TG	murine coronin-1 locus: bp(+7687) <- bp(+7706)	Reverse primer used for the amplification of the digoxigenin labeled DNA probe DIG5
ORTC1for	AAA CCA CTT GGG ACA GTG GCT	Okumura et al., 1998	Forward primer for the detection of coronin-1 transcripts by RT-PCR
ORTC1rev	CAT CCG GGC CCA GCG TCA GCA	Okumura et al., 1998	Reverse primer for the detection of coronin-1 transcripts by RT-PCR
ORTC2for	GTG AGC GGT CAG GAT GCT AAT CCA A	Okumura et al., 1998	Forward primer for the detection of coronin-2 transcripts by RT-PCR
ORTC2rev	TTC TCC CTG CTC CTT GAC CAG	Okumura et al., 1998	Reverse primer for the detection of coronin-2 transcripts by RT-PCR
ORTC3for	TTT GAG GGG AAG AAC GCG GAC	Okumura et al., 1998	Forward primer for the detection of coronin-3 transcripts by RT-PCR
ORTC3rev	AGT GTC TCC CTC TCT GCC CTC	Okumura et al., 1998	Reverse primer for the detection of coronin-3 transcripts by RT-PCR

Table 3 *(continued) Primers used in this study. Primers were obtained from Microsynth GmbH, Balgach, Switzerland. As a source of the sequence for primers annealing to the murine coronin-1 locus, the position is given relative to the start codon of coronin-1 (position of the start codon arbitrarily set to +1). Negative position values indicate position of the primer 5' of the coronin-1 start codon, positive position values indicated location of the primer 3' of the coronin-1 start codon.*

Name	Sequence (5' -> 3')	Source of sequence	Application
RTC4/2for	CGA CTA GGG ATT GTC CTC CA	murine coronin-4 cDNA: bp969 -> bp988	Forward primer for the detection of coronin-4 transcripts by RT-PCR
RTC4/2rev	GGT CAG GTG AGG TTT CTC CA	murine coronin-4 cDNA: bp1246 <- bp1265	Reverse primer for the detection of coronin-4 transcripts by RT-PCR
RTC5for	GAT CCC CAT CAC CAA GAA TG	murine coronin-5 cDNA: bp477 -> bp496	Forward primer for the detection of coronin-5 transcripts by RT-PCR
RTC5rev	GGC TGC CGT CTG TAT TGA AG	murine coronin-5 cDNA: bp939 <- bp958	Reverse primer for the detection of coronin-5 transcripts by RT-PCR
RTC6for	GTG CTG GAC ATT GAC TGG TG	murine coronin-6 cDNA: bp250 -> bp269	Forward primer for the detection of coronin-6 transcripts by RT-PCR
RTC6rev	TTG CTT GTG TCC ATC TCC TG	murine coronin-6 cDNA: bp781 <- bp800	Reverse primer for the detection of coronin-6 transcripts by RT-PCR
RTC7for	GAG CTG CCA GTG GAG GTA CT	murine coronin-7 cDNA: bp491 -> bp510	Forward primer for the detection of coronin-7 transcripts by RT-PCR
RTC7rev	GCA ACT CAT GAC AGC CAG TG	murine coronin-7 cDNA: bp1071 <- bp1090	Reverse primer for the detection of coronin-7 transcripts by RT-PCR
beta-actinfor	GTG GGA ATT CGT CAG AAG GAC TCC TAT GTG	murine beta-actin cDNA: bp213 -> bp242	Forward primer for the detection of beta-actin transcripts by RT-PCR
beta-actinrev	GAA GTC TAG AGC AAC ATA GCA CAG CTT CTC	murine beta-actin cDNA: bp720 <- bp749	Reverse primer for the detection of beta-actin transcripts by RT-PCR
GAPDHfor	ACC ACA GTC CAT GCC ATC AC	murine GAPDH cDNA: bp578 -> bp597	Forward primer for the detection of GAPDH transcripts by RT-PCR
GAPDHrev	TCC ATC ACC CTG TTG CTG TA	murine GAPDH cDNA: bp1010 <- bp1029	Reverse primer for the detection of GAPDH transcripts by RT-PCR
RTS2for	TCT AGA GGC TTT TGG GAA GAG TTT GAG	Okumura et al., 1998	Forward primer for the detection of SHP-2 transcripts by RT-PCR
RTS2rev	AGA AAA GGA GGT GCC AAT TAG	Okumura et al., 1998	Reverse primer for the detection of SHP-2 transcripts by RT-PCR

Table 3 *(continued) Primers used in this study. Primers were obtained from Microsynth GmbH, Balgach, Switzerland.*

2.6 Antibodies

Name	Isotype	Antigen/Target	Source	Application (dilution)
Antiserum 1002	rabbit, polyclonal	GST-coronin-1 (mouse)	Gatfield et al., 2005	Western blot (1:1000) Immunofluorescence (1:1000)
AlexaFluor633-labeled IgG fraction of 1002	rabbit, polyclonal IgG	GST-coronin-1 (mouse)	J.Massner, this thesis	Flow cytometry (1:250) (stock conc.: 1 mg/ml)
AlexaFluor633-labeled IgG fraction of pre1002	rabbit, polyclonal IgG	preimmune serum of antiserum 1002	J.Massner, this thesis	Flow cytometry (1:250) (stock conc.: 1 mg/ml)
Anti-actin (MAB1501)	monoclonal mouse $IgG_{1\kappa}$	G- and F-actin	Chemicon	Western blot (1:2000)
Anti-tubulin (clone E7)	monoclonal mouse IgG_1	tubulin	Dev. Studies Hybridoma Bank	Immunofluorescence (1:4000)
anti-GFP, mixture of clones 7.1 and 13.1	monoclonal mouse $IgG_{1\kappa}$	GFP	Roche	Western blot (1:1000)
FITC-anti-F4/80	rat	mouse F4/80	Serotec	Flow cytometry (1:200)
PE-anti-B220, clone RA3-6B2	monoclonal rat IgG_{2a}	mouse B220 (CD45R)	BD Pharmingen	Flow cytometry (1:200)
anti-CD3, clone 145-2C11 purified, sterile	monoclonal hamster IgG1	mouse CD3	BD Pharmingen	Activation of thymocytes (100 μg/ml)
PE-anti-CD3, clone 145-2C11	monoclonal hamster IgG1	mouse CD3	BD Pharmingen	Flow cytometry (1:200)
Biotin-anti-CD4, clone RM4-5	monoclonal rat IgG_{2a}	mouse CD4	A.Rolink, University of Basel	Flow cytometry (1:2000)
PE-anti-CD4, clone RM4-5	monoclonal rat IgG_{2a}	mouse CD4	BD Pharmingen	Flow cytometry (1:200)
PECy7-anti-CD4, clone RM4-5	monoclonal rat IgG_{2a}	mouse CD4	BD Pharmingen	Flow cytometry (1:200)
PE-anti-CD8a, clone 53-6.7	monoclonal rat IgG_{2a}	mouse CD8a	eBioscience	Flow cytometry (1:200)
APC-anti-CD8a, clone 53-6.7	monoclonal rat IgG_{2a}	mouse CD8a	BD Pharmingen	Flow cytometry (1:200)

Table 4 *Antibodies and flow cytometry reagents used in this study.*

Name	Isotype	Antigen/Target	Source	Application (dilution)
PE-anti-CD11b, clone M1/70	monoclonal rat IgG_{2b}	mouse CD11b	BD Pharmingen	Flow cytometry (1:200)
Biotin-anti-CD19, clone 1D3	monoclonal rat IgG_{2a}	mouse CD19	A.Rolink, University of Basel	Flow cytometry (1:4000)
PE-anti-CD19, clone 1D3	monoclonal rat IgG_{2a}	mouse CD19	BD Pharmingen	Flow cytometry (1:200)
PECy7-anti-CD19, clone 1D3	monoclonal rat IgG_{2a}	mouse CD19	BD Pharmingen	Flow cytometry (1:200)
Biotin-anti-CD21, clone 7G6	monoclonal rat IgG_{2b}	mouse CD21	A.Rolink, University of Basel	Flow cytometry (1:800)
PE-anti-CD23, clone B3B4	monoclonal rat IgG_{2a}	mouse CD23	BD Pharmingen	Flow cytometry (1:200)
anti-CD28, clone 37.51 purified, sterile	monoclonal hamster IgG2	mouse CD28	BD Pharmingen	Activation of thymocytes (100 μg/ml)
Biotin-anti-CD44, clone IM7	monoclonal rat IgG_{2b}	mouse CD44	BD Pharmingen	Flow cytometry (1:200)
APC-anti-CD44, clone IM7	monoclonal rat IgG_{2b}	mouse CD44	BD Pharmingen	Flow cytometry (1:200)
AlexaFluor647-anti-CD45.1, clone A20	monoclonal mouse IgG_{2a}	mouse CD45.1 (Ly5.1)	A.Rolink, University of Basel	Flow cytometry (1:800)
AlexaFluor647-anti-CD45.2, clone 104	monoclonal mouse IgG_{2a}	mouse CD45.2 (Ly5.2)	A.Rolink, University of Basel	Flow cytometry (1:800)
APC-anti-CD62L, clone MEL-14	monoclonal rat IgG_{2a}	mouse CD62L	BD Pharmingen	Flow cytometry (1:200)
Biotin-anti-CD117, clone ACK4	monoclonal rat IgG_{2b}	mouse CD117 (c-kit)	A.Rolink, University of Basel	Flow cytometry (1:800)
Biotin-anti-IgM, clone M41	refer to: Leptin, 1985	mouse IgM	refer to: Leptin, 1985	Flow cytometry (1:1000)
AlexaFluor568-anti-mouse IgG (H+L)	goat, polyclonal	mouse IgG (heavy and light chains)	Molecular Probes	Immunofluorescence (1:200)
AlexaFluor633-anti-rabbit IgG (H+L)	goat, polyclonal	rabbit IgG (heavy and light chains)	Molecular Probes	Immunofluorescence (1:200)
HRP-anti-mouse IgG (H+L)	goat, polyclonal	mouse IgG (heavy and light chains)	SBTA*	Western blot (1:20'000)

Table 4 *(continued) Antibodies and flow cytometry reagents used in this study. * SBTA: Southern Biotechnology Associates.*

Name	Isotype	Antigen/Target	Source	Application (dilution)
HRP-anti-rabbit IgG (H+L)	goat, polyclonal	rabbit IgG (heavy and light chains)	SBTA*	Western blot (1:20'000)
AlexaFluor568-Phalloidin	-	F-actin	Molecular Probes	Immunofluorescence (1:100)
PE-Streptavidin	-	biotin	BD Pharmingen	Flow cytometry (1:400) (second step reagent)
PECy7-Streptavidin	-	biotin	BD Pharmingen	Flow cytometry (1:400) (second step reagent)
APC-Streptavidin	-	biotin	BD Pharmingen	Flow cytometry (1:400) (second step reagent)
APC-AnnexinV	-	phosphatidylserine (apoptotic cells)	BD Pharmingen	Flow cytometry (1:33)

Table 4 *(continued) Antibodies and flow cytometry reagents used in this study. * SBTA: Southern Biotechnology Associates.*

2.7 Bacteria and cell lines

2.7.1 Bacterial strains and culture conditions

Name	Source	Culture medium	Culture conditions	Application
E.coli DH10B	S. Arber, Biozentrum, University Basel,	LB-media	37°C, 200 rpm	propagation of plasmid DNA for cloning purposes
Lactobacillus casei -GFP	M. Shaw, TNO, the Netherlands	*Lactobacillus* medium + erythromycin (5 μg/ml)	37°C, 200 rpm	flow cytometric phagocytosis assay

Table 5 *Bacterial strains used in this study.*

2.7.2 Mammalian cells, cell lines and culture conditions

Name	Cell type	Source	Culture medium	Application
BMM	Bone marrow derived macrophages	prepared by differentiation of murine bone marrow cells	DMEM / 10% FCS 2mM L-glutamine 50 μM β-mercaptoethanol 30% L929-conditioned medium	activation, phago-cytosis assays
L929	Fibroblasts	(Wiltschke et al., 1989), obtained from M.Kopf, ETH Zürich, Switzerland	DMEM / 10% FCS 2mM L-glutamine 50 μM β-mercaptoethanol	production of conditioned medium for BMM culture
E14.1	murine embryonic stem cells	Transgenic Mouse Core Facility (TMCF), Biozentrum, University Basel	see special section in paragraph 2.10.1	gene targeting and generation of coronin-1 deficient mice

Table 6 *Mammalian primary cells and cell lines used in this study. If not otherwise stated, cells and cell lines were cultured at 37°C / 5 % CO_2.*

2.8 Molecular biological methods

2.8.1 Agarose gel electrophoresis of DNA fragments

For analytical as well preparative purposes DNA was separated on agarose gels prepared in 0.5 % TBE. Agarose was purchased from Eurobio and used at 0.8 % for the separation of DNA fragments of 25 –2 kb size or at 1.6 % to separate 0.1 to 2 kb sized fragments. To visualize DNA fragments using UV-light (280 nm) ethidium bromide (final concentration 10 μg/ml) was added to the liquid agarose solution prior to casting the gel. DNA samples were prepared for gel electrophoresis by adding 6x DNA loading buffer. Gel electrophoresis was performed at 50 – 80 V in electrophoresis chambers (type: M.A.K. I, Baechler, Switzerland).

2.8.2 Preparation of chemically competent *E.coli* DH10B and transformation

2.8.2.1 Preparation of ultra-competent *E.coli* DH10B

Materials:

- SOB medium — 0.5% (w/v) yeast extract, 2% (w/v) tryptone, 10 mM NaCl, 2.5 mM KCl, 10 mM $MgCl_2$, 10 mM $MgSO_4$ dissolved in 1l ddH_2O and sterilized by autoclaving.
- TB solution — 10 mM PIPES, 15 mM $CaCl_2$, 250mM KCl dissolved in ddH_2O. pH was adjusted to 6.7 with KOH or HCl prior to the addition of $MnCl_2$ at a final concentration of 55 mM. The solution was brought to a total volume of 1l by adding ddH_2O and then sterilized by filtration (0.45 μm).
- DMSO — before use stored at –20°C o/n.

Ultra-competent *E.coli* (strain: DH10B, kind gift from S.Arber, Biozentrum, University of Basel) were prepared based on a protocol from Inoue et al. (1990). 250 ml SOB medium were inoculated with 10 colonies of *E.coli* DH10B grown on LB plates. The culture was incubated in a 1l Erlenmeyer flask at 19°C with vigorous agitation to an OD_{600} of 0.5. Bacteria were harvested by centrifugation for 10 min, 4°C at 4000 rpm (Sorvall RC5C, rotor GS3). The resulting pellet was gently resuspended by pipetting in 80 ml ice-cold TB solution and stored on ice for 10 min. By centrifugation at 4000 rpm (10 min, 4°C) the bacteria were pelleted again and then resuspended in 20 ml TB solution supplemented with 1.4 ml DMSO. Bacteria

were flash-frozen in liquid nitrogen and stored at –80°C in 1.5 ml Eppendorf tubes as 250 µl aliquots.

2.8.2.2 Transformation of ultra-competent *E.coli* DH10B

For transformation, 50 µl of ultra-competent *E.coli* DH10B were used after thawing the bacteria on ice. An appropriate amount of plasmid DNA or 5 – 10 µl of a ligation reaction were gently mixed with the bacteria (maximal 5 pipetting strokes) followed by 5 min incubation on ice. For recovery and expression of the resistance gene bacteria were then transferred to 1 ml antibiotic-free LB supplemented with 0.1% glucose in 14 ml polypropylene round-bottom tubes (BD Falcon) and incubated for 1 hr at 37°C with agitation (150 rpm, Kuehner shaker). After incubation, bacteria were plated on LB agar plates containing the appropriate antibiotic and incubated o/n at 37°C. The resulting colonies were then used to inoculate 5 ml cultures for mini-prep of plasmid DNA.

2.8.3 General cloning methods

2.8.3.1 Preparation of plasmid DNA from *E.coli* cultures

Plasmid DNA from *E.coli* cultures was prepared using Maxi- and Mini-Prep Kits from QIAGEN according to the manufacturer's protocol. Purified plasmid DNA was dissolved in either molecular biology grade H_2O (Eppendorf) for immediate use in cloning procedures or in TE buffer for long-term storage at –20°C.

2.8.3.2 Ethanol precipitation of DNA

Precipitation of DNA was performed by adding 1/10 volume of 3M Na-acetate pH 5.2 and 2 volumes of 100% ethanol to the DNA solution. After mixing by inverting the tube a few times, the solution was incubated at –20°C for at least 15 min. The precipitated DNA was then pelleted by centrifugation (20'000 *x g*, 15 min, 4°C), washed twice with 70% ethanol (5 min centrifugation steps) and air-dried. The DNA pellet was dissolved in ddH_2O or TE buffer depending on further use.

2.8.3.3 Restriction enzyme digest of plasmid DNA and PCR products

For restriction enzyme digest of plasmid DNA or PCR products restriction enzymes were purchased from New England Biolabs (NEB) and used with the supplied buffers. Generally, 0.5 – 5 µg DNA were digested at 37°C in a total volume of 30 µl with 5 – 60 U of restriction enzyme either for 1 – 2 hrs for analytical purposes or o/n for preparative purposes as required for further cloning steps.

2.8.3.4 Dephosphorylation of DNA

To prevent religation of digested vectors 5'-phosphate groups were removed by treating linearized plasmid DNA with shrimp alkaline phosphatase (SAP, Roche). 1U SAP per 250 ng DNA together with the supplied SAP reaction buffer were directly added to the restriction digest reaction and incubated for 10 min at 37°C. SAP was inactivated by incubation at 65 °C for 15 min and the linearized and dephosphorylated vector was isolated by agarose gel electrophoresis and subsequent gel extraction.

2.8.3.5 Purification of DNA fragments from agarose gels

DNA fragments of interest as visualized by UV light were excised from the agarose gel with a ethanol cleaned razor blade and purified using the gel extraction kit (QIAGEN) according to the manufacturer's protocol.

2.8.3.6 Ligation of DNA fragments

Ligation of DNA fragments with cohesive or blunt ends was performed at a molar ratio between vector and insert of 1: 2 – 4 in a volume of 20 µl using the T4 ligase from New England Biolabs (NEB) or the Rapid DNA Ligation Kit (Roche). Ligation reactions with T4 ligase were set up at RT as follows:

x µl vector DNA (up to 100 ng vector)
x µl insert DNA (as required for a certain ratio relative to the vector DNA)
2 µl 10x ligation buffer
1 µl T4 ligase
x µl molecular biology grade water (to a total reaction volume of 20 µl)

Ligation reactions were then incubated for 1 hr at RT and 2 – 5 µl of the reaction were transformed into ultra-competent *E.coli* DH10B.
Ligations with the Rapid DNA Ligation Kit were set up as given below:

x µl vector DNA (up to 100 ng vector)
x µl insert DNA (as required for a certain ratio relative to the vector DNA)
2 µl 5x DNA dilution buffer
10 µl 2x T4 DNA ligation buffer
1 µl T4 ligase
x µl molecular biology grade water (to a total reaction volume of 20 µl)

Ligation reactions were then incubated for 30 min at RT and 2 – 5 µl of the reaction were transformed into ultra-competent *E.coli* DH10B.

2.8.3.7 Polymerase chain reaction (PCR) for the construction of the coronin-1 targeting vectors

Materials:

- Molecular biology grade water (Eppendorf, Cat.No. 0032 006 302)
- 10 mM PCR nucleotide mix (Roche, Cat.No. 11 581 295 001)
- Expand Long Template PCR System (Roche, Cat.No. 1 681 834)
- Primer (15 µM solution in molecular biology grade water)
- T3 thermocycler (Biometra)

The individual parts of the targeting vector for the coronin-1 locus were amplified by PCR using ES cell genomic DNA as a template and the Expand Long Template PCR System. Primers were designed to insert appropriate restriction sites for subcloning the PCR products. PCR products were purified using the gel extraction kit (Qiagen) and subcloned either directly in pBluescript SK(+) or via T/A cloning in the vector pGEM®-T easy (Promega) according to the manufacturer's protocol. PCR reactions were set up as follows:

x µl template DNA (500 ng)
1 µl 10 mM PCR nucleotide mix
1 µl 15 µM forward primer
1 µl 15 µM reverse primer

5 µl 10x PCR buffer 1

0.75 µl polymerase mix (corresponds to 2.5 units)

x µl molecular biology grade water (to a total reaction volume of 50 µl)

PCR reactions were then run on a T3 thermocycler employing the following program:

Step 1	**94°C, 2 min**	*(initial denaturation of DNA)*
Step 2	**94°C, 20 sec**	*(denaturation of DNA)*
Step 3	**56 – 62°C, 30 sec**	*(annealing temperature depending on primer)*
Step 4	**68°C, 1 - 4 min**	*(elongation time depending on product length)*
Return to step 2, 10 times		
Step 5	**94°C, 20 sec**	*(denaturation of DNA)*
Step 6	**56 – 62°C, 30 sec**	*(annealing temperature depending on primer)*
Step 7	**68°C, 1 - 4 min + 20 sec each cycle** *(elongation time depending on product length, 20 sec elongation of time to compensate for loss in enzyme activity)*	
Step 8	**68°C, 10 min**	*(elongation of incomplete products)*
Step 9	**4°C,**	*(storage until further processing)*

2.8.3.8 Sequencing of plasmid DNA

Sequencing of plasmid DNA was performed according to the manufacturer's protocol supplied with the Big Dye 1.1® Terminator v 1.1 Sequencing Kit.

Materials:

- Big Dye 1.1® Terminator v 1.1 Sequencing Kit
  (Applied Biosystems, Cat No. 4337452)
- 96 well optical reaction plate (Applied Biosystems, Cat No. 4306737)
- Primus 96 plus thermocycler (MWG Biotec)
- Molecular biology grade water (Eppendorf)
- 95% and 70% ethanol
- Hi-Di™ formamide (Applied Biosystems, Cat.No. 4311320)
- Plasmid DNA to be sequenced in ddH_2O or TE buffer
- Sequencing primers (Microsynth) as 5 µM solution in ddH_2O

For sequencing of plasmid DNA the following components were mixed in one well of a 96 well optical reaction plate:

x µl plasmid DNA (100 – 500 ng)
1 µl primer (equals 5 pmol)
4 µl Big Dye 1.1 Terminator Ready Reaction Mix
x µl molecular biology grade H_2O (to a total reaction volume of 10 µl)

These reactions were run in a Primus 96 plus thermocycler with the following program:

Step 1	96°C, 2 min	(initial denaturation of DNA)
Step 2	96°C, 30 sec	(denaturation of DNA)
Step 3	50°C, 15 sec	(annealing of primers)
Step 4	60°C, 4 min	(elongation)
Return to step 2, 25 times		
Step 5	4°C for storage until further processing	

Prior to analysis the DNA needed to be precipitated from the sequencing reaction according to the following protocol:

- per well 8 µl molecular biology grade H_2O were added
- 32 µl 95% ethanol were added and the solution was gently mixed by pipetting up and down 2 – 3 x
- the samples were incubated at room temperature for 15 min to allow precipitation
- the 96 well plates were then centrifuged for 45 min at 2'000 *x g*
- the supernatant was discarded by inverting the plate onto a papertowel
- 150 µl 70% ethanol were used to wash the barely visible pellets by pipetting up and down 2 – 3 x
- another centrifugation at 2'000 *x g* for 10 min was performed to pellet the DNA
- the supernatant was discarded by inverting the plate onto a papertowel
- the DNA pellets were dried by placing the 96 well reaction plate inverted onto a papertowel in the plate holder of the centrifuge and spinning at 700 *x g* for 1 min
- the pellets were resuspended in 20 µl diluted Hi-Di™ formamide for analysis (2 parts Hi-Di™ formamide + 1 part molecular biology grade H_2O)

Analysis of the sequencing reactions was performed by capillary electrophoresis on an ABI PRISM Genetic Analyzer 3700. Sequences were analysed using the MacVector software package (version 7.2.2).

2.8.4 Southern blot analysis of genomic DNA isolated from ES cells and tail biopsies

(protocol courtesy of S.Arber, Biozentrum, University of Basel)

2.8.4.1 Isolation of genomic DNA from ES cells and mouse tail biopsies

Materials:

- Tail buffer: 100 mM Tris-HCl pH 8.5, 5 mM EDTA, 0.2 % SDS, 200 mM NaCl, 100 µg/ml Proteinase K (stock solution: 20 mg/ml Proteinase K in destilled water)
- Phenol:Chloroform:Isoamylalcohol (25:24:1, Sigma, Cat.No. P3803)
- 3 M sodium-acetate pH 5.2
- 100 % and 70 % ethanol (prepared with molecular biology grade water)
- Isopropanol

Lysates for the isolation of genomic DNA from ES cells were prepared by incubating a confluent ES cell layer in a 10 cm tissue culture dish with 5 ml tail buffer o/n at 37 °C. Tail biopsies were lysed o/n in 500 µl tail buffer at 55°C on a thermoshaker (600 rpm, Eppendorf). 500 µl of the lysates were then cleared by centrifugation in a table top centrifuge (20'000 *x g*, 5 min, RT) and the supernatant was transferred to a fresh 1.5 ml Eppendorf tube. An equal volume of phenol:chloroform:isoamylalcohol was added to the tubes which were subsequently vigorously shaken for 3 min at RT. To allow phase separation tubes were spun at 20'000 *x g* for 5 min at RT and the upper, aqueous phase was transferred to a fresh tube. DNA was then precipitated as described in paragraph 2.8.3.2.
For PCR screening purposes genomic DNA was precipitated from ES cell lysates by isopropanol. To that end, ES cells grown to confluency in 24-well plates were lysed with 500 µl tail buffer per well o/n at 37°C. The next day 300 µl isopropanol were added to each well and the plates were incubated for 1 hr at RT on a shaking platform. Genomic DNA precipitated as a clearly visible string under these conditions which was taken out with a forceps, dipped 2 x into fresh 70 % ethanol for washing, briefly air-dried and finally resuspended in 50 µl molecular biology grade water.

2.8.4.2 Preparation of digoxigenin labeled DNA probes

Materials:

- 1 mM DIG DNA labeling mix (Roche Cat.No. 127 70 65)
- Taq DNA polymerase + corresponding 10 x PCR buffer (Pharmacia, Cat.No. 270799)
- Primer (50 µM solution in molecular biology grade water)
- T3 thermocycler (Biometra)

Digoxigenin labeled DNA probes for Southern blot analysis of genomic DNA were prepared by PCR. As template for the PCR genomic fragments of the coronin-1 locus cloned in the pBluescript SK(+) vector were used. PCR reactions were set up as follows:

x µl plasmid DNA (100 ng)
1 µl forward primer (equals 50 pmol)
1 µl reverse primer (equals 50 pmol)
5 µl 1 mM DIG DNA labeling mix
5 µl 10 x PCR buffer
0.5 µl Taq polymerase (5U/µl stock)
x µl molecular biology grade H_2O (to a total reaction volume of 50 µl)

The PCR reactions were run on a T3 thermocyler using the following program:

Step 1	95°C, 5 min	(initial denaturation of DNA)
Step 2	95°C, 45 sec	(denaturation of DNA)
Step 3	58°C, 60 sec	(annealing of primers)
Step 4	72°C, 2 min	(elongation)
Return to step 2, 40 times		
Step 5	72°C, 5 min	(elongation of incomplete products)
Step 6	4°C for storage until further processing	

PCR products were separated by electrophoresis on 1.5 % agarose gels and purified using the gel extraction kit (as described in paragraph 2.8.3.5). The digoxigenin labeled probes were stored in molecular biology grade water at –20°C until use.

2.8.4.3 Digest of genomic DNA, gel electrophoresis and transfer to nylon membranes

Five to ten microgram genomic DNA were digested o/n at 37 °C with 60 U of restriction enzyme in a total volume of 30 µl. DNA fragments were separated by electrophoresis on 0.8 % agarose gels at 60 V. Under UV light the position of the DNA molecular weight marker bands was marked by cutting the gel with a syringe needle. In order to prepare the gel for transfer to nylon membranes it was first incubated with 0.25 M HCl for 10 min and then two times for 15 min with 0.4 M NaOH under agitation at RT. For transfer positively charged nylon membranes (Roche, Cat. No. 1 209 272) were used. On a saran wrap 15 ml 0.4 M NaOH were supplied, the DNA gel was inverted on the solution and covered with the nylon membrane which has been soaked in destilled water and 0.4 M NaOH before hand. Finally 3 sheets of filter paper (type: 3MM Chr, Whatman) and a pile of paper towel (10 cm height) was placed on the membrane. To promote close contact between the layers a plate and weight were put on top of the sandwich. Transfer was performed o/n at RT.

2.8.4.4 Hybridization of the nylon membrane

After transfer the blot was disassembled, the position of the wells and the molecular weight markers were marked on the membrane with a pen and the membrane was neutralized in 0.5 M Tris-HCl for 1 min. The membrane was dried between two filter papers (type: 3MM Chr, Whatman) and crosslinked by UV light on both sides (AutoCrosslink function, UV Stratalinker, Strategene). Prehybridization of the membrane was performed in hybridization tubes in a hybridization oven with rotating wheel at 42°C for 1 hr using 15 ml of hybridization solution (5 x SSC, 2 % (w/v) blocking reagent, 0.1 % (w/v) sarcosyl, 0.02 % SDS, 50 % formamide in destilled water; blocking reagent for Southern blot was obtained from Roche, Cat.No. 11 0961 76001).
For hybridization 100 ng digoxigenin labeled DNA probe were added to 10 ml hybridization solution, denatured for 10 min at 68°C and filtered through a 0.2 µm syringe filter prior to addition to the prehybridized membrane. Hybridization was performed o/n at 42°C in a hybridization oven.

2.8.4.5 Detection of digoxigenin labeled DNA probes on the nylon membrane

After hybridization the membrane was subjected to the following stringency washing steps:

- 2 x 15 min at RT with 50 ml 2 x SSC, 0.1 % SDS (performed in trays on a rocking platform)

- 2 x 15 min at 68°C with 50 ml 0.2 x SSC, 0.1 % SDS (performed in hybridization tubes and oven)

The membrane was then washed with DIG wash buffer (0.1 M maleic acid, 0.15 M NaCl, 0.3 % Tween 20, pH 7.5) for 1 min in a tray under agitation. Subsequent blocking of the membrane was performed with 20 ml 1 % (w/v) blocking solution (blocking reagent dissolved in 0.1 M maleic acid, 0.15 M NaCl, pH 7.5) in hybridization tubes and oven at RT for 1 hr. After blocking, the membrane was incubated with alkaline phosphatase labeled anti-digoxigenin Fab fragments (anti-DIG-AP, Roche Cat.No. 1 093 274, diluted 1:20'000 in 1 % blocking solution) for 30 min at RT in hybridization tubes. Following 2 x 15 min washing steps in 100 ml DIG wash buffer at RT in trays under agitation the membrane was incubated for 2 min in CDP-Star detection buffer (0.1 M Tris-HCl, 0.1 M NaCl, pH 9.5). Detection of alkaline phosphatase labeled anti-digoxigenin Fab fragments bound to the nylon membrane was performed using the CDP-Star reagent (Roche, Cat.No. 1 759 051) diluted 1:100 in CDP-Star detection buffer. The membrane was incubated with CDP-Star (2 ml) inverted on a layer of Parafilm for 5 min at RT. For exposure to ECL film (Amersham) the membrane was drained from excess liquid with a filter paper and mounted into an autoradiography cassette between transparent plastic sheets.

2.8.5 Reverse transcriptase-PCR (RT-PCR)

2.8.5.1 Isolation of RNA from cell lines and murine tissue

Materials:

- Sterile filter tips (Rainin)
- Molecular biology grade water, fresh vial (Eppendorf, Cat.No. 0032 006 302)
- Isopropanol, chloroform and ethanol p.a. (to be used for RNA work only)
- TriZOL reagent (Invitrogen Cat.No. 15596-026)
- Lysing matrix D: tubes containing beads to lyse tissue samples on the FastPrep device (Qbiogen, Cat.No. 6913-100), in the following referred to as ‚lysis tubes'
- FastPrep FP120 device (Qbiogen)

After dissection, 50 –100 mg of murine tissue of interest were placed on ice into lysis tubes which have been supplied with 1 ml TriZOL reagent. Tissue homogenization was performed at 4°C by running the lysis tubes for 2 x 45 sec at speed 6 in the FastPrep device. Lysates

from cell lines were prepared by homogenizing 5 x 10^6 cells with a syringe and a 22G needle (10 strokes) in 1 ml TriZOL reagent.
The resulting lysate was cleared by centrifugation (10'000 *x g*, 10 min, 4°C) and transferred to a fresh 1.5 ml Eppendorf tube. After incubation at RT for 5 min 0.2 ml chloroform were added to the lysate and tubes were vigorously shaken for 15 sec. An additional incubation step at RT for 3 min followed by centrifugation at 12'000 *x g* (15 min, 4°C) allowed phase separation. The upper aqueous phase was collected, transferred to a fresh 1.5 ml Eppendorf tube and mixed with 0.5 ml isopropanol by inverting the tube to precipitate the RNA. The RNA pellet was recovered after a 10 min incubation at RT and subsequent centrifugation (12'000 *x g*, 10 min., 4°C). 75 % Ethanol was used to wash the RNA pellet twice (centrifugation steps for washing: 7'500 *x g*, 5 min, 4°C). Finally, the RNA pellet was dissolved in molecular biology grade water by gentle pipetting before and after heating the sample to 55°C for 10 min.
The concentration and quality of the isolated RNA was determined using a RNA NanoChip and the corresponding 2100 BioAnalyzer instrument according to the manufacturer's protocol (AGILENT Technologies).

2.8.5.2 DNAse I treatment and reverse transcription

Materials:

- DNA-free kit (Ambion, Cat.No. 1906): contains DNAse I and appropriate buffer
- PCR nucleotide mix (Roche, Cat.No. 11 581 295 001)
- Random primers at 0.5 □g/□l (Promega, Cat.No. C 1181)
- SuperScript III (Invitrogen, Cat.No. 18080-044): reverse transcriptase + corresponding buffers
- rRNAsin (40 U/□l, Promega, Cat.No. N 251 A): RNAse inhibitor
- 0.1 M DTT (supplied with SuperScript III)
- T3 thermocycler (Biometra)

In order to remove DNA contamination from the RNA preparation 10 □g purified RNA were treated with DNAse I according to the following protocol:

- in a total reaction volume of 50 □l 10 □g RNA were mixed with 1x DNAse I buffer and 2 □l DNAse I (corresponds to 4U)
- samples were incubated for 1 hr at 37°C in a waterbath

- 10 µl inactivation reagent (supplied with the DNA-free kit) were added, the sample was mixed by pipetting and incubated for 2 min at RT
- after centrifugation at 10'000 *x g* for 1 min the supernatant was transferred to a fresh 1.5 ml Eppendorf tube and incubated for 3 min at 90°C for full DNAse I inactivation
- prior to reverse transcription RNA concentration and integrity was checked on a RNA NanoChip as described in paragraph 2.8.5.1

Reverse transcription of DNAse I treated RNA was performed using random hexanucleotide primers. The reverse transcription reactions were set up in two steps according to the following scheme:

STEP 1: in a PCR tube were first combined:

1 µl random primers (stock concentration: 0.5 µg/µl)
x µl DNAse I treated RNA (corresponding to 2 µg RNA)
1 µl PCR nucleotide mix (dNTPs at 10 mM)
x µl molecular biology grade water (to a total volume of 13 µl)

STEP 2: in a separate tube the following components were mixed:

4 µl 5 x first strand buffer (supplied with SuperScript III)
1 µl 0.1 M DTT
1 µl rRNAsin (corresponds to 40 U)
1 µl SuperScript III (as a control for amplification from contaminating DNA, samples were also prepared without SuperScript III)

Finally, the 7 µl from step 2 were added to the reagents from step 1, mixed by pipetting and run on a T3 thermocycler with the following program for reverse transcription:

Step 1	25°C, 5 min	(annealing of random primers)
Step 2	50°C, 1 hr	(reverse transcription)
Step 3	70°C, 15 min	(inactivation of reverse transcriptase)
Step 4	4°C,	(storage until further processing)

2.8.5.3 PCR on reversely transcribed RNA

Materials:

- 10 mM PCR nucleotide mix (Roche Cat.No. 11 581 295 001)
- Taq DNA polymerase + corresponding 10 x PCR buffer (Pharmacia, Cat.No. 270799)
- Primer (10 µM solution in molecular biology grade water)
- T3 thermocycler (Biometra)

Reversely transcribed RNA was diluted 1:10 in molecular biology grade water and used for the setup of PCR reactions as follows:

1 µl 1:10 diluted reversely transcribed RNA
0.5 µl forward primer
0.5 µl reverse primer
0.5 µl PCR nucleotide mix
2.5 µl 10 x PCR buffer
0.3 µl Taq polymerase
x µl molecular biology grade water (to a total reaction volume of 25 µl)

The PCR reactions were run on a T3 thermocycler with the program given below:

Step 1	95°C, 3 min	(initial denaturation of DNA)
Step 2	95°C, 30 sec	(denaturation of DNA)
Step 3	56°C, 30 sec	(annealing of primers)
Step 4	72°C, 1 min	(elongation)
Return to step 2, 35 times		
Step 5	72°C, 10 min	(elongation of incomplete products)
Step 6	4°C for storage until further processing	

10 µl of the samples were then run on 1.8 % agarose gels to analyze them for the presence of coronin and control transcripts.

2.9 Cell culture methods

2.9.1 Determination of cell numbers

Cell counting was performed using a Neubauer counting chamber (0.1 mm depth). An aliquot of the cell suspension was diluted 1:10 in trypan blue solution (0.1%, Sigma) to distinguish living from dead cells. Living and therefore colourless cells present in the 4 outer squares were counted and the cell number per ml was calculated by dividing the result by 4 and subsequently multiplying it with $1x10^4$.

2.9.2 Preparation of L929-conditioned medium

In order to condition cell culture medium 10^7 L929 cells were plated out in 100 ml L929 medium in 15 cm cell culture dishes (BD Falcon). After seven days in culture at 37°C, 5% CO_2 the medium was harvested, filtersterilized (0.22 µm) and stored at 4°C until further use. New medium was added to the dish and the procedure was repeated 3 times before the cells were discarded.

2.9.3 Preparation of bone marrow-derived macrophages

Bone marrow-derived macrophages (BMM) were obtained by differentiation of bone marrow cells in the following medium (referred to as ‚BMM-culture medium'): DMEM / 10% FCS / 2mM glutamine / 50µM β-mercaptoethanol / 30% L929-conditioned medium. Bone marrow cell suspensions were prepared from 6 – 8 week old, female C57Bl/6 mice (RCC, Füllinsdorf). Mice were sacrified by CO_2 asphyxiation, their hind legs were isolated and freed from all muscle tissue. Subsequently, the femura were cut open at the upper most part and placed in a blunt-ended yellow pipette tip with the open end of the femur pointing downwards. The loaded pipette tip was placed in a 5 ml polystyrene tube (BD Falcon, Cat.No. 352063) supplied with 500 µl BMM-culture medium. Centrifugation (7 min, 800 *x g*, RT) allowed retrieval of the bone marrow cells into a pellet which was subsequently resuspended. The resulting cell suspension was added to 10 cm Teflon dishes (one plate per femur) with 15 ml BMM-culture medium. Cells were cultured for at least 5 days to allow their differentation into BMM at 37°C, 5% CO_2. BMM were used for experiments at day 6. Their identity was assessed by microscopy looking at typical macrophage morphology and by flow cytometry analysing the expression of macrophage markers such as CD11b and F4/80.

2.9.4 Preparation of single cell suspensions from murine tissue

In order to obtain single cell suspensions of spleen, thymus or lymph nodes mice were sacrified by CO_2 asphyxiation. The dissected organs were placed in a tissue culture dish containing 10 ml DMEM / 10 % FCS / 2 mM glutamine and mashed between two nylon nets with a syringe plunger. Single cell suspensions of bone marrow were prepared by flushing isolated hind leg femura with a syringe and a needle (22 Gauge) loaded with 2 ml DMEM / 10 % FCS / 2 mM glutamine. To ensure full dissociation of the tissue the homogenate was passed 2 – 3 times through and collected with a Gilson P1000 (blue pipette tip) and eventually transferred to a 15 ml polystyrene tube (BD Falcon, Cat.No. 352095). After centrifugation at 300 *x g* for 5 min at 4°C the pellet was resuspended with several gentle pipetting strokes (Gilson P1000) in an appropriate volume of DMEM / 10 % FCS / 2 mM glutamine for further processing.

2.9.5 MACS-based isolation of murine T-lymphocytes

Materials:

- Cell culture medium (e.g. the medium used for mixed lymphocyte reactions as described in paragraph 2.9.6)
- Pan T-cell isolation kit (Miltenyi, Cat.No. 130-090-861): contains the cocktail of biotin-labeled antibodies and streptavidin-coated magnetic microbeads. Both solutions are ready for use.
- MACS LS Separation Columns (Miltenyi, Cat.No. 130-042-401)
- ACK erythrocyte lysis buffer
- MACS buffer: PBS / 0.5 % (w/v) BSA / 2mM EDTA

T-lymphocytes were isolated from splenic cell suspensions using magnet assisted cell sorting (MACS). The principle of this method relies on the incubation of a splenic cell suspension with biotin-labeled antibodies directed against B-lymphocytes and myeloid/erythroid cells. Following an incubation with streptavidin coated magnetic beads, the labeled cell suspension is run over a column placed in a magentic field which allows collection of non-labeled T-lymphocytes in the flow-through whereas the labeled fraction of the cell suspension remains bound to the column (i.e. negative selection of T-lymphocytes).
As described in paragraph 2.9.4 single cell suspensions were prepared from isolated spleen and transferred to 50 ml polypropylene tubes (BD Falcon, Cat.No. 352070). Cells were pelleted by centrifugation (300 *x g*, 5 min, RT), resuspended in ACK erythrocyte lysis buffer

(5 ml per spleen) and incubated at RT for 5 min with slight, occasional agitation. To quench the lysis buffer culture medium was added to a total volume of 30 ml and cells were harvested by centrifugation. Cells were resuspended in 10 ml culture medium, counted and pelleted again by centrifugation. The resulting pellet was then taken up in 40 µl cold MACS buffer per 10^7 cells and 10 µl of biotin-labeled antibody cocktail were added per 10^7 cells. The cell suspension was mixed by swirling the tube and incubated at 4 – 8°C (fridge !) for 10 min. After incubation, 30 µl cold MACS-buffer and 20 µl streptavidin-coated microbeads per 10^7 cells were added to the suspension, samples were mixed by swirling the tube and incubated for 15 min in the fridge. In order to wash away excess antibodies and microbeads the sample volume was then brought to a total volume of 20 ml with cold MACS buffer and the cells were harvested by centrifugation (300 *x g*, 10 min, 4°C). The supernatant was removed completely, the cells were resuspended in 1.2 ml cold MACS buffer and filtered through a syringe equipped with parachute silk to remove cell clumps. For magnetic separation at RT a MACS LS separation column was installed into the magnetic holder and equilibrated by running 3 ml MACS buffer through the column. Subsequently, the cell suspension was loaded onto the column and allowed to flow through. The flow through from the loading and the three following washing steps (each with 3 ml MACS buffer) was collected in a 15 ml polystyrene tube (BD Falcon) on ice. Cells were finally pelleted by centrifugation (300 *x g*, 10 min, 4°C), resuspended in culture medium, counted and checked by FACS staining for purity.

2.9.6 Mixed lymphocyte reaction

Splenic T-lymphocytes were isolated from homozygous coronin-1 knock-out mice and wildtype littermates using magnetic bead isolation as described in paragraph 2.9.5. For allogeneic stimulation of T-lymphocytes spleen cell suspensions were isolated from BALB/c mice (RCC) and treated with 50 µg/ml Mitomycin C (Sigma) in PBS for 30 min at 37°C after erythrocyte lysis. Cocultures of responding T-lymphocytes ($2x10^5$) and either $2x10^5$ (1:1 ratio) or $4x10^5$ (2:1 ratio) stimulating spleen cells were set up in flat-bottom 96-well plates (BD Falcon) using the following medium: RPMI-1640 (Gibco BRL) / 1x MEM non-essential amino acids (Gibco BRL) / 1 mM sodium pyruvate (Gibco BRL) / 100 U/ml Penicillin (Sigma) / 100 µg/ml Streptomycin (Sigma) / 10 µM β-Mercaptoethanol (Gibco BRL) / 10% FCS (Gibco BRL). After 3 days incubation at 37°C / 6% CO_2 and 20 hours before harvesting, 1 µCi [^{3}H]-thymidine (Amersham) was added to each well. Incorporation of the isotope was measured in a liquid scintillation counter (Packard TopCount) and expressed as the average cpm (± SD) per well of triplicate cultures.

2.10 Generation and maintenance of coronin-1 deficient mice

2.10.1 ES cell culture, transfection and selection

The culture and manipulation of murine ES cells for the generation of coronin-1 deficient mice was performed in the tissue culture facility of the transgenic mouse core facility (TMCF) at the Biozentrum. The ES cell strain used (E14.1, supplier: TMCF, Biozentrum) was originally isolated from blastocysts of Sv129/Ola background. In contrast to other protocols ES cell culture procedures at the TMCF were carried out in the absence of a layer of mouse embryonic fibroblasts as feeder cells. This required special care in handling ES cells in order to keep them in the undifferentiated stage necessary for successful germline transmission.
In the following, general ES culture procedures will be intoduced (paragraph 2.10.1.1) before the scheme of ES cell transfection and selection will be described in more detail (paragraph 2.10.1.2 and 2.10.1.3).

2.10.1.1 ES cell culture: general methods

Preparation of complete ES cell medium:

Materials:

- DMEM 500 ml (PAN Biotech)
- MEM non-essential amino acids (100x stock, Gibco BRL)
- Glutamine (100x stock, Gibco BRL)
- Sodium pyruvate (100x stock, Gibco BRL)
- 50 mM □-mercaptoethanol for cell culture purposes (Gibco BRL)
- Murine recombinant LIF (ESGRO, $1x10^6$ units/ml, Gibco BRL)
- ES culture qualified FCS (HyClone)
- 10x G418 stock (concentration: 3 mg/ml, Sigma) in complete ES cell medium

To prepare complete ES cell medium the following components were mixed

500 ml DMEM
5.2 ml 100x Non-essential amino acids
5.2 ml 100x Glutamine
5.2 ml 100x Sodium pyruvate
520 □l 50 mM □-mercaptoethanol

60 µl murine recombinant LIF
52 ml FCS

For the selection of ES cells after transfection complete ES cell medium containing G418 at a final concentration of 300 µg/ml was prepared freshly before use by mixing complete ES cell medium with an appropriate amount of 10x G418 stock.

Preparation of culture dishes:

Materials:

- 10 cm tissue culture dishes (BD Falcon)
- 6-well tissue culture dishes (BD Falcon)
- 24-well tissue culture dishes (BD Falcon)
- 96-well tissue culture dishes (BD Falcon)
- 0.1 % (w/v) gelatine (Sigma) solution

All tissue culture dishes were gelatinized before adding ES cells by incubating tissue cultures plates with an appropriate amount of 0.1 % gelatine for 5 min at RT followed by aspiration of the solution.

Passaging of ES cells:

Materials:

- Prewarmed PBS (PAN Biotech)
- Trypsin-EDTA in HBSS (Gibco BRL)
- Prewarmed complete ES cell medium

Confluent ES cell culture were passaged by aspirating the medium, washing the cells once with prewarmed PBS and incubation with Trypsin-EDTA (2 ml per 10 cm dish, 500 µl per well of a 6-well plate, 100 µl per well of a 24-well plate, 20 µl per well of a 96-well plate) at 37 °C until the cell layer lost contact to the substrate (this usually took 0.5 - 5 min). Incubation with Trypsin-EDTA was kept as short as possible to avoid damage of ES cells after prolonged contact to trypsin and was supported by agitation of the culture dish. Cells were collected from the culture dish by adding an excess of prewarmed complete ES cell medium (4 x the volume of trypsin-EDTA), dissociated by gentle pipetting and transferred to 15 ml polystyrene

tubes (BD Falcon, Cat No. 352095). ES cells were then pelleted by centrifugation (300 *x g*, 3 min, RT) and resuspended in complete ES cell medium. Cells were seeded onto new gelatinized culture dishes. Trypsinized cultures in 96-well plates were quenched by adding per well 200 µl of a prewarmed 1:1 mixture of complete ES cell medium and FCS. Cells were then seeded into a new, gelatinized 24-well plate (100 µl cell suspension + 900 µl prewarmed, complete ES cell medium per well). To avoid any harmful effect of trypsin the medium was exchanged after 4 hrs. Generally, ES cells were cultured in a cell culture incubator at 37°C / 6 % CO2.

Thawing and freezing cells in 96-well plates and cryovials:

Materials:

- 2 ml cryogenic vials (NUNC)
- 2x freezing mix (20% DMSO (Fluka) in complete ES cell medium)

At multiple steps of the selection process ES cells were frozen. Picked ES cells clones were first grown in 96-well plates until confluency, then trypsinized as described above and 100 µl were transferred in one well of a 24-well plate. After expansion in these 24-well plates the ES cells were used for the preparation of genomic DNA. The remaining 100 µl cell suspension were mixed by gentle pipetting with 100 µl 2x freezing mix and the whole 96-well plate was transferred to a –80°C freezer. Positive ES cell clones frozen in 96-well plates were taken in culture by thawing the plate at 37°C in the cell culture incubator. The cell suspension of one well was then transferred as passage 1 to one well of a 24-well plate containing 2 ml of prewarmed, complete ES cell medium. To avoid any harmful effects of residual DMSO the medium was exchanged after o/n incubation at 37°C / 6% CO2.
Passage 1 cells were split 1:6 into 6 wells of a new 24-well plate as passage 2, grown to confluency and trypsinized as described above. The resulting cells suspensions out of 6 wells of passage 2 cells were then pooled, pelleted by centrifugation and resuspended in 2.5 ml complete ES medium. Of this suspension 1 x 0.1 ml were transferred for DNA preparation into one well of a new 24-well plate containing 900 µl prewarmed, complete ES cell medium, 1x 0.5 ml together with 1.5 ml prewarmed, complete ES medium were added per well of a new 6-well plate (=passage 3) and 4x 0.5 ml were transferred to cryogenic vials. The cell suspensions for freezing were mixed with 2x freezing mix, frozen at –80°C and finally transferred to liquid nitrogen for long-term storage.

Passage 3 cells from one well of a 6-well plate were splitted as described above into 5 wells of a new 6-well plate resulting in passage 4. As soon as passage 4 was grown to confluency cells of these 5 wells were trypsinized, pooled and resuspended in 2 ml ES cell medium. 4x 0.5 ml cell suspension were then frozen as described above for passage 2 cells.
Cells frozen in cryogenic vials were thawed in a waterbath at 37°C then transferred to a 15 ml polystyrene tube (BD Falcon, Cat.No. 352095) containing 10 ml of prewarmed, complete ES cell medium, pelleted by centrifugation and resuspended in prewarmed, complete ES cell medium for seeding onto new culture dishes.

2.10.1.2 ES cell transfection and selection

Electroporation with the linearized targeting construct:

100 µg of the targeting vector were digested o/n at 37°C with 400 U ClaI (NEB) in a total digest volume of 200 µl. After having confirmed linearization on an agarose gel, the plasmid DNA was precipitated from the digestion reaction as described in paragraph 2.8.3.2. After the last 70% Ethanol washing step the DNA pellet was air-dried under sterile conditions and resuspended in sterile PBS to a final concentration of 30µg/100µl. ES cells were trypsinized and resuspended in sterile PBS to a final density of $1x10^8$ cells/ml. 1 ml ES cell suspension was mixed with 100 µl of above mentioned DNA solution (i.e. 30 µg DNA per $1x10^8$ ES cells) and transferred to an electroporation cuvette (4 mm gap, Biorad). Following an incubation of the cuvette on ice for 10 min cells were electroporated in a GenePulser II electroporator (Biorad) under the following conditions: 0.8 kV, 3 µFd, time constant: 0.08. After electroporation the cuvette was incubated for another 10 min on ice and subsequently the cells were added to 8 ml prewarmed complete ES cell medium. The resulting 9 ml cell suspension were seeded according to the following scheme onto a total of 20 gelatinized 10 cm culture dishes containing each 10 ml complete ES cell medium:

4x 1ml seeded on 4 x 10 cm dishes (= 1 ml aliquots)
4ml new medium added to the remaining 5ml cell suspension, then:
4x 1 ml seeded on 4 x 10 cm dishes (= 0.5 ml aliquots)
4ml new medium added to the remaining 5ml cell suspension, then:
4x 1 ml seeded on 4 x 10 cm dishes (=0.25 ml aliquots)
4 ml new medium added to the remaining 5 ml cell suspension, then:
8x 1 ml seeded on 8 x 10 cm dishes (=0.125 ml aliquots)

This seeding scheme served the purpose of having plates with the optimal density of clones independently of the transfection efficiency. Cells were incubated o/n at 37°C / 6 % CO2. The next morning the medium was exchanged by complete ES cell medium. Only 24 hrs after electroporation the selection with 300 µg/ml G418 was started. Regular medium changes were then performed every 2-3 days until the appearance of the first clones. 8 –12 days after transfection clones were picked into 96-well plates.

Further processing and expansion of picked ES cell clones:

ES cell clones initially picked in 96-well plates were grown in these plates until confluency. As described in paragraph 2.10.1.1, the cells were then on one hand frozen in these 96-well plates and on the other hand splitted to 24-well plates. ES cell clones in 24-well plates were grown until confluency and then used for the preparation of genomic DNA as described in paragraph 2.8.4.1. Positive ES cell clones were selectively thawed from the original 96-well plate and expanded over four passages as described in paragraph 2.10.1.1.

2.10.1.3 PCR based screening of ES cell clones

Materials:

- 10 mM PCR nucleotide mix (Roche Cat.No. 11 581 295 001)
- Taq DNA polymerase + corresponding 10 x PCR buffer (Pharmacia, Cat.No. 270799)
- Forward primer PSC1 (10 µM solution in molecular biology grade water)
- Reverse primer PSC2 (10 µM solution in molecular biology grade water)
- T3 thermocycler (Biometra)

ES cell clones were screened for integration of the targeting construct first by PCR in pools of five. Primers used for the PCR were designed to give a 2.5 kb product only if the targeting vector has integrated in the coronin-1 locus. Pools giving the expected PCR product were then split up and the positive clones within a pool were identified by PCR and confirmed by subsequent Southern blot analysis. The genomic DNA pool was made by mixing 1 µl genomic DNA of each of the five ES cell clones. PCR reactions were set up and run on a T3 thermocycler as follows:

1 µl	genomic DNA pool
2 µl	10x PCR buffer
0.4 µl	10mM PCR nucleotide mix
0.4 µl	10 µM forward primer PSC1
0.4 µl	10 µM reverse primer PSC2
0.2 µl	Taq polymerase (5U/µl stock)
15.6 µl	molecular biology grade water

PCR program:

Step 1	96°C, 5 min	(initial denaturation of DNA)
Step 2	95°C, 30 sec	(denaturation of DNA)
Step 3	51°C, 30 sec	(annealing of primers)
Step 4	72°C, 2 min	(elongation)
Return to step 2, 40 times		
Step 5	72°C, 10 min	(elongation of incomplete products)
Step 6	4°C,	(storage until further processing)

The PCR reactions were mixed with 4 µl 6x DNA loading buffer and 10 µl were loaded onto a 0.8 % agarose gel for the visualization of PCR products.

2.10.2 Blastocyst injection and generation of chimaeric animals

Identified and confirmed positive ES cell clones were expanded from passage 2 frozen stocks by Daniela Nebenius-Oosthuizen in the TMCF and used for injection into blastocysts derived from a cross of a C57Bl/6 female with a BDF-1 male. Injected blastocysts were then transferred into pseudo-pregnant NMRI foster mothers. The offspring was checked for coat colour chimaerism. Since the injected ES cell clones were of Sv129/Ola background they carried a dominant *agouti* allele that was lacking in the C57Bl/6 x BDF-1 blastocysts. Highly chimaeric animals were therefore identified by a high degree of *agouti* (brown) coat colour.
Only highly chimaeric animals were used for further crosses to C57Bl/6 females to check for germline transmission of the coronin-1 K.O. transgene by PCR.

2.10.3 Breeding of mice and backcrosses

Mice were kept under special pathogen free (SPF) conditions in the mouse facility of the Biozentrum of the University of Basel. C57Bl/6 mice were obtained from RCC (Füllinsdorf, Switzerland).
In order to bring the coronin-1 K.O. allele into the defined C57Bl/6 inbred background male mice heterozygous for the coronin-1 K.O. allele were crossed to C57Bl/6 females (RCC, Füllinsdorf, Switzerland). The offspring was genotyped by PCR and male, heterozygous animals were again crossed to C57Bl/6 females. This procedure is referred to as backcrossing and is currently going on. For the experiments presented in this thesis homozygous coronin-1 K.O. and wildtype littermates were used which originated from breedings of backcross 3 heterozygous male and female coronin-1 K.O. mice.

2.10.4 PCR based genotyping of coronin-1 deficient mice

Materials:

- Tail buffer: 100 mM Tris-HCl pH 8.5, 5 mM EDTA, 0.2 % SDS, 200 mM NaCl, 100 □g/ml Proteinase K
- 10 mM PCR nucleotide mix (Roche Cat.No. 11 581 295 001)
- Taq DNA polymerase + corresponding 10 x PCR buffer (Pharmacia, Cat.No. 270799)
- Forward primer WTCor1 (10 □M solution in molecular biology grade water)
- Reverse primer WTCor2 (8 □M solution in molecular biology grade water)
- Reverse primer KOCor1 (8 □M solution in molecular biology grade water)
- T3 thermocycler (Biometra)

For routine genotyping of coronin-1 K.O. mice a PCR was performed using three primers simultaneously. The forward primer WTCor1 and the reverse primer WTCor2 were used for the detection of the wildtype allele by amplifying a 392 bp product whereas the forward primer WTCor1 together with the reverse primer KOCor1 led to the amplification of a 478 bp product specific for the K.O. allele. PCR reactions were performed using diluted tail biopsie lysates as a template. To do so, tail biopsies (5-8 mm in size) were digested in 500 □l tail buffer o/n at 55°C on a thermoshaker (600 rpm, Eppendorf) and subsequently cleared by centrifugation (20'000 *x g*, 5 min, RT). For dilution 10 □l tail lysate were then added to 100 □l

molecular biology grade water. PCR reactions were set up and run on a T3 thermocycler as follows:

1 µl	diluted lysate
2 µl	10x PCR buffer
0.4 µl	10mM PCR nucleotide mix
0.4 µl	10 µM forward primer WTCor1
0.4 µl	8 µM reverse primer WTCor2
0.4 µl	8 µl reverse primer KOCor1
0.2 µl	Taq polymerase (5U/µl stock)
15.2 µl	molecular biology grade water

PCR program:

Step 1	96°C, 5 min	(initial denaturation of DNA)
Step 2	95°C, 30 sec	(denaturation of DNA)
Step 3	56°C, 30 sec	(annealing of primers)
Step 4	72°C, 45 sec	(elongation)
Return to step 2, 35 times		
Step 5	72°C, 10 min	(elongation of incomplete products)
Step 6	4°C,	(storage until further processing)

The PCR reactions were mixed with 4 µl 6x DNA loading buffer and 10 µl were loaded onto a 1.8 % agarose gel for the visualization of PCR products.

2.11 Flow cytometry based techniques

2.11.1 Staining of cells for flow cytometric (FACS) analysis

For FACS staining single cell suspensions were prepared as described in paragraph 2.9.4 and adjusted to contain 10 – 20 x 10^6 cell/ml. Antibodies used for staining were either directly labeled with fluorescent dyes or were coupled to biotin and detected in a second staining step with fluorescently labeled streptavidin. The appropriate dilution for the antibodies was determined before hand by titration. Commercial antibodies were mostly used at a dilution of 1:200 (see table 2.6 Antibodies). Staining, washing and analysis of the cells was performed in PBS / 2 % FCS (referred to as FACS buffer).

In 96-well V-bottom plates (Corning Costar) 200 µl of antibody solution in FACS buffer were provided per well and 50 µl single cell suspensions were added. Samples were then mixed by pipetting and incubated on ice in the dark for 30 min. As a first washing step after incubation 100 µl FACS buffer were added, cells were pelleted by centrifugation (300 *x g*, 4°C, 3 min) and the supernatant was discarded by rapidly inverting the plate and draining off excess liquid from the inverted plate with a paper towel. Cells were resuspended in the remaining drop of FACS buffer by vortexing the 96-well plate. Subsequently, the cells were washed additional two times with 200 µl FACS buffer. The cells were then either resuspended in 200 µl FACS buffer for analysis or in 200 µl 1:400 diluted fluorescently labeled streptavidin. Incubation with streptavidin was performed on ice in the dark for 15 min and cells were washed two times in 200 µl FACS buffer prior to analysis.

For intracellular coronin-1 staining, cells were stained for surface markers as described above, then resuspended in 100 µl PBS and fixed by adding 100 µl of 3 % paraformaldehyde in PBS. Incubation with paraformaldehyde was performed for 1 hr on ice and cells were subsequently washed two times with PBS / 2% (w/v) BSA / 0.2 % saponin for quenching of paraformaldehyde and permeabilization. AlexaFluor® 633 labeled anti-coronin-1 IgGs were diluted 1:250 in PBS / 2% (w/v) BSA / 0.2 % saponin. Cells were incubated with this solution (200 µl per well) for 30 min on ice in the dark, then washed two times in 200 µl PBS / 2% (w/v) BSA / 0.2 % saponin and resuspended in 200 µl FACS buffer for analysis.

For all stainings negative (no staining or second step reagent only), background stainings (AlexaFluor® 633 labeled anti-coronin-1 preimmune IgGs) and single stained compensation controls were always included. Flow cytometric analysis was carried out on a FACSCalibur (Becton Dickinson) and data were analyzed with the FlowJo software (version 4.3.2).

2.11.2 Collection and flow cytometric analysis of peripheral blood

Materials:

- Microvette® blood collection tubes (Sarstedt, Cat.No. 20.1288)
- Ketalar (50 mg Ketamine/ml, Parke-Davis)
- Rompun (23 mg/ml Xylazine/ml, Bayer Healthcare)
- Liquemine® (Heparin solution at 5'000 U/ml, Roche)
- ACK erythrocyte lysis buffer
- 0.9 % physiological NaCl solution (Bichsel, Interlaken, Switzerland)

Peripheral blood for flow cytometric analysis was collected in two ways: either by bleeding of mice via the tail vein which keeps the animals alive (referred to as tail blood, 200 – 300 µl collection volume, for small scale analysis) or by bleeding out anaesthesized mice to collect large amounts of peripheral blood for the preparation of peripheral blood lymphocytes (PBLs).

Tail blood was collected in blood collection tubes after cutting the tail vein with a clean scalpell. The collected volume of tail blood was then determined with a Gilson P200 (yellow pipette tip). After addition of 200 µl 0.9 % physiological NaCl solution, samples were mixed by pipetting and analyzed on a fully-automated ADVIA 120 hematology system (Bayer) at the Hämatologielabor, Kantonspital Basel. Blood cell counts were then corrected taken the initial tail blood sample volume and dilution factors into account.

For the preparation of PBLs mice were anaethesized by peritoneal injection of 200 µl of the following mix: 0.5 ml Ketalar / 0.25 ml Rompun / 2 ml 0.9 % physiological NaCl solution. Peripheral blood was collected through the retro-orbital vene into 1.5 ml Eppendorf containing 30 µl liquemine. In order to open the retro-orbital vene one eye of anaesthesized mice was torn out with a forceps. The collected volume of peripheral blood (usually between 500 - 800 µl) was determined with a Gilson P1000 (blue pipette tip) pipette and then brought to a total volume of 10 ml by adding PBS. Cells were pelleted by centrifugation (300 *x g*, 7 min, RT) and resuspended in 10 ml ACK erythrocyte lysis buffer. After incubation for 2 min at RT with occasional agitation (inverting the tubes), 20 ml PBS / 2 % FCS were added and cells were collected by centrifugation (300 *x g*, 5 min, RT). The resulting pellet was resuspended in DMEM / 10 % FCS / 2 mM glutamine and total cell counts were determined. PBLs prepared in this way were analysed by flow cytometry after staining as described in the previous paragraph. Lymphocyte specific cell counts per ml of blood were calculated under consideration of the sample volume by referring the percentage of a particular lymphocyte subset (as determined by flow cytometry) to the total cell counts.

2.11.3 Analysis of apoptotic cells with Annexin V

Materials:

- Recombinant human Annexin V coupled to allophycocyanin (AV-APC, BD Pharmingen, Cat.No. 550 474)
- 10x Annexin V binding buffer: 0.1 M Hepes (pH 7.4), 1.4 M NaCl, 25 mM $CaCl_2$ (always prepared freshly)
- 2 µg/ml propidium iodide (Sigma) in destilled water

One hundred thousand ($1x10^5$) cells per well of a 96-well V-bottom plate were stained for leukocyte surface markers as described in paragraph 2.11.1. Following antibody incubation cells were washed two times with 200 µl ice-cold PBS and one time with 200 µl 1x Annexin V-binding buffer (centrifugation steps: 300 *x g*, 3 min, 4°C). The cells were then resupended by gentle pipetting in 100 µl Annexin V-binding buffer containing propidium iodide (diluted 1:30'000 from above mentioned stock). 3 µl AV-APC was added per well and the cells were incubated 15 min at RT in the dark after gentle mixing of the suspension by pipetting. Cells were then pelleted by centrifugation (300 *x g*, 3 min, 4°C) and resuspended in 200 µl 1x Annexin V-binding buffer. Analysis was performed within one hour after staining on a BD FACSCalibur flow cytometer. Whereas specific binding of Annexin V identified apoptotic cells, cells positive for propidium iodide are considered to be necrotic.

2.11.4 Generation and analysis of mixed bone marrow chimaeras

Donor bone marrow cells were isolated from either Ly5.2 positive homozygous coronin-1 knock-out mice or from Ly5.1 positive C57Bl/6 mice. Bone marrow cells were harvested by flushing isolated femurs and tibias with a syringe and needle using serum-free IMDM. Six weeks old recipient C57Bl/6 mice (Ly5.2 positive) were irradiated with 950 rad and received then 2 x 10^6 bone marrow cells comprising of a 1:1 mixture of $Ly5.2^+$ coronin-$1^{-/-}$ and $Ly5.1^+$ C57Bl/6 cells. As controls irradiated recipients also received 2 x 10^6 of either $Ly5.2^+$ coronin-$1^{-/-}$ or $Ly5.1^+$ C57Bl/6 cells alone. Composition and origin of lymphoid cells in chimaeric mice was analyzed six weeks later by flow cytometry employing antibody stainings specifically detecting the Ly5.1 or Ly5.2 markers.

2.11.5 T-lymphocyte homing assay

In order to assess the capacity of coronin-1 deficient T-cells to survive in the periphery and to home to lymph nodes of wildtype mice a T-lymphocyte homing assay was performed in collaboration with Daniela Finke at the University of Basel. To that end, single cell suspensions of spleen were prepared in PBS as described in paragraph 2.9.4 from either 6 weeks old coronin-1 deficient mice or as a control for the homing of wildtype T-cells from 6 weeks old C57Bl/6 mice transgenic for GFP under the control of the ubiquitin promotor (kind gift of D. Finke, University of Basel). After having determined the percentage of CD4 and CD8 positive cells by flow cytometry, the cell suspensions were adjusted with PBS to contain an equivalent amount of CD4 and CD8 positive cells ($8x10^6$ CD4 and CD8 positive T-cells per 200 µl PBS). Six weeks old recipient C57Bl/6 wildtype mice then received via tail vein

injection 200 µl cell suspension. Four or twenty hours post injection the mice were sacrified and peripheral blood lymphocytes (PBLs) as well as single cell suspensions of spleen, inguinal and mesenteric lymphnodes were prepared. Flow cytometry using fluorophore-labeled monoclonal antibodies directed against CD4 and CD8 allowed to determine the percentage of GFP positive T-cells (this means injected T-cells) within a given cell suspension.

2.11.6 Assessing phagocytosis by flow cytometry

To study Fc-receptor mediated phagocytosis 10 µl of a 2% aqueous suspension of yellow-green fluorescent polystyrene beads (Molecular Probes FluoSpheres beads) were washed twice with PBS and then incubated for 1 hour at 37°C on a shaking thermoblock in 1 ml PBS containing 50 µg/ml rabbit IgG (Cappel/ICN). After two additional washing steps in PBS, the IgG-opsonized beads were resupended in 3 ml DMEM / 10% FCS / 2mM glutamine.
For complement receptor-mediated uptake *Lactobacillus casei* expressing GFP was treated at an OD_{600} of 0.2 with 1:10 diluted fresh or heat-inactivated (56°C, 30 min) human serum in PBS for 30 min at 37°C on a rotator. Serum treated bacilli were then washed twice in an excess volume of PBS and resuspended in DMEM / 10% FCS / 2mM glutamine at an OD_{600} of 2. Bone marrow derived macrophages were seeded to 80 % confluency in 24-well cell culture plates (BD Falcon) and shifted to 4°C followed by the addition of 250 µl per well of the above mentioned suspensions of fluorescent beads or serum treated Lactobacilli. To allow phagocytosis, cells were then incubated for 30 min at either 37°C or 4°C (cold control) and subsequently washed five times with 1 ml PBS / 5% FCS on ice. Cells were harvested by scraping and subjected to flow cytometry (FACSCalibur, Becton Dickinson) to determine uptake of fluorescent cargo in the FL-1 channel.
Only living cells as assessed by the forward- and side-scatter profile were considered for the analysis. Rate of uptake was measured as the increase in fluorescence as expressed by the median fluorescence intensity.

2.12 Microscopical techniques

2.12.1 Staining of cells for indirect immunofluorescence

Materials:

- Teflon-coated 10-well slides (Polyscience Inc., Cat.No. 18357)
- 20 x 55 mm cover slips (Menzel)
- Staining buffer: PBS / 2 % BSA (w/v) / 0.1 % (w/v) saponin
- Washing buffer: PBS / 0.1 % saponin (w/v)
- Q-tips (cotton swaps)
- Wet chamber (assembled from a slide archive box and wet paper towels)
- Slide jars (Glaswerk, Germany)
- FluoroGard Antifade Reagent (Biorad)
- Nail polish
- 3 % paraformaldehyde in PBS

Microscopes and associated software:

- Confocal laser scanning microscope: Axiovert 200M with the laser scanning module LSM 510 Meta (Zeiss), LSM 510 software (version 3.2 SP2)
- Fluorescence microscope: Axiovert 100 TV (Zeiss), OpenLab software (version 2)

For the detection of intracellular membrane components and cytosolic proteins, cells were stained with appropriate antibodies under permeabilizing conditions employing the mild detergent saponin. Cells were either grown o/n on teflon-coated 10-well slides or adhered to these slides to an approximate density of 10'000 cells/well. After aspiration of the medium, cells were briefly washed by transferring the slide into a slide jar containing PBS. The cells were then fixed in a slide jar containing 3 % paraformaldehyde in PBS for 10 min at 37°C. For the complete removal and quenching of remaining paraformaldehyde after fixation cells were washed 1x 5 min PBS / 1x 5 min PBS + 5 mM glycine / 1x 5 min PBS.

Permeabilization and blocking was performed by incubating the slides first for 15 min in washing buffer and then in staining buffer for 15 min at RT. Slides were placed in a wet chamber, liquid around the wells was removed with Q-tips and 30 µl of primary antibody solution or undiluted hybridoma supernatant was added to the wells. Primary antibodies were diluted in staining buffer. Incubation with primary antibodies was carried out at RT for 30 – 60

min depending on the affinity of the antibody. Following incubation with the primary antibody slides were washed in slide jars at RT: 2x 5 min washing buffer / 1x 10 min staining buffer. Slides were transferred back into the wet chamber, the space around the wells was dried with Q-tips and the secondary antibodies or phalloidin coupled to appropriate fluorescent dyes were added to the wells. Secondary antibodies and/or phalloidin were diluted in staining buffer. Incubation with secondary antibodies and/or phalloidin was performed for 30 min at RT with 30 µl antibody solution per well. Subsequently slides were washed 1x 5 min staining buffer / 2x 5 min washing buffer/ 3x 5 min PBS. For mounting, slides were briefly dipped in destilled water, then dried with Q-tips around each well and received a drop of Fluorogard Antifade reagent on each well. A cover slip was placed on top, excess liquid was removed by gently pressing the slides between two paper towels and finally slides were sealed with nail polish. If not analyzed immediately slides were stored at 4°C in the dark to avoid bleaching of the fluorophores.

2.12.2 Adherence of thymocytes on poly-L-lysine and antibody coated glass slides

Materials:

- Poly-L-lysine solution (stock obtained from Sigma, Cat.No. P8920, for use diluted 1:10 in destilled water)
- Anti-mouse-CD3 (clone 145-2C11, BD Pharmingen, Cat.No. 553057) and anti-CD28 (clone 37.51, BD Pharmingen, Cat.No. 553294) antibody
- Teflon-coated 10-well slides (Polyscience Inc., Cat.No. 18357)

Teflon-coated 10-well slides were coated with poly-L-lysine for the adherence of cell suspensions by adding 50 µl poly-L-lysine solution to each well. After incubation for 5 min at RT, liquid was aspirated and the slides were dried at 60°C for 1 hr. Thymocyte cell suspensions were prepared in PBS as described in paragraph 2.9.4 and $4x10^5$ thymocyte in 50 µl PBS were added per well of poly-L-lysine coated slides. Slides were incubated on ice for 20 min, then dipped in ice-cold PBS to remove non-adherent cells and fixed in 3 % paraformaldehyde in PBS for 10 min at 37°C.

Antibody coated slides for the adherence of thymocytes were prepared as follows. Anti-mouse-CD3 and –CD28 antibodies were diluted in PBS to a final concentration of 100 µg/ml. Each well of teflon-coated 10-well slides received 10 µl of this antibody mix and slides were subsequently incubated o/n at 37°C in a cell culture incubator. The next day, slides were washed 3 times well by well and blocked with DMEM / 10 % FCS / 2mM glutamine for 30 min

at 37°C. Thymocyte cell suspensions were prepared in DMEM / 10 % FCS / 2mM glutamine and $4x10^5$ thymocyte were incubated on antibody coated slides for 30 min in a cell culture incubator at 37°C / 5% CO_2. Following adherence slides were dipped in PBS to remove non-adherent cells and fixed for staining with 3 % paraformaldehyde in PBS for 10 min at 37°C.

2.12.3 Activation of bone marrow derived macrophages (BMM)

Materials:

- Teflon-coated 10-well slides (Polyscience Inc., Cat.No. 18357)
- Culture medium: DMEM / 10 % FCS / 2 mM glutamine
- Phorbol-12-myristate-13-acetate (PMA, Sigma, 1 mM stock solution in DMSO)
- Recombinant mouse Interferon-γ (BD Pharmingen, Cat.No. 554 587, 9.25 U/µl)

$1x10^5$ day 6 bone marrow derived macrophages (BMM) were allowed to adhere per well of teflon-coated 10-well slides in DMEM / 10 % FCS / 2 mM glutamine for 2 hrs at 37°C / 5 % CO_2. After adherence the culture medium was replaced by normal culture medium (for stimulation with PMA) or by culture medium containing 1000U/ml interferon-γ. BMM were incubated o/n at 37°C / 5 % CO_2. The next day, medium was replaced by culture medium containing either 100nM PMA or 1000 U/ml interferon-γ and the cells were incubated at 37°C / 5 % CO_2 for additional 4 hrs. Finally, the slides were dipped in PBS and fixed in 3 % paraformaldehyde in PBS (37°C, 10 min) for subsequent staining.

2.12.4 Immunohistological analysis of cryosections (courtesy of C. Blum and H.R. Rodewald, University of Ulm, Germany)

Organs (spleen, thymus and lymph nodes) were embedded in OCT medium (Sakura Finetek), snap-frozen and 5-µm sections were cut with a cryostat. Sections were air-dried, acetone-fixed for 8 min and stored at –70°C. Sections were then rehydrated and blocked in PBS / 2% (w/v) BSA with 0.1% NaN_3. and 220 µg/ml mouse IgG (Jackson ImmunoResearch Laboratories,). Antibodies, diluted in PBS / 2% (w/v) BSA, were added directly onto the sections and incubated for 60 min at room temperature in a wet chamber. Antibodies used were: Allophycocyanin (APC)-labeled anti-mouse CD4 (rat IgG2a, clone RM4-5) (Caltag Laboratories), fluorescein isothiocyanate (FITC)-labeled anti-mouse CD8 (rat IgG2a, clone 53-6.7) (BD Biosciences), fluorescein isothiocyanate (FITC)-labeled anti-mouse B220 / CD45R (rat IgG2a, clone RA3-6B2) (BD Biosciences), R-Phycoerythrin (PE)-labeled anti-

mouse Thy1.2 / CD90.2 (mouse IgG2b, clone 5a-8) (Caltag Laboratories) and R-Phycoerythrin (PE)-labeled anti-mouse I-A^b (mouse IgG2a, clone AF6-120.1) (BD Biosciences). Sections were counterstained with DAPI (Serva) for 5 min. After washing the sections were mounted in Fluoromount (Southern Biotechnology Associates). Images were taken on a Zeiss Axioskop with ORCA ER camera (Hamamatsu) and images were processed by using OPENLAB software (Improvision, Coventry, U.K.).

2.13 Biochemical methods

2.13.1 Preparation of total cell lysates from murine tissue

Materials:

- 1x lysis buffer
- Protease inhibitors (1x CLAAP, 1x PMSF)

Single cell suspensions were prepared as described in paragraph 2.9.4. One million ($1x10^6$) cells were transferred to a 1.5 ml Eppendorf tube and washed three times in 1 ml ice-cold PBS (centrifugation steps: 300 *x g*, 2 min, 4°C). After centrifugation the supernatant was removed and the pellet was resuspended with several pipetting strokes in 10 pellet volumes of 1x lysis buffer supplemented with protease inhibitors. The lysate was subsequently cleared by centrifugation at 20'000 *x g*, 4°C for 10 min and the supernatant was transferred to a new 1.5ml Eppendorf tube. The lysate was either further processed immediately or stored after quick-freezing in liquid nitrogen at –80°C until use.

2.13.2 Determination of protein concentrations

Materials:

- Bradford reagent (Biorad)
- BCA reagent (Pierce)
- Standard protein solution at 1 mg/ml dissolved in dH_2O (Biorad, Cat No. 500-0005)
- 96-well flat bottom plates (Corning Costar)
- Microplate reader (Bucher) and corresponding software (SoftMax Pro, version 1.2.0)

Protein concentrations were determined using the Bradford method (Bradford, 1976) or alternatively the BCA method (Smith et al., 1985) if the protein solution of interest contained detergents such as Triton X-100 or NP40.
Measurements were performed in 96-well flat bottom plates supplied with different volumes of the sample (1 – 10 µl) and the standard protein solution (0, 1, 2, 3, 5, 7, 10 µl). 200 µl of either 1x Bradford reagent or BCA solution (prepared according to the manufacturer's protocol) were then mixed with the samples by pipetting. After incubation for 5 min at RT in case of the Bardford assay or 30 min at 37°C for the BCA assay samples were measured on a microplate reader determining either the OD_{595} (Bradford) or the OD_{562} (BCA). Protein concentrations were calculated from the resulting OD values using the standard curve and taking sample volume and dilution factors into account.

2.13.3 SDS-PAGE using the Biorad Protean II minigel system

Materials:

- Protean II minigel system (Biorad)
- 5 x reducing sample buffer
- 10 x SDS-PAGE electrophoresis running buffer
- 30 % (w/v) acrylamide / 0.8 % (w/v) bisacrylamide in destilled water (filtered through 0.2 µm filter and stored at 4°C)
- 2 M Tris-HCl, pH 8.8
- 0.5 M Tris-HCl, pH 6.8
- 10 % ammonium persulfate (APS) dissolved in destilled water (stored at 4°C)
- TEMED
- Biorad broad range SDS-PAGE standard

Using the casting station supplied with the Protean II minigel system two minigels (7 x 10 cm in size, 0.75 mm thick) were prepared simultaneously using gel solutions as indicated in table 2. First the running gel was prepared and overlaid with isopropanol until complete polymerization. After complete removal of the isopropanol layer the stacking gel was poured on top of the running gel and an appropriate comb was inserted avoiding trapping of air bubbles. Fully polymerized gels were mounted into the Protean II minigel running chamber, SDS-PAGE electrophoresis running buffer was added and the comb was gently removed to free the sample slots which were subsequently flushed with buffer. Protein samples of interest were mixed with 5 x reducing sample buffer, heated to 95°C for 5 min and loaded onto the gel after brief centrifugation (Eppendorf 5415D table top centrifuge, 13'000 rpm, 1

min, RT). Empty slots were loaded with an equivalent amount of 1 x reducing sample buffer. Gels were run at constant voltage (60 V for the stacking gel, 80 – 100 V for the running gel).

	Running gel			Stacking gel
	12.5%	10 %	7.5%	4%
30% acrylamide/0.8% bisacrylamide	4.2	3.3	2.5	0.65
2 M Tris-HCl pH 8.8	2	2	2	-
0.5 M Tris-HCl pH 6.8	-	-	-	1.25
20% SDS	0.05	0.05	0.05	0.025
Destilled water	3.7	4.6	5.4	3.05
APS	0.05	0.05	0.05	0.025
TEMED	0.01	0.01	0.01	0.005

Table 7 *Gel components required for the preparation of two minigels. Volumes in ml.*

2.13.4 Coomassie staining of polyacrylamide gels

Materials:

- Staining solution (0.25 % (w/v) Coomassie Brilliant Blue R-250 in fixation solution)
- Fixation solution (10 % acetic acid, 45 % methanol in destilled H_2O)

After SDS-PAGE, minigels were incubated in staining solution for 1 hr at RT under slight agitation. Destaining and fixation was performed by incubation of stained gels in fixation solution on a rocking platform. Fixation solution was exchanged several times. For documentation fixed gels were transferred on a filter paper and dried under vacuum at 60°C o/n.

2.13.5 Western blot analysis

2.13.5.1 Transfer of proteins after SDS-PAGE on nitrocellulose membranes

Materials:

- Semi-dry transfer cell (Biorad)
- Semi-dry transfer buffer
- Ponceau S solution (0.1 % in 5 % acetic acid, Sigma)
- Hybond C super nitrocellulose membrane (Amersham Bioscience)

- Thin and thick filter paper, 7 x 10 cm in size (Whatman, type: 3MM Chr and Schleicher&Schuell, type: GB002)

After SDS-PAGE, the gel, the membrane and the filter paper were soaked in semi-dry transfer buffer. Using this components a sandwich was build up on the lower electrode (=anode) of the semi-dry transfer cell in the following order: 1x thick filter paper, 1x thin filter paper, nitrocellulose membrane, gel, 1x thin filter paper, 1x thick filter paper. Prior to fitting the upper electrode (=cathode) air bubbles between the layers were removed by tightly rolling a glass pipette over the sandwich. Transfer was performed for 36 min at 2.5 mA/cm^3 = 0.17 A per minigel and appropriate voltage (usually between 12 and 25 V). To check the effciency of the transfer the nitrocellulose membrane was incubated in Ponceau S solution for 2 min at RT and subsequently rinsed with destilled water to visualize the protein bands. The positions of the molecular weight marker bands were marked with a pen and the stained membrane was digitalized as a reference using a desktop scanner (Hewlett-Packard, scanjet 8290).

2.13.5.2 Immunodetection

Prior to immunodetection Ponceau S stained nitrocelluose membranes were blocked by incubation for at least 1 hr at RT or at 4°C o/n in 5% low fat milk powder in PBST (PBST/milk) under agitation. The primary antibody was appropriately diluted in PBST/milk and added as a drop (2 ml per 7 x 10 cm membrane) on a layer of Parafilm. Subsequently, the blocked membrane was inverted on the drop of antibody solution avoiding the formation of air bubbles and incubated for 30 – 60 min (depending on the affinity of the antibody) at RT. After incubation with the primary antibody the membrane was washed extensively with PBST/milk (6x 5 min, 100 ml per washing step) under agitation. Incubation with the secondary HRP-labeled antibody (diluted 1:20'000 in PBST/milk) was performed for 30 min at RT under agitation with 10 ml antibody solution per 7 x 10 cm membrane. Finally, the membrane was washed 4 x 5 min with PBST/milk, 2 x 5 min with PBST and incubated with ECL solution for 1 min at RT inverted on a layer of Parafilm. For exposure to ECL film the membrane was drained from excess liquid with a filter paper and mounted into an autoradiography cassette between transparent plastic sheets.

2.13.6 Preparation of an IgG fraction from rabbit serum

Materials:

- 1 M Tris-HCl pH 8.0
- 100 mM Tris-HCl pH 8.0
- 10 mM Tris-HCl pH 8.0
- 100 mM glycine pH 3.0
- HiTrap® Protein A HP column (Amersham Cat.No. 17-0402-01)
- Slide-A-Lyzer 10'000 MWCO unit (Pierce, Cat.No. 66 425)
- Äkta P-920 FPLC system (Amersham)

IgGs of the rabbit anti-coronin-1 serum No. 1002 were affinity purified using a Protein A column connected to an Äkta FPLC system. All solutions including the diluted starting material were filtered through 0.2 µm filters to avoid clogging of the system. The whole purification procedure was performed in a 4°C coldroom. As starting material, 2 ml serum (No. 1002, third bleed or preimmune) were diluted in a 50 ml polypropylene tube (BD Falcon) by adding 18 ml 100mM Tris-HCl pH 8.0. Prior to loading on the column the FPLC system as well as the column were washed with 30 ml 100 mM Tris-HCl pH 8.0 (0.5 ml/min). The diluted serum was then run over the column three times at 0.3 ml/min. Subsequently, the column was first washed with 30 ml 100 mM Tris-HCl pH8.0 and then with 30 ml 10 mM Tris-HCl pH8.0 (0.5 ml/min). Elution of the IgGs from the column was performed at 0.2 ml/min with 100 mM glycine pH 3.0. 500 µl fractions were collected into 1.5 ml Eppendorf tubes containing 100 µl 1 M Tris-HCl pH 8.0 for the rapid neutralization of the fraction. Fractions with the highest UV absorption were pooled (pool volume: 2 ml) and dialyzed o/n at 4°C against 4 liters of PBS using a Slide-A-Lyzer 10'000 MWCO unit.

2.13.7 AlexaFluor® 633 labelling of rabbit IgGs

Materials:

- IgG fraction of serum 1002 (third bleed or preimmune serum) in PBS at a concentration of 2 mg/ml
- AlexaFluor® 633 Protein labeling kit (Molecular Probes, Cat.No. A-20170) which contains:
  - AlexaFluor® 633 reactive dye in a vial with magnetic stirring bar
  - 1 M sodium bicarbonate solution

- Purification resin
- 10x elution buffer
- purification columns

Using the AlexaFluor® 633 protein labeling kit IgGs of the rabbit anti-coronin-1 serum No.1002 were labeled with the fluorescent dye AlexaFluor® 633 for intracellular FACS staining of coronin-1. 0.5 ml IgG fraction (concentration 2 mg/ml) were mixed with 50 µl 1 M sodium bicarbonate by briefly vortexing the tube and transferred to a vial containing the reactive AlexaFluor® 633 dye and a magnetic stirring bar. The sample was then incubated on a magnetic stirrer for 1 hr at RT in the dark. During incubation the gel filtration column was prepared by packing the provided purification resin into the supplied purification column. The sample was then loaded onto the column, allowed to enter the resin and 1x elution buffer (= PBS / 2 mM NaN_3) was added until elution was completed. While the sample was running over the column two blue coloured bands formed: a faster running one which represented the labeled IgGs and a slower running one which consisted of the non-coupled dye. The first band was collected into 1.5 ml Eppendorf tubes. Coupling efficiency and concentration of the AlexaFluor® 633 labeled IgGs was determined as described in the protocol of the AlexaFluor® 633 protein labeling kit. Finally, the concentration of the AlexaFluor® 633 labeled IgGs was adjusted to 1 mg/ml with 1x elution buffer and the samples were stored at 4°C until use.

3 RESULTS

3.1 Analysis of coronin expression

Coronin-1 has first been described in the slime mold *Dictyostelium discoideum* as an actin binding protein localised to cell surface projections. Subsequently, coronin-like proteins have been found in many species, from yeast to mammals. In mammalian organisms, the coronin family of proteins consists of seven members (coronin 1 – 7) for which the degree of homology ranges beyond 60% amino acid identity (reviewed in de Hostos, 1999, Rybakin and Clemen, 2005). Expression of individual members of the coronin protein family has been analysed by several authors but comprehensive expression data for all family members are so far not available. We therefore analysed the expression of coronin 1 - 7 in murine tissues by RT-PCR. Furthermore, coronin-1 expression in cells of the hematopoietic lineage was analysed by flow cytometry. With respect to the generation and phenotypic analysis of coronin-1 K.O. mice these expression data will be valuable in understanding a defect in different cell types and will allow to assess to which extent a phenotype caused by coronin-1 deficiency could be masked by the expression of and potential functional redundancy between members of the coronin protein family.

3.1.1 Analysis of the expression of coronin-1 - 7 in murine tissues and cell lines by RT-PCR

Expression of the seven members of the coronin family of proteins in the mouse was analysed by RT-PCR. For this purpose, specific primers have been either taken from published data (for coronin 1 – 3: Okumura et al., 1998) or newly designed. Total RNA was isolated from murine tissues or mouse cell lines, reversely transcribed and analysed for the presence of coronin 1 - 7 transcripts by PCR. In order to allow a semi-quantitative determination of coronin expression RT-PCR analysis of beta-actin or glyceraldehyde 3-phosphate dehydrogenase (GAPDH) transcripts was performed.

RT-PCR analysis of coronin expression in bone marrow, thymus and spleen revealed that all members of the coronin family of proteins except coronin-4 are expressed (Fig.9). With respect to the signal intensity obtained for beta-actin it can be concluded that in hemato- and lymphopoietic tissues coronin-1, -2, -3 and -7 are prominently expressed, whereas coronin-5 and -6 are only present at low levels. For the analysis of the expression of coronin 1 - 7 in neural tissues, reversely transcribed total RNA from the cerebellum and the diencephalon

was used. Consistent with the restricted expression of coronin-1 in leukocytes only weak expression in the brain was found (Fig.10). Of the other members of the coronin family coronin-2 and -5 were found to be abundantly and coronin-3 and -7 weakly present in the brain. Expression of coronin-4 and -6 could not be detected.

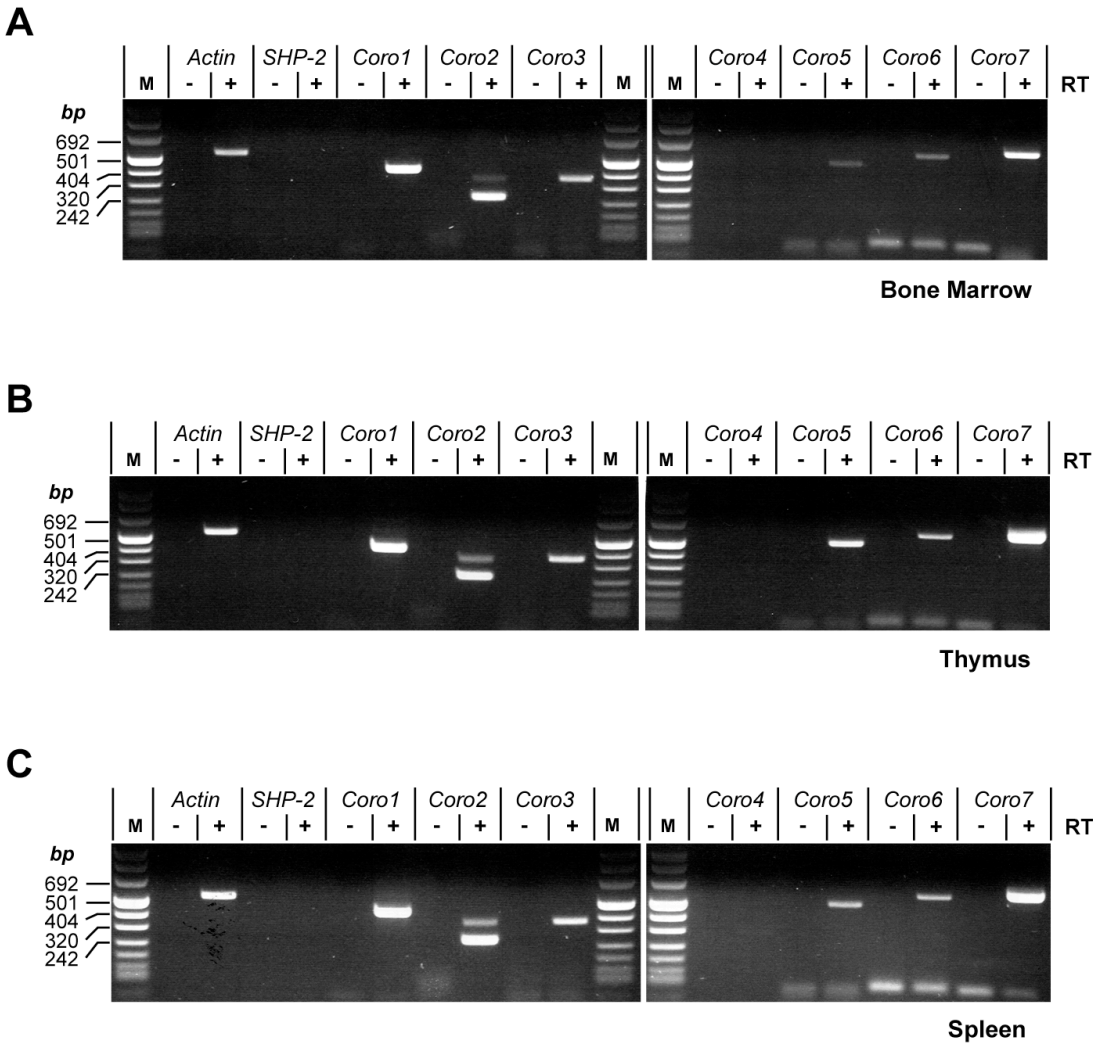

Fig. 9 Expression of coronin-1 - 7 in bone marrow, thymus and spleen as determined by RT-PCR. Total RNA was extracted from the indicated tissues, reversely transcribed and analysed for the presence of coronin-1 - 7 transcripts by PCR. To control for background amplification from genomic DNA, RNA extracts not treated with reverse transcriptase (- RT) were also subjected to PCR. As an internal standard, PCR reactions were performed to detect the transcripts of ubiquitously expressed beta-actin and protein tyrosine phosphatase SHP-2. (**A**) Bone Marrow. (**B**) Thymus. (**C**) Spleen. RT: reverse transcriptase.

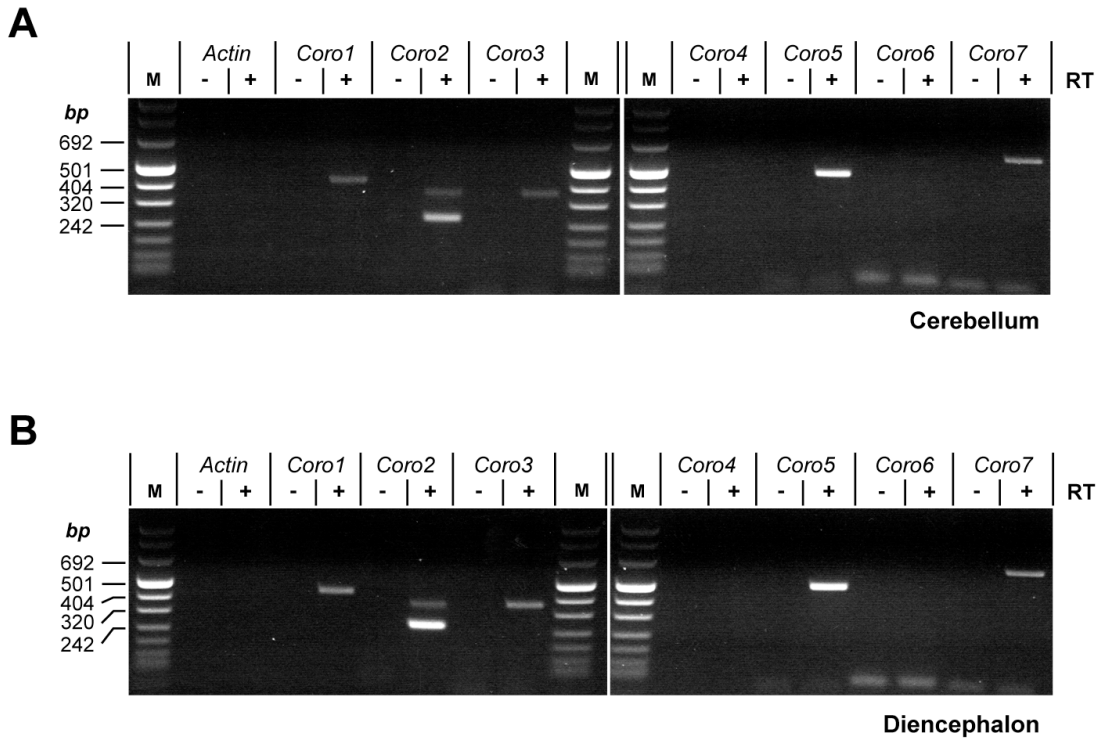

Fig. 10 Expression of coronin-1 - 7 in brain tissue as determined by RT-PCR. Total RNA was extracted from the indicated brain tissues, reversely transcribed and analysed for the presence of coronin-1 - 7 transcripts by PCR. To control for background amplification from genomic DNA, RNA extracts not treated with reverse transcriptase (- RT) were also subjected to PCR. As an internal standard, PCR reactions were performed to detect the transcript of ubiquitously expressed beta-actin. (**A**) Cerebellum. (**B**) Diencephalon. RT: reverse transcriptase.

In heart, skeletal muscle, kidney and liver (Fig.11) coronin-1 was found to be weakly expressed which is probably due to the presence of blood cells in these tissues. The most abundantly expressed members of the coronin family in these tissues were coronin-2 and -7. Coronin-3 and -5 expression was detected but with tissue specific variations in its intensity. Coronin-4 was absent as in all other tissues tested. Interestingly, coronin-6 showed a clearly tissue-specific expression by being present in heart and muscle tissue but absent in kidney and liver. To summarise, our results revealed that of the coronin family of proteins coronin-2, -3 and -7 are cleary ubiquitously expressed in murine tissue. This is in accordance with published data (for review see de Hostos, 1999, Rybakin and Clemen, 2005 and references therein). Also Coronin-5 that was thus far described to be restricted in its expression to nervous tissue (Nakamura et al., 1999) could be identified as being ubiquitously present. Coronin-1, -4 and -6 can be considered as coronins with tissue-specific expression. It is noteworthy that for coronin-4 and -6 any description of the gene product is thus far lacking. The expression data for coronin-4 provided by Okumura et al., 1998 are not reliable since our analysis of the published primer sequences revealed no sequence specificity for coronin-

4. Coronin-6 has been only identified during a genome annotation project leaving the question open whether a functional protein is expressed from this locus.

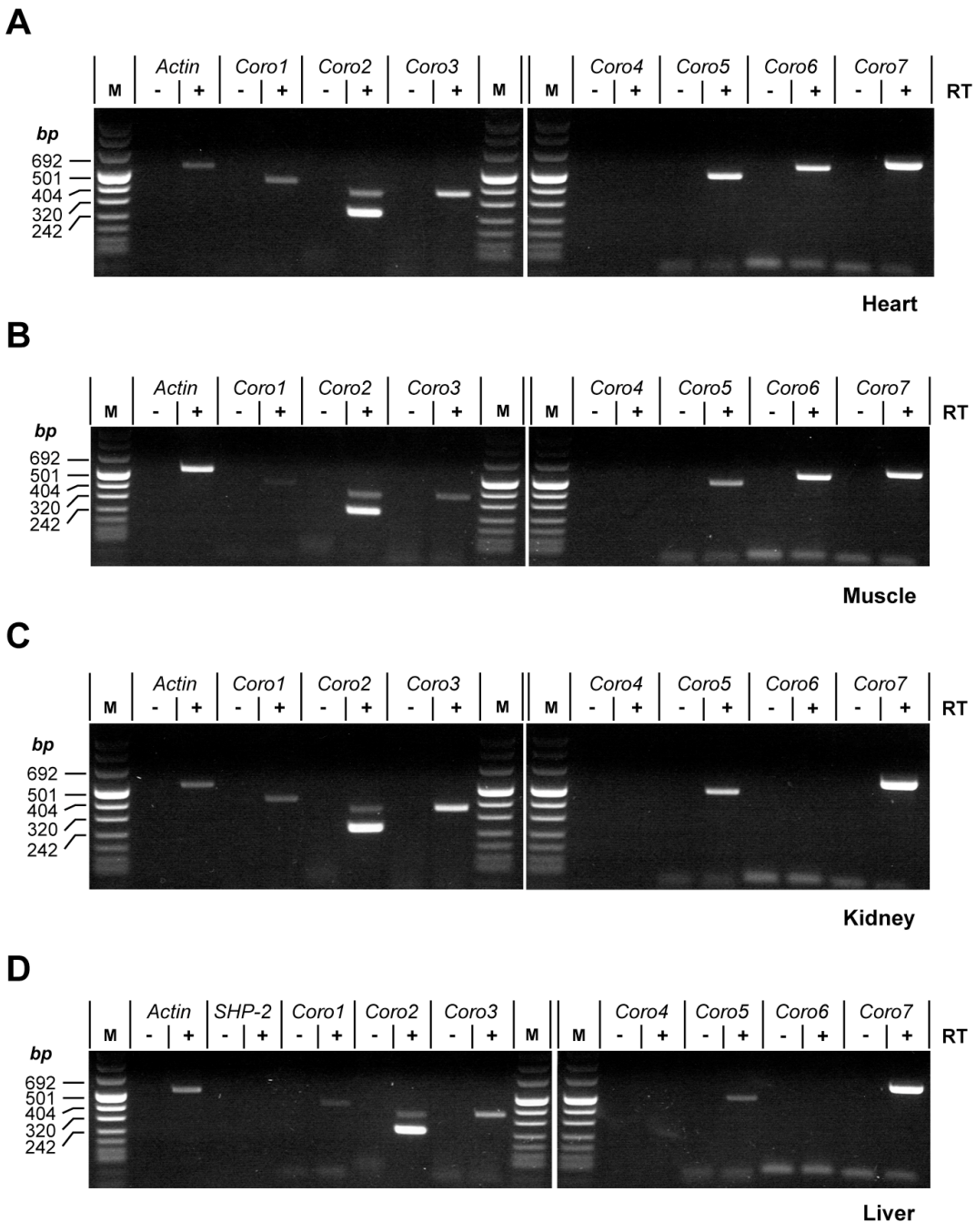

Fig. 11 Expression of coronin-1 - 7 in heart, skeletal muscle, kidney and liver tissue as determined by RT-PCR. Total RNA was extracted from the indicated tissues, reversely transcribed and analysed for the presence of coronin-1 - 7 transcripts by PCR. To control for background amplification from genomic DNA, RNA extracts not treated with reverse transcriptase (- RT) were also subjected to PCR. As an internal standard, PCR reactions were performed to detect the transcripts of ubiquitously expressed beta-actin and protein tyrosine phosphatase SHP-2 (only used for liver). (**A**) Heart, (**B**) Muscle, (**C**) Kidney and (**D**) Liver. RT: reverse transcriptase.

Generation of antibodies directed against the members of the coronin family of proteins is currently under progress. These antibodies will then allow to analyse coronin expression in murine tissues at the level of the protein.

Currently available functional and biochemical data for coronin-1 were mainly obtained from studies using murine primary cells and cell lines. In order to gain insight into the expression of the seven coronin protein family members and therefore potential functional reduncancy in murine primary cells and cell lines, coronin expression was analysed by RT-PCR in bone marrow derived macrophages (BMM) and in the two murine macrophage-like cell lines J774 and RAW 264.7. As a respresentative for a non-leukocytic cell type, the murine fibroblast cell line NIH3T3 was included in this analysis. All coronin family members except coronin-5 were found to be expressed in murine macrophages (Fig.12 B-D). In NIH3T3 only expression of coronin-2, -3 and -7 was detected (Fig.12 A). For the cell lines tested it can therefore be concluded that coronin-1, together with coronin-4 and -6, is predominantly expressed in leukocytes whereas coronin-2, -3 and -7 are ubiquitously present. Coronin-5 was absent from all the cell types tested. In summary, the RT-PCR based analysis of the expression of members of the coronin family of proteins confirmed the leukocyte-specific expression of coronin-1. However, having established the presence of other coronin family members in leukocytes a potential functional redundancy between the coronin famliy members should be taken into account when analysing the phenotype of coronin-1 deficient leukocytes. In order to gain insight into the expression of coronin-1 in distinct subset of cells originating from the hematopoietic lineage, flow cytometric analysis was employed as described in the following.

3.1.2 Analysis of coronin-1 expression in leukocytes by flow cytometry

Coronin-1 expression was shown to be restricted to hemato- and lymphopoietic tissue (Suzuki et al., 1995, Okumura et al., 1998, Ferrari et al., 1999, Nal et al., 2004). However, a detailed analysis of coronin-1 expression in cells of the hematopoietic lineage is currently not available. To determine coronin-1 expression in cells of the hematopoietic lineage by flow cytometry, IgGs of the polyclonal rabbit anti-coronin-1 serum No.1002 (Gatfield et al., 2005) were purified and coupled to the fluorophore AlexaFluor® 633. Single cell suspensions of bone marrow, thymus, spleen and lymph nodes from wildtype C57Bl/6 mice were first subjected to a staining with fluorophore-labeled monoclonal antibodies identifying the various leukocyte subsets. Monoclonal antibodies directed against the pan B-cell markers B220 and CD19 were used to detect on one hand all stages of B-cell development ($B220^+/CD19^+$) in the bone marrow and on the other hand B-cells in the spleen and lymph nodes

(B220^{+}/CD19^{+}). Mature B-cells in bone marrow, spleen and lymph nodes were identified by being positive for CD19 and IgM (CD19^{+}/IgM^{+}).

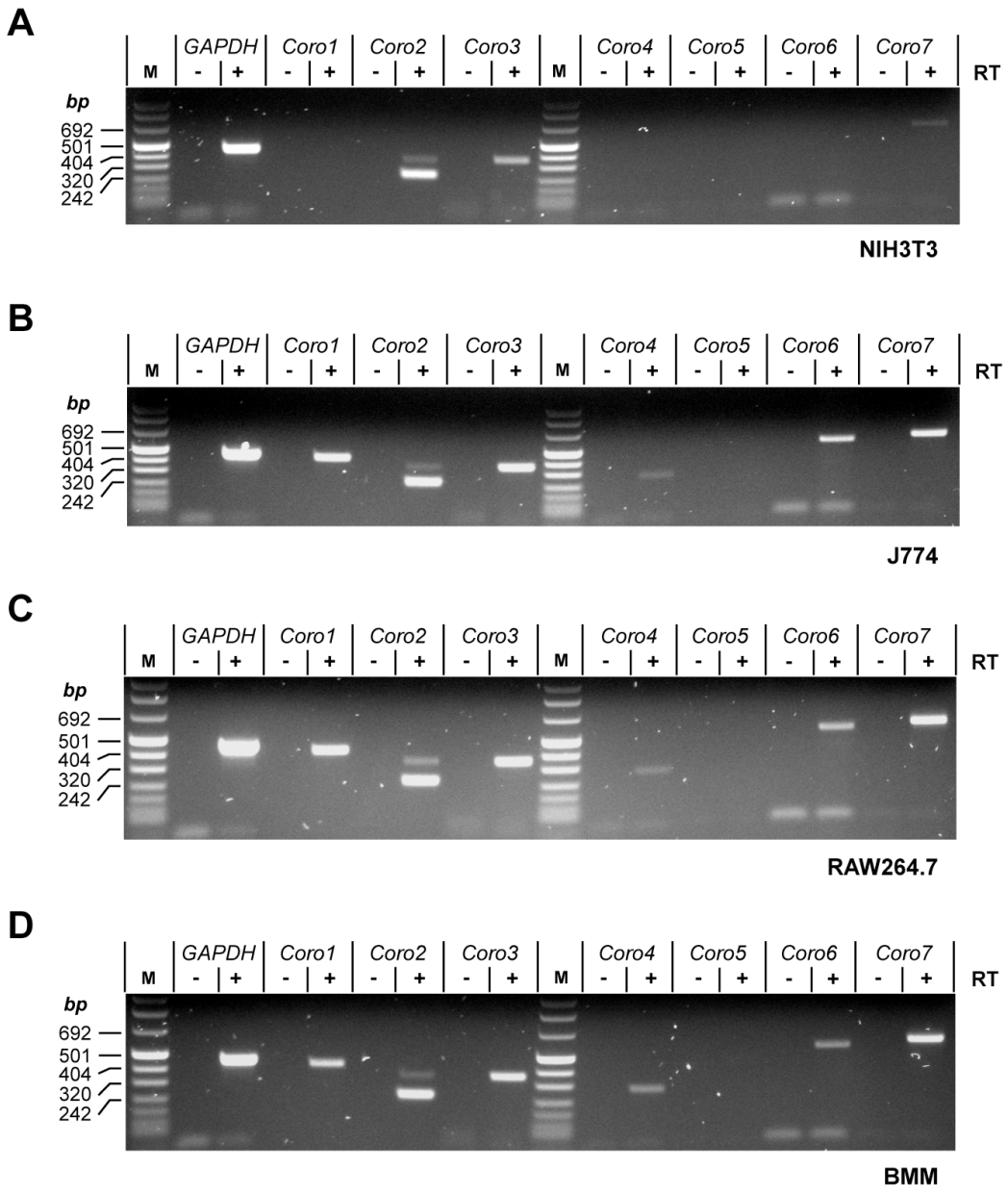

Fig. 12 Expression of coronin-1 - 7 in different cell lines and primary cells as determined by RT-PCR. Total RNA was extracted from the indicated cell types, reversely transcribed and analysed for the presence of coronin-1 - 7 transcripts by PCR. To control for background amplification from genomic DNA, RNA extracts not treated with reverse transcriptase (- RT) were also subjected to PCR. As an internal standard, PCR reactions were performed to detect the transcripts of ubiquitously expressed beta-actin. (**A**) NIH3T3, (**B**) J774, (**C**) RAW264.7, and (**D**) Bone marrow derived macrophages (BMM). RT: reverse transcriptase.

A monoclonal antibody directed against CD11b was used to stain cells of the myeloid lineage (CD11b^{+}). The various stages of T-cell development in the thymus (double negative (CD4^{-}

CD8$^-$), double positive (CD4$^+$CD8$^+$), CD4 (CD4$^+$CD8$^-$) and CD8 (CD4$^-$CD8$^+$) single positive thymocytes) as well as peripheral T-cells (CD4$^+$ or CD8$^+$) were detected by expression of CD4 and CD8. Following staining for leukocyte surface markers, the cells were fixed with PFA and stained for coronin-1 using the AlexaFluor®633-coupled anti-coronin-1 IgGs. Flow cytometric analysis and determination of the median fluorescence intensity for the coronin-1 staining (Fig. 13) revealed that coronin-1 is expressed throughout the development of the B-cell and myeloid lineage in the bone marrow. In the thymus, coronin-1 expression was found to be upregulated within single positive thymocytes compared to the double-positive and double-negative thymocytes. Among the various peripheral leukocyte populations coronin-1 is expressed without any cell type specific differences.

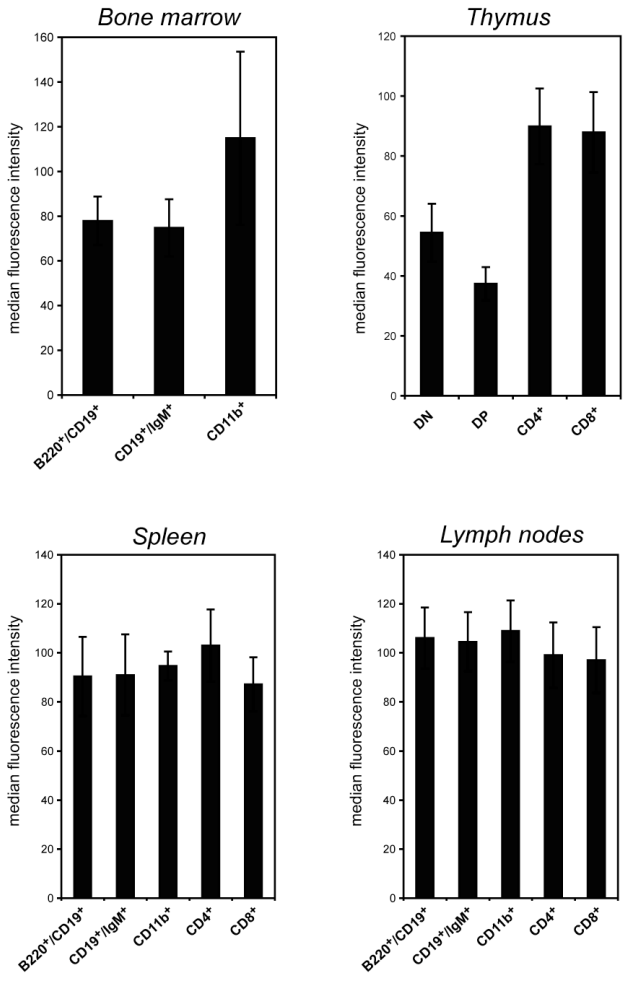

Fig. 13 Coronin-1 expression in leukocytes. Single cell suspensions of the indicated organs were first stained with antibodies directed against the indicated leukocyte markers, then fixed with PFA, permeabilized and stained with AlexaFluor633-labeled polyclonal rabbit anti-coronin-1 IgGs. Analysis by flow cytometry and subsequent determination of the median fluorescence intensity for the AlexaFluor633 signal allowed to quantitate the coronin-1 expression of cells within the indicated gates. Data are medians in arbitrary units ± SD based on the analysis of three C57Bl/6 animals (n=3). Courtesy of I. Albrecht.

3.1.3 Summary

Expression of the seven members of the coronin family of proteins was analysed by RT-PCR. Coronin-2, -3, -5 and -7 were found to be ubiquitously expressed, whereas coronin-1, -4 and -6 showed a restricted expression pattern. Detailed analysis of the expression of coronin-1 in cells of the hematopoietic lineage by flow cytometry established the presence of the coronin-1 protein in all leukocyte subsets. Phenotypic analysis of coronin-1 K.O. mice should therefore account for this by focusing on the analysis of potential defects in cells of

the immune system. With respect to the ubiquitous expression of some of the coronins, functional redundancy between members of the coronin protein family can be expected.

3.2 Analysis of the coronin-1 locus and generation of coronin-1 knock-out mice by targeting the coronin-1 gene in mouse embryonic stem cells

The cell biological function of coronin-1 in non-infected macrophages as well as in leukocytes in general is unknown. Generation of coronin-1 deficient mice was chosen as a strategy to gain insight into a role for coronin-1 in cells of the immune system.
Knock-out mice are generated from embryonic stem cells in which the functional gene sequence is disrupted by the integration of a targeting cassette via homologous recombination (Thomas and Capecchi, 1987, Capecchi, 1989, Joyner, 1999). The targeting cassette usually carries a neomycin resistance marker (alternatively a hygromycin resistance gene) for the positive selection of targeted ES cell clones. The neomycin resistance gene is often flanked by recognition sites for Cre recombinase (loxP sites) which allows excision of the resistance marker in cells expressing Cre recombinase (Lakso et al., 1992, Gu et al., 1994). Excision of the resistance marker is required if ES cell clones are used for a second round of gene targeting or if proximity of the strong promotor of the resistance gene could interfere with the expression of adjacent genes (Joyner, 1999). In order to allow negative selection of ES cell clones which have excised the resistance gene upon Cre expression, the gene for thymidine kinase (TK) is often used together with the neomycin resistance gene in the targeting cassette. Whereas the neomycin resistance marker confers resistance to G418, expression of thymidine kinase renders cells sensitive to gancyclovir which is metabolized by thymidine kinase into toxic compounds (Joyner, 1999).

In addition to resistance markers a reporter gene like the green fluorescent protein can be included in the targeting cassette. Integration of the reporter gene in frame with the start codon of the targeted gene allows analysis of the cell types in which the original promotor is active. Positive ES cell clones are injected into blastocysts that are subsequently transferred to foster mothers where they develop into chimaeric mice. Chimaeric mice are then analysed for germline transmission of the transgene by crossing them to C57Bl/6 mice. Once germline transmission has been established, appropriate breeding results in mice being homozygous for the mutated locus.
Construction of the targeting vector requires intimate knowledge about the organisation of the genomic locus for the gene of interest in order to ensure the precise integration of the

targeting cassette. Integration of the targeting cassette via homologous recombination is mediated by homologous genomic sequence flanking the targeting cassette.

3.2.1 *In silico* analysis of the coronin-1 locus

The mouse coronin-1 locus has been described to be located on chromosome 7 in an area that corresponds to cytogenetic band 7F3 (Kung et al., 1999). Interestingly, a variety of hematopoietic genes also map into this region which is noteworthy taking the leukocyte specific expression of coronin-1 into account. These hematopoietic genes are involved in signal transduction and/or adhesion-related processes (Kung et al., 1999).

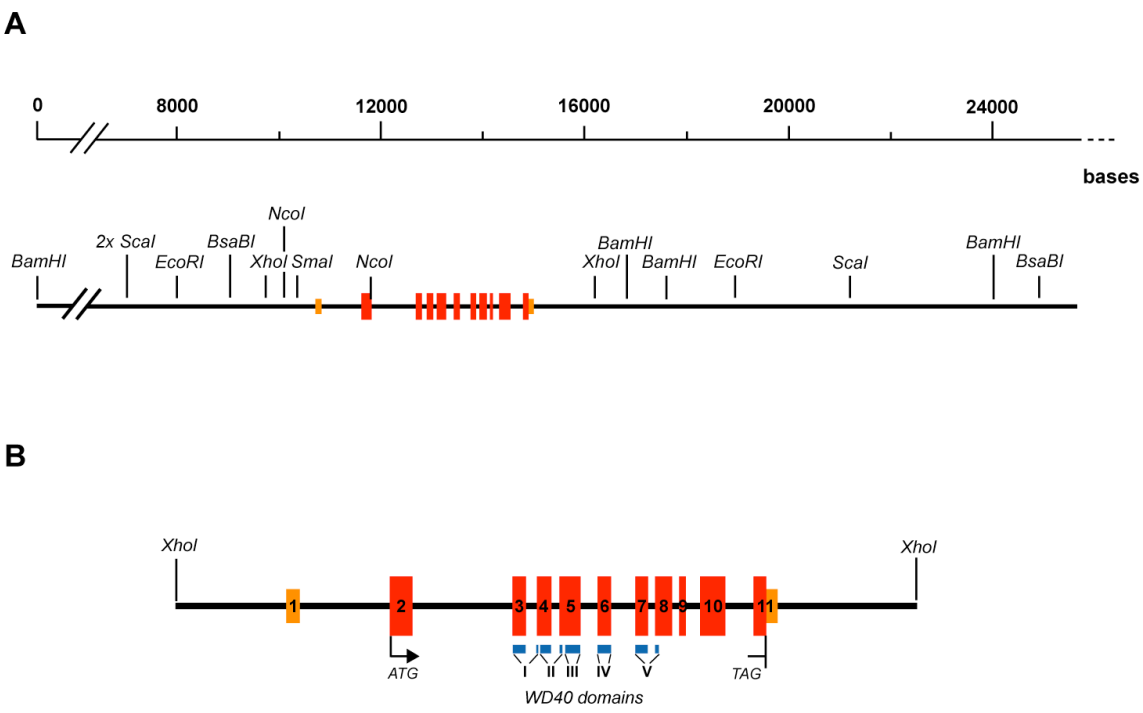

Fig. 14 Structure of the coronin-1 genomic locus (**A**) Schematic representation of the genomic locus of coronin-1. Coding exons are represented in red, the exonic regions encoding the 5' and 3' untranslated regions (UTR) in orange. Restriction sites are shown that were relevant for the construction of appropriate targeting constructs or for Southern blot analysis of the coronin-1 locus. For NcoI which cuts 8x within the depicted region and SmaI (cuts 6x) not all sites are shown. NotI and ClaI have no restriction sites within the genomic region of interest. Genomic sequence information was retrieved from web based databases accessible via the Genome Browser Tool Suite (http://genome.ucsc.edu). Restriction site analysis as well as alignments to determine published exon/intron boundaries (Kung et al., 1999) were performed using the MacVector Software. (**B**) Detailed scheme of the coronin-1 gene. The coronin-1 locus consists of eleven exons of which exon 1 encodes the 5' UTR and exon 11 contains the stop codon and the 3' UTR. The start codon is found in exon 2. Exons 1 - 11 are shown in scale. Sequence regions encoding the 5 WD40 domains (I - V) present in coronin-1 are indicated by the blue, hyphenated line (adapted from Kung et al., 1999).

The coronin-1 locus itself was shown to consist of eleven exons of which exon 1 encodes the 5' untranslated region (UTR) and exon 11 contains the stop codon and the 3' UTR. The start codon is found in exon 2. Fig.14 displays a schematic overview of the coronin-1 locus.

The design of flanking homology regions for the targeting construct requires detailed information on the genomic sequence. For this purpose the coronin-1 locus has been analysed using the genome browser (*http://genome.ucsc.edu*) a web based tool suite provided by the Genome Bioinformatics Group at the University of California, Santa Cruz (Kent et al., 2002; Karolchik et al., 2003). Genomic sequence 12 kb 5' and 14 kb 3' of the start codon of coronin-1 was retrieved from the databases and analysed for the localization of restriction enzyme sites required for the targeting vector construction (as indicated in Fig. 14). *In silico* analysis of the coronin-1 locus also allowed the characterisation of regions rich in repeats using the repeat masker algorithm available at the UCSC Genome Browser web site. Especially long stretches of repetitive sequence were found to be closely located 3' of exon 11 (see Fig.15). Repetitive sequences should be excluded from the flanking homology regions since they lead to unspecific, non-homologous integration of the targeting constructs.

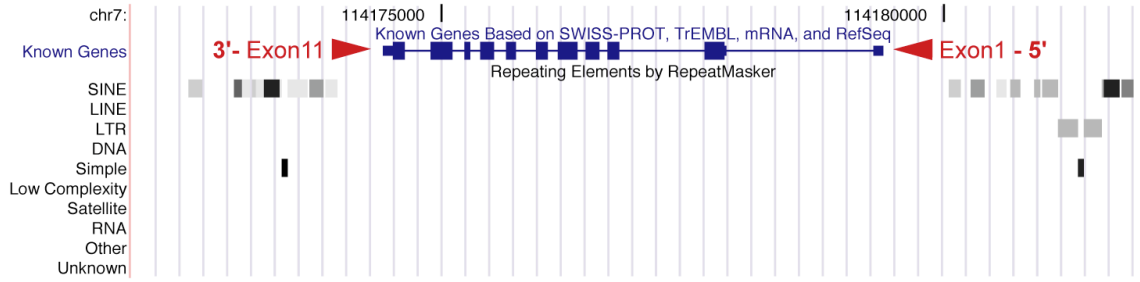

Fig. 15 Regions rich in repetitive sequences are found adjacent to the coronin-1 locus. Using the RepeatMasker algorithm at the UCSC Genome Browser web site regions rich in repetitive sequences could be identified. These repetitive sequences are very closely located to the 5' and 3' end of the coronin-1 locus. This raised the issue of excluding these sequences from the flanking homology regions of gene-targeting constructs if maximal efficiency in homologous recombination is desired. The track labeled 'Known Genes' gives a schematic representation of the coronin-1 locus with its 11 exons. Note that due to the definition of the orientation of genes on the chromosomes the coronin-1 locus is here shown in 3' to 5' orientation (as indicated by red arrowheads). Below the 'Known Genes' track, tracks for nine different classes of repeats are found. Boxes of different shades from grey to black indicate the position of identified repeats. The level of color shading reflects the amount of base mismatch, base deletion and base insertion associated with a repeat element. The higher the combined number of these, the lighter the shading. Based on this the region 3' of exon 11 is considered as a repeat rich region (rich in SINE sequence). The nine different classes of repeats are: **SINE**: short interspersed nuclear elements. **LINE**: long interspersed nuclear elements. **LTR**: long terminal repeats. **DNA**: DNA repeat elements. **Simple**: simple repeats (microsatellites). **Low complexity**: low complexity repeats. **Satellite**: satellite repeats. **RNA**: tRNA repeats. **Other**: other classes of repeats. **Unknown**: not yet classified type of repeats. This figure is a screenshot from the Genome Browser web site (http://genome.ucsc.edu). The RepeatMasker analysis was done on the May 2004 mouse genome assembly.

3.2.2 Overview of the different targeting vectors

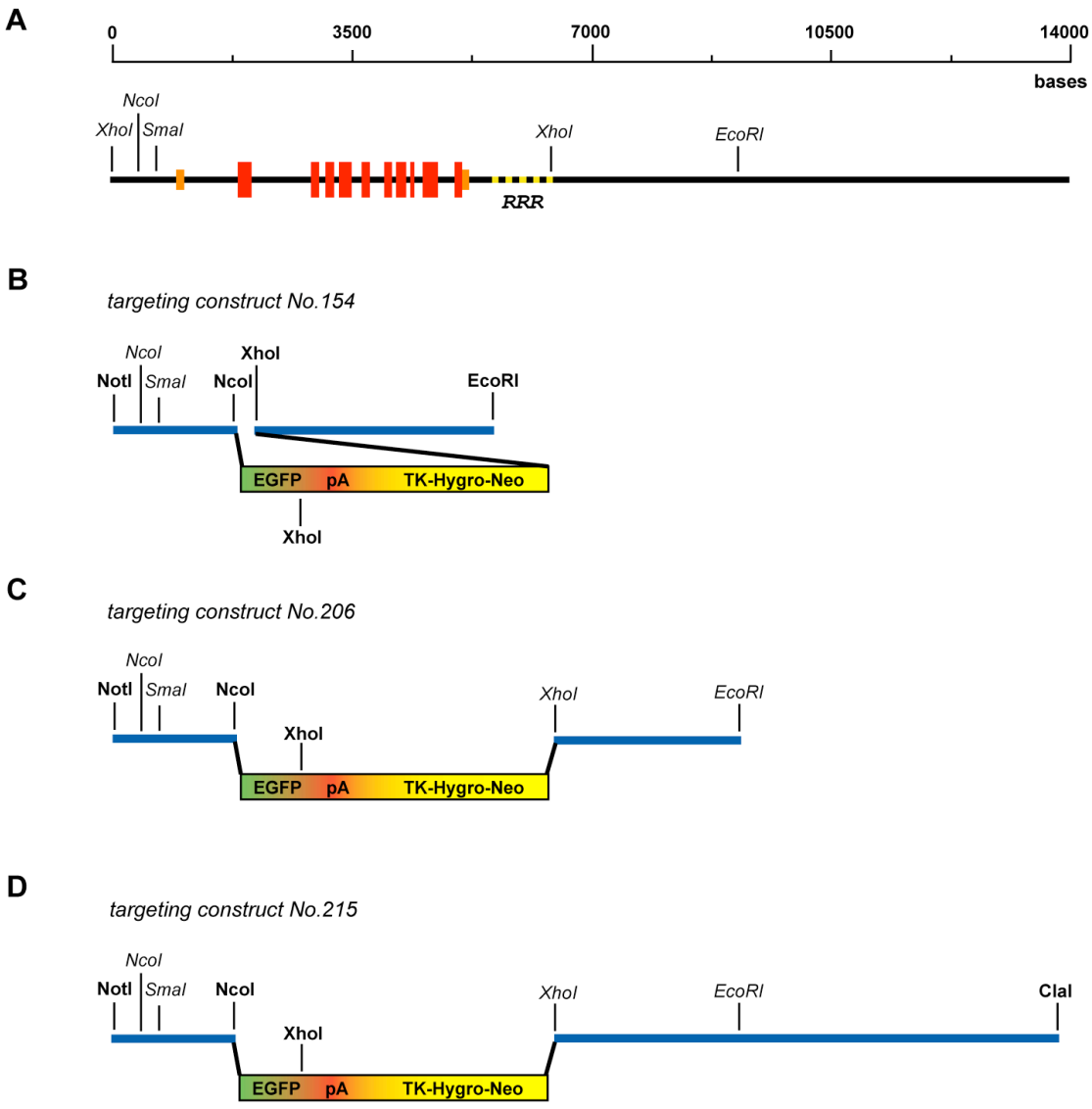

Fig. 16 Overview of the three different constructs made to allow targeting of the coronin-1 gene in mouse embryonic stem cells. (**A**) Schematic representation of the genomic locus of coronin-1. Coding exons are represented in red, the 5' and 3' untranslated regions (UTR) in orange. The dashed yellow line indicates the position of the repeat rich region (***RRR***). (**B - D**) Structure of the targeting constructs. Blue heavy lines represent flanking homology regions. Restrictions sites in bold represent sites that have been added by PCR in the course of construction. Restriction sites in italic are those originally present in the genomic locus. The gene of the enhanced green fluorescent protein (EGFP, represented by green colour) is positioned in frame with exon 2 allowing EGFP expression under the control of regulatory elements of the coronin-1 locus. A SV40 polyadenylation signal (pA, red) and the neomycin resistance cassette (TK-Hygro-Neo, yellow) follow the EGFP coding region. Construct No. 154 (**B**) is intended to delete exon 2 only, whereas the constructs No. 206 (**C**) and No. 215 (**D**) will result in deletion of the whole coding region. Construct No. 215 is identical to construct No. 206 but with an extension of the right flanking homology region by 4.7 kb. Construct No. 215 is made to allow successful gene targeting in case that the homology regions of construct No. 206 are not sufficiently long to result in efficient homologous recombination. All constructs have been cloned in a modified pBluescript SK+ (modpBSK) vector. A unique restriction site for linearization of all three constructs is the ClaI site in the multiple cloning site of the modpBSK vector.

The efficiency of homologous recombination depends on a variety of factors such as the accessibility of the locus, the length of the genomic sequence to be replaced by the targeting cassette, and the length of the flanking homology regions and their content of repetitive sequences. These factors and their influence on homologous recombination differ from locus to locus and can only be determined empirically. Generally, it is believed that flanking homology regions should be as long as possible and that the shorter the targeted sequence is the higher is the efficiency of homologous recombination. It was therefore decided to construct three targeting vectors to enhance the rate of homologous recombination at the coronin-1 locus. Furthermore, targeting vectors were designed to replace the coronin-1 coding sequence by the coding sequence for enhanced green fluorescent protein (EGFP). The fusion of the open reading frame (ORF) of EGFP with the original start codon of the coronin-1 coding sequence should result in expression of EGFP as a reporter. Since exon 1 (encoding the coronin-1 5' UTR) remains intact after successful homologous recombination we expected EGFP to be expressed under the control of regulatory elements of the coronin-1 locus.

As shown in Fig.16 construct No.154 was designed to knock out exon 2 only whereas the constructs No.206 and No.215 should result in the knock-out of the whole coding region (exon2 - 11). All constructs consist of the same 1.8 kb long 5' flanking homology region (referred to as ‚left arm') but differ in the length and position of the 3' flanking homology regions (referred to as ‚right arm'). The right arm of construct No.154 is 3.5 kb long, the constructs No.206 and No.215 are identical but have a right arm of 2.7 kb and 7.3 kb length, respectively. With respect to the repeat rich region 3' of exon 11 the targeting vectors have been constructed to either not include this region in the flanking homology sequence (as in construct No.154) or to knock it out together with the coding region for coronin-1 (constructs No.206 and No.215).

3.2.3 Construction of the targeting vectors

Construction of the targeting vectors is schematically shown in Fig.17 and Fig.18. Generally, the targeting vectors No.154, 206 and 215 have been built up sequentially by first amplifying corresponding genomic sequences by PCR, cloning them then into pBluescript SK(+) (pBSK) and finally subcloning them together with the EGFP sequence into a modified pBluescriptSK(+) (modpBSK) as a carrier which does not contain the XhoI site any more. As a last step the sequences comprising of a SV40 polyadenylation signal (SV40 pA) and the neomycin resistance cassette (*SV40pA-lox-TK-Neo-Hygro-lox*, described in Hippenmeyer et al., 2005) have been introduced.

In particular, the left arm was amplified by PCR (*PCR I*, Fig.17) using the primers TCP2860/TCP4675 and genomic DNA isolated from ES cells (Sv129/Ola).

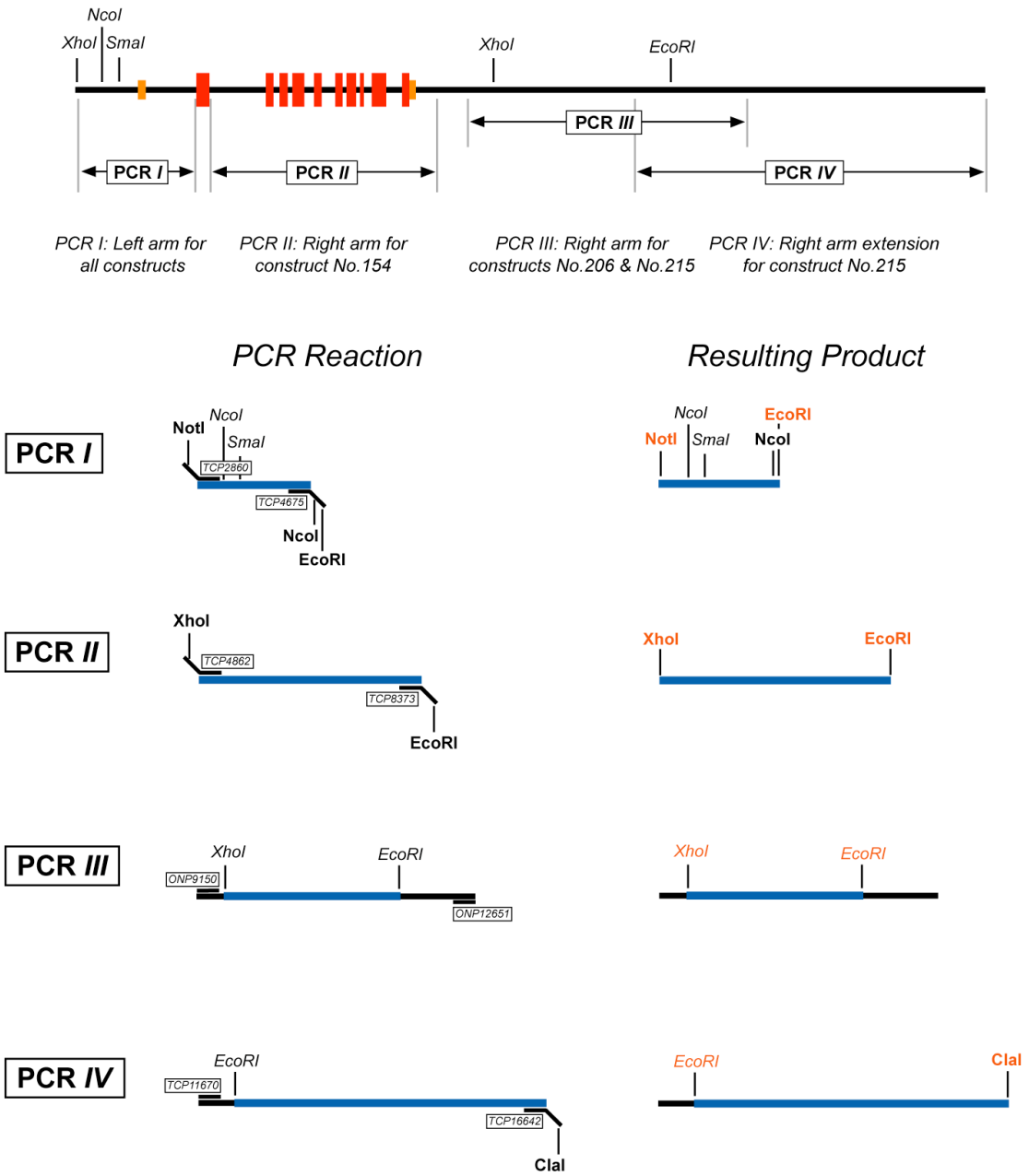

Fig. 17 Construction of targeting vectors for the coronin-1 locus. The flanking homology regions (represented in blue colour) of the different targeting constructs were amplified by PCR from genomic DNA as a template. In the top panel the relative position of the genomic regions serving as a template for the respective PCR reactions are shown between grey lines. Restriction sites in italics are those originally present in the coronin-1 locus. Restriction sites that have been included in PCR primers are shown in bold letters. Red coloured restriction sites are those used to clone the PCR products (shown on the right side) in pBluescriptSK(+) (pBSK). **PCR *I***: the left arm for all three targeting constructs is amplified using the primers TCP2860 and TCP4675; the resulting product is cloned in pBSK via NotI and EcoRI. **PCR *II***: the right arm for construct No.154 is generated by PCR using the primers TCP4862/TCP8373 and subsequently cloned in pBSK via XhoI and EcoRI. **PCR *III***: the right arm for the constructs No. 206 and No. 215 is amplified using the primers ONP9150/ONP12651. The XhoI/EcoRI portion of the PCR product was then cloned in pBSK. **PCR *IV***: the right arm of construct No.215 was further extended by using the product of a PCR with the primers TCP11670/TCP16642 which was subsequently cloned in pBSK via EcoRI and ClaI.

The primer TCP2860 included a NotI and the primer TCP4675 a NcoI and EcoRI into the PCR product. Using the NotI and EcoRI sites, the PCR product was cloned into pBSK. For the right arm of construct No.154 a PCR (*PCR II*, Fig.17) was performed with the primers TCP4862 (includes a XhoI site)/TCP8373 (includes an EcoRI site) followed by cloning the PCR product via XhoI and EcoRI in pBSK. The right arm for the constructs No.206 and No.215 was generated by PCR employing the primers ONP9150/ONP12651 (*PCR III*, Fig.17) and cloned into pBSK using the XhoI and EcoRI sites. As a 4.7 kb extension for the right arm of construct No.215, the product of a PCR (*PCR IV*, Fig.17) using the primers TCP11670/TCP16642 (includes a ClaI site) was cloned into pBSK via EcoRI and ClaI. In order to appropriately introduce the coding sequence of EGFP a PCR was performed with the primers GFP605/GFP1400 (includes a XhoI and EcoRI site) and plasmid DNA (pEGFP-N2) as a template. The product of this PCR was cloned into pGEM®-T Easy using single deoxyadenosine overhangs. Before building up the final targeting vectors the individual parts cloned into pBSK were sequenced to confirm the correctness of the sequences.

For the sequences of genomic origin it needed to be established whether found errors in the sequence are due to error-prone PCR reactions or due to strain based individual differences in the genomic sequence such as single nucleotide polymorphisms (SNPs). Whereas for the PCR genomic DNA of Sv129/Ola origin was used, the sequence of the coronin-1 locus retrieved from web based databases is of C57Bl/6J origin. In order to solve this problem, two independent PCR reactions for each flanking homology region to be amplified from genomic DNA were set up and the products were cloned into pBSK independently. Sequencing of multiple plasmids allowed to settle the issue of the origin of sequence mismatches. Practically, the sequences of multiple plasmids for a particular part of the targeting vectors have been aligned to the genomic sequence of C57Bl/6J origin. A particular single nucleotide mismatch of all plasmid sequences with the genomic reference was considered to be a mouse strain specific SNP. As soon as single nucleotide mismatches occured between the plasmid sequences an error was considered to originate from the PCR reaction. The independent setup of two PCR reactions allowed to trace back which reaction was error prone. Finally, only those plasmids were used for further cloning steps which had only mismatches categorized as single nucleotide polymorphisms between Sv129/Ola and C57Bl/6J genomic sequences.

By sequential subcloning steps the targeting vectors were then built up from the individual parts as shown in Fig.18. First, a SmaI/EcoRI fragment of the left arm was subcloned into modpBSK followed by inserting the EGFP sequence via NcoI/EcoRI. The left arm was then completed by inserting the NotI/SmaI portion into the plasmid carrying the SmaI/EcoRI left

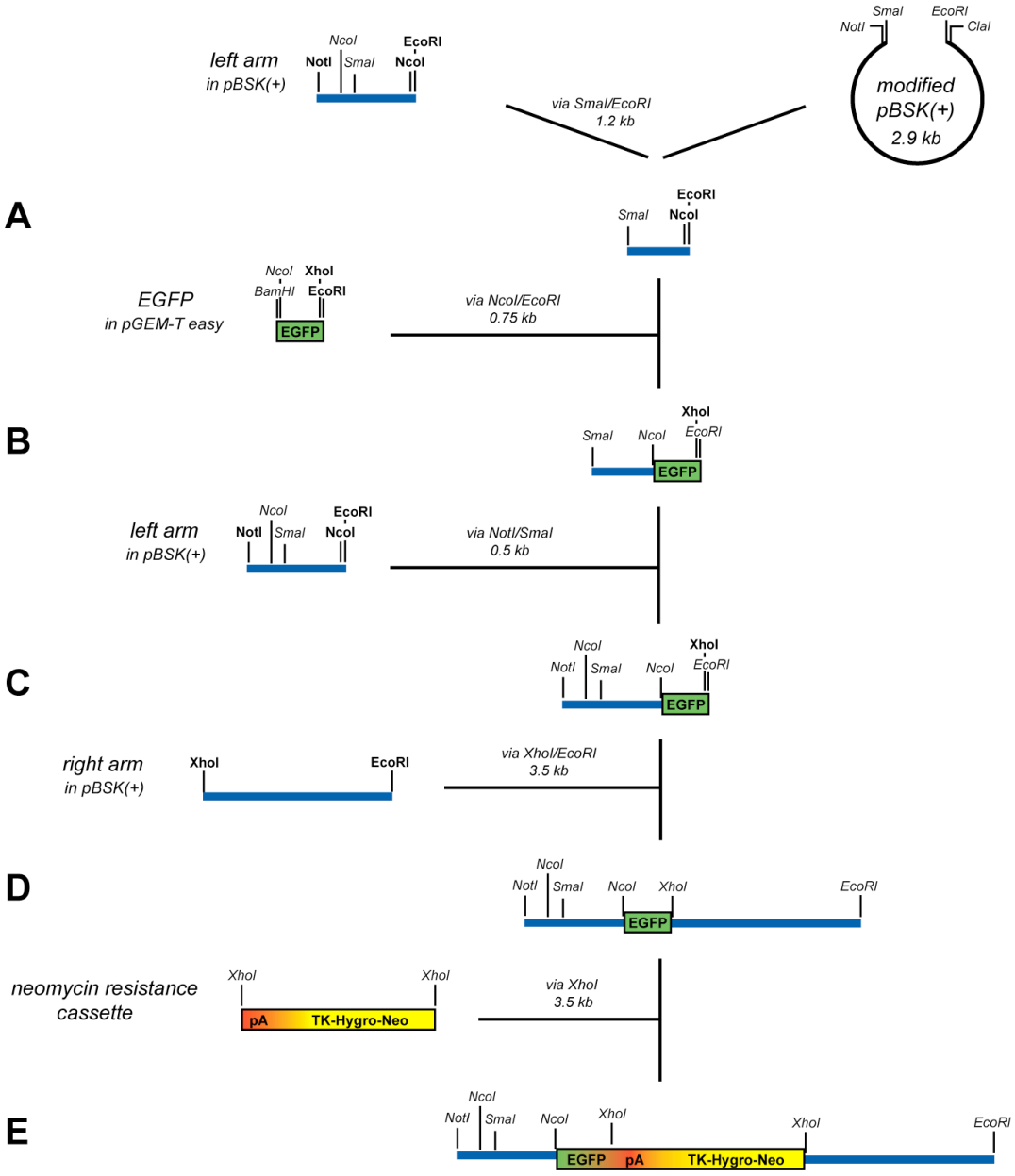

Fig. 18 Construction of targeting vectors for the coronin-1 locus. Building up the targeting constructs from individual parts. (**A**) Construction of all three targeting vectors started from subcloning the SmaI/EcoRI portion of the left arm in a modified pBluescriptSK(+) which no longer contains the XhoI in its multiple cloning site (MCS). The XhoI site from pBluescriptSK(+) was deleted by cutting the vector with SalI and XhoI and religating the plasmid. (**B**) Subsequently the EGFP sequence was subcloned in the vector containing the left arm fragment by NcoI/EcoRI. (**C**) The left arm was then completed by subcloning the NotI/SmaI portion into the resulting plasmid. (**D**) 3' of EGFP the appropriate right arms were then introduced using XhoI/EcoRI. The right arms for the three constructs differ in length and sequence homology to the coronin-1 locus. Shown here is the right arm for construct No.154 (3.5 kb in size). The right arm for constructs No.206 and No.215 is 2.7 kb in length. (**E**) As a last step of construction the neomycin resistance cassette was inserted by XhoI. For construct No.215 it was necessary to introduce the extension of its right arm (4.7 kb in size) via EcoRI/ClaI before insertion of the neomycin resistance cassette. Restriction sites in bold represent those introduced by PCR. The size of the subcloned fragments for each cloning step is indicated in kilobases (kb). For a better overview the plasmid backbone is not shown, the inserts are displayed in a linearized fashion.

arm fragment and 3’ of it the EGFP sequence. Based on the resulting plasmid the three different targeting constructs were assembled by subcloning the appropriate right arms via

XhoI/EcoRI 3' of the EGFP sequence. For construct No.215 it was furthermore necessary to introduce the right arm extension using EcoRI and ClaI sites. As a last step the polyadenylation signal and the neomycin resistance cassette (*SV40pA-lox-TK-Neo-Hygro-lox*) were inserted via XhoI. To confirm the proper assembly of all three targeting vectors the final plasmids were sequenced around the restriction sites used for the sequential construction of the targeting vectors from the individual parts.

3.2.4 Screening of gene-targeted ES cell clones by Southern blot analysis

For the targeting of the coronin-1 gene mouse ES cells (strain: E14.1, isolated from mouse strain background Sv129/Ola) were transfected with the ClaI linearized targeting vectors by electroporation and selected with G418. Table 8 provides an overview of the electroporations performed and the clones picked. For construct No.154 an initial round of electroporation and selection was performed in collaboration with Toru Miyazaki (University of Texas). 191 clones were picked and screened by Southern blot. In order to obtain more clones for construct No.154 and to also apply constructs No.206 and No.215 for gene-targeting, ES cells were electroporated with all three constructs independently at the transgenic mouse core facility (TMCF) of the Biozentrum. 576 clones were picked for each construct and prescreened by PCR in pools of five clones. Pools being positive according to the PCR analysis were then split up and the positive clone within a pool was identified by Southern blot.

Construct		Electroporation	Clones picked		Screening		Positive clones	
No.	Purpose	Date	Date	Number	Method	Date	Pos.	Clone No.
154	Exon 2 K.O.	July 2003 T. MIYAZAKI	Aug. 2003	191	Southern	Sept. 2003	1	No. 143
154	Exon 2 K.O.	28. Oct. 2003 TMCF, Basel	Nov. 2003	576	PCR/Southern	Dec. 2003/Jan. 2004	2	No. 106 and No. 205
206	ORF K.O.	28. Oct. 2003 TMCF, Basel	Nov. 2003	576	PCR/Southern	Dec. 2003/Jan. 2004	1	No. 831
215	ORF K.O.	7. Nov. 2003 TMCF, Basel	Nov. 2003	576	PCR/Southern	Dec. 2003/Jan. 2004	0	-

Table 8 Summary of the electroporations and the clones picked for the targeting of the coronin-1 gene in mouse ES cells. Construct No.154 was designed to replace exon 2 of the coronin-1 locus whereas the constructs No.206 and No.215 were used to delete the whole open reading frame (ORF). Electroporation of all three constructs was performed in collaboration with the transgenic mouse core facility (TMCF) at the Biozentrum, University of Basel. Construct No.154 was in addition used for electroporation by Toru Miyazaki (University of Texas) in July 2003 who also picked the corresponding 191 clones. These clones have been screened for homologous recombination at the coronin-1 locus by Southern blot. The clones picked at the TMCF have been first prescreened by PCR in pools of five and then identified by Southern blot analysis of splitted positive pools.

Homologous recombination is a rare event and therefore most of the clones are expected to display a random and/or multiple integration of the targeting construct. Successful

homologous recombination is detected by Southern blot. The integration of the targeting construct introduces new restriction sites into the genomic locus that lead to changes in the restriction digest pattern of the genomic locus.

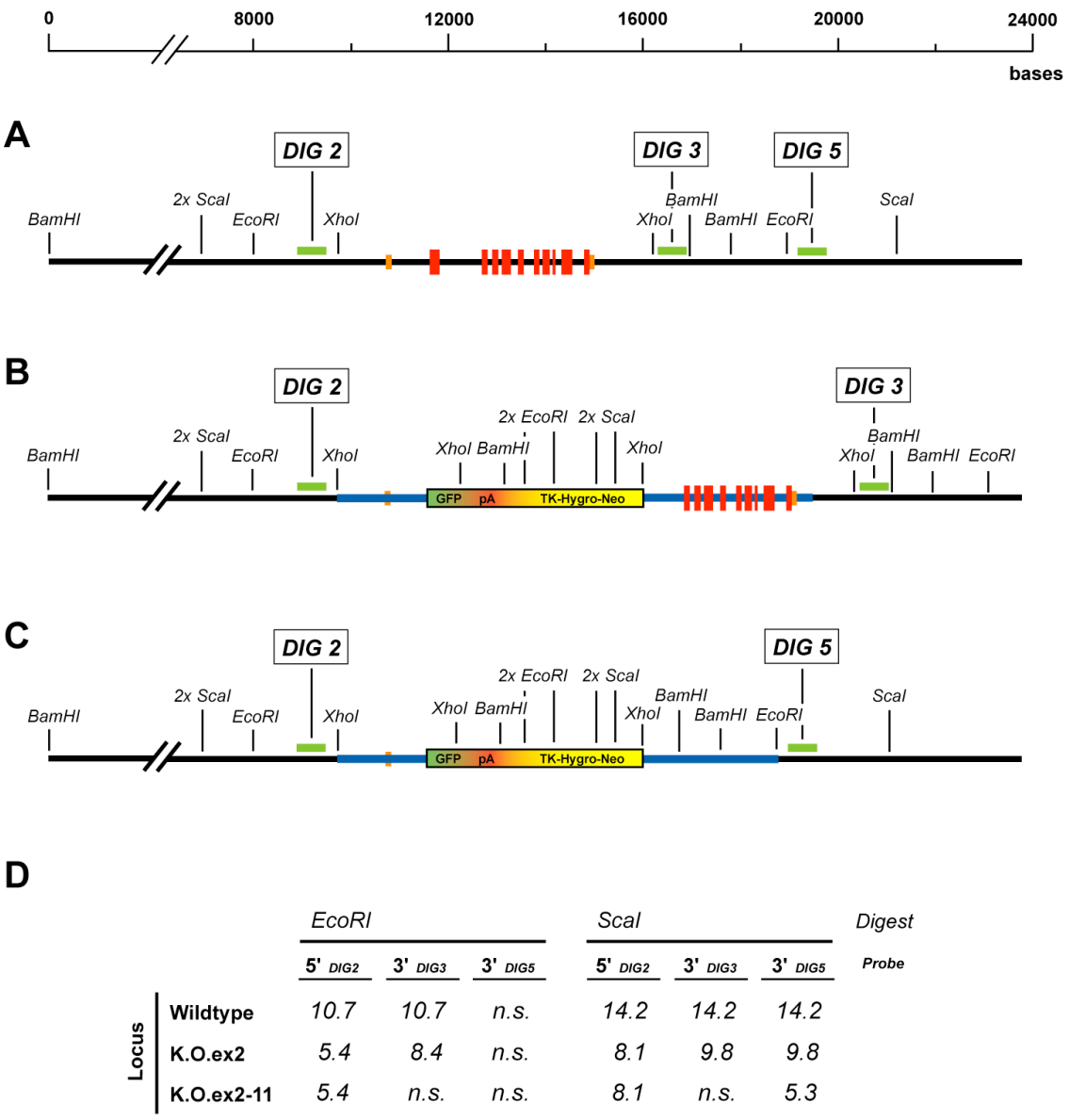

		EcoRI			ScaI			Digest
		5' DIG2	3' DIG3	3' DIG5	5' DIG2	3' DIG3	3' DIG5	Probe
Locus	Wildtype	10.7	10.7	n.s.	14.2	14.2	14.2	
	K.O.ex2	5.4	8.4	n.s.	8.1	9.8	9.8	
	K.O.ex2-11	5.4	n.s.	n.s.	8.1	n.s.	5.3	

Fig. 19 Screening strategy to detect homologous recombination at the coronin-1 locus by Southern blot. (**A**) Schematic representation of the wildtype coronin-1 locus. (**B**) Structure of the coronin-1 K.O. locus after successful homologous recombination of construct No.154 which leads to the deletion of exon 2 of coronin-1. (**C**) Once construct No.206 has been inserted into the coronin-1 locus by homologous recombination exon 2-11 are replaced by EGFP and the neomycin resistance cassette. Integration of the targeting vector into the genomic locus results in the appearance of new restriction sites, such as XhoI, BamHI, EcoRI and ScaI. The resulting changes in the digest pattern for the coronin-1 locus can be employed to screen for homologous recombination by Southern blotting. Shown are the positions of the digoxigenin labeled probes (*DIG2*, *DIG3* and *DIG5*) in the wildtype and K.O. loci. Size of the probes (in green) is not drawn in scale. In (**B**) the position of *DIG5* is outside of the image frame. (**D**) After digest with the indicated restriction enzymes and Southern blotting with the appropriate probes, bands of distinct size (here shown in kb) are detected. This allows to differentiate homologous from non-homologous integration of the targeting vectors into the coronin-1 locus. *n.s.* = probe not suited, either due to position outside of restriction sites of interest or due to location within the flanking homology regions of the targeting vector.

As shown in Fig.19 the correct integration of the EGFP-*SV40pA-lox-TK-Neo-Hygro-lox* cassette into the coronin-1 locus introduces new EcoRI, BamHI and ScaI restriction sites which results in distinct fragment patterns for the wildtype and the knock-out locus. For the Southern blot analysis of the positive ES cells, probes located at the positions indicated in Fig.19 were used. The first round of screenings was performed with the 5' probe *DIG2* only and allowed to identify the following positive ES cell clones for construct No.154: No.143 (clone selected by Toru Miyazaki), No.106 and No.205 (clones selected at the TMCF). For construct No.206 only one positive clone (No.831) out of 576 clones picked could be identified. Among the 576 clones picked from an electro-poration of construct No.215 no positive clone was found. The positive ES cell clones had then to be also tested for the correct integration at the 3' end. The results of the Southern blot analysis of the four positive ES cell clones are shown in Fig.20. For all clones bands of the expected size could be detected. These results demonstrate the

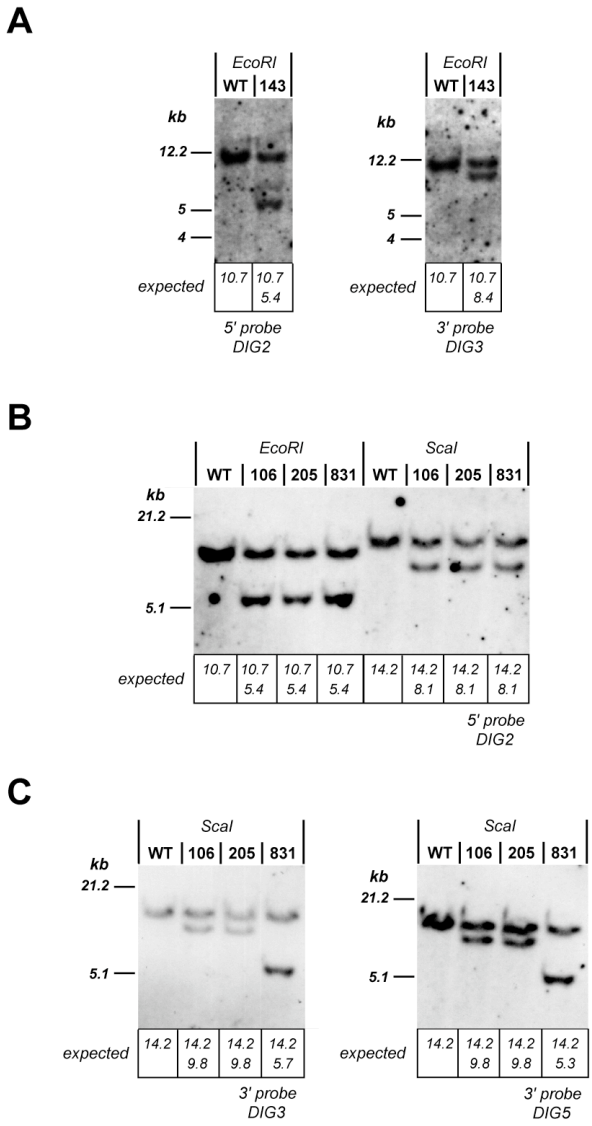

Fig. 20 Southern blot analysis of positive ES cell clones. Genomic DNA was isolated from wildtype ES cells and the positive ES cell clones No.143, 106, 205 and 831 and subjected to a digest with the indicated enzymes. After separation on a 0.8% agarose gel and transfer to nylon membrane the DNA was probed using the indicated digoxigenin labeled probes (*DIG2*, *DIG3* and *DIG5*). Below the gels, the size of the expected bands is shown in kilobases (kb). (**A**) Southern blot analysis of clone No.143 (Exon 2 K.O.) after EcoRI digest. (**B**) Southern blot analysis using the 5' probe *DIG2* of the clones No.106 and 205 (Exon 2 K.O.) and No.831 (Exon 2-11 K.O.) after EcoRI and ScaI digest. (**C**) The same clones as shown in (**B**) but probed with the 3' probes *DIG3* (not suited for clone No. 831 due to its position in the flanking homology region of the targeting vector) and *DIG5* (probe developed to detect proper 3' end integration for clone No. 831).

correct integration of the targeting constructs at the expected position within the coronin-1 locus.

3.2.5 Blastocyst injection of positive ES cell clones and establishment of transgenic mouse lines

The establishment of transgenic mouse lines for the coronin-1 K.O. locus required the generation of chimaeric animals. Injection of ES cells into blastocysts and transplantation of these blastocysts into pseudo-pregnant foster mothers leads to chimaeric animals that are derived to a certain extent from the injected ES cells. The ES cells that were used for the gene-targeting are of Sv129/Ola origin and therefore carry an *agouti*-allele. This allele is not present in the blastocyts of C57Bl/6xBDF-1 origin used for injection.

ES-Clone	Injection date	Inj. No.	Embryos transferred	Birth	Born	Black	Chimaeras Sex (% chimaerism)
106	13.Feb. 2004	OP 507	13	4. March 2004	2	1	m (80%)
106	13.Feb. 2004	OP 508	9	4. March 2004	2	2	-
106	19.Aug. 2004	OP 789	11	8. Sept. 2004	6	4	m (80%), m (40%)
106	19.Aug. 2004	OP 790	8	8. Sept. 2004	2	0	m (50%), m (30%)
106	19.Aug. 2004	OP 791	9	8. Sept. 2004	2	2	-
106	20.Aug. 2004	OP 792	10	8. Sept. 2004	5	1	m (100%), m(100%), m (90%), f (50%)
106	20.Aug. 2004	OP 793	9	8. Sept. 2004	5	3	m (80%), m (50%)
106	20.Aug. 2004	OP 794	10	9. Sept. 2004	5	5	-
106	20.Aug. 2004	OP 795	10	8. Sept. 2004	3	3	-
143	10. Feb. 2004	OP 493	11	28. Feb. 2004	2	1	f (10%)
143	10. Feb. 2004	OP 494	11	29. Feb. 2004	2	1	m (80%)
143	10. Feb. 2004	OP 495	13	1. March 2004	6	6	-
143	10. Feb. 2004	OP 496	12	29. Feb. 2004	1	1	-
143	17. Aug. 2004	OP 780	26	8. Sept. 2004	9	9	-
143	23. Aug. 2004	OP 801	8	-	0	0	-
143	23. Aug. 2004	OP 802	7	14. Sept. 2004	3	2	f (40%)
143	23. Aug. 2004	OP 803	7	-	0	0	-
205	17. Feb. 2004	OP 509	7	-	0	0	-
205	18. Aug. 2004	OP 784	11	7. Aug. 2004	3	3	-
205	18. Aug. 2004	OP 785	12	-	0	0	-
205	18. Aug. 2004	OP 786	12	8. Sept. 2004	9	8	m (40%)
205	18. Aug. 2004	OP 787	12	8. Sept. 2004	8	8	-
205	18. Aug. 2004	OP 788	12	8. Sept. 2004	8	8	-
831	17. Aug. 2004	OP 778	10	8. Sept. 2004	4	4	-
831	17. Aug. 2004	OP 779	10	7. Sept. 2004	4	4	-
831	17. Aug. 2004	OP 781	10	8. Sept. 2004	3	3	-
831	20.Aug. 2004	OP 796	10	8. Sept. 2004	8	6	m (70%), m (70%)
831	20.Aug. 2004	OP 797	10	8. Sept. 2004	3	3	-
831	20.Aug. 2004	OP 798	11	8. Sept. 2004	4	4	-
831	23. Aug. 2004	OP 799	9	-	0	0	-
831	23. Aug. 2004	OP 800	10	11. Sept. 2004	4	1	m (100%), m (70%), f (30%)

Table 9 Results of the blastocyst injection of the ES cell clones No.106, No.143, No.205 and No.831. For all four ES cell clones chimaeric animals could be obtained. Injections which gave rise to chimaeric animals are highlighted in orange. The degree of chimaerism (given in %) was estimated based on the extent of *agouti* (brown) coat colour of a particular animal. **m**: male; **f**: female.

The *agouti*-allele which results in brown coat colour allows to estimate the degree of chimaerism of a particular animal since regions of brown coat colour are of injected ES cell

origin and black coat colour is contributed by the recipient blastocyst. ES cells clones being positive for the coronin-1 K.O. locus were injected into blastocysts at the TMCF. Table 9 shows the results of the several injections. In summary, for all four ES cell clones chimaeric animals could be obtained.

Highly chimaeric animals are likely to have also germ cells of ES cell origin which is a prerequisite for germline transmission of the mutated locus. Germline transmission of the mutated locus is tested by breeding chimaeric male animals to C57Bl/6 females and genotyping the *agouti* coloured offspring. Heterozygous founder animals can subsequently be bred to generate homozygous K.O. animals.

Concerning the chimaeric animals listed in table 9 only the male animals with a high degree of chimaerism where used to test them for the germline transmission of the coronin-1 K.O. locus. Female chimaeras were generally not used because they are often sterile due to the contribution of the male ES cells to their germline. In chimaeric females most of the cells of ES cell origin are expected to have a X0-genotyp.

Out of the total of the 14 chimaeras tested, 3 were shown to transmit the mutated coronin-1 allele to the next generation (see table 10). The resulting heterozygous animals were used as founders for the generation of coronin-1 K.O. mouse lines by crossing them to C57Bl/6 animals.

Clone	Chimaera		Birth	Litters	Offspring	Germline	Comment
	Inj. No.	Sex (%chimaerism)			*agouti* ?	transmission	
106	507	male (80%)	4. Mar. 2004	4	yes (1.)	no	chimaera died (6. Oct. 2004), agouti only in first litter
106	789	male (80%)	8. Sept. 2004	12	yes (1.)	yes (2.)	discontinued, chimaera sacrified (3. Mar. 2006)
106	789	male (40%)	8. Sept. 2004	-	-	-	not tested, chimaera sacrified (6. Jul. 2005)
106	790	male (50%)	8. Sept. 2004	-	-	-	not tested, chimaera sacrified (6. Jul. 2005)
106	790	male (30%)	8. Sept. 2004	-	-	-	not tested, chimaera sacrified (6. Jul. 2005)
106	792	male (100%)	8. Sept. 2004	6	no	no	discontinued, chimaera sacrified (8. Jul. 2005)
106	792	male (100%)	8. Sept. 2004	3	yes (1.)	no	discontinued, chimaera sacrified (22. Nov. 2005)
106	792	male (90%)	8. Sept. 2004	9	yes (2.)	yes (2.)	discontinued, chimaera sacrified (3. Mar. 2006)
106	792	female (50%)	8. Sept. 2004	-	-	-	not tested, chimaera sacrified (6. Jul. 2005)
106	793	male (80%)	8. Sept. 2004	7	no	no	discontinued, chimaera sacrified (8. Jul. 2005)
106	793	male (50%)	8. Sept. 2004	-	-	-	not tested, chimaera sacrified (6. Jul. 2005)
143	493	female (10%)	28. Feb. 2004	6	no	no	discontinued, chimaera sacrified (8. Dec. 2004)
143	494	male (80%)	29. Feb. 2004	10	yes (5.)	yes (6.)	discontinued, chimaera sacrified (8. Jul. 2005)
143	802	female (40%)	14. Sept. 2004	3	no	no	discontinued, chimaera sacrified (8. Jul. 2005)
205	786	male (40%)	8. Sept. 2004	3	no	no	discontinued, chimaera sacrified (8. Jul. 2005)
831	796	male (70%)	8. Sept. 2004	8	no	no	discontinued, chimaera sacrified (3. Mar. 2006)
831	796	male (70%)	8. Sept. 2004	8	no	no	discontinued, chimaera sacrified (3. Mar. 2006)
831	800	male (100%)	11. Sept. 2004	5	no	no	discontinued, chimaera sacrified (3. Mar. 2006)
831	800	male (70%)	11. Sept. 2004	8	no	no	chimaera died (31. Oct. 2005)
831	800	female (30%)	11. Sept. 2004	-	-	-	not tested, chimaera sacrified (6. Jul. 2005)

Table 10 Results of testing chimaeric animals for germline transmission of the coronin-1 K.O. locus. Generally, only highly chimaeric male animals were tested by crossing them to C57Bl/6 females. Germline transmission of the coronin-1 K.O. locus was assessed by PCR in *agouti* coloured offspring only since the *agouti* allele and the coronin-1 K.O. locus are transmitted together. For some clones also female chimaeras and animals with a low degree of chimaerism were tested due to the lack of better candidates. Chimaeric animals for which germline transmission could be demonstrated are highlighted in orange.

Southern blot analysis using an EcoRI digest and the 5' probe *DIG2* confirmed the proper configuration of the coronin-1 K.O. locus (Fig.21). For future genotyping purposes a PCR based screening strategy was developed as shown in Fig.21.

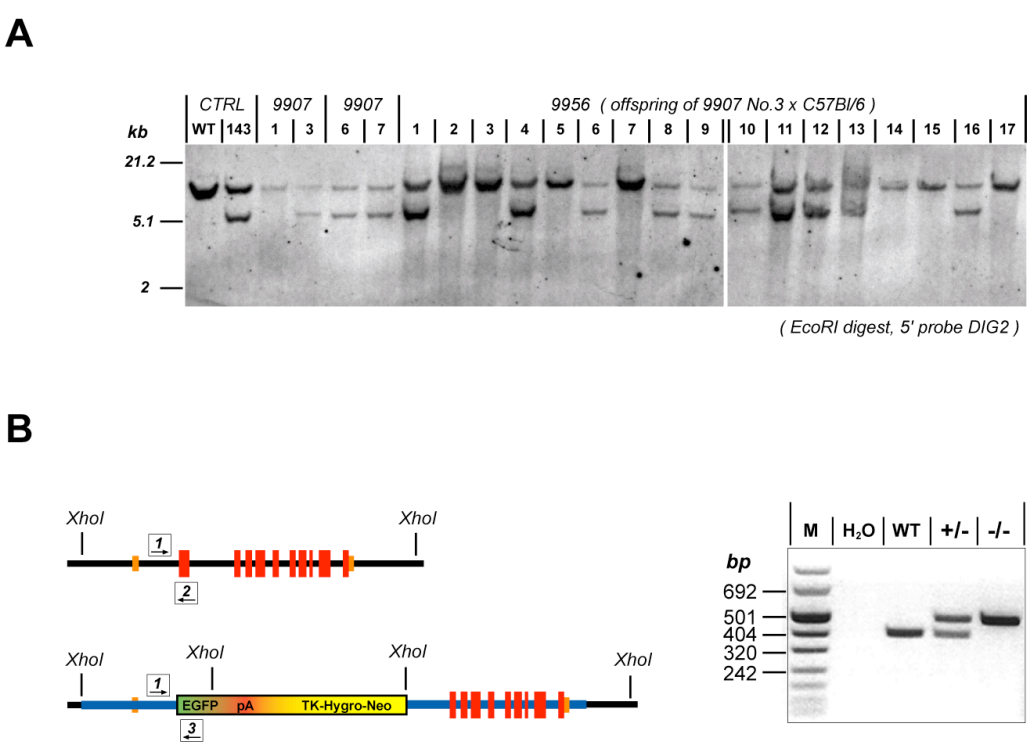

Fig. 21 Genotyping of coronin-1 knock-out mice by Southern blot and PCR. (**A**) Germline transmission of the coronin-1 K.O. locus. Shown is a Southern blot of genomic DNA isolated from tail biopsies, digested with EcoRI and probed with the 5' probe *DIG2*. The number *9907* refers to the code of the breeding of a male chimaera (clone No.143, injection no.494, birth: 29.Feb.2004) with a C57Bl/6 female. Animal No. 3 turned out to be heterozygous (10.7 kb band for the WT allele, 5.4 kb band for the K.O. allele) and was chosen to be founder for the coronin-1 K.O. line. Animal No.3 was backcrossed to C57Bl/6 under the code *9956* of which the Southern blot analysis of two litters (in total 17 animals) is shown. As a control (*CTRL*) genomic DNA isolated from ES cells (wildtype and exon 2 K.O. clone No.143) was used. (**B**) Genotyping of coronin-1 K.O. mice by PCR is performed using three primers simultaneously. The position of these primers relative to the coronin-1 WT and KO locus is shown in the left hand panel. Primer 1 (WTCor1) anneals between exon 1 and the start codon of coronin-1 or EGFP, respectively. Primer 2 (WTCor2) anneals within exon 2, primer 3 (KOCor1) is specific for EGFP. WT animals are identified by the detection of a single band at 400 bp, for homozygous coronin-1 animals the PCR gives a single product of 500 bp size. Heterozygous coronin-1 locus configuration allows amplification of both products as shown for a representative PCR in the right hand panel. As a template, genomic DNA from tail biopsies was used (**WT** = wildtype animal identical to code *9907* No.1 in (**A**), **+/-** = heterozygous animal identical to code *9907* No. 3 in (**A**), **-/-** = homozygous coronin-1 K.O. animal from an intercross of heterozygous animals of code *9956* as genotyped in (**A**), **H_2O** = no template added to the PCR as a control, **M** = marker).

Continous crossing of heterozygous coronin-1 K.O. mice to C57Bl/6 animals is referred to as backcrossing and is required to generate a so-called congenic mouse line. The genetic background can very often have a profound influence on the phenotype of a transgenic mouse line (Sanford et al., 2001; Doetschman, 1999). The rationale behind generating a congenic mouse line by backcrossing is to bring the mutated allele into a defined inbred

background such as C57Bl/6. The founder animals of a line still have a mixed background consisting of Sv129/Ola (contributed by the gene-targeted ES cells) and C57Bl/6 (of blastocyst origin and from crossing chimaeric males to C57Bl/6 females). With each backcross of heterozygous animals with animals of a defined inbred background the contribution of other genetic backgrounds is reduced. In a congenic mouse line all individual animals are genetically identical for all alleles of a particular inbred background. Per definition a mouse line is considered to be congenic after the tenth backcross generation (Silver, 1995).

During the course of this work a coronin-1 K.O. mouse line originating from ES cell clone No.143 could be backcrossed up to the third generation. Further backcrossing for this line and others is in progress. The phenotypic analysis of coronin-1 K.O. mice presented in this thesis was performed using homozygous animals and appropriate control littermates generated by intercrossing heterozygous animals of the third backcross generation.

3.2.6 Summary

Genomic sequence of the coronin-1 locus was retrieved from web based databases. A detailed characterisation of the locus allowed to design targeting vectors for gene-targeting in mouse ES cells. Three targeting vectors (No.154, No.206 and No.215) have been constructed and used for the electroporation of ES cells. A total of 1919 clones was picked and screened for homologous recombination at the coronin-1 locus by PCR and Southern blot. A total of four clones was identified, three clones for the knock-out of exon 2 (construct No.154) and one clone for the knock-out of the whole coding region (construct No.206). Blastocyst injection resulted in chimaeric animals for all of the four clones. Nevertheless, germline transmission of the transgene could only be achieved for the exon 2 K.O. clones No.143 and No.106. Appropriate congenic mouse lines are currently established by backcrossing heterozygous coronin-1 K.O. mice to C57Bl/6 mice.

3.3 Phenotypic analysis of coronin-1 K.O. mice

Coronin-1 was found to be specifically expressed in leukocytes. During embryogenesis expression of coronin-1 appears at stage E14 and goes along with the development of hematopoietic tissue (Nal et al., 2004). Due to this late and specific expression during embryogenesis and in the adult mouse homozygous coronin-1 K.O. mice can be expected to be viable. The phenotypic analysis of coronin-1 K.O. mice initially focused on the description of the development of the immune system. It needed to be shown whether the deficiency for coronin-1 affected generation of leukocyte subsets and whether these leukocytes are found in normal numbers in the peripheral organs such as spleen and lymph nodes.

3.3.1 Homozygous Coronin-1 K.O. mice do not display an obvious phenotype

Homozygous coronin-1 K.O. mice and wildtype litttermates as a control were generated by intercrossing heterozygous coronin-1 K.O. mice. Heterozygous animals originated from blastocyst injection of ES cell clone No.143 and subsequent backcrosses of coronin-1 K.O. mice to C57Bl/6 mice up to the third generation. Homozygous coronin-1 K.O. mice were born at normal mendelian ratio and were viable. No obvious abnormalities in behaviour or mortality were observed for these animals compared to wildtype littermates. Homozygous coronin-1 K.O. were found to be fertile since appropriate breedings did not show any alterations in average litter size and time between setting up the breeding and weaning of the offspring.

3.3.2 Homozygous coronin-1 K.O. mice do not express coronin-1

Homozygous coronin-1 K.O. were analysed for the correct configuration of the coronin-1 K.O. locus by Southern blot. Genomic DNA was extracted from tail biopsies of homozygous and heterozygous coronin-1 K.O. mice and wildtype littermates. The DNA was then digested with EcoRI and analysed by Southern blot using the 5' probe *DIG2*. As shown in Fig.22 A wildtype mice are characterised by the detection of a single band at 10.7 kb whereas for homozygous coronin-1 K.O. mice a single band of 5.4 kb could be identified. As expected, heterozygous coronin-1 K.O. show both bands (see also Fig.21 A).
Analysis of coronin-1 expression was performed by subjecting lysates of single cell suspensions of spleen and thymus to SDS-PAGE and subsequent Western blot analysis using a polyclonal rabbit anti-coronin-1 serum (No.1002, third bleed, Gatfield et al., 2005). No detectable coronin-1 expression was found in homozygous coronin-1 K.O. mice (Fig.22 B). In addition, no lower molecular weight products were detected which would have been

indicative for the generation of shorter versions of the coronin-1 protein from the remaining exons 3 –11 in the coronin-1 K.O. locus.

Corresponding to the disappearance of coronin-1 expression in homozygous coronin-1 K.O. mice appearance of EGFP expression was detected by Western blot in thymus and spleen (Fig.22 B). EGFP was therefore found to be expressed under the control of regulatory elements of the coronin-1 locus.

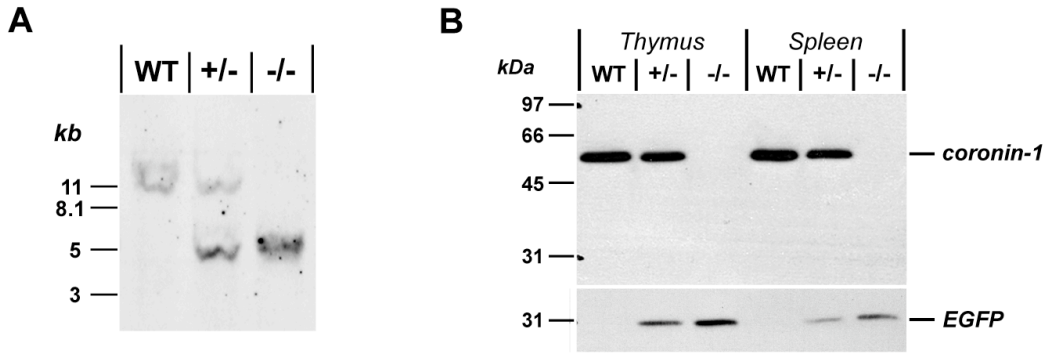

Fig. 22 Coronin-1 expression in homozygous coronin-1 K.O. mice. (**A**) Southern blot analysis of coronin-1 K.O. mice. Genomic DNA was isolated from tail biopsies, digested with EcoRI and analysed using the 5' probe *DIG2*. EcoRI digest of the coronin-1 wildtype allele results in a single 10.7 kb band whereas the coronin-1 K.O. locus is characterized by the appearance of a single 5.4 kb fragment. (**B**) Lysates of single cell suspensions of the indicated organs were prepared and equal protein amounts were subjected to SDS-PAGE followed by Western blot analysis to detect coronin-1 (polyclonal rabbit anti-coronin-1 serum No.1002) or EGFP (mixture of the two monoclonal antibodies clones 7.1 and 13.1). **WT**: wildtype; **+/-**: heterozygous and **-/-**: homozygous coronin-1 K.O. mice.

3.3.3 EGFP as a reporter for coronin-1 expression

The EGFP expression under the control of regulatory elements of the coronin-1 locus was further analysed by flow cytometry. For this purpose IgGs of the polyclonal rabbit anti-coronin-1 serum No.1002 (Gatfield et al., 2005) were purified and coupled to the fluorophore AlexaFluor®633. AlexaFluor®633 labeled IgGs of the corresponding rabbit preimmune serum served as a control for background binding. Single cell suspensions of bone marrow, thymus and spleen of homozygous, heterozygous coronin-1 K.O. mice and wildtype littermates were fixed with 2% PFA and stained with the appropriate AlexaFluor®633 labeled rabbit IgGs. The results of the flow cytometric analysis are shown in Fig.23. The AlexaFluor®633 labeled anti-coronin-1 IgGs reliably detected coronin-1 expression in bone marrow, thymus and spleen of wildtype and heterozygous coronin-1 K.O. mice and confirmed the absence of coronin-1 expression in homozygous coronin-1 K.O. mice. For homozygous coronin-1 K.O. mice, which possess two alleles of the coronin-1 K.O. locus, a two-fold higher signal intensity for EGFP expression was found compared to their heterozygous littermates (see Fig.23).

The analysis of heterozygous coronin-1 K.O. animals allowed to test to which extend EGFP expression matches the expression of coronin-1. As shown in Fig.23 (A and B) for cells of the bone marrow as well as of the thymus a perfect match between the signal intensities for EGFP and coronin-1 staining could be detected in heterozygous coronin-1 K.O. mice. All events were aligned on a diagonal line in EGFP versus coronin-1 flow cytometry dot plots. For the spleen this perfect match between EGFP and coronin-1 signal intensities was not observed (Fig.23 C). We therefore further analysed coronin-1 and EGFP expression in splenic lymphocyte subsets of wildtype and heterozygous coronin-1 deficient mice. As shown in Fig.24 A, CD4 and CD8 positive T-lymphocytes were found to express both coronin-1 and EGFP at high and discrete levels. In contrast to this finding, the two major splenic B-cell subsets, marginal zone as well as follicular B-cells, displayed discrete and high expression of coronin-1 but not of EGFP. Taken together, these results demonstrate that EGFP expression from the coronin-1 K.O. locus is well suited as a reporter for coronin-1 expression in cells of the bone marrow and the thymus but not in all splenic cell subsets. Especially for splenic B-cells EGFP cannot be used as a reporter for coronin-1 expression. This could be explained on one hand by differences in protein stability between EGFP and coronin-1 and on the other hand by differences in expression of coronin-1 and EGFP under the control of regulatory elements of the coronin-1 locus. The mRNA for EGFP transcribed from the coronin-1 K.O. locus does not contain the original coronin-1 3'-UTR which could be responsible for regulating mRNA stability and translation depending on the cell type. Further

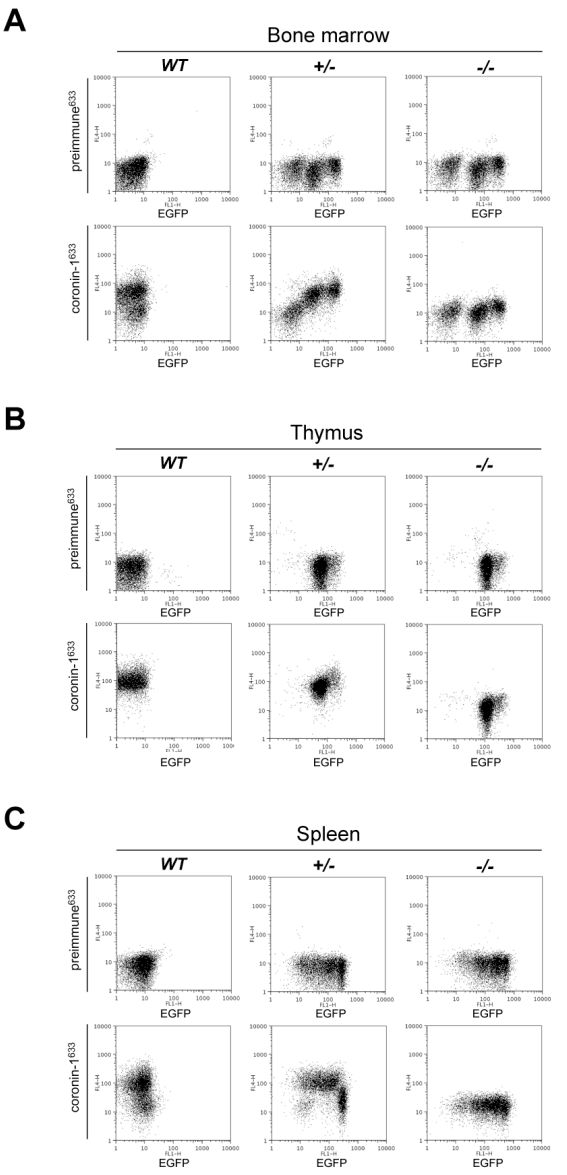

Fig. 23 Coronin-1 and GFP expression in coronin-1 knock-out mice. Single cell suspensions of the indicated organs of homozygous (-/-), heterozygous (+/-) and wildtype (WT) coronin-1 knock-out mice were fixed in 2% paraformaldehyde for one hour on ice and stained with AlexaFluor633-conjugated IgGs of either the preimmune (background staining control) or anti-coronin-1 rabbit serum No.1002. Antibody incubations were performed in 0.2% saponin / 2% BSA in PBS to permeabilize the cells. AlexaFluor633 and GFP fluorescence were then analysed by flow cytometry. Representative FACS profiles of coronin-1 and GFP expression in **(A)** bone marrow **(B)** thymus and **(C)** spleen.

functional characterisation of the UTRs of the coronin-1 locus would allow to gain insight into the regulation of coronin-1 expression dependent on the developmental stage of leukocyte subsets and its corresponding functional requirements for coronin-1.

3.3.4 Homozygous coronin-1 K.O. mice do not display developmental defects in the bone marrow and the thymus

Leukocytes are generated from precursors originating from the bone marrow (see Fig.2). Specifically, the crucial developmental stages of the entire B-cell and myeloid lineage are found in the bone marrow (see paragraph 1.4.1). T-lymphocytes develop in the thymus from so far unidentified precursors which immigrate from the bone marrow into the thymus (Miller and Osoba, 1967, and Fig.7). Taking the specific expression of coronin-1 in all leukocyte subsets into account it was investigated whether coronin-1 expression was required for the development of leukocyte subsets.

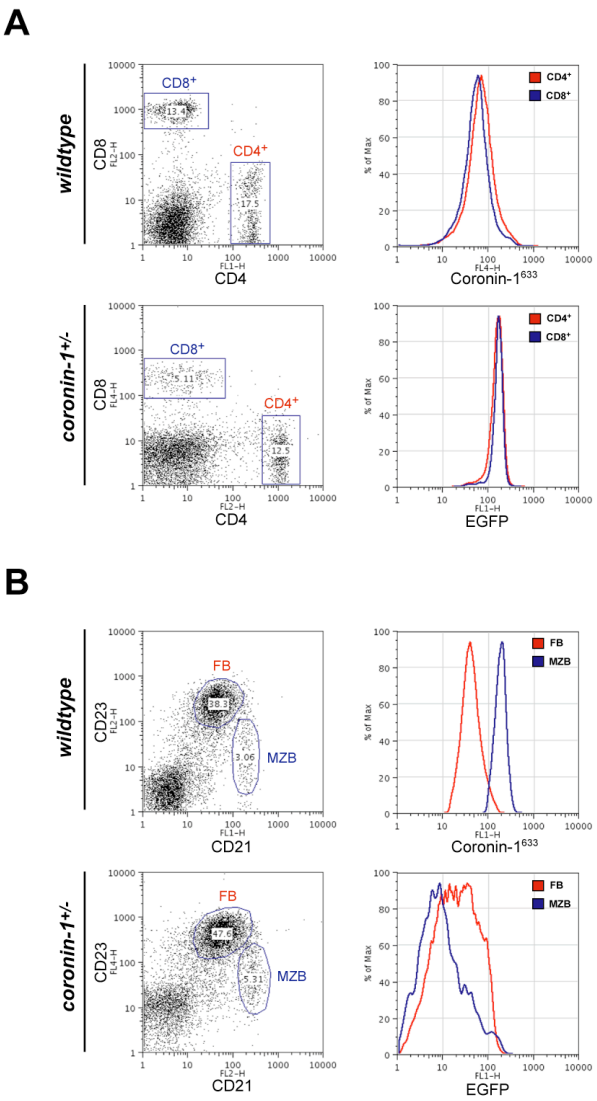

Fig. 24 Analysis of coronin-1 and EGFP expression in lymphocyte subsets of the spleen. Single cell suspensions of the spleen of either heterozygous coronin-1 K.O. mice (coronin-$1^{+/-}$) or wildtype littermates were stained with fluorophore labeled monoclonal antibodies directed against the indicated lymphocyte subsets. Subsequently, cells were fixed with 2% PFA, stained with AlexaFluor633 anti-coronin-1 IgGs in the presence of 0.2% saponin and analysed by flow cytometry. Gates were set to identify CD4 and CD8 positive T-lymphocytes (**A**) or follicular (FB) and marginal zone (MZB) B-cells (**B**). Signal intensities for EGFP and the coronin-1 staining for cells within the indicated gates were then displayed in histograms.

3.3.4.1 Flow cytometric analysis of leukocyte subsets in the bone marrow

Using flow cytometry and antibodies directed against the various leukocyte subtypes the composition of leukocyte populations in bone marrow and thymus was analysed. B-lymphocyte development in the bone marrow can be tracked using CD19 (or equivalently B220), c-kit and IgM surface expression as markers (Fig.4, for review see Ceredig and Rolink, 2002, and references therein). The earliest stage

being specific for the B-cell lineage is referred to as Pro-B and is characterised by being negative for CD19/B220 but highly positive for c-kit. Pro-B cells give raise to first Pre-BI and subsequently Pre-B2 cells which are positive for CD19/B220 but gradually loose c-kit expression. From Pre-B2 cells immature B-cells ($CD19^{+}/B220^{+}/IgM^{+++}/IgD^{-}$) are generated which then develop into mature B-cells ($CD19^{+}/B220^{+}/IgM^{++}/IgD^{++}$). Analysis of the myeloid lineage was performed employing antibodies directed against CD11b which is expressed by all developmental stages. The results of the flow cytometric analysis of B-cell and myeloid cell development in the bone marrow is shown in Fig.25. All analysed subsets appeared normal with no differences in relative numbers indicating that coronin-1 deficiency does not affect B-cell or myeloid cell development.

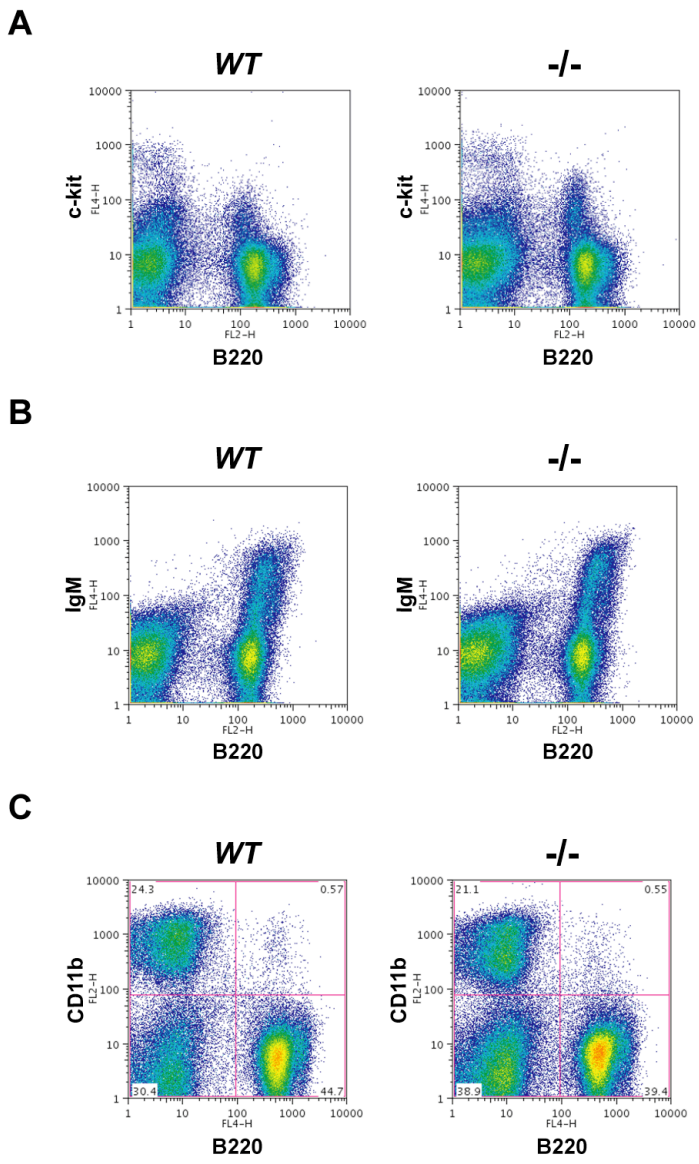

Fig. 25 Development of leukocyte subsets in the bone marrow of coronin-1 deficient mice. Single cell suspensions of the bone marrow of 6 weeks old homozygous (**-/-**) or wildtype (**WT**) coronin-1 K.O. mice were analysed by flow cytometry using antibodies directed against the indicated leukocyte markers. Shown are flow cytometry profiles of bone marrow cell suspensions detecting (**A**) the early stages of B-lymphocyte development using the stem cell marker c-kit and the B-cell lineage marker B220, (**B**) the intermediate and mature stages of B-lymphocyte development using IgM and B220 as markers and (**C**) cells of the myeloid lineage as assessed by the expression of CD11b but not B220.

3.3.4.2 Analysis of T-cell development by flow cytometry and histology

T-lymphocyte development in the thymus proceeds through a series of well-defined differentiation steps which are classically characterised based on the surface expression of CD4 and CD8 (Zuniga-Plücker, 2004 and Fig.7). $CD4^{-}CD8^{-}$ double negative (DN) thymocytes

represent the earliest stage of T-cell development. DN thymocytes then become $CD4^+CD8^+$ double positive (DP) thymocytes and lastly mature into single positive (SP) $CD4^+$ or $CD8^+$ T-cells which emigrate from the thymus to establish the peripheral T-cell pool. T-cell development is dependent on the organisation of the thymus into discrete cortical and medullary areas, each of which is characterised by the presence of particular stromal cell types, as well as thymocyte subsets at defined maturation stages. DN and DP thymocytes are found in cortical regions whereas maturation of single positive T-cells through positive and negative selection occurs in the medulla (refer to Fig.7).

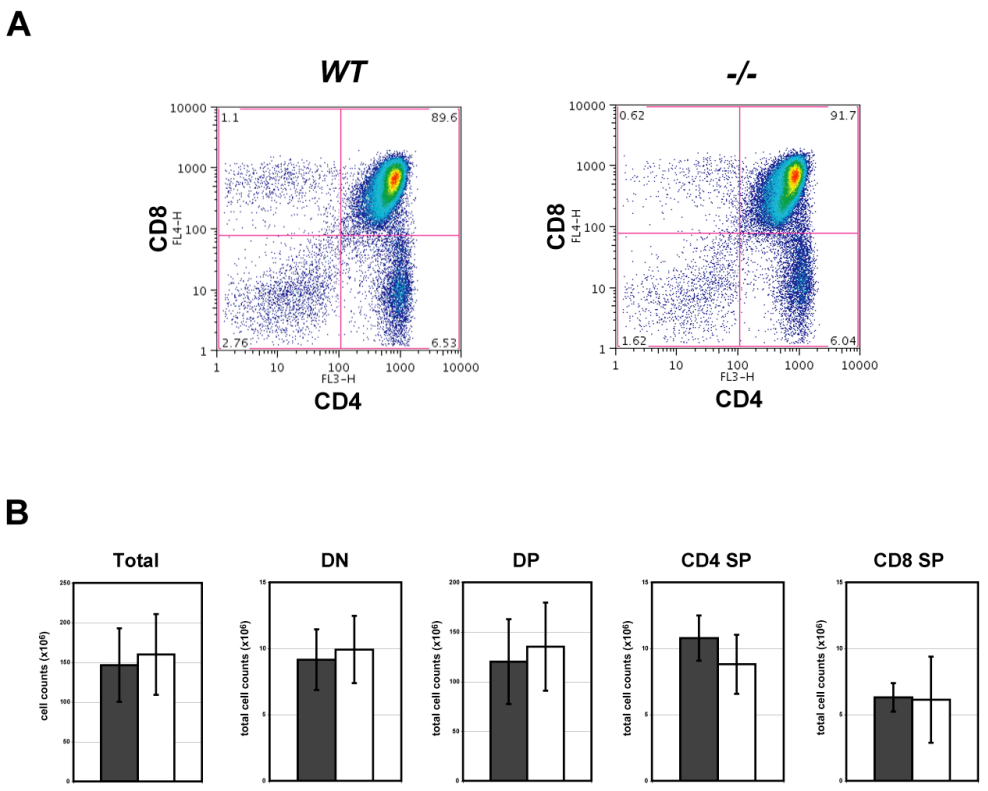

Fig. 26 T-cell development in the thymus of coronin-1 deficient mice. Single cell suspensions of the thymus of 6 weeks old homozygous (**-/-**) or wildtype (**WT**) coronin-1 K.O. mice were analysed by flow cytometry using antibodies directed against the indicated thymocyte subsets (CD4/CD8 double-negative (**DN**), double-positive (**DP**) and single-positive (**SP**) thymocytes). Cells were counted using a Neubauer chamber. Subset specific cell numbers were calculated by referring the percentage of a certain cell type (as determined by flow cytometry) to the total cell counts. (**A**) Representative flow cytometry profiles of thymic cell suspensions. (**B**) Total and subset specific thymocyte cell counts. Filled bars: wildtype, open bars: coronin-1 K.O.. Data are means +/- SD of 5 animals (n=5).

To assess T-cell development in coronin-1 deficient mice, flow cytometry of single cell suspensions as well histological analysis of thymic cryosections were employed. For flow cytometry, single cell suspensions of thymi of homozygous coronin-1 K.O. mice and wildtype littermates were subjected to a staining with antibodies directed against CD4 and CD8 which allowed the determination of the relative numbers of the various thymocyte subsets. Absolute numbers for DN, DP and SP thymocytes were obtained by determining first the total cell

count of the thymic cell suspension and then referring the percentage of a certain cell type (as determined by flow cytometry) to the total cell counts. As shown in Fig.26 all analysed thymocyte subsets (DN, DP and SP) were found to be present in normal relative and absolute numbers. No detectable difference between wildtype and homozygous coronin-1 K.O. mice was observed.

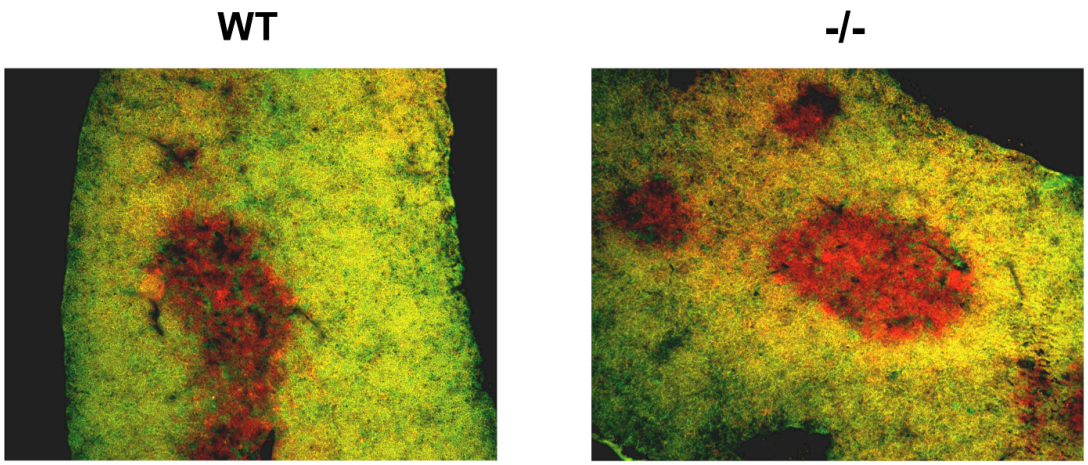

Fig. 27 Immunohistochemical analysis of thymic cryosections from wildtype (**WT**) and homozygous (**-/-**) coronin-1 K.O. mice. Cryosections were acetone-fixed and stained with an APC-labeled monoclonal antibody against CD4 (red staining) and a FITC-labeled monoclonal anti-CD8 antibody (green staining). Magnification: 10x. Courtesy of C. Blum and H. R. Rodewald.

In collaboration with Hans-Reimer Rodewald and Carmen Blum at the University Ulm, Germany, thymi of homozygous coronin-1 K.O. and wildtype littermates were analysed histologically. For this purpose, cryosections were fixed in acetone and stained with fluorophore-labeled monoclonal antibodies directed against CD4 and CD8. Consistent with the results of the flow cytometric analysis of thymocyte subsets in the thymus no differences in the overall structure as well as in the distribution of thymocyte subsets in cortical and medullary regions within the sections was observed (Fig.27). We therefore conclude that T-cell development in the thymus occured normally in the absence of coronin-1 expression.

3.3.5 Coronin-1 deficiency affects the peripheral immune system

Mature lymphocytes generated in the bone marrow and the thymus emigrate into the periphery to establish defined lymphocyte pools with their discrete, organ-dependent function. Having shown no developmental defects for the B-, T- and myeloid cell lineage in the bone marrow and thymus of coronin-1 K.O. mice it was analysed whether coronin-1 deficiency could affect lymphocyte populations in the periphery, namely peripheral blood, spleen and lymph nodes.

3.3.5.1 Analysis of leukocyte populations in the spleen and lymph nodes of coronin-1 deficient mice

Analogous to the analysis of T-cell development in the thymus (section 3.3.4.2) the composition of leukocyte populations in the spleen and lymph nodes of coronin-1 deficient mice was analysed by flow cytometry of single cell suspensions and by histology of cryosections. For flow cytometry fluorophore labeled monoclonal antibodies were used to detect B-cells by CD19 ($CD19^+$), T-lymphocytes by CD4 ($CD4^+$) or CD8 ($CD8^+$) and myeloid cells by CD11b ($CD11b^+$) expression. Relative and absolute numbers for the various leukocyte subsets in spleen and lymph nodes were determined as described in section 3.3.4.2.

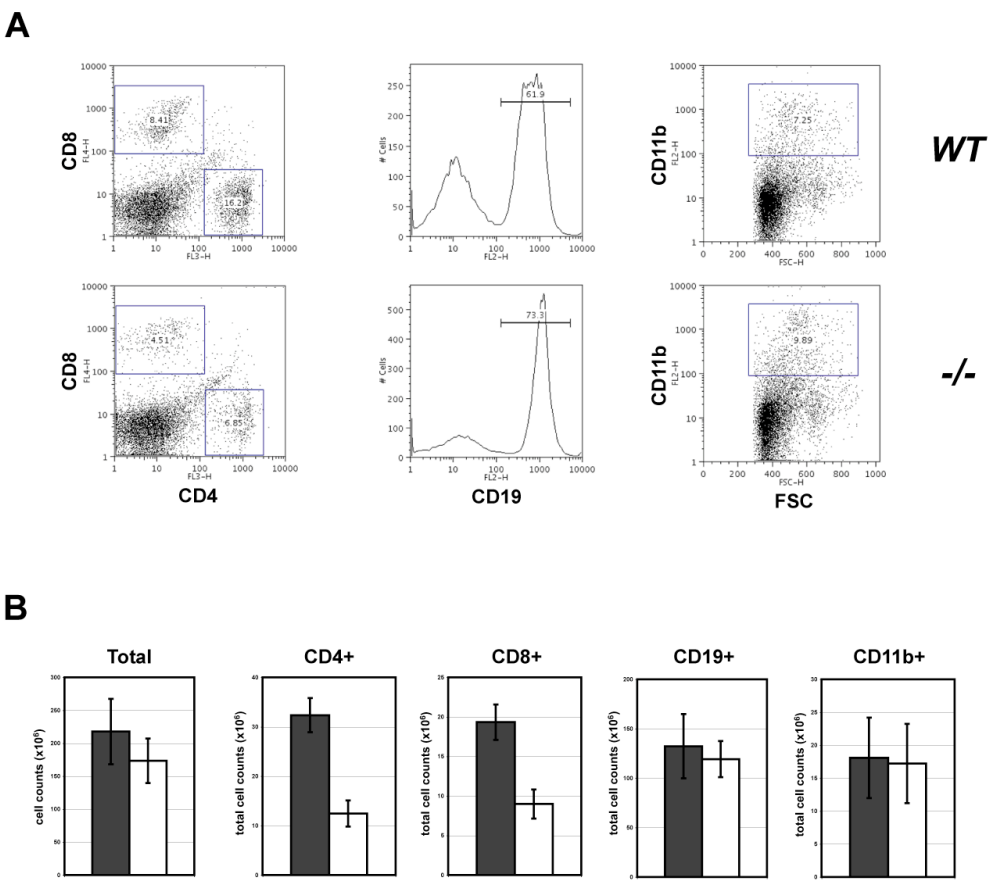

Fig. 28 Splenic leukocyte populations in coronin-1 deficient mice. Single cell suspensions of the spleen of 6 weeks old homozygous (**-/-**) or wildtype (**WT**) coronin-1 K.O. mice were analysed by flow cytometry using antibodies directed against the indicated leukocyte markers. Cells were counted using a Neubauer chamber. Leukocyte specific cell numbers were calculated by referring the percentage of a certain cell type (as determined by flow cytometry) to the total cell counts. (**A**) Representative flow cytometry profiles of spleen cell suspensions. (**B**) Total and leukocyte specific cell counts. Filled bars: wildtype, open bars: coronin-1 K.O.. Data are means +/- SD of 5 animals (n=5).

In the spleen, numbers of both $CD4^+$ and $CD8^+$ T-lymphocytes were found to be reduced by about 50% in homozygous coronin-1 K.O. mice compared to wildtype littermates. In contrast, $CD19^+$ B-cells as well as $CD11b^+$ myeloid cells were only slightly diminished (Fig.28). For lymph nodes, an about 5-fold reduction in total cell counts was observed due to an absolute reduction of T-, B- and myeloid cells. However, the relative proportions of B- and myeloid cells were enriched, whereas T-cells were strongly diminished (Fig.29).

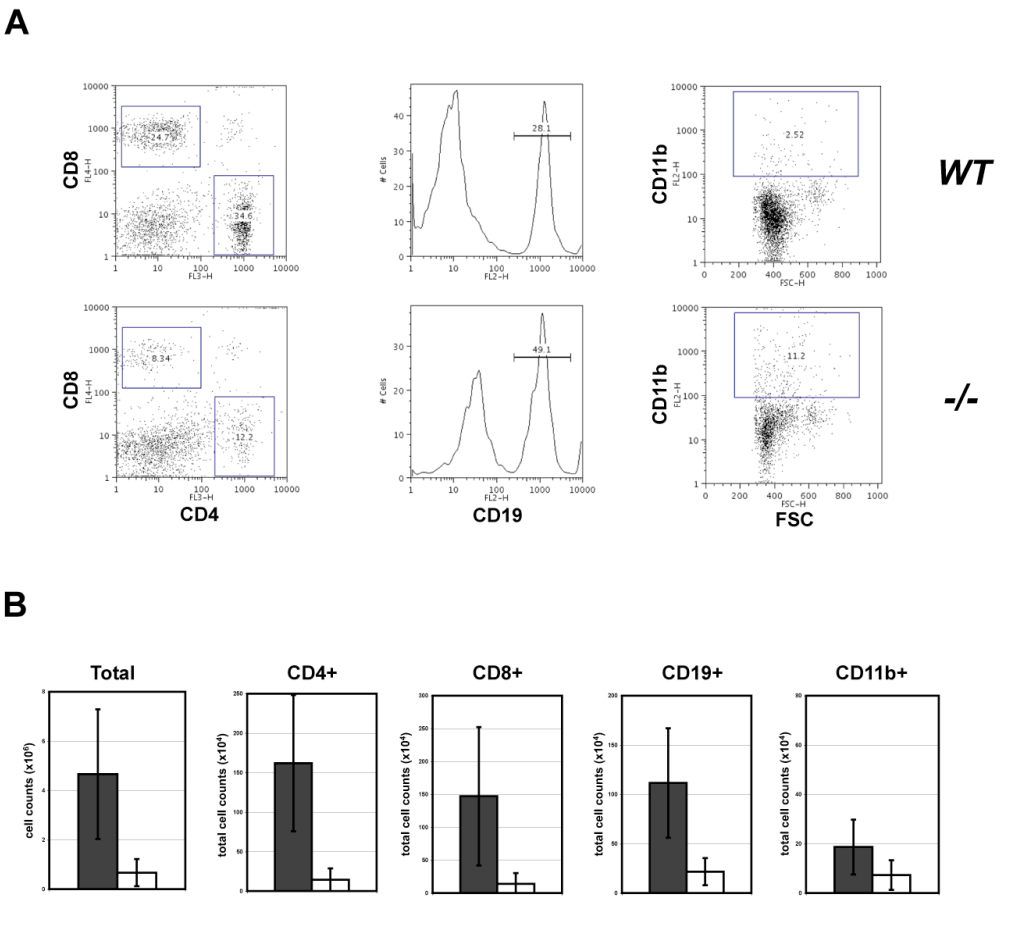

Fig. 29 Leukocyte populations in lymph nodes of coronin-1 deficient mice. Single cell suspensions of inguinal lymph nodes of 6 weeks old homozygous (**-/-**) or wildtype (**WT**) coronin-1 K.O. mice were analysed by flow cytometry using antibodies directed against the indicated leukocyte markers. Cells were counted using a Neubauer chamber. Leukocyte specific cell numbers were calculated by referring the percentage of a certain cell type (as determined by flow cytometry) to the total cell counts. (**A**) Representative flow cytometry profiles of inguinal lymph node cell suspensions. (**B**) Total and leukocyte specific cell counts. Filled bars: wildtype, open bars: coronin-1 K.O.. Data are means +/- SD of 5 animals (n=5).

These observations were further substantiated by histological analysis of cryosections. Generally, the bulk of the spleen is composed of red pulp, where removal of red blood cells takes place. Lymphocytes surround the arterioles entering the spleen, forming areas of white pulp. The inner region of the white pulp is divided into a periarteriolar sheet (PALS), containing mainly T-cells and a flanking B-cell corona (see Fig.5 A). Compared to wildtype littermates splenic cryosections of homozygous coronin-1 K.O. mice (Fig.30) were

characterised by a strong depletion of T-cells (as detected by anti-Thy1.2 staining) from the PALS, which were, instead, enriched in B-cells (as detected by anti-B220 staining).

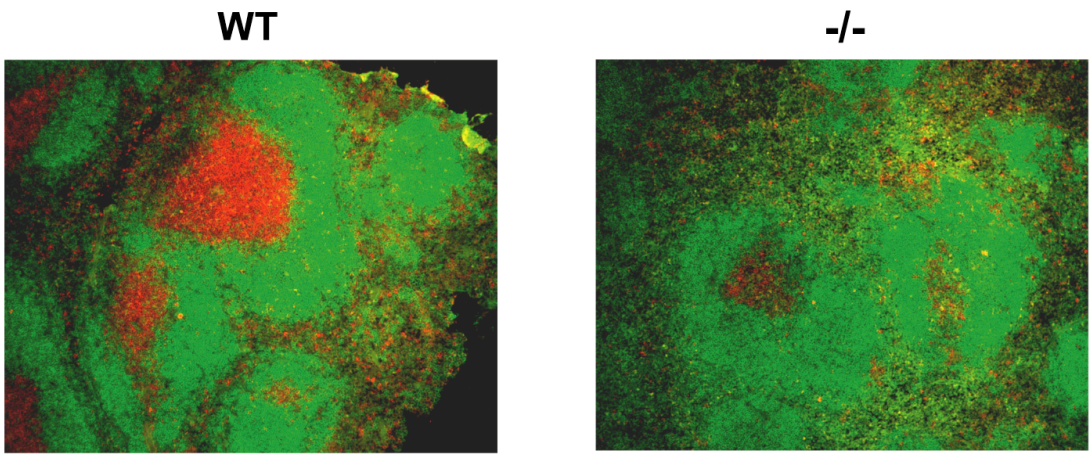

Fig. 30 Immunohistochemical analysis of splenic cryosections from wildtype (**WT**) and homozygous (**-/-**) coronin-1 K.O. mice. Cryosections were acetone-fixed and stained with an FITC-labeled monoclonal antibody against B220 (green staining) and a PE-labeled monoclonal anti-Thy1.2 antibody (red staining). Magnification: 10x. Courtesy of C. Blum and H. R. Rodewald.

Histologically, lymph nodes consist of an outermost cortex and an inner medulla. The cortex is composed of an outer layer of B-cells which are organised into lymphoid follicles, and extensive paracortical areas (also referred to as T-cell zones) made up mainly of T-cells (see Fig.5 B). In comparison to wildtype littermates, lymph nodes of coronin-1 deficient mice were found to be severly reduced in overall size and to be largely depleted of T-cells in the paracortical areas (Fig.31). In conclusion, the absence of coronin-1 expression leads to a paucity of T-lymphocytes in secondary lymphoid organs.

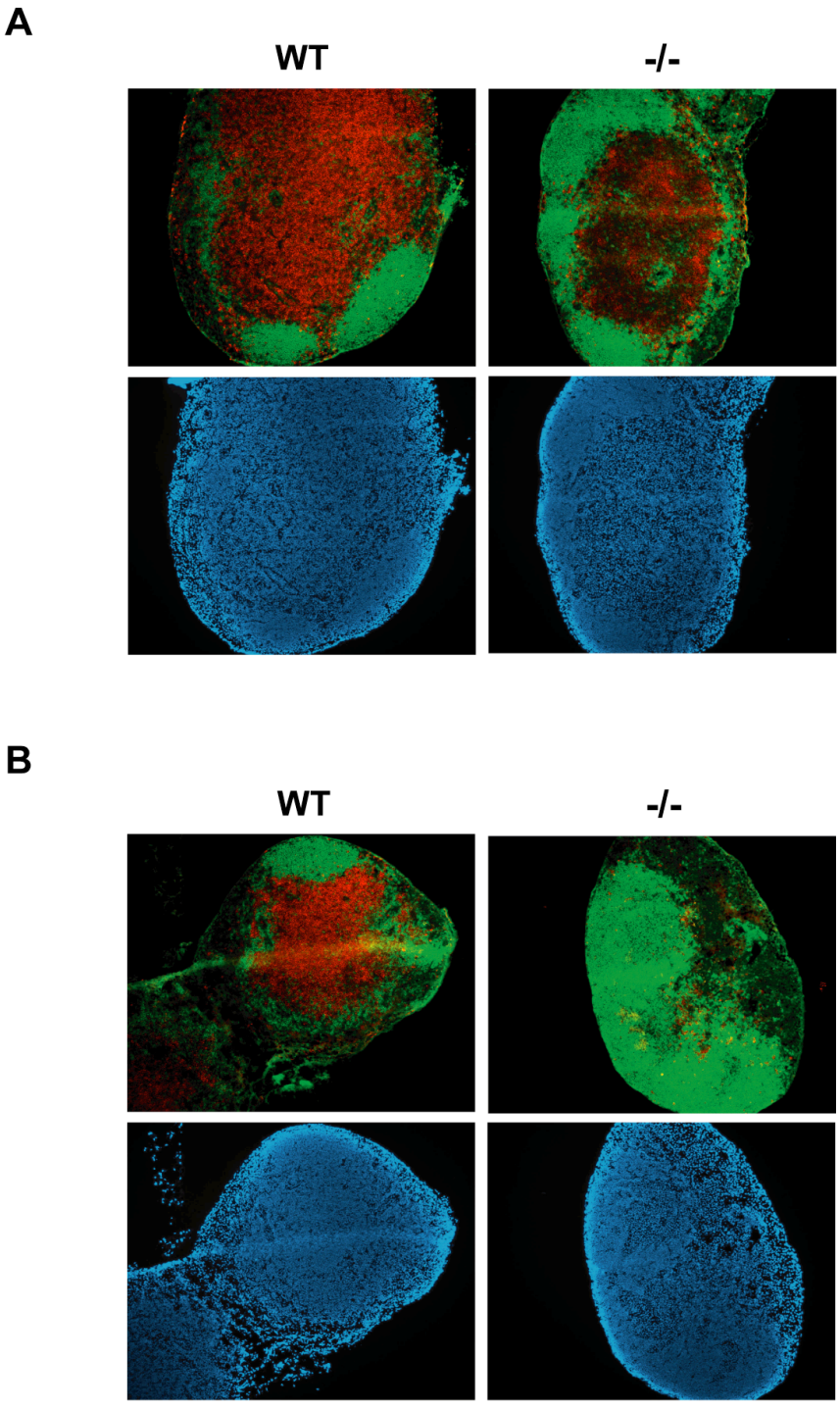

Fig. 31 Immunohistochemical analysis of lymph node cryosections from wildtype (**WT**) and homozygous (**-/-**) coronin-1 K.O. mice. Cryosections were acetone-fixed and stained with a FITC-labeled monoclonal antibody against B220 (green staining), a PE-labeled monoclonal anti-Thy1.2 antibody (red staining) and DAPI (blue staining). (**A**) inguinal, (**B**) cervical lymph nodes. Magnification: 10x. Courtesy of C. Blum and H. R. Rodewald.

3.3.5.2 Coronin-1 deficient mice display abnormalities in peripheral blood composition

Given the specific depletion of T-lymphocytes from secondary lymphoid organs, the blood composition of homozygous coronin-1 K.O. mice was analysed. For this purpose, tail blood of homozygous coronin-1 K.O. mice and wildtype littermates was subjected to hematological analysis on an automated ADVIA hematology system (done in collaboration with Imke Albrecht and the Hämatologielabor, Kantonspital Basel, Switzerland). As summarised in table 11 leukocyte counts were found to be reduced in homozygous coronin-1 K.O. mice when compared to wildtype littermates. In contrast, all other parameters were not affected. Since the ADVIA analysis revealed that a reduction of lymphocyte counts accounts for the reduction in peripheral leukocyte numbers, peripheral blood lymphocytes (PBL) were prepared and stained for flow cytometry to assess the contribution of individual lymphocyte subsets. Results of this analysis are shown in table 12. Absolute T-lymphocyte numbers in peripheral blood were drastically reduced whereas B-cells ($CD19^+$) and myeloid cells ($CD11b^+$) were less severly affected. These results further corroborate the finding that the absence of coronin-1 expression leads to a strong deficiency within the peripheral T-lymphocyte population.

		WT	-/-
Leukocytes	($x10^9$/l)	15.64 ± 5.77	4.77 ± 1.4
Erythrocytes	($x10^{12}$/l)	10.4 ± 2	10.12 ± 1.47
Hemoglobin	(g/l)	161.6 ± 22.53	164.05 ± 28.9
Thrombocytes	($x10^9$/l)	1419.88 ± 265	1101.5 ± 265
Reticulocytes	($x10^9$/l)	413.54 ± 116.1	393.4 ± 138.1
Neutrophils	($x10^9$/l)	1.18 ± 1.37	0.54 ± 0.3
Lymphocytes	($x10^9$/l)	13.45 ± 5.17	3.74 ± 1.36
Monocytes	($x10^9$/l)	0.54 ± 0.43	0.22 ± 0.19
Eosinophils	($x10^9$/l)	0.4 ± 0.23	0.25 ± 0.09
Basophils	($x10^9$/l)	0.03 ± 0.02	0

Table 11 Peripheral blood composition as determined on an ADVIA hematology system. Tail blood of homozygous coronin-1 K.O. mice (**-/-**, n = 19) and wildtype littermates (**WT**, n = 13) was analysed using an ADVIA hematology system in collaboration with the Hämatologielabor, Kantonspital Basel. Courtesy of I. Albrecht.

		WT	-/-
$CD4^+$	($x10^4$/ml)	76.6 ± 12.7	4.4 ± 2.4
$CD8^+$	($x10^4$/ml)	51.2 ± 9.7	3.6 ± 2
$CD19^+$	($x10^4$/ml)	168.5 ± 48.9	48.6 ± 16.9
$CD11b^+$	($x10^4$/ml)	64.7 ± 25.4	25.8 ± 13

Table 12 Leukocyte populations in peripheral blood as determined by FACS analysis. Peripheral blood of homozygous (**-/-**) or wildtype (**WT**) coronin-1 knock-out mice was analysed by flow cytometry using antibodies directed against the indicated leukocyte subsets. Before subjecting to staining, erythrocytes were lysed. Cells were counted using a Neubauer chamber and total cell counts were corrected to 1 ml peripheral blood. Subset specific cell numbers were calculated by referring the percentage of a certain cell type (as determined by flow cytometry) to the total cell counts. Data are means +/- SD of 5 animals (n=5).

3.3.6 Reconstitution of hematopoietic and lymphoid organs in wildtype and coronin-1$^{-/-}$ mixed bone marrow chimaeras

Homozygous coronin-1 knock-out mice were shown to have a strong deficiency within the peripheral T-lymphocyte population. In order to adress the question at which stages of T-lymphocyte development the defect occurs the ability of coronin-1 deficient bone marrow cells to reconstitute peripheral lymphocyte compartments was analysed. Therefore, a 50:50 mixture of bone marrow cells of WT (Ly5.1^{+}/GFP^{-}) and coronin-1$^{-/-}$ (Ly5.2^{+}/GFP^{+}) origin was transferred into sub-lethally irradiated six weeks old C57Bl/6 mice. As a control, mice were reconstituted with either WT or coronin-1$^{-/-}$ cells only. Six weeks later the chimaeric mice were analysed by flow cytometry for reconstitution of B- and T-lymphocyte compartments and for the relative contribution of WT and coronin-1$^{-/-}$ cells. The same experiment was performed with coronin-1$^{-/-}$ mice as recipients which allowed to test whether the absence of coronin-1 expression in cells other than those of the hematopoietic lineage (such as stroma cells) would have an effect on the reconstitution of hematopoietic and lymphoid organs.
Flow cytometric analysis employed monoclonal antibodies directed against the various leukocyte subsets. The origin of the cells in the different cell populations was determined by expression of the Ly5 allelic marker (Ly5.1 or Ly5.2 positive).

3.3.6.1 Reconstitution of the bone marrow

In the bone marrow of mixed bone marrow chimaeras the following B-cell and myeloid cell compartments were analysed: early stages of B-cell development (CD19^{lo}/c-kit^{hi}), intermediate to mature stages of B-cell development (CD19^{hi}/IgM^{lo-hi}) and cells of the myeloid lineage (CD11b^{+}). For all leukocyte compartments in the bone marrow an approximate 50:50 ratio of cells of wildtype (Ly5.1^{+}/GFP^{-}) versus coronin-1$^{-/-}$ (Ly5.2^{+}/GFP^{+}) origin was observed reflecting the capacity of coronin-1$^{-/-}$ cells to reconstitute the bone marrow equally well as their wildtype counterparts (Fig.32 A). These results were independent of the genetic background of the recipient mice (Fig.32 B) indicating that the absence of coronin-1 expression in hematopoietic as well as non-hematopoietic cells does not affect the development of leukocyte subsets in the bone marrow.

3.3.6.2 Reconstitution of the thymus

Analysis of the reconstitution of thymic cell compartments in mixed bone marrow established an approximate 60:40 ratio of cells of wildtype (Ly5.1^{+}/GFP^{-}) versus coronin-1$^{-/-}$ (Ly5.2^{+}/GFP^{+}) origin (Fig.33). Similar to the reconstitution of the bone marrow no strong

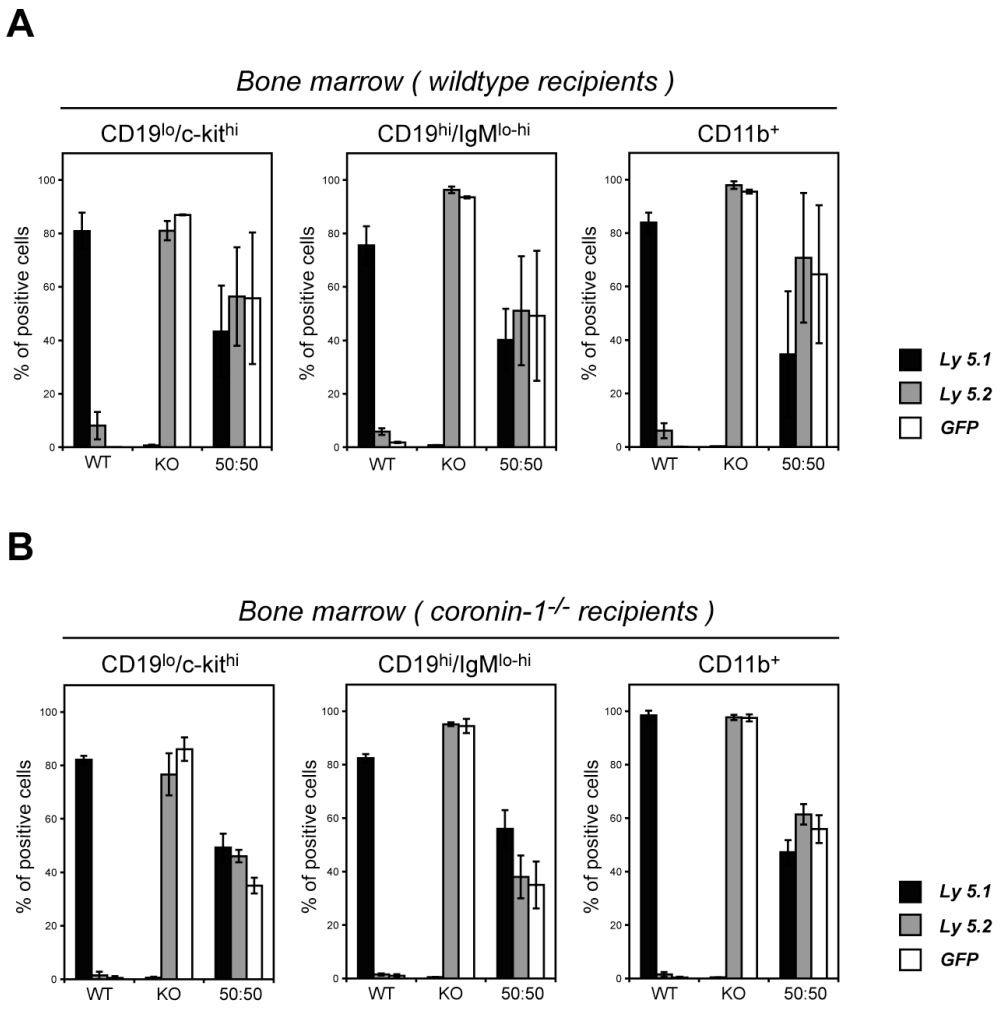

Fig. 32 Bone marrow chimaeras. Sub-lethally irradiated recipient mice of either wildtype (**A**) or coronin-1$^{-/-}$ origin (**B**) received either a 50:50 mixture (**50:50**) of wildtype (Ly 5.1^{+}) and coronin-1$^{-/-}$ (Ly5.2^{+}) bone marrow cells or bone marrow cells of either origin only (**WT** or **KO**). Composition and origin of lymphoid cells in chimaeric mice was analysed six weeks later by flow cytometry employing antibody stainings specifically detecting the indicated lymphocyte subsets and the expression of the allelic Ly5.1 and Ly5.2 markers. The percentage of Ly5.1, Ly5.2 and GFP positive cells within gates identifying specific lymphocyte subsets was determined. Depicted are means ± SD of three mice (n=3) in each group (for (**B**): for transplantation of wildtype bone marrow cells two (n=2) animals were used). Shown is the reconstitution of the bone marrow in (**A**) wildtype and (**B**) coronin-1$^{-/-}$ recipients.

dependence of thymic reconstitution on the background of the recipient mice was observed (Fig.33 B). It should be nevertheless noted that for the CD4 and CD8 single-positive cells a deviation from the 60:40 ratio found for DN and DP subsets towards a 80:20 ratio was apparent which was more pronounced in mixed bone marrow chimaeras set up with coronin -1$^{-/-}$ recipients. This could be indicative for a role of coronin-1 in the late steps of T-cell development just before exit of the T-cells from the thymus. It remains to be established to which extent coronin-1 could be required at this stage either on the side of the T-cell itself or in antigen-presenting cells (and perhaps also stroma cells) which interact with T-cells to ensure proper maturation. However, cells of coronin-1$^{-/-}$ origin gave rise to the various

thymocyte subsets which supports the earlier described finding (section 3.3.4.2) that coronin-1 deficiency does not affect T-cell development in the thymus.

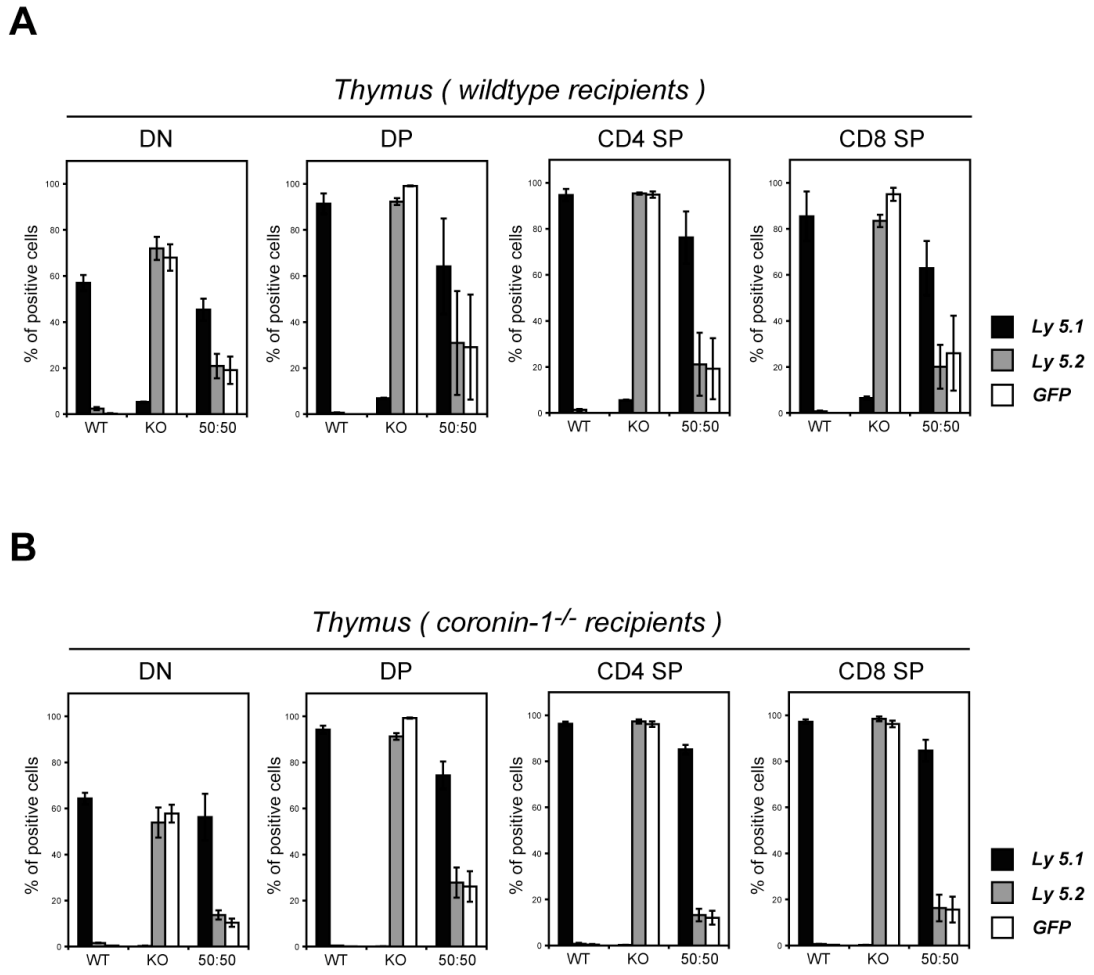

Fig. 33 Bone marrow chimaeras. Sub-lethally irradiated recipient mice of either wildtype (**A**) or coronin-1$^{-/-}$ origin (**B**) received either a 50:50 mixture (**50:50**) of wildtype (Ly 5.1^{+}) and coronin-1$^{-/-}$ (Ly5.2^{+}) bone marrow cells or bone marrow cells of either origin only (**WT** or **KO**). Composition and origin of lymphoid cells in chimaeric mice was analysed six weeks later by flow cytometry employing antibody stainings specifically detecting the indicated lymphocyte subsets and the expression of the allelic Ly5.1 and Ly5.2 markers. The percentage of Ly5.1, Ly5.2 and GFP positive cells within gates identifying specific lymphocyte subsets was determined. Depicted are means ± SD of three mice (n=3) in each group (for (**B**): for transplantation of wildtype bone marrow cells two (n=2) animals were used). Shown is the reconstitution of the thymus in (**A**) wildtype and (**B**) coronin-1$^{-/-}$ recipients. **DN**: CD4 and CD8 double-negative thymocytes; **DP**: CD4 and CD8 double-positive thymocytes; **SP**: CD4 or CD8 single positive thymocytes.

3.3.6.3 Reconstitution of peripheral lymphoid organs

The B-cell compartment in spleen and lymph nodes was found to comprise on average of 60% WT Ly5.1^{+} and 40% coronin-1$^{-/-}$ Ly5.2^{+} cells (Fig.34 and Fig.35). Since the peripheral B-cell compartments were found to be not severly compromised in the absence of coronin-1

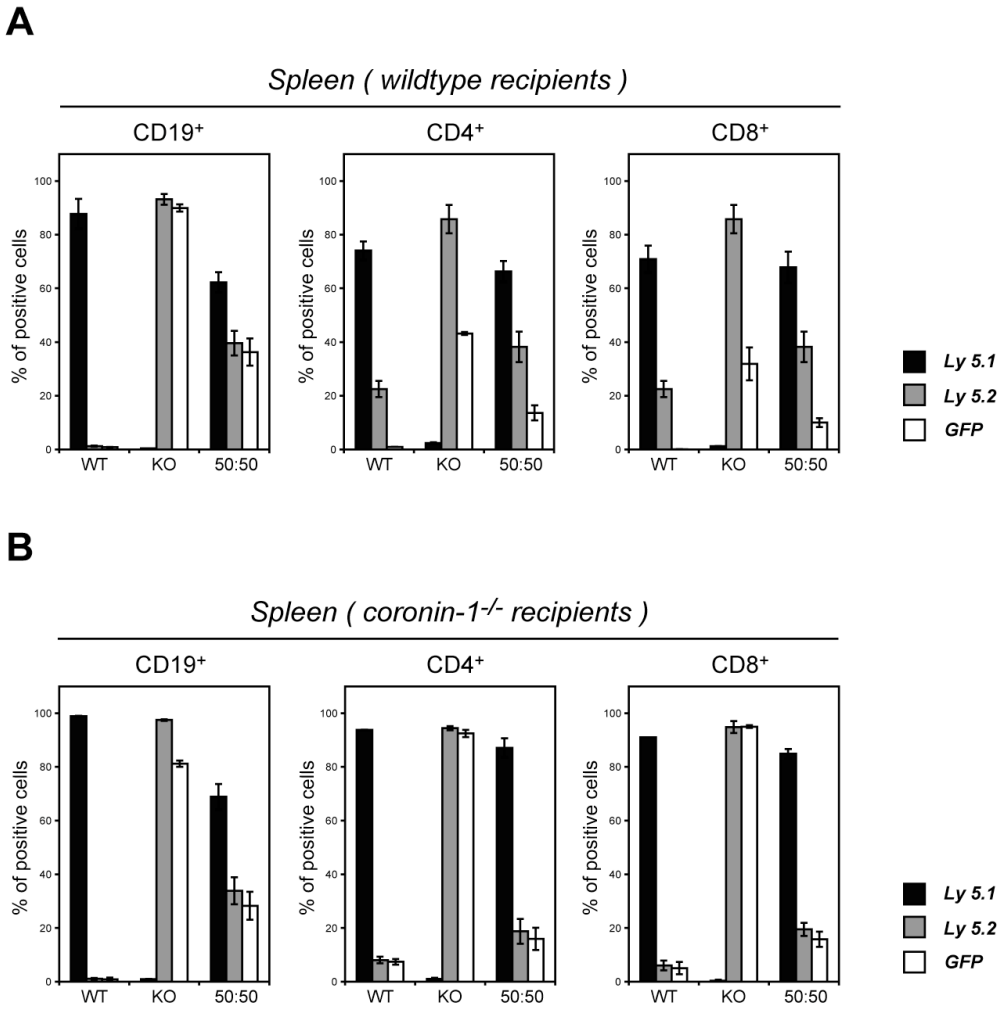

Fig. 34 Bone marrow chimaeras. Sub-lethally irradiated recipient mice of either wildtype (**A**) or coronin-1$^{-/-}$ origin (**B**) received either a 50:50 mixture (**50:50**) of wildtype (Ly 5.1^{+}) and coronin-1$^{-/-}$ (Ly5.2^{+}) bone marrow cells or bone marrow cells of either origin only (**WT** or **KO**). Composition and origin of lymphoid cells in chimaeric mice was analysed six weeks later by flow cytometry employing antibody stainings specifically detecting the indicated lymphocyte subsets and the expression of the allelic Ly5.1 and Ly5.2 markers. The percentage of Ly5.1, Ly5.2 and GFP positive cells within gates identifying specific lymphocyte subsets was determined. Depicted are means ± SD of three mice (n=3) in each group (for (**B**): for transplantation of wildtype bone marrow cells two (n=2) animals were used). Shown is the reconstitution of the spleen in (**A**) wildtype and (**B**) coronin-1$^{-/-}$ recipients.

expression (see paragraph 3.3.5), this ratio was used as a reference for the relative contribution of coronin-1$^{-/-}$ cells to the reconstitution of those populations not affected by coronin-1 deficiency. Not all Ly5.2^{+}/CD19^{+} positive cells were found to express EGFP which is due to specific downregulation of EGFP expression in B-cells (see section 3.3.3 and Fig.24). In contrast to the B-cell compartment, the T-lymphocyte populations in spleen and lymph nodes were mostly derived from WT cells indicating that coronin-1 deficient cells are unable to efficiently reconstitute the peripheral T-cell compartments (Fig.34 and Fig.35). The analysis of chimaerism in peripheral T-cell populations is hampered by the presence of

Ly5.2^{+} cells which most probably are of recipient origin and reflect a pool of radiation resistant peripheral T-cells. Since all T-lymphocytes in homozygous coronin-1$^{-/-}$ deficient mice were found to express EGFP, EGFP instead of Ly5.2 is a reliable marker to determine the contribution of coronin-1 deficient cells to the reconstitution of peripheral T-cell compartments. Taking this into account, we conclude that coronin-1 is involved in peripheral T-lymphocyte survival in and/or homing to peripheral lymphoid organs.

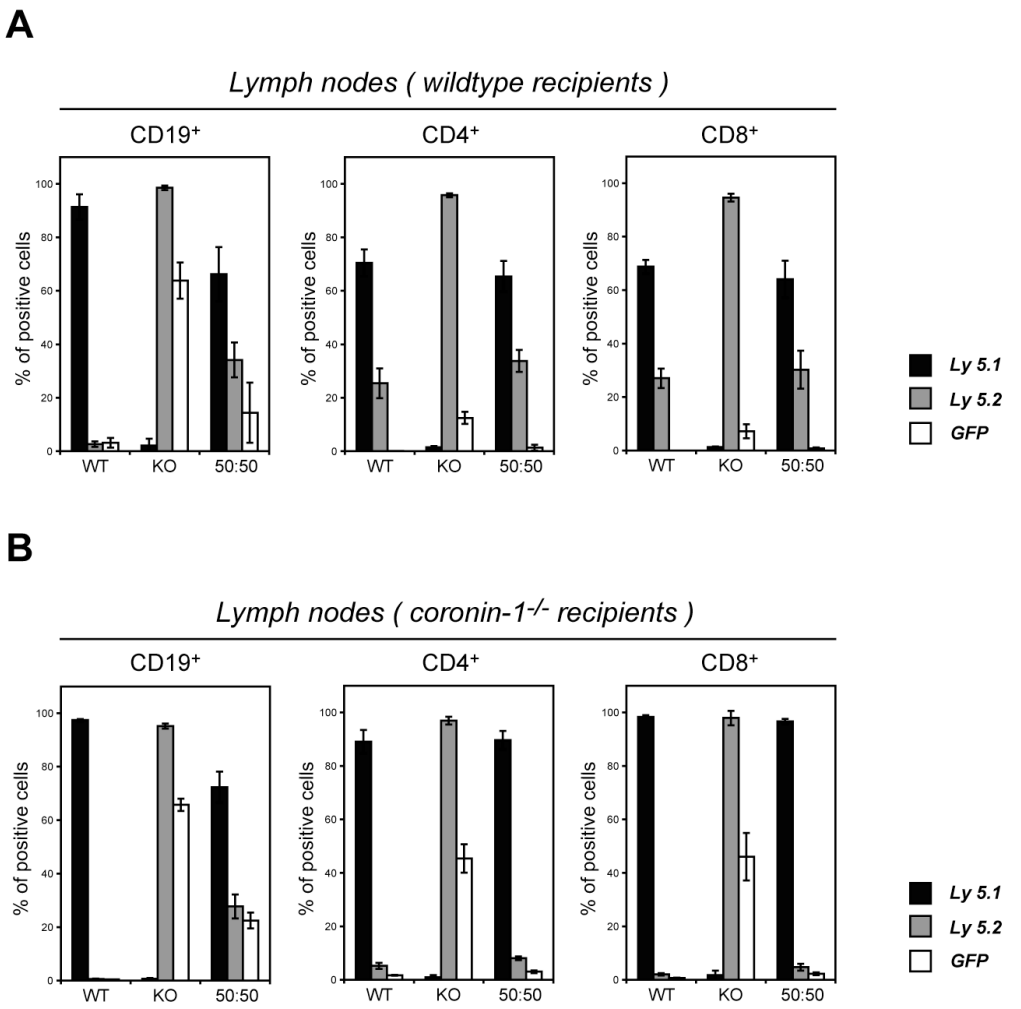

Fig. 35 Bone marrow chimaeras. Sub-lethally irradiated recipient mice of either wildtype (**A**) or coronin-1$^{-/-}$ origin (**B**) received either a 50:50 mixture (**50:50**) of wildtype (Ly 5.1^{+}) and coronin-1$^{-/-}$ (Ly5.2^{+}) bone marrow cells or bone marrow cells of either origin only (**WT** or **KO**). Composition and origin of lymphoid cells in chimaeric mice was analysed six weeks later by flow cytometry employing antibody stainings specifically detecting the indicated lymphocyte subsets and the expression of the allelic Ly5.1 and Ly5.2 markers. The percentage of Ly5.1, Ly5.2 and GFP positive cells within gates identifying specific lymphocyte subsets was determined. Depicted are means ± SD of three mice (n=3) in each group (for (**B**): for transplantation of wildtype bone marrow cells two (n=2) animals were used). Shown is the reconstitution of the lymph nodes in (**A**) wildtype and (**B**) coronin-1$^{-/-}$ recipients.

3.3.7 Summary

Homozygous coronin-1 deficient mice appeared healthy and fertile. These mice do not show any detectable coronin-1 expression but instead do express EGFP under the control of coronin-1 regulatory elements. EGFP expression was shown to be a reliable reporter for coronin-1 expression in T-lymphocyte and myeloid cell subsets, but not for certain B-lymphocyte subsets. Analysis of the development of the immune system employing flow cytometry of bone marrow and thymic cell suspensions and histological analysis of the thymus revealed no differences between homozygous coronin-1 deficient mice and wildtype littermates. However, in the periphery of homozygous coronin-1 deficient mice a strong deficiency within the T-lymphocyte population was observed. Relative and absolute numbers of CD4 and CD8 positive T-cells in spleen, peripheral blood and lymph nodes were found to be strongly reduced whereas other leukocyte subsets were not as severely affected. In mixed bone marrow chimaeras coronin-1 deficient bone marrow precursors were shown to be unable to reconstitute peripheral T-lymphocyte subsets but not the B-lymphocyte and myeloid compartments. In conclusion, the deficiency for coronin-1 expression does not affect the development of the immune system but leads to a specific depletion of T-lymphocytes from secondary lymphoid organs.

3.4 Phenotypic analysis of coronin-1 deficient T-cells

Homozygous coronin-1 deficient mice were found to display a strong deficiency within the peripheral T-lymphocyte population. In order to explain this specific defect, coronin-1 deficient T-lymphocyte were subjected to an in-depth functional analysis. The absence of T-cells from the peripheral lymphoid organs could be due a failure to properly develop in the thymus, a deficiency in T-cell homing or the inability of T-cells to survive in the periphery. Since both the cellularity as well as the organisation of the thymus in wildtype and coronin-1 deficient mice were normal (section 3.3.4.2) coronin-1 is unlikely to play a major role during T-cell development.

3.4.1 Coronin-1 deficient T-cells undergo apoptosis

Lymphocytes that fail to receive survival signals, and those that are clonally deleted because they are self-reactive, undergo apoptosis. T-lymphopenia as observed in coronin-1 deficient mice could be due to increased apoptosis within the peripheral T-cell pool. Apoptosis was studied using flow cytometry and APC-labeled AnnexinV. AnnexinV binds to phosphatidylserine exposed on the cell surface of apoptotic cells and can therefore be used to determine the percentage of apoptotic cells within a given cell population. Counterstaining with propidium iodide (PI) was used to differentiate between apoptotic and necrotic cells the latter being propidium iodide positive since they fail to extrude the dye from the cytoplasm. Including fluorophore-labeled monoclonal antibodies directed against CD3 and CD19 allowed to independently check for apoptosis in T-cells and B-cells, respectively.

Staining of thymic cell suspensions of homozygous coronin-1 K.O. mice and wildtype littermates revealed identical annexinV and PI positive cell populations (Fig.36 A). This confirms the finding that coronin-1 deficiency does not lead to defects in thymic T-cell development since a defect in the processes of positive and negative selection would have resulted in increased apoptosis of certain subsets of thymocytes. In contrast, both within the spleen and the lymph nodes the percentage of CD3 positive cells undergoing apoptosis was significantly increased (Fig.36 A). Interestingly, the percentage of apoptotic cells within the B-lymphocyte compartment (as identified by CD19 surface expression) was similar between wildtype and coronin-1 K.O. mice (Fig.36 B). We therefore conclude that apoptosis occurs specifically in the peripheral T-cell populations of coronin-1 deficient mice resulting in peripheral T-cell depletion.

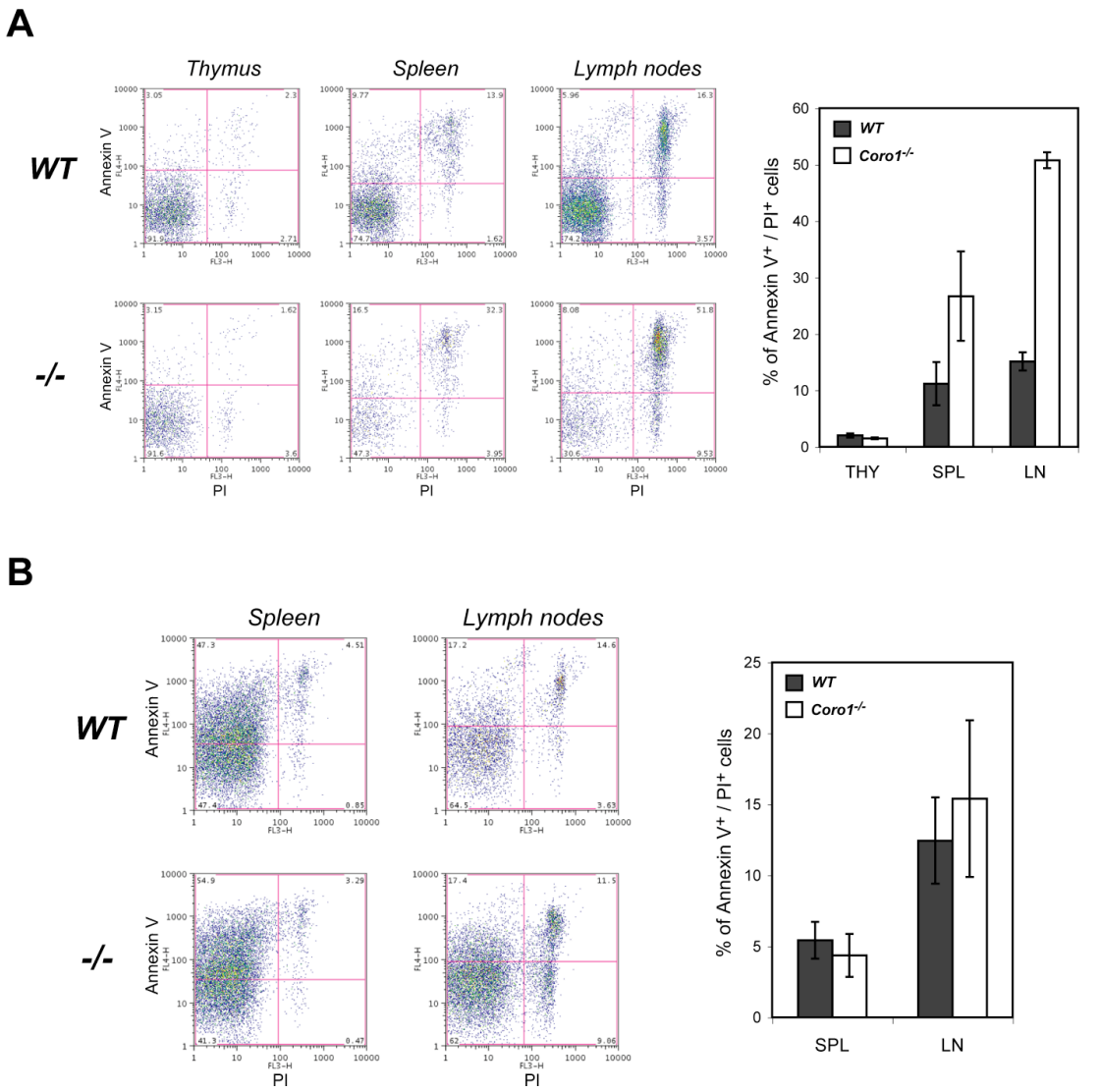

Fig. 36 Apoptosis within lymphocyte subsets in coronin-1 K.O. mice. (**A**) Single cell suspensions of the indicated organs were stained with a monoclonal anti-CD3 antibody, annexin V and propidium iodide (**PI**) and analysed by flow cytometry. The left hand panels show representative PI / Annexin V FACS profiles of CD3 positive cells. The graph on the right shows the percentage of PI / Annexin V double positive cells within the $CD3^+$ gate. Data are means ± SD of 2 animals (n=2). (**B**) Single cell suspensions of the indicated organs were stained with a monoclonal anti-CD19 antibody, annexin V and propidium iodide (**PI**) and analysed by flow cytometry. The left hand panels show representative PI / Annexin V FACS profiles of CD19 positive cells. The graph on the right shows the percentage of PI / Annexin V double positive cells within the $CD19^+$ gate. Data are means ± SD of 2 animals (n=2). **WT**: wildtype, **-/-**: coronin-1 K.O. mice.

3.4.2 Characterisation of T-cell subsets in coronin-1 K.O. mice

Further flow cytometric characterisation of peripheral T-cell subsets for the surface expression of markers identifying naïve versus memory and regulatory T-cells was required to analyse to which extent the subset composition of peripheral T-cell pools in wildtype and coronin-1 K.O. mice differs. As an initial set of markers CD62L and CD44 were chosen.

Naïve T-cells emigrating from the thymus are characterised by the expression of CD62L (L-selectin) which is required for homing of lymphocytes to lymphoid organs (Gallatin et al., 1983). As shown in Fig.37 A analysis of CD62L expression by T-lymphocytes ($CD3^+$) from spleen and lymph nodes revealed that, in contrast to wildtype mice, the few T-cells present in coronin-1 deficient mice were mostly CD62L negative. In thymic cell suspensions of coronin-1 K.O. mice and wildtype littermates the fraction of CD62L positive cells was found to be similar indicating that the lack of CD62L positive cells in the periphery is not due to defects in the thymus. Rather, the absence of CD62L positive cells may be the result of the deletion of naïve, CD62L positive cells in the periphery or due to the expansion of the small number of CD62L negative coronin-1 deficient T-cells.

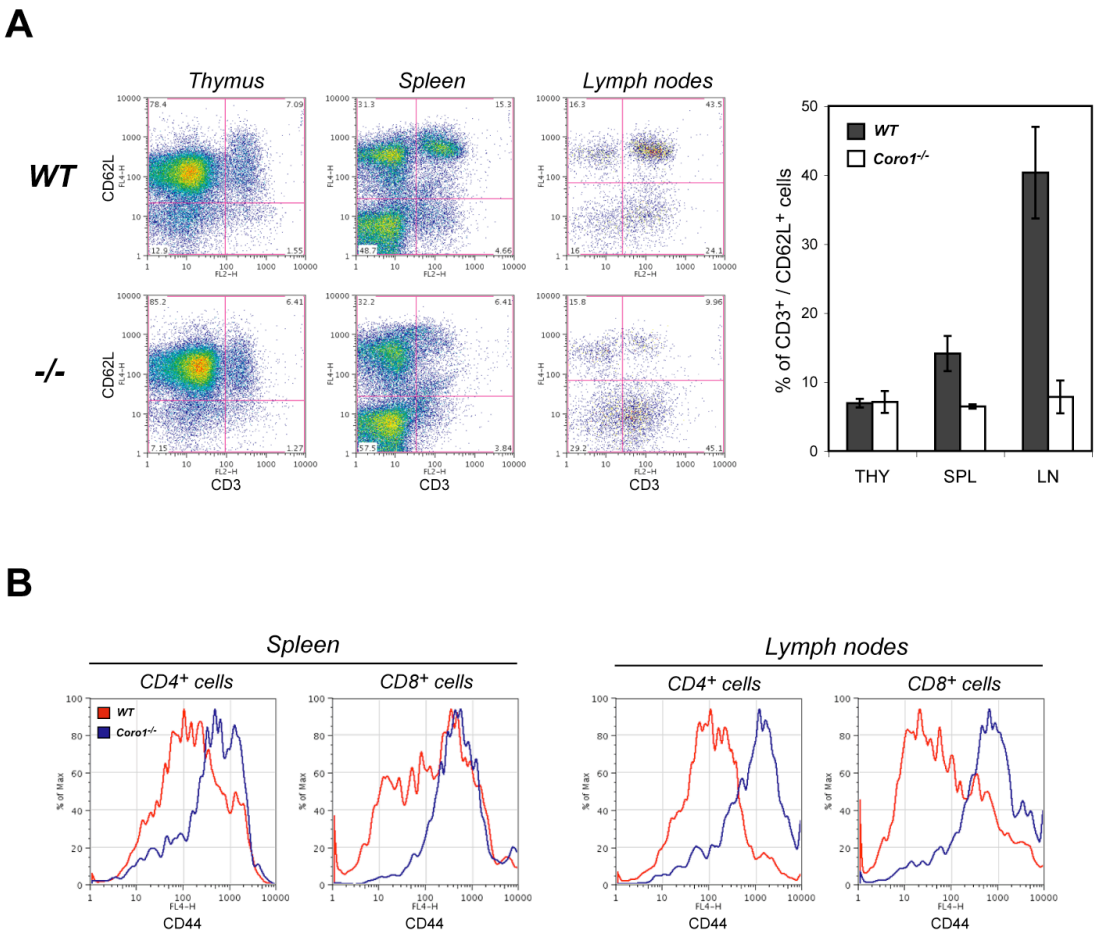

Fig. 37 Characterisation of T-lymphocyte subsets in coronin-1 K.O. mice. (**A**) Single cell suspensions of the indicated organs were stained with monoclonal antibodies directed against CD3 and CD62L and analysed by flow cytometry. The left hand panels show representative CD3 / CD62L FACS profiles. The graph on the right shows the percentage of CD3 / CD62L double positive cells. Data are means ± SD of 3 animals (n=3). **WT**: wildtype, **-/-**: coronin-1 K.O. mice. THY: thymus, SPL: spleen, LN: lymph nodes (**B**) Single cell suspensions of the indicated organs were stained with monoclonal antibodies directed against CD4, CD8 and CD44 and analysed by flow cytometry. Shown are histogram plots for CD44 expression of cells within the indicated gates (CD4 or CD8 positive).

In a depleted lymphoid compartment, i.e. under lymphopenic conditions, naïve T-cells were shown to begin slow proliferation which is independent of cognate antigen recognition but

nevertheless requires recognition of MHC-bound self-peptides (Goldrath and Bevan, 1999, Seddon and Zamoyska, 2002). These expanding subsets of T-cells have an activated or memory-like phenotype as characterised by an increase in CD44 expression (Greenberg and Ridell, 1999; Mackall et al., 1997). Flow cytometric analysis of CD44 expression on T-cells in splenic and lymph node cell suspensions from wildtype and coronin-1 deficient mice showed that coronin-1 deficient T-cell have increased CD44 expression levels (Fig.37 B). This suggests that T-lymphopenia caused by coronin-1 deficiency leads to lymphopenia-driven proliferation of T-cells with a memory-like phenotype to compensate for the depletion of naïve, CD62L positive T-cells.

3.4.3 Homing and survival of coronin-1 deficient T-cells *in vivo*

The observations that coronin-1 deficient T-cells are more prone to apoptosis and are mostly CD62L negative prompted us to assess the capacity of coronin-1 deficient T-cells to home to lymph nodes and to survive within the periphery *in vivo*. To do so, splenic cell suspensions were prepared from either homozygous coronin-1 deficient mice or as wildtype control from mice transgenic for GFP expressed under the ubiquitin promotor (Ubi-GFP, kind gift from D.Finke, University of Basel). These cell suspensions were then adjusted to contain an equivalent amount of CD4 and CD8 positive T-cells. A suspension equivalent of $8x10^6$ T-cells was injected into C57Bl/6 recipient mice via the tail vein. Four or twenty hours post injection the mice were sacrified and peripheral blood lymphocytes (PBLs) as well as single cell suspensions of spleen, inguinal and mesenteric lymph nodes were prepared. Flow cytometry using fluorophore-labeled monoclonal antibodies directed against CD4 and CD8 allowed to determine the percentage of GFP positive T-cells within a given cell suspension.

Four hours post injection CD4 and CD8 positive cells of wildtype (Ubi-GFP) origin could be detected in spleen, inguinal and mesenteric lymph nodes. At the later, twenty hour timepoint wildtype cells were found at similar percentages among the PBL and spleen cell populations whereas their percentage in mesenteric and inguinal lymph nodes increased (Fig.38). This is indicative for the successful homing of wildtype cells to the lymph nodes. In contrast, coronin-1 deficient CD4 and CD8 positive T-cells were found to home to inguinal and mesenteric lymph nodes less efficiently. Between the four and twenty hour timepoint no pronouced increase in the percentage of coronin-1 deficient CD4 and CD8 positive T-cells in mesenteric and inguinal lymph nodes was observed. We therefore conclude that coronin-1 deficient T-cells are defective in homing to the lymph nodes. At the four timepoint this is also reflected by a two-fold higher percentage of coronin-1 deficient T-cells among the PBLs compared to wildtype cells. Given the same number of wildtype and coronin-1 deficient T-cells injected per

recipient animal, this suggests that T-cells of coronin-1 K.O. origin accumulated in the blood due to their inability to home to the lymph nodes. Interestingly, at the twenty hour timepoint percentages of wildtype and coronin-1 deficient T-cells among the PBLs were then found to be similar. Since at the same time the percentage of coronin-1 deficient T-cells in the inguinal and mesenteric lymph nodes did not significantly increase, we conclude that T-cells of coronin-1 K.O. origin not only display a defect in homing to the lymph nodes but also in survival in an *in vivo* context.

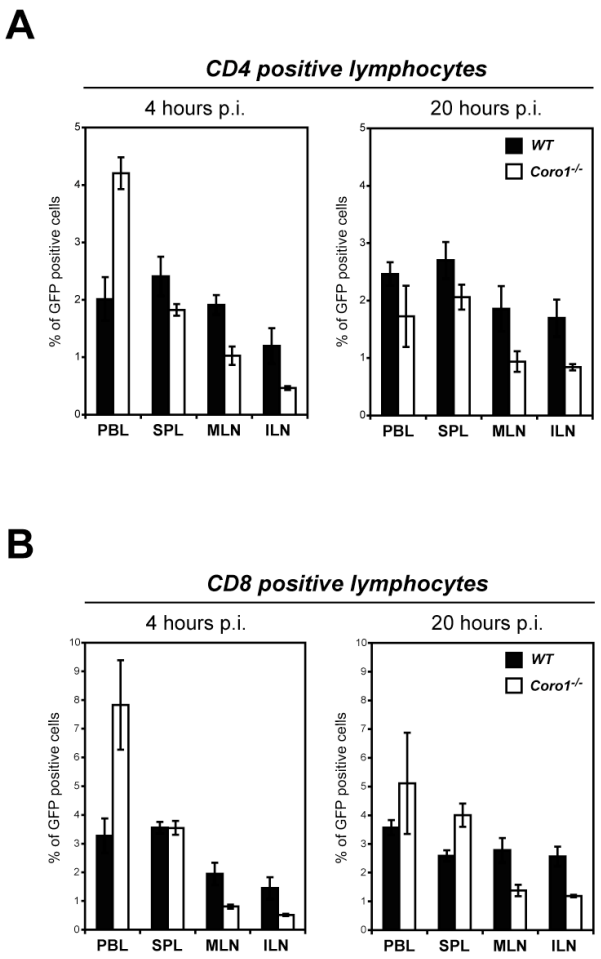

Fig. 38 Homing of coronin-1$^{-/-}$ T-lymphocytes. Splenic cell suspensions in PBS were prepared from either C57Bl/6 mice expressing GFP under the ubiquitin promotor (referred to as **WT**) or from coronin-1$^{-/-}$ (**Coro1$^{-/-}$**) mice and adjusted to contain 4x10^7/ml CD4 and CD8 positive T-cells. Wildtype C57Bl/6 recipient mice then received by tail vein injection 200 µl of this cell suspensions (equals 8x10^6 CD4 and CD8 positive T-cells per mouse). Four or twenty hours post injection peripheral blood lymphocytes (**PBL**) as well as single cell suspensions of spleen (**SPL**), mesenteric (**MLN**) and inguinal (**ILN**) lymph nodes were stained with fluorophore-labeled antibodies directed against CD4 and CD8. Analysis by flow cytometry then allowed to determine the percentage of GFP-positive cells within gates identifying either (**A**) CD4 or (**B**) CD8 positive T-lymphocytes. Shown are mean values ± SD of three mice in each group (n=3).

These findings are in agreement with the observations that coronin-1 deficient T-cells are on one hand more prone to apoptosis (see paragraph 3.4.1) and on the other hand are mostly CD62L negative (see paragraph 3.4.2). Whether coronin-1 deficient T-cells undergo apoptosis because they do not enter the lymph nodes where they would receive stimuli promoting their survival or whether they undergo apoptosis before they reach the lymph nodes needs to be adressed in future experimental work. This further investigations could include performance of homing assays using defined CD62L positive or negative coronin-1 deficient T-cell subsets and analysis of the requirements, such as cytokines, for the survival of coronin-1 deficient T-cells in *in vitro* culture.

3.4.4 Coronin-1 deficient T-cells do not respond to allogeneic MHC stimuli in a mixed lymphocyte reaction

As the depletion of peripheral T-lymphocytes can occur as a result of deficient T-cell stimulation, the capacity of wildtype and coronin-1 deficient T-cells to respond to allogeneic MHC stimuli was analysed. For this purpose, purified splenic T-cells were cocultured with Mitomycin C treated BALB/c spleen cells in a mixed lymphocyte reaction (MLR). The allogeneic MHC stimuli present on non-proliferating BALB/c spleen cells lead to the stimulation of the C57Bl/6 T-cells of wildtype and coronin-1 K.O. origin. As a result of stimulation T-cells start to proliferate. In a MLR, this proliferation is used as a read-out for the ability of T-cells to respond to allogeneic MHC stimuli.

The results of a MLR with wildtype and coronin-1 deficient splenic T-cells are shown in Fig.39 A. In contrast to wildtype T-cells, which responded as expected to the presence of appropriate stimuli by proliferation, the proliferation of coronin-1 deficient T-cells was drastically reduced. These results can be explained on one hand by defects in TCR signaling leading to defective proliferation or on the other hand by a severe defect of coronin-1 deficient cells to survive in the coculture.

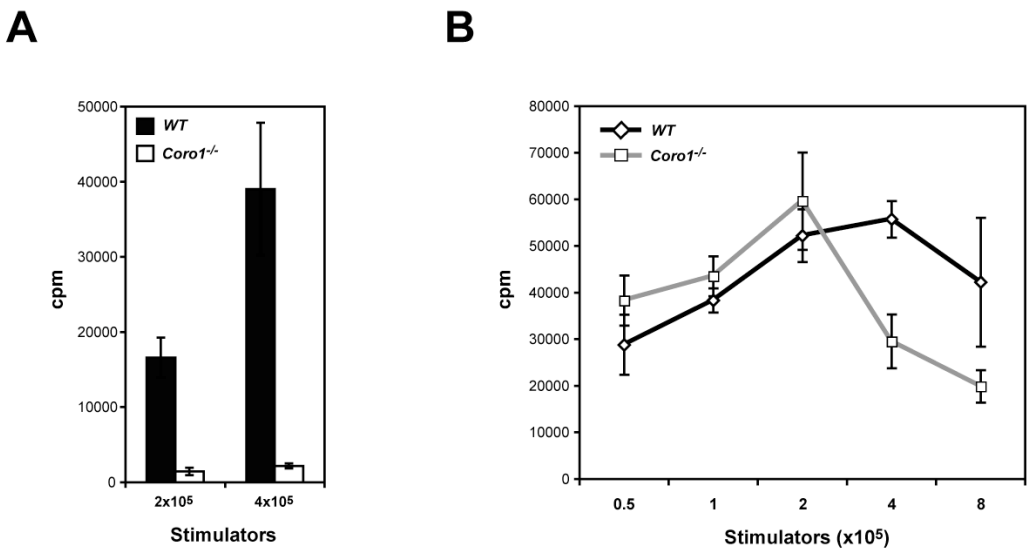

Fig. 39 Mixed Lymphocyte Reaction. (**A**) Mixed lymphocyte reaction using MACS purified splenic T-lymphocytes as responders and allogeneic BALB/c spleen cells as stimulators. $1x10^5$ purified splenic T-cells were cocultured with the indicated amount of mitomycin C treated BALB/c spleen for 3 days. Proliferation upon stimulation by allogeneic MHC stimuli was performed by measuring [^{3}H]-thymidine incorporation by scintillation counting. Shown are mean values of triplicate cultures ± SD. (**B**) Mixed lymphocyte reaction using the indicated amounts of coronin-$1^{-/-}$ or wildtype spleen cells as stimulators and $4x10^5$ BALB/c spleen cells as responders. Cocultures were incubated for 3 days before measuring [^{3}H]-thymidine incorporation by scintillation counting. Shown are mean values of triplicate cultures ± SD.

Further experimental work like analysis of TCR stimulation and downstream signaling pathways or a cytokine mediated (e.g. IL-2) rescue of coronin-1 defcient T-cells in *in vitro* culture is required to thouroughly understand the inability of coronin-1 deficient T-cells to respond to allogeneic MHC stimuli by proliferation.

In order to check whether coronin-1 has a role in antigen presenting cells such as dendritic cells, coronin-1 deficient spleen cells were analysed for their capacity to stimulate BALB/c derived splenic T-cells. In a MLR using varying amounts of wildtype or coronin-1 deficient spleen cells as stimulators and a fixed amount of BALB/c spleen cells as responders, no difference in proliferation was observed up to a 1:2 ratio of stimulators versus responders (Fig.39 B). Increasing the amount of stimulators relative to the responders resulted in a reduction of proliferation of BALB/c spleen cells stimulated by coronin-1 deficient spleen cells. In contrast, using increasing amounts of wildtype spleen cells as stimulators revealed as expected a plateau in proliferation of the responding BALB/c spleen cells. In conclusion, in the absence of coronin-1 expression spleen cells show a similar capacity as wildtype cells to stimulate responding BALB/c cells as long as the responders are provided in excess. It needs to be adressed by additional experiments why as soon as coronin-1 deficient stimulators are in excess over the responding cells a reduction in proliferation of the responders is seen. It has to be noted at this point that from a total of $8x10^5$ cells per well proliferation data could be inconsistent due to the high density of cells per well. It might be that under circumstances of high cell density coronin-1 deficient cells are more prone to cell death due to limiting nutrients or cytokines which would ultimately lead to a less efficient stimulation of responding cells.

3.4.5 Coronin-1 deficient T-lymphocytes show no defects in the actin and tubulin cytoskeleton

Upon encountering an antigen presented on APCs T-cells rapidly undergo substantial membrane and cytoskeletal rearrangements which result in the formation of the immunological synapse between the T-cell and the APC. Formation of the immunological synapse is required for the specificity of the immune response by stabilizing and favoring continous TCR-antigen interaction and consequent activation of T-cells (reviewed in Dustin et al., 2000; Krummel et al., 2002; van den Merwe, 2002). The immunological synapse is characterised by a tight collar of polymerized actin at the T-cell-APC interface and the reorientation of the microtubule-organizing center (MTOC) towards the bound APC (Geiger et al., 1982; Ryser et al., 1982). Coronin-1 has been described as an F-actin interacting molecule that crosslinks the leukocyte plasma membrane with the F-actin cytoskeleton

(Gatfield et al., 2005). This opens the possibility that coronin-1 has a role in T-cell activation events involving membrane dynamisms and regulating actin cytoskeleton rearrangements.

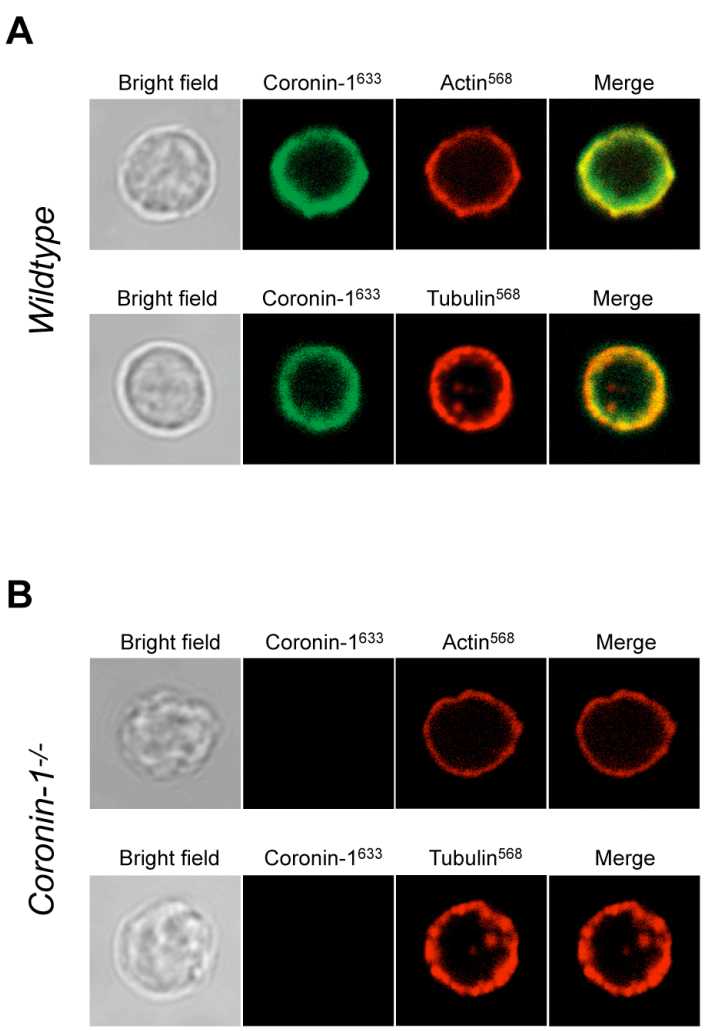

Fig. 40 Actin and tubulin cytoskeleton organisation in resting thymocytes. Thymocytes isolated from coronin-1 K.O. mice and wildtype littermates were allowed to adhere to poly-L-lysine coated glass-slides, fixed with 3% PFA and stained with antibodies directed against coronin-1 and tubulin and appropriate secondary antibodies (coupled to AlexaFluor633 for coronin-1 and to AlexaFluor568 for tubulin). The actin cytoskeleton was stained using AlexaFluor568 coupled Phalloidin. Shown are representative confocal microscopy images for (**A**) wildtype and (**B**) coronin-1$^{-/-}$ thymocytes.

To analyse potential defects of cytoskeletal organisation in coronin-1 deficient T-cells, thymocytes from wildtype and coronin-1 deficient mice were analysed by immunofluorescence staining for F-actin and tubulin and subsequent confocal microscopy. In non-activated thymocytes the morphological appearance as well as the F-actin and the tubulin cytoskeleton were indistinguishable comparing thymocytes from coronin-1 K.O. mice and wildtype littermates (Fig.40) suggesting no gross defects in T-lymphocyte cytoskeletal structure and/or morphology. Adhesion of thymocytes on glass slides coated with anti-CD3 and anti-CD28 antibodies allowed to study the cytoskeletal rearrangements occuring upon crosslinking of the TCR. CD3 and CD28 are essential components of the TCR signaling complex and crosslinking these molecules with appropriate substrate-bound antibodies mimicks the clustering of the TCR during formation of the immunological synapse. As shown in Fig.41, adhesion of thymocytes on glass slides coated with poly-L-lysine and subsequent staining for F-actin or tubulin revealed an indistinguishable cortical localization of these cytoskeletal components in wildtype and coronin-1 deficient thymocytes. Upon adhesion to anti-CD3/anti-CD28 coated glass slides, thymocytes of both wildtype and coronin-1 K.O.

origin were similarly capable to polarize the actin and the tubulin cytoskeleton towards the site of adhesion. In summary, these data demonstrate that coronin-1 deficiency does not affect the morphological appearance and cytoskeletal organisation of non-activated as well as activated T-lymphocytes. We therefore conclude that the absence of coronin-1 does not affect cytoskeletal organisation in T-cells upon activation.

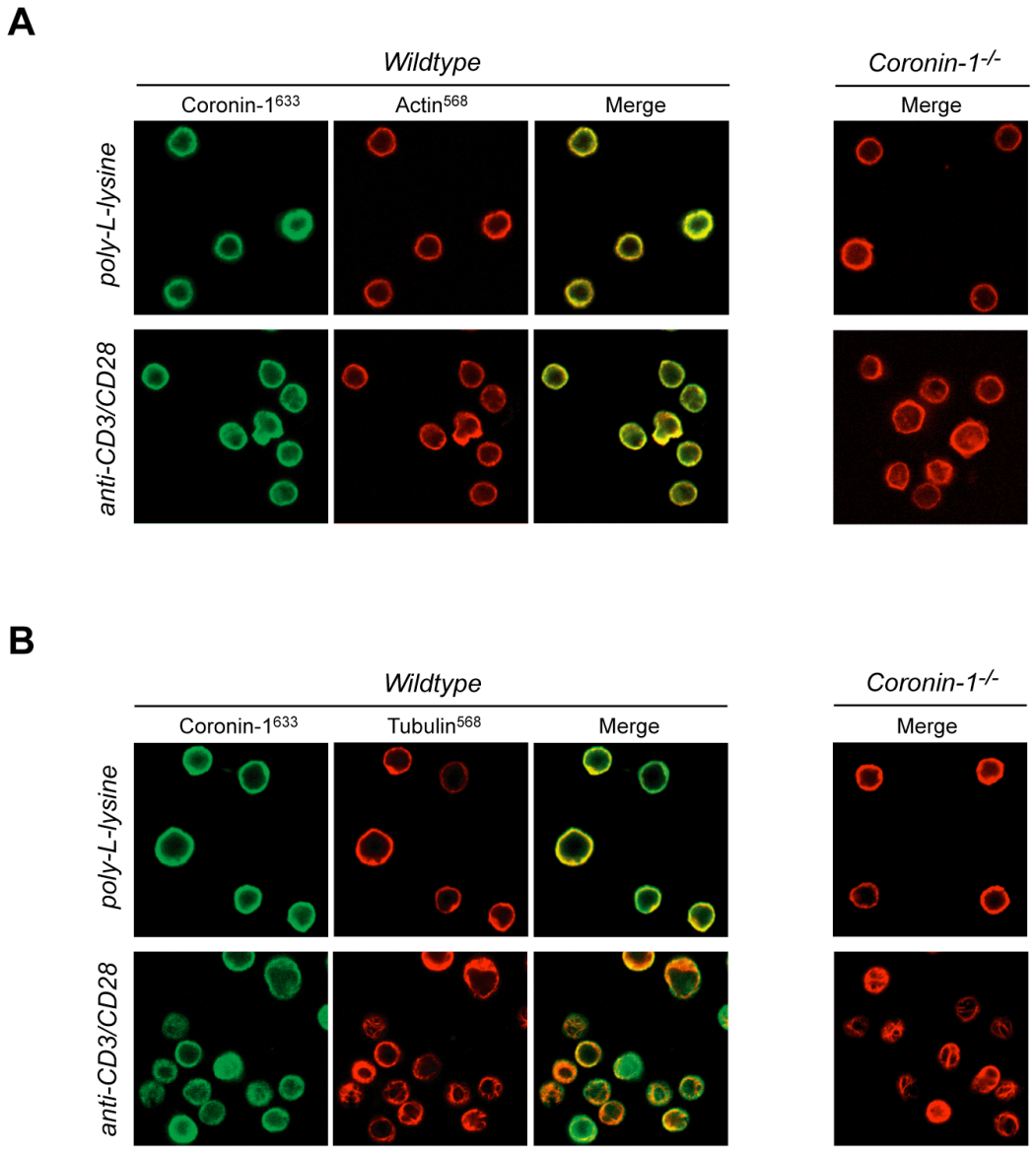

Fig. 41 Actin and tubulin cytoskeleton organisation in resting thymocytes. Thymocytes isolated from coronin-1 K.O. mice and wildtype littermates were allowed to adhere either to poly-L-lysine coated glass-slides for 30 min on ice or to anti-CD3/anti-CD28 antibody coated slides for 30 min at 37°C. After fixation with 3% PFA the cells were stained with antibodies directed against coronin-1 and tubulin and appropriate secondary antibodies (coupled to AlexaFluor633 for coronin-1 and to AlexaFluor568 for tubulin). The actin cytoskeleton was stained using AlexaFluor568 coupled Phalloidin. Shown are representative confocal microscopy images of (**A**) the actin cytoskeleton and (**B**) the tubulin cytoskeleton.

3.4.6 Summary

In order to explain the defect in peripheral T-lymphocyte compartments of homozygous coronin-1 K.O. mice, coronin-1 deficient T-lymphocytes were subjected to an in-depth functional characterisation. Absence of coronin-1 was found to result in enhanced apoptosis of T-cells in spleen and lymph nodes. In the thymus, no differences in apoptosis were detected further corroborating the finding that T-cell development is not defective in coronin-$1^{-/-}$ mice. T-cells in the periphery of homozygous coronin-1 K.O. mice were mostly CD62L negative which may be the result of the specific deletion of naïve, CD62L positive cells in the periphery or due to the expansion of a subset of CD62L low expressing T-cells. Furthermore, peripheral, coronin-1 deficient T-cells showed increased expression of CD44 which indicates lymphopenia-driven proliferation of T-cells with a memory-like phenotype to compensate for the depletion of naïve, CD62L positive T-cells.

CD62L is crucial for the homing of T-lymphocytes to lymph nodes therefore a homing assay was performed assessing the ability of coronin-1 deficient T-lymphocytes to home to the lymph nodes of wildtype recipient mice. This experiment revealed that coronin-1 deficient T-cells were not only defective in homing to secondary lymphoid organs but to be also incapable of surviving in the periphery. Since coronin-1 was shown to interact with F-actin the organisation of the actin and tubulin cytoskeleton in coronin-1 deficient thymocytes was investigated. The morphological appearance of the F-actin as well as the tubulin cytoskeleton in resting and anti-CD3/CD28 activated thymocytes were indistinguishable comparing thymocytes from homozygous coronin-1 K.O. mice and wildtype littermates.

In a mixed lymphocyte reaction coronin-1 deficient T-cells were severly affected in their ability to proliferate as a response to allogeneic MHC stimuli. In summary, we conclude that coronin-1 plays a crucial role in the maintainance of T-cell functions such as activation through the TCR, homing to secondary lymphoid organs and survival in the periphery.

3.5 Phenotypic analysis of coronin-1 deficient macrophages

Coronin-1 was identified as a crucial factor in mediating mycobacterial survival in macrophages (Ferrari et al., 1999). As in T-cells, coronin-1 could play a role in regulating actin dependent processes in macrophages such as cell motility, phagocytosis and activation. Using macrophages derived from the bone marrow of coronin-1 deficient mice we adressed in an initial series of experiments actin cytoskeleton organisation and phagocytosis in these cells.

3.5.1 Coronin-1 deficient bone marrow-derived macrophages do not show defects in actin cytoskeleton organisation

The organisation of the actin cytoskeleton was studied in resting as well activated BMM by immunofluorescence staining for F-actin and subsequent microscopic analysis. Macrophage activation is characterised by an enhancement of microbicidal mechanisms and antigen presentation by extracellular stimuli (Janeway et al., 2001). Morphologically, activated macrophages can be identified by their ability to spread on a glass substratum which requires rearrangements of the actin cytoskeleton (Bechard et al., 1988). *In vitro* macrophage activation can be achieved by either cytokines such as Interferon-γ or by phorbolesters, such as phorbol-12-myristate-13-acetate (PMA), which are potent stimulators of protein kinase C.

Activation of BMM isolated from wildtype and coronin-1 K.O. mice with either Interferon-γ or PMA resulted in spreading of the cells on glass slides. Neither morphological differences nor abnormalities in F-actin cytoskeleton organisation were observed between wildtype and coronin-1 deficient BMM (Fig.42 A). In order to measure the area covered by spreaded macrophages digital image analysis was used. Determination of the area covered by wildtype or coronin-1 deficient macrophages upon activation revealed no significant differences (Fig.42 B). We therefore conclude that absence of coronin-1 expression does not affect actin cytoskeleton organisation and activation of BMM as determined by their ability to spread on a glass substratum. Further experimental work needs to adress to which extent coronin-1 deficiency affects other activation-induced macrophage functions, e.g. increased phagocytosis rates, increased phagosome-lysosome fusion (Ishibashi and Arai, 1990), activation of NADPH oxidase and induction of NO-synthase (Bogdan et al., 2000).

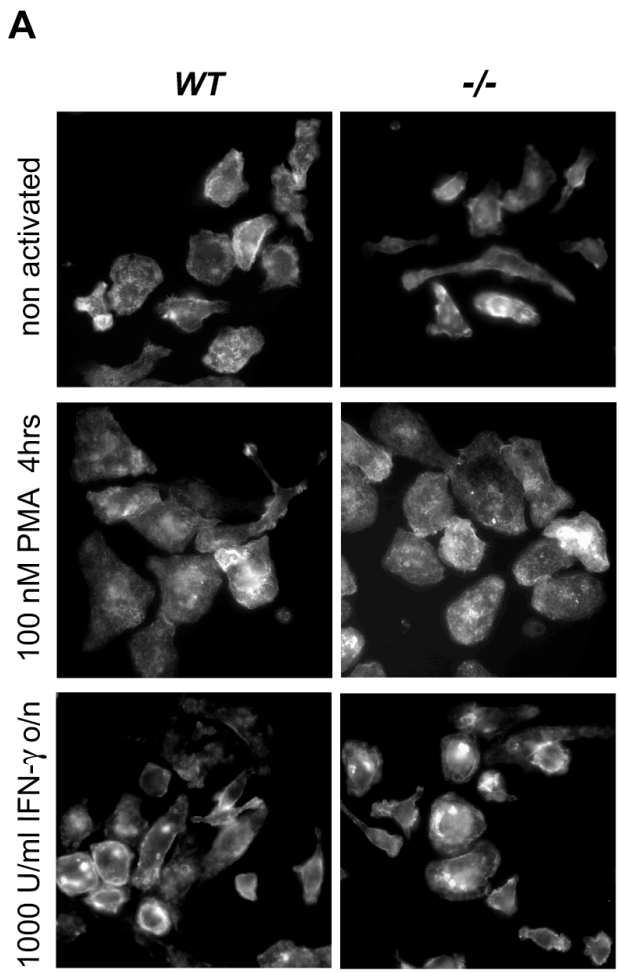

Fig. 42 Actin cytoskeleton organisation in coronin-1 deficient bone marrow-derived macrophages (BMM). BMM of either wildtype (***WT***) or coronin-1$^{-/-}$ (**-/-**) origin were cultured overnight (o/n) on glass-slides in the absence (non activated) or presence of activating stimuli (100 nM PMA or 1000 U/ml Interferon-γ). The cells were then fixed with 3% PFA and permeabilised with 0.2% saponin to stain the F-actin cytoskeleton with AlexaFluor568-labeled phalloidin. (**A**) Representative images taken on a conventional fluorescence microscope (Zeiss Axioskop). (**B**) The occupied area of BMM spread out on the glass slide upon activation was determined by digital image analysis using the ImageJ software. Data are means ± SD of 40 cells (n=40).

3.5.2 Coronin-1 deficient bone marrow-derived macrophages are not defective in phagocytosis

Phagocytosis of microorganisms by host phagocytic cells is a crucial host defense mechanism. The process of phagocytosis involves rearrangement of the cytoskeleton and cell membrane to ingest the microbial particle (Greenberg, 1999; Underhill and Ozinsky, 2002). Coronin-1 as an actin-associated protein has been implicated in phagocytosis in *Dictyostelium* and murine macrophage cell lines since deletion or RNAi mediated downregulation of the coronin-1 gene resulted in cells with impaired phagocytosis (de Hostos et al., 1993, Yan et al., 2005).

To analyse the contribution of coronin-1 to receptor mediated phagocytosis, bone marrow macrophages derived from either coronin-1$^{-/-}$ mice or wildtype littermates were incubated with human serum treated GFP expressing *Lactobacillus casei* or IgG coated fluorescent polystyrene beads for 30 min at 37°C. The rate of uptake was determined using flow

cytometry (Fig.43). Both wildtype as well as coronin-1$^{-/-}$ macrophages were found to have a similar capacity to internalize cargo by either complement receptor or Fc receptor-mediated phagocytosis. These data show that coronin-1 is not essential for proper receptor-mediated phagocytosis.

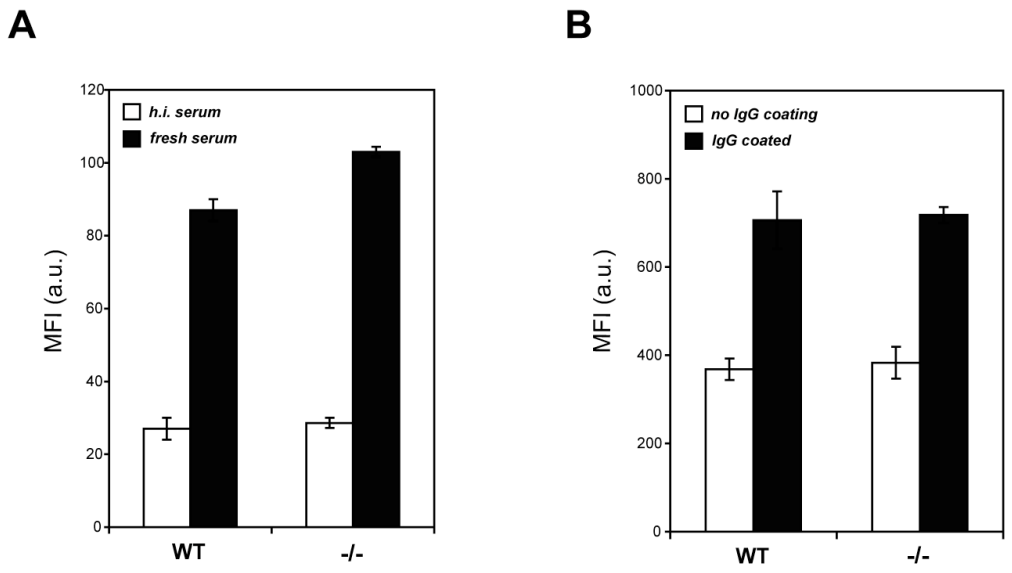

Fig. 43 Flow cytometric analysis of receptor mediated phagocytosis by bone marrow derived macrophages isolated from coronin-1 knock-out mice (-/-) or wildtype (WT) littermates. (**A**) To study complement receptor 3 (CR3)-mediated uptake adherent macrophages were incubated with GFP expressing *Lactobacillus casei* that have either been treated with fresh or heat inactivated (h.i.) human serum (as control for background uptake). After internalization for 30 min at 37°C the cells were washed to remove adherent bacteria, harvested by scraping and analysed by flow cytometry. Rate of uptake is determined as the increase in fluorescence as expressed by the median fluorescence intensity (MFI). Shown are median values in arbitrary units (a.u.) of duplicate assays. (**B**) Fc receptor-mediated uptake was analysed by incubating adherent macrophages with fluorescent polystyrene beads that have either been coated with IgGs or not (as control for background uptake). Flow cytometric analysis of Fc receptor mediated phagocytosis was performed as described for CR3-mediated uptake.

3.5.3 Summary

Due to the prominent role of coronin-1 in mediating mycobacterial survival in macrophages coronin-1 deficient bone marrow-derived macrophages were functionally analysed. Fc receptor- as well complement receptor-mediated phagocytosis occurred normally in the absence of coronin-1. The F-actin cytoskeleton in resting and activated coronin-1 deficient BMM was found to be indistinguishably organised compared to their wildtype counterparts. To that end, we conclude that coronin-1 plays a crucial role in maintaining T-cell but not macrophage functions.

4 DISCUSSION

Coronin-1 represents a member of the coronin family of proteins which are widely expressed in eukaryotic organisms. Although a substantial body of functional and biochemical data concerning coronin-1 has been delineated from the work with several eukaryotic organisms, such as *Dictyostelium* and yeast, a precise functional activity in mammalian organisms has not been defined for coronin-1 and other members of the coronin protein family. The aim of the work described in this thesis was to gain insight into the cell biological function of coronin-1 through the generation and phenotypic characterization of coronin-1 deficient mice.
Coronin-1 deficient mice appeared healthy and fertile. Taking the specific expression of coronin-1 in leukocytes into account further analysis of cells of the immune system revealed a strong defect within the peripheral T-lymphocyte population in coronin-1 deficient mice. Whereas no developmental defects of the T-lymphocyte lineage in the thymus were observed, the peripheral T-lymphocyte pool was strongly depleted in coronin-1 K.O. mice. Peripheral T-lymphocytes were prone to apoptosis, expressed markers characteristic for lymphopenia-driven proliferation and turned out to be unable to mount a proliferative response to allogeneic MHC stimuli. This argues for a role of coronin-1 in differentially regulating T-cell fate through the modulation of signaling pathways downstream of the T-cell receptor.

4.1 Coronin-1 is required for peripheral T-cell survival but not for T-cell development

The lack of peripheral T-cells, constituting a T-lymphopenic situation, as observed in coronin-1 deficient mice could be on one hand a consequence of defects in T-cell development and therefore T-cell output from the thymus or on the other hand be a result of defects in the survival of peripheral T-cells.
The observation that T-cell development in the thymus occured normally in coronin-1 deficient mice as well as the ability of coronin-1 deficient bone marrow cells to reconstitute the thymus indicate that coronin-1 is not required for T-cell development. Positive and negative selection of T-cells in the thymus seemed to occur independently of coronin-1 since coronin-1 deficient mice showed neither accumulation nor reduction in single-positive thymocyte numbers. Consistent with this, no increase in apoptotic cell numbers compared to wildtype littermates was found among the thymocyte subpopulations in coronin-1 deficient mice.

The reduction in peripheral T-cell numbers in coronin-1 K.O. mice is reminiscent of the phenotype of mice with mutations in genes involved in lymphocyte migration (Fukui et al., 2001, Matloubian et al., 2004). However, our data on the cellularity and composition of thymocyte subsets argue against a defect of single positive thymocytes to egress from the thymus which would otherwise result in the accumulation of mature T-cells. Furthermore, compared to wildtype littermates normal numbers of single positive thymocytes in coronin-1 deficient mice acquired CD62L expression. CD62L as a crucial lymphocyte homing determinant is expressed by mature single-positive thymocyte prior to their migration out of the thymus into the periphery (Gallatin et al., 1983, Zuniga-Pflücker, 2004). Taken together, these data indicate that the absence of coronin-1 does not affect the development of T-cells which are competent to leave the thymus to establish the peripheral T-cell pool.

Once in the periphery, T-cells circulate for prolonged times between the secondary lymphoid organs and the blood in a naïve state (Sprent and Tough, 2001). The survival of naïve T-cells in the periphery requires continous engagement of their TCR as well as the exposure to certain cytokines (Takeda et al., 1996, Tanchot et al., 1997, Rathmell et al., 2001, Vivien et al., 2001). In coronin-1 deficient mice we found not only a drastic reduction of T-cell numbers in secondary lymphoid organs and the peripheral blood but could also demonstrate that coronin-1 deficient T-cells are more prone to apoptosis. In addition, the majority of peripheral T-cells that are left in coronin-1 deficient mice lack CD62L expression. These data suggest that after egress from the thymus, coronin-1 peripheral T-cells could have either a defect in homing to secondary lymphoid organs or in survival within the periphery.

As outlined above, the thymus in coronin-1 deficient mice has the capacity to constantly seed the periphery with mature T-cells. Judged by the normal CD62L expression of thymocytes, thymic emigrants could be expected to be compentent to home to secondary lymphoid organs. Since the organization of neither the actin nor the tubulin cytoskeleton was found to be affected in coronin-1 deficient thymocytes we propose that also the migration of mature T-cells is not disturbed. Nevertheless, peripheral T-cell numbers are strongly reduced in coronin-1 K.O. mice. The increase in apoptosis of peripheral coronin-1 deficient T-cells indicates that the absence of coronin-1 causes a constant clearance of T-cells from the peripheral T-cell pool. Apoptosis of peripheral T-cells could have several reasons and further experimental work is required to determine the sequence of events leading to peripheral T-cell death. Naïve T-cells that fail to interpret TCR dependent signals as well as the presence of cytokines are elimininated through apoptosis (Nagata, 1997, Refaeli et al., 1998, Inaba et al., 1999, Rathmell and Thompson, 1999). Analysis of the capacity of peripheral T-cells to mount a proliferative response to allogeneic MHC stimuli revealed that coronin-1 deficient T-

cells did not proliferate suggesting that T-cell activation through TCR engagement is defective. To which extent coronin-1 deficient T-cells could be rescued *in vitro* by the addition of cytokines such as interleukin-2 or -7 needs to be addressed. T-cell activation via the TCR occurs in the T-cell zones of secondary lymphoid organs. Histological analysis of spleen and lymph nodes from coronin-1 deficient mice demonstrated the absence of T-cells from T-cell zones.

A homing assay performed with coronin-1 deficient peripheral T–cells supported the inability of coronin-1 deficient T-cells to home to secondary lymphoid organs. However, the majority of peripheral T-cells isolated from coronin-1 deficient mice does not express CD62L rendering these cells in principle incapable of homing to secondary lymphoid organs. Furthermore, the homing assay demonstrated that coronin-1 deficient T-cells are defective in surviving in the periphery. Whether coronin-1 deficient T-cells undergo apoptosis because they do not enter the lymph nodes where they would receive stimuli promoting their survival or whether they undergo apoptosis before they reach the lymph nodes needs to be adressed in future experimental work. These further investigations could include performance of homing assays using defined CD62L positive or negative coronin-1 deficient T-cell subsets and analysis of the requirements, such as cytokines, for the survival of coronin-1 deficient T-cells in *in vitro* culture.

4.2 Towards a role of coronin-1 in regulating T-cell homeostasis

The composition of the peripheral T-cell pool in coronin-1 deficient mice compared to wildtype littermates showed pronounced differences. Beside its reduction in overall T-cell numbers, the coronin-1 deficient T-cell pool is characterized by a decrease in the percentage of $CD3^+CD62L^{hi}$ cells and an increase of the relative number of $CD44^{hi}$ cells (see Table 13). The relative reduction of CD62L positive T-cells could be either explained by the deletion of naïve, CD62L positive cells or by the expansion of the small number of $CD62L^{lo}$ T-cells. The latter explanation is further substantiated by the relative increase of $CD44^{hi}$ T-cells in coronin-1 deficient mice which is indicative for T-cells with a memory-like phenotype which have been

Cell type	% of total cells in (gate)	
	Wildtype	*Coronin-1* $^{-/-}$
$CD3^+CD62L^{hi}$ (spleen)	14.1 ± 2.6 (FSC/SSC)	6.5 ± 0.3 (FSC/SSC)
$CD3^+CD62L^{hi}$ (lymph nodes)	40.3 ± 6.6 (FSC/SSC)	7.9 ± 2.4 (FSC/SSC)
$CD44^{hi}$ (spleen)	43.8 ± 0.5 ($CD4^+$)	71.8 ± 2.2 ($CD4^+$)
	41.1 ± 9.3 ($CD8^+$)	75.2 ± 6.7 ($CD8^+$)
$CD44^{hi}$ (lymph nodes)	32.6 ± 3.5 ($CD4^+$)	65.2 ± 5.4 ($CD4^+$)
	28.7 ± 5.4 ($CD8^+$)	70.6 ± 13.9 ($CD8^+$)

Table 13 Relative proportion of CD62L and CD44 highly positive ($CD62L^{hi}$ and $CD44^{hi}$) T-cells in the spleen and inguinal lymph nodes of wildtype and coronin-1 deficient mice. Data are derived from the experiments described in paragraph 3.4.2 (Fig.37). To assess CD62L expression, a forward/side scatter gate (FSC/SSC) was set to identify living cells and the percentage of CD3 positive and CD62L highly positive cells ($CD3^+CD62L^{hi}$) within this gate was determined. For the analysis of CD44 expression, a gate was set for CD4 or CD8 positive cells followed by determination of the percentage of CD44 highly positive cells within this gate.

generated in the course of lymphopenia-driven proliferation (see paragraph 1.5.3). The drastic reduction of peripheral T-cell numbers as observed in coronin-1 deficient mice constitutes a T-lymphopenic situation which could induce the proliferation of memory-like T-cells to compensate for the lack of peripheral T-cells.

To which extent T-cells generated by lymphopenia-driven proliferation are functionally equivalent to naïve T-cells found in a non-lymphopenic environment is not yet fully understood. Future experiments investigating homing, survival and stimulation of coronin-1 deficient peripheral T-cells should take this issue into account by for example using specifically enriched populations of T-cells. It might be - as shown for the homing assay - that functional differences between wildtype and coronin-1 deficient peripheral T-cells rather reflect the altered composition of the peripheral T-cell pool than a defect in a particular T-cell function *per se*. Only an in-depth characterization of the peripheral T-cell pool in coronin-1 K.O. mice would allow to draw further conclusions on how coronin-1 is involved in regulating T-cell homeostasis. Markers employed for such kind of analysis should include CD5, CD25, CD44, FoxP3, CD122, Ly6C, LFA-1 and CCR7. CD5 expression by double positive thymocytes plays a significant role in modulating TCR signaling during positive and negative selection (Azzam et al., 2001) and would therefore be a valuable marker in further analysing potential defects in T-cell development in the absence of coronin-1. Currently it cannot be excluded that subtle defects at the level of thymic T-cell development are responsible for generating mature T-cells which ultimately can not survive in the periphery. At the level of single positive coronin-1 deficient thymocytes these subtle defects could include the lack of expression of molecules required for the homing to secondary lymphoid organs such LFA-1 and CCR7. Peripheral T-cells from coronin-1 K.O. mice should be carefully analysed for the expression of markers which are expressed by T-cells which underwent lymphopenia driven proliferation such as CD122, Ly6C and CD44 (Surh and Sprent, 2000).

Finally, coronin-1 K.O. mice should be analysed for a relative increase in naturally arising CD4+CD25+ regulatory T-cells (T_{reg}) using FoxP3 as a marker (Fontenot et al., 2003, Hori et al., 2003, Khattri et al., 2003). Several reports have shown an relative increase in T_{reg} numbers under lymphopenic conditions (Peschon et al., 1994, von Freeden-Jeffry et al., 1995). In addition to the characterization of the precise composition of the T-cell pool in coronin-1 deficient mice by analysing the expression of surface markers, the turnover and differentiation of identified subsets should be studied using BrdU labeling experiments (Tough and Sprent, 1994) possibly resolving whether there is lymphopenia driven proliferation and which T-cell subsets are subject to apoptosis in coronin-1 deficient mice. The detailed characterization of the peripheral T-cell pool in coronin-1 deficient mice will be

instructive in defining a functional role of coronin-1 in regulating T-cell homeostasis. Depending on the subset of T-cells most affected by the absence of coronin-1 predictions can be made in which signaling pathway downstream of the TCR, of molecules required for homing and migration or cytokine receptors coronin-1 could play a regulatory role. Furthermore, together with experiments specifically analysing the function of the immune system it could be assessed to which extent coronin-1 K.O. mice are immunocompromised or prone to develop autoimmune disease.

The disturbance of the peripheral T lymphocyte pool under lymphopenic conditions would not only affect the response of coronin-1 K.O. mice to T-cell dependent as well as independent antigens but could also render them more susceptible to autoimmune diseases. Several studies have established a link between lymphopenia and autoimmune diseases based on the lymphopenia driven proliferation of potentially autoreactive T-cells (Gleeson et al., 1996, King et al., 2004, Khoruts and Fraser, 2005). Although these T-cells could be kept in check by regulatory T-cells coronin-1 K.O. mice should be carefully analysed for typical symptoms of autoimmune diseases such as diarrhoea, inflammatory bowel disease, the presence of autoreactive antibodies and lymphocytic infiltration of organs like the intestine, the liver, the lung and salivary glands.

4.3 Potential molecular mechanims of coronin-1 function in leukocytes

The phenotypic analysis of coronin-1 deficient mice as presented in this thesis established a role for coronin-1 in regulating peripheral T-cell homeostasis. T-cell homeostasis relies on a variety of receptor based mechanisms of which the most prominent ones are those downstream of the TCR and cytokine receptors. As discussed in the following, coronin-1 might be involved in modulating the strength of downstream signaling through organizing cytoskeletal structures or by providing a scaffold for the assembly of signaling complexes.

4.3.1 Coronin-1 could participate in regulating cytoskeletal rearrangements as required for the function of immune receptors

The function of cells of the immune system relies on a variety of mechanisms which are dependent on an actively reorganizing actin cytoskeleton. These mechanisms include phagocytosis and macropinocytosis, cellular movements, formation of the immunological synapse and subsequent T-cell activation (Das et al., 2002, Vincente-Manzanares et al., 2002, Fenteany and Glogauer, 2004, Meiri, 2004). A common feature of these functions is the induction of rapid rearrangements of the actin cytoskeleton by signaling through

receptors expressed on the surface of immune cells. These receptors include the BCR, the TCR, phagocytic receptors and adhesion molecules (Allen and Aderem, 1996, Fischer et al., 1998, Fuller et al., 2003, Gruenheid and Finlay, 2003). The extracellular signals transduced by these receptors are connected to intracellular actin reorganization by molecules linking the plasma membrane with the actin cytoskeleton (Das et al., 2002, Schafer, 2002, Ivetic and Ridley, 2004).

Coronin-1 was recently shown to link the leukocyte cytoskeleton to the plasma membrane via two distinct domains (Gatfield et al., 2005). This suggests that coronin-1 may integrate extracellular receptor-based signals with the rearrangement of cytoskeletal structures. Such a role is supported by the work performed on coronin in *Dictyostelium* and yeast. Coronin in *Dictyostelium* was shown to be required for the proper function of a variety of actin-based processes such as phagocytosis, macropinocytosis, cell motility and cytokinesis (de Hostos, 1991 and 1993, Maniak, 1995, Hacker, 1997). *Saccharomyces cerevisiae* Crn1p was shown to be able to crosslink the actin and microtubule cytoskeleton as well as to modulate the activity of the actin regulating Arp2/3 complex *in vitro* (Heil-Chapdelaine et al., 1998, Goode et al., 1999, Humphries et al., 2002). Interestingly, coronin-1 was found to accumulate at sites of actin cytoskeleton remodeling such as the cortical region, sites of phagocytosis and the immunological synapse (Ferrari et al., 1999, Nal et al., 2004). However, to which extent, with which consequences for downstream signaling and how coronin-1 exactly modulates actin cytoskeletal dynamics in response to extracellular signals in mammalian cells remains to be adressed.

Our analysis of cytoskeletal structures in resting and TCR stimulated thymocytes as well resting and activated bone marrow derived macrophages did not reveal any differences in actin or tubulin cytoskeleton organization between coronin-1 deficient and wildtype cells. Phagocytosis as a macrophage function being strongly dependent on actin cytoskeleton rearrangements was also found to be not defective in the absence of coronin-1. Although these results argue against a role of coronin-1 in regulating T-cell and macrophage function via cytoskeletal structures further experimental work is required to exclude this possibility. Depending on the analysed function and the stimuli used coronin-1 could be differentially required for inducing cytoskeletal rearrangements. Especially for T-cells a clear distinction should be made between thymocytes and peripheral T-cells when analysing the organization of cytoskeletal structures. Furthermore, actin dependent processes such as migration and immunological synapse formation by T-cells in the presence and absence of coronin-1 need extensive characterization.

4.3.2 Coronin-1 could function in modulating the strength of signaling downstream of the T-cell receptor

Based on its localization to the immunological synapse coronin-1 has been suggested to be involved in the activation of T-cells (Das et al., 2002, Nal et al., 2004). Our observations that coronin-1 deficiency does not affect T-cell development but their maintenance in the periphery suggest that coronin-1 may modulate the strength of signaling downstream of the TCR. Supporting evidence for this comes from the inability of coronin-1 deficient T-cells to respond to allogeneic MHC stimuli. Besides its potential function in modulating actin cytoskeleton dynamics coronin-1 could be required for appropriately assembling the TCR sginaling complex. Coronin-1 binds to cholesterol enriched membrane microdomains also refered to as rafts (Gatfield and Pieters, 2000) which have been shown to be essential for proper functioning of TCR signaling (Harder, 2004). In addition, coronin-1 contains WD40 domains which represent an evolutionary conserved motif for protein-protein interaction (Neer et al., 1994, Li and Roberts, 2001) and which could allow coronin-1 to recruit signaling partners to sites of raft induced clustering of the TCR complex. An additional noteworthy feature of coronin-1 is the presence of several putative PKC phosphorylation sites (Gatfield et al., 2005). Two studies suggest a regulation of the subcellular localization and function of coronin-1 in dependence of its phophorylation state (Itoh et al., 2002, Gatfield et al., 2005). This opens the possibility that the capacity of coronin-1 to not only regulate cytoskeletal organization but to also recruit certain interacting partners could be regulated differentially dependent on the signals to be transduced.

In summary, these characteristics of coronin-1 could provide an explanation on how coronin-1 is involved in differentially regulating TCR signaling in thymocytes and peripheral T-cells. Activation of T lymphocytes through the TCR is based on the same principles both in the thymus to regulate selection processes as well as in the periphery to allow the survival of naïve T-cells. Currently it is hypothesized that the interpretation of signals received in the thymus leading to positive and negative selection is distinct from the one that results in survival or death of peripheral T-cells (Takeda et al., 1996, Kirberg et al., 1997, Starr et al., 2003). Although it is not yet well understood how thymocytes and peripheral T-cells differ in transducing TCR-based signals a further characterization of the involvement of coronin-1 in signaling downstream of the TCR could provide valuable insight into differential regulation of TCR signaling pathways. Further experimental work should adress activation of the various subsets of coronin-1 deficient T-cells. In detail, the appropriate recruitment of important downstream signaling partners to the TCR such as Lck, LAT, ZAP70 and PKC□ should be analysed. Are important signaling pathways downstream of the TCR such as Ca2+

mobilization, Erk, Jnk and MAP kinase pathways affected in the absence of coronin-1 ? The analysis of the phosphorylation state of coronin-1 in dependence of different TCR stimuli ranging from anti-CD3 antibody mediated clustering of the TCR complex to peptide/MHC stimulation of transgenic TCRs might allow to draw conclusions on the capacity of coronin-1 to modulate downstream signaling by being differentially phosphorylated.

4.3.3 The absence of coronin-1 expression does not affect other leukocyte subsets

Our analysis of the phenotype of coronin-1 deficient mice established a regulatory function of coronin-1 in peripheral T-cell survival. Yet an open question is why other leukocyte subsets such as macrophages and B cells seem to be not affected by the absence of coronin-1. Analysis of the activation and phagocytic properties of bone marrow derived macrophages detected no defect induced by the lack of coronin-1 expression. B cell numbers and subsets were interestingly found to be not disturbed in the spleen of coronin-1 K.O. mice. However, in peripheral blood and lymphnodes B cell numbers were found to be reduced but never to such an extent as seen for T-cells. Whether the partial reduction of B cell numbers is a direct effect of the deficiency of coronin-1 or whether it is a secondary effect either due to the absence of T-cells in secondary lymphoid organs or the inability of T-cells to interact with B cells remains to be analysed. Like T-cells, B cells require exposure to cytokines as well as BCR dependent signals to survive in the periphery (Lam et al., 1997, Niiro and Clark, 2002, Kalia et al., 2006, Milne and Paige, 2006). Signaling downstream of the BCR also relies on the concerted recruitment of a variety of signaling molecules and rearrangements of the cytoskeleton (Graziadei et al., 1990, Jugloff and Jongstra-Bilen, 1997, Niiro and Clark, 2002, Pierce, 2002, Harnett et al., 2005). Coronin-1 could be involved in regulating BCR signaling along similar principles as in T-cells. Nevertheless, B cells are not as strongly affected by the absence of coronin-1 as T-cells. Further experimental work on the activation of coronin-1 deficient B cells is required to determine to which extent coronin-1 is involved in regulating B cell functions. In addition, functional redundancy among the different mamalian coronins should be taken into account. The RT-PCR based expression analysis of the seven mammalian coronins revealed ubiquitous expression of coronin-2,-3,-5 and -7. Given the high degree in structural similarity, subcellular localization and potential regulation by phosphorylation these coronins could take over functions of coronin-1. This would provide an explanation why some leukocyte subsets are more affected by coronin-1 deficiency than others. RT-PCR based expression analysis and antibodies specifically recognizing the various mammalian coronins in isolated leukocyte subsets could be used in the future to further assess a potential functional redundancy among the mammalian coronins.

5 SUMMARY

Coronins represent an evolutionary conserved family of WD-repeat actin-binding proteins for which a role in regulating membrane and cytoskeleton related functions have been proposed. In mammalian organisms seven members of the coronin protein family have been described of which coronin-1 respresents the thus far best characterized molecule. Coronin-1 is specifically expressed in leukocytes and was originally identified as a key player in mediating the survival of pathogenic mycobacteria in infected murine macrophages by inhibiting the fusion of the mycobacterial phagosome with lysosomes. Further analyses demonstrated the capacity of coronin-1 to link the leukocyte plasma membrane with the underlying actin cytoskeleton suggesting a regulatory role of coronin-1 in leukocyte specific functions. However, a precise biological activity of coronin-1 in leukocytes and in mammalian organisms in general has not yet been defined. The aim of this thesis was to contribute to our understanding of the function of coronin-1 by generating and phenotypically characterizing coronin-1 knock-out mice.

Coronin-1 deficient mice were found to be viable and fertile. In-depth analysis of the immune system revealed that the lack of coronin-1 expression severly affected the homeostasis of the peripheral T-cell pool. Whereas T-cell development could be shown to be independent on coronin-1, peripheral T-cell numbers were found to be strongly reduced. The reduction of peripheral T-cell numbers in coronin-1 deficient mice was accompanied by changes in the composition and function of the peripheral T-cell pool. Coronin-1 deficient peripheral T-cells were prone to apoptosis, expressed markers characteristic for lymphopenia driven proliferation of T-cells and were unable to mount a proliferative response to allogeneic MHC stimuli. These data suggest a regulatory role of coronin-1 in T-cell homeostasis most likely by modulating the strength of signaling downstream of the T-cell receptor.

Based on the proposed role of coronin-1 in regulating cytoskeletal dynamics coronin-1 deficient T-cells as well as bone marrow derived macrophages were analysed for defects in the organization of the cytoskeleton and for the functionality of actin based processes such as phagocytosis. In both cell types no defects in the organization of the actin or the microtubule cytskeleton could be detected in the absence of coronin-1. Coronin-1 deficient bone marrow derived macrophages were not defective in phagocytosis. We therefore conclude that the phenotype established for coronin-1 deficient mice is specific for T-cells and is not due to the impairment of functionally relevant rearrangements of the actin cytoskeleton. Coronin-1 might well play a regulatory role on cytoskeletal dynamics, but

probably not to such an extent that it would affect all coronin-1 deficient cells in a drastic manner. As shown by RT-PCR based expression analysis of the seven members of the mammalian coronin family of proteins other coronins could take over some of the funcions of coronin-1 in a cell-type specific manner. In summary, the phenotypic analysis of coronin-1 deficient mice as presented in this thesis allowed to assign a function of coronin-1 in maintaining T-cell homeostasis. The specificity of the defect caused by the absence of coronin-1 will promote further analysis of a potential role of coronin-1 in modulating T-cell functions such as activation through the TCR. The signals differentiating between the life or the death of a T-cell in the periphery are largely ill-defined. The analysis of coronin-1 deficient mice established coronin-1 as a candidate molecule in differentially regulating T-cell fate.

6 REFERENCES

Abbas, A.K., Murphy, K.M. and Sher, A. (1996). Functional diversity of helper T-lymphocytes. *Nature* **383**, 787 – 793.

Acuto, O. and Cantrell, D. (2000). T cell activation and the cytoskeleton. *Annu Rev Immunol* **18**, 165 – 184.

Aderem, A. and Underhill, D.M. (1999). Mechanisms of phagocytosis in macrophages. *Annu Rev Immunol* **17**, 593 – 623.

Allen, L.A. and Aderem, A. (1996). Mechanisms of phagocytosis. *Curr Opin Immunol* **8**, 36 – 40.

Amit, A.G., Mariuzza, R.A., Phillips, S.E. and Poljak, R.J. (1985). Three-dimensional structure of an antigen-antibody complex at 6 A resolution. *Nature* **313**, 156 – 158.

Amit, A.G., Mariuzza, R.A., Phillips, S.E. and Poljak, R.J. (1986). Three-dimensional structure of an antigen-antibody complex at 2.8 A resolution. *Science* **233**, 747 – 753.

Amigorena, S., Drake, J.R., Webster, P. and Mellman, I. (1994). Transient accumulation of new class II MHC molecules in a novel endocytic compartment in B lymphocytes. *Nature* **369**, 113 – 120.

Anderson, G. and Jenkinson, E.J. (2001). Lymphostromal interactions in thymic development and function. *Nat Rev Immunol* **1**, 31 – 40.

Androlewicz, M.J., Anderson, K.S. and Cresswell, P. (1993). Evidence that transporters associated with antigen processing translocate a major histocompatibility complex I-binding peptide into the endoplasmic reticulum in an ATP-dependent manner. *Proc Natl Acad Sci USA* **90**, 9130 – 9134.

Appleton, B.A., Wu, P. and Wiesmann, C. (2006). The crystal structure of murine coronin-1: a regulator of actin cytoskeleton dynamics in lymphocytes. *Structure* **14**, 87 – 96.

Arcaro, A., Gregoire, C., Bakker, T.R., Baldi, L., Jordan, M., Goffin, L., Boucheron, N. et al. (2001). CD8 beta endows CD8 with efficient coreceptor function by coupling T cell receptor/CD3 to raft-associated CD8/p56(lck) complexes. *J Exp Med* **194**, 1485 – 1495.

Aroian, R.V., Field, C., Pruliere, G., Kenyon, C. and Alberts, B.M. (1997). Isolation of actin-associated proteins from Caenorhabditis elegans oocytes and their localization in the early embryo. *EMBO J* **16**, 1541 – 1549.

Asnagli, H. and Murphy, K.M. (2001). Stability and commitment in T helper cell development. *Curr Opin Immunol* **13**, 242 – 247.

Asano, S., Mishima, M. and Nishida, E. (2001). Coronin forms a stable dimer through its C-terminal coiled coil region: an implicated role in its localization to cell periphery. *Genes Cells* **6**, 225 – 235.

Azzam, H.S., DeJarnette, J.B., Huang, K., Emmons, R., Park, C.S., Sommers, C.L., El-Khoury, D., Shores, E.W. and Love, P.E. (2001). Fine tuning of TCR signaling by CD5. *J Immunol* **166**, 5464 – 5472.

Bacik, I., Snyder, H.L., Anton, L.C., Russ, G., Chen, W., Bennink, J.R. et al. (1997). Introduction of a glycosylation site into a secreted protein provides evidence for an alternative antigen processing pathway: transport of precursors of major histocompatibility complex class I-restricted peptides from the endoplasmic reticulum to the cytosol. *J Exp Med* **186**, 479 – 487.

Bakke, O. and Dobberstein, B. (1990). MHC class II-associated invariant chain contains a sorting signal for endosomal compartments. *Cell* **63**, 707 – 716.

Banchereau, J. and Steinman, R.M. (1998). Dendritic cells and the control of immunity. *Nature* **392**, 245 – 252.

Baumeister, W., Walz, J., Zuhl, F. and Seemueller, E. (1998). The proteasome: paradigm of a self-compartmentalizing protease. *Cell* **92**, 367 – 380.

Bechard, D.E., Fisher, B.J., Kessler, F.K., Carchman, R.A. and Fowler, A.A. (1988). Macrophage spreading disparity: alveolar vs peritoneal. *J Clin Lab Immunol* **26**, 67 – 71.

Becker, T.C. et al. (2002). IL-15 is required for proliferative renewal of virus-specific memory CD8 T cells. *J Exp Med* **195**, 1541 – 1548.

Berke, G. (1997). Killing mechanisms of cytotoxic lymphocytes. *Curr Opin Hematol* **4**, 32 – 40.

Bevan, M.J. (1976). Minor H antigens introduced on H-2 different stimulating cells cross-react at the cytotoxic T cell level during in vivo priming. *J Immunol* **117**, 2233- 2238.

Bharathi, V., Pallavi, S.K., Bajpai, R., Emerald, B.S. and Shashishara, L.S. (2004). Genetic characterization of the Drosophila homologue of coronin. *J Cell Sci* **117**, 1911 – 1922.

Bogdan, C., Rollinghoff, M. and Diefenbach, A. (2000). Reactive oxygen and reactive nitrogen intermediates in innate and specific immunity. *Curr Opin Immunol* **12**, 64 – 67.

Boise, L.H., Minn, A.J., June, C.H., Lindsten, T. and Thompson, C.B. (1995). Growth factors can enhance lymphocyte survival without committing the cell to undergo cell division. *Proc Natl Acad Sci USA* **92**, 5491 – 5495.

Boon, T. and Van Pel, A. (1989). T cell recognized antigenic peptides derived from the cellular genome are not protein degradation products but can be generated directly by transcription and translation of short subgenic regions. A hypothesis. *Immunogenetics* **29**, 75 – 79.

Bosselut, R., Kubo, S., Guinter, T., Kopacz, J.L., Altman, J.D., Feigenbaum, L. and Singer, A. (2000). Role of CD8 beta domains in CD8 coreceptor function: importance for MHC I binding, signaling, and positive selection of CD8+ T cells in the thymus. *Immunity* **12**, 409 – 418.

Brachet, V., Raposo, G., Amigorena, S. and Mellman, I. (1997). Ii controls the transport of major histocompatibility class II molecules to and from lysosomes. *J Cell Biol* **137**, 51 – 55.

Bradford, M.M. (1976). A rapid and sensitive method for the quantitation of microgram quantities of protein utilizing the principle of protein-dye binding. *Anal Biochem* **72**, 248 – 254.

Bromley, S.K., Burack, W.R., Johnson, K.G., Somersalo, K., Sims, T.N. et al. (2001). The immunological synapse. *Annu Rev Immunol* **19**, 375 – 396.

Brown, M.R. and Chew, C.S. (1989). Carbachol-induced protein phosphorylation in parietal cells: regulation by [Ca2+]. *Am J Physiol* **257**, G99 – G110.

Bullock, T.N. and Eisenlohr, L.C. (1996). Ribosomal scanning past the primary initiation codon as a mechanism for expression of CTL epitopes encoded in the alternative reading frames. *J Exp Med* **184**, 1319 – 1329.

Cai, L., Holoweckyj, N., Schaller, M.D. and Bear J.E. (2005). Phosphorylation of coronin 1B by protein kinase C regulates interaction with Arp2/3 and cell motility. *J Biol Chem* **280**, 31913 – 31923.

Capecchi, M.R. (1989). Altering the genome by homologous recombination. *Science* **244**, 1288 - 1292.

Catron, D.M., Itano, A.A., Pape, K.A., Mueller, D.L. and Jenkins, M.K. (2004). Visualizing the first 50 hr of the primary immune response to a soluble antigen. *Immunity* **21**, 341 – 347.

Cella, M., Engering, A., Pinet, V., Pieters, J. and Lanzavecchia, A. (1997). Inflammatory stimuli induce accumulation of MHC class II complexes on dendritic cells. *Nature* **388**, 782 – 787.

Ceredig, R., Dialynas, D.P., Fitch, F.W. and MacDonald, H.R. (1983). Precursors of T-cell growth-factor-producing cells in the thymus: ontogeny, frequency and quantitative recovery in a subpopulation of phenotypically mature thymocytes defined by monoclonal antibody GK-1.5. *J Exp Med* **158**, 1654 – 1671.

Ceredig, R. and Rolink, T. (2002). A positive look at double-negative thymocytes. *Nature Rev Immunol* **2(11)**, 888 – 897.

Cerottini, J.C. and Brunner, K.T. (1972). Reversible inhibition of lymphocyte-mediated cytotoxicity by cytochalasin B. *Nat New Biol* **237**, 272 – 273.

Chambers, C.A. and Allison, J.P. (1997). Co-stimulation in T cell responses. *Curr Opin Immunol* **9**, 396 – 404.

Chew, C.S., Zhou, C.J. and Parente, J.A. Jr. (1997). Ca2+-independent protein kinase C isoforms may modulate parietal cell HCl secretion. *Am J Physiol* **272**, G246 – G256.

Chu, D.H., Morita, C.T. and Weiss, A. (1998). The Syk family of protein kinases in T-cell activation and development. *Immunol Rev* **165**, 167 – 180.

Clements, J.L., Boerth, N.J., Lee, J.R. and Koretzky, G.A. (1999). Integration of T cell receptor-dependent signaling pathways by adapter proteins. *Annu Rev Immunol* **17**, 89 – 108.

Colman, P.M., Laver, W.G., Varghese, J.N., Baker, A.T., Tulloch, P.A., Air, G.M. and Webster, R.G. (1987). Three-dimensional structure of a complex of antibody with influenza virus neuraminidase. *Nature* **326**, 358 – 363.

Crabtree, G.R. (1999). Generic signals and specific outcomes: signaling through Ca2+, calcineurin, and NF-AT. *Cell* **96**, 611 – 614.

Crowley, M., Inaba, K. and Steinman, R.M. (1990). Dendritic cells are the principal cells in mouse spleen bearing immunogenic fragments of foreign proteins. *J Exp Med* **172**, 383 – 386.

Das, V., Nal, B., Roumier, A., Meas-Yedid, V., Zimmer, C., Olivo-Marin, J.C. et al. (2002). Membrane- cytoskeleton interactions during the formation of the immunological synapse and subsequent T-cell activation. *Immunol Rev* **189**, 123 – 135.

Das, V., Nal, B., Dujeancourt, A., Thoulouze, M.I., Galli, T., Roux, P., Dautry-Varsat, A. and Alcover, A. (2004). Activation-induced polarized recycling targets T cell antigen receptors to the immunological synapse: involvement of SNARE complexes. *Immunity* **20**, 577 – 588.

David, V., Gouin, E., Troys, M.V., Grogan, A., Segal, A.W. et al. (1998). Identification of cofilin, coronin, Rac and capZ in actin tails using a Listeria affinity approach. *J Cell Sci* **111**, 2877 – 2884.

De Hostos, E.L., Bradtke, B., Lottspeich, F., Guggenheim, R. and Gerisch, G. (1991). Coronin, an actin binding protein of Dictyostelium discoideum localized to cell surface projections, has sequence similarities to G protein beta subunits. *EMBO J* **10**, 4097 – 4104.

De Hostos, E.L., Rehfeu, B.C., Bradtke, B., Waddell, D., Albrecht, R., Murphy, J. and Gerisch, G. (1993). Dictyostelium mutants lacking the cytoskeletal protein coronin are defective in cytokinesis and cell motility. *J Cell Biol* **120**, 163 – 173.

De Hostos, E.L. (1999). The coronin family of actin-associated proteins. *Trends Cell Biol* **9**, 345 – 350.

Denzin, L.K. and Creswell, P. (1995). HLA-DM induces CLIP dissociation from MHC class II alpha beta dimers and facilitates peptide loading. *Cell* **82**, 155 – 165.

Di Giovanni, S., De Biase, A., Yakovlev, A., Finn, T., Beers, J., Hoffman, E.P. and Faden, A.I. (2005). In vivo and in vitro characterization of novel neuronal plasticity factors identified following spinal cord injury. *J Biol Chem* **280**, 2084 – 2091.

Doetschman, T. (1999). Interpretation of phenotype in genetically engineered mice. *Lab Anim Sci.* **49(2)**, 137-43.

Dornan, S., Sebestyen, Z., Gamble, J., Nagy, P., Bodnar, A., Alldridge, L., Doe, S. et al. (2002). Differential association of CD45 isoforms with CD4 and CD8 regulates the actions of specific pools of p56lck tyrosine kinase in T cell antigen receptor signal transduction. *J Biol Chem* **277**, 1912 – 1918.

Doucey, M.A., Legler, D.F., Boucheron, N., Cerottini, J.C., Bron, C. and Luescher, I.F. (2001). CTL activation is induced by cross-linking of TCR/MHC-peptide-CD8/p56lck adducts in rafts. *Eur J Immunol* **31**, 1561 – 1570.

Dummer, W., Ernst, B., LeRoy, E., Lee, D. and Surh,C. (2001). Autologous regulation of naive T cell homeostasis within the T cell compartment. *J Immunol* **166**, 2460 – 2468.

Dustin, M.L. and Cooper, J.A. (2000). The immunological synapse and the actin cytoskeleton: molecular hardware for T cell signaling. *Nat Immunol* **1**, 23 –29.

Early, P., Rogers, J., Davis, M., Calame, K., Bond, M., Wall, R. and Hood, L. (1980). Two mRNAs can be produced from a single immunoglobulin mu gene by alternative mRNA processing pathways. *Cell* **20**, 313 – 319.

Engering, A.J., Richters, C.D., Fluitsma, D.M., Van Pelt, A.M., Kamperdijk, E.W., Hoefsmit, E.C. and Pieters, J. (1998). MHC class II and invariant chain biosynthesis and transport during maturation of human precursor dendritic cells. *Int Immunol* **10**, 1713 – 1723.

Ernst, B., Lee, D.S., Chang, J.M., Sprent, J. and Surh, C.D. (1999). The peptide ligands mediating positive selection in the thymus control T cell survival and homeostatic proliferation in the periphery. *Immunity* **11**, 173 – 181.

Eynon, E.E., Schlax, C. and Pieters, J. (1999). A secreted form of the major histocompatibility complex class II-associated invariant chain inhibiting T cell activation. *J Biol Chem* **274**, 26266 – 26271.

Fehling, H.J., Krotkova, A., Saint-Ruf, C. and von Boehmer, H. (1995). Crucial role of the pre-T-cell receptor-□ gene in development of □□ but not □□ T cells. *Nature* **375**, 795 – 798.

Fenteany, G. and Glogauer, M. (2004). Cytoskeletal remodeling in leukocyte function. *Curr Opin Hematol* **11**, 15 – 24.

Ferrari, G., Knight, A.M., Watts, C. and Pieters, J. (1997). Distinct intracellular compartments involved in invariant chain degradation and antigenic peptide loading of major histocompatibility complex (MHC) class II molecules. *J Cell Biol* **139(6)**, 1433 – 1446.

Ferrari, G., Langen, H., Naito, M. and Pieters, J. (1999). A coat protein on phagosomes involved in the intracellular survival of mycobacteria. *Cell* **97**, 435 – 447.

Fischer, K.D., Tedford, K. and Penninger, J.M. (1998). Vav links antigen-receptor signaling to the actin cytoskeleton. *Semin Immunol* **10**, 317 – 327.

Fontenot, J.D., Gavin, M.A. and Rudensky, A.Y. (2003). Foxp3 programs the development and function of CD4+CD25+ regulatory T cells. *Nat Immunol* **4**, 330 – 336.

Fowlkes, B. J. and Pardoll, D.M. (1989). Molecular and cellular events of T-cell development. *Adv Immunol* **44**, 207 – 264.

Freeman, G.J., Long, A.J., Iwai, Y., Bourque, K., Chernova, T., Nishimura, H. et al. (2000). Engagement of the PD-1 immunoinhibitory receptor by a novel B7 family member leads to negative regulation of lymphocyte activation. *J Exp Med* **192**, 1027 – 1034.

Fukui, Y., de Hostos, E.L. and Inoue, S. (1997). Dynamics of GFP-coronin and eupodia in live Dictyostelium observed with real-time confocal optics. *Biol Bull* **193**, 224 – 225.

Fukui, Y., Engler, S., Inoue, S., de Hostos, E.L. (1999). Architectural dynamics and gene replacement of coronin suggest its role in cytokinesis. *Cell Motil Cytoskeleton* **42**, 204 – 217.

Fukui, Y., Hashimoto, O., Sanui, T., Oono, T., Koga, H., Abe, M. et al. (2001). Haematopoietic cell-specific CDM family protein DOCK2 is essential for lymphocyte migration. *Nature* **412**, 826 – 831.

Fuller, C.L., Braciale, V.L. and Samelson, L.E. (2003). All roads lead to actin: the intimate relationship between TCR signaling and the cytoskeleton. *Immunol Rev* **191**, 220 – 236.

Gallatin, W.M., Weissman, I.L. and Butcher, E.C. (1983). A cell-surface molecule involved in organ-specific homing of lymphocytes. *Nature* **304**, 30-34.

Garcia, K.C., Teyton, L. and Wilson, I.A. (1999). Structural basis of T cell recognition. *Annu Rev Immunol* **17**, 369 – 397.

Garrett, W.S., Chen, L.M., Kroschewski, R., Ebersold, M., Turley, S., Trombetta, S., Galan, J.E. and Mellman, I. (2000). Developmental control of endocytosis in dendritic cells by Cdc42. *Cell* **102**, 325 – 334.

Gatfield, J. and Pieters, J. (2000). Essential role for cholesterol in entry of mycobacteria into macrophages. *Science* **288**, 1647 – 1650.

Gatfield, J. (2001). Studies on the tryptophan aspartate-containing coat protein (TACO) in *Mycobacterium*-infected and non-infected macrophages. PhD-thesis, Ruprecht-Karls-Universität, Heidelberg, Germany.

Gatfield, J., Albrecht, I., Zanolari, B., Steinmetz, M.O. and Pieters, J. (2005). Association of the leukocyte plasma membrane with the actin cytoskeleton through coiled coil-mediated trimeric coronin 1 moelcules. *Mol Biol Cell* **16**, 2786-2798.

Geiger, B., Rosen, D. and Berke, G. (1982). Spatial relationships of microtubule-organizing centers and the contact area of cytotoxic T lymphocytes and target cells. *J Cell Biol* **95**, 137 – 143.

Germain, R.N. and Stefanova, I. (1999). The dynamics of T cell receptor signaling: complex orchestration and the key roles of tempo and cooperation. *Annu Rev Immunol* **17**, 467 – 522.

Gleeson, P.A., Toh, B.H. and van Driel, I.R. (1996). Organ-specific autoimmunity induced by lymphopenia. *Immunol Rev* **149**, 97 – 125.

Godfrey, D.I., Kennedy, J., Suda, T. and Zlotnik, A. (1993). A developmental pathway involving four phenotypically and functionally distinct subsets of CD3-CD4-CD8-triple negative adult mouse thymocytes defined by CD44 and CD25 expression. *J Immunol* **150**, 4244 – 4252.

Goldrath, A.W. and Bevan, M.J. (1999). Low affinity ligands for the TCR drive proliferation of mature CD8+ T cells in lymphopenic hosts. *Immunity* **11**, 183 – 190.

Goldrath, A.W., Bogatzki, L.Y. and Bevan, M.J. (2000). Naive T cells transiently acquire a memory-like phenotype during homeostasis-driven proliferation. *J Exp Med* **192**, 557 – 564.

Goldrath, A.W. et al. (2002). Cytokine requirements for acute and basal homeostatic proliferation of naive and memory CD8+ T cells. *J Exp Med* **195**, 1515 – 1522.

Goldsby, R.A., Kindt, T.J., Osborne, B.A. and Kuby, J. (2003). Immunology. 5th edition. W.H. Freeman and Company, New York.

Gong, Q., Jin, X., Akk, A.M., Foger, N., White, M., Gong, G., Wardenburg, J.B. and Chan, A.C. (2001). Requirement for tyrosine residues 315 and 319 within zeta chain-associated protein 70 for T cell development. *J Exp Med* **194**, 507 – 518.

Goode, B.L., Wong, J.J., Butty, A.C., Peter, M., McCormack, A.L., Yates, J.R. et al. (1999). Coronin promotes the rapid assembly and cross-linking of actin filaments and may link the actin ann microtubule cytoskeleton in yeast. *J Cell Biol* **144**, 83 – 98.

Gordon, S. (1995). The macrophage. *BioEssays* **17**, 977 – 986.

Grakoui, A., Bromley, S.K., Sumen, C., Davis, M.M., Shaw, A.S., Allen, P.M. and Dustin, M.L. (1999). The immunological synapse: a molecular machine controlling T cell activation. *Science* **285**, 221 – 227.

Grandea, A.G., III, Golovina, T.N., Hamilton, S.E., Sriram, V., Spies, T., Brutkiewicz, R.R., Harty, J.T., Eisenlohr, L.C. and Van Kaer, L. (2000). Impaired assembly but yet normal trafficking of MHC class I molecules in Tapasin mutant mice. *Immunity* **13**, 213 – 222.

Grawunder, U., Leu, T.M., Schatz, D.G., Werner, A., Rolink, A.G., Melchers, F. and Winkler, T.H. (1995). Down-regulation of RAG1 and RAG2 gene expression in preB cells after functional immunoglobulin heavy chain rearrangement. *Immunity* **3**, 601 – 608.

Graziadei, L., Riabowol, K., Bar-Sagi, D. (1990). Co-capping of ras proteins with surface immunoglobulins in B lymphocytes. *Nature* **347**, 396 – 400.

Greenberg, P.D. and Ridell, S.R. (1999). Deficient cellular immunity – finding and fixing the defects. *Science* **285**, 546 – 551.

Greenberg, S. (1999). Modular components of phagocytosis. *J Leukocyte Biol* **66**, 712 – 717.

Groettrup, M., Ungewiss, K., Azogui, O., Palacios, R., Owen, M.J., Hayday, A.C. and von Boehmer, H. (1993). A novel disulfide-linked heterodimer on pre-T cells consists of the T cell receptor beta chain and a 33 kD glycoprotein. *Cell* **75(2)**, 283 – 294.

Groettrup, M. and von Boehmer, H. (1993). A role for a pre-T-cell receptor in T-cell development. *Immunol Today* **14**, 610 – 614.

Grogan, A., Reeves, E., Keep, N., Wientjes, F., Totty, N.F., Burlingame, A.L. et al. (1997). Cytosolic phox proteins interact with and regulate the assembly of coronin in neutrophils. *J Cell Sci* **110**, 3071 – 3081.

Gruenheid, S. and Finlay, B.B. (2003). Microbial pathogenesis and cytoskeletal function. *Nature* **422**, 775 – 781.

Gu, H., Marth, J.D., Orban, P.C., Mossmann, H. and Rajewsky, K. (1994). Deletion of a DNA polymerase beta gene segment in T cells using cell type-specific gene targeting. *Science* **265**, 103 - 106.

Hacker, U., Albrecht, R. and Maniak, M. (1997). Fluid-phase uptake by macropinocytosis in Dictyostelium. *J Cell Sci* **110**, 105 – 112.

Harder, T. and Simons, K. (1999). Clusters of glycolipid and glycosylphosphatidylinositol-anchored proteins in lymphoid cells: accumulation of actin regulated by local tyrosine phosphorylation. *Eur J Immunol* **29**, 556 – 562.

Harder, T. and Kuhn, M. (2000). Selective accumulation of raft-associated membrane protein LAT in T cell receptor signaling assemblies. *J Cell Biol* **151**, 199 – 208.

Harder, T. (2001). Raft membrane domains and immunoreceptor functions. *Adv Immunol* **77**, 45 – 92.

Harder, T. (2004). Lipid raft domains and protein networks in T-cell receptor signal transduction. *Curr Opin Immunol* **16**, 353 – 359.

Harnett, M.M., Katz, E. and Ford, C.A. (2005). Differential signalling during B-cell maturation. *Immunol Lett* **98**, 33 – 44.

Hasse, A., Rosentreter, A., Spoerl, Z., Stumpf, M., Noegel, A.A. et al. (2005). Coronin 3 and its role in murine brain morphogenesis. *Eur J Neurosci* **21**, 1155 – 1168.

Heil-Chapdelaine, R.A., Tran, N.K. and Cooper, J.A. (1998). The role of Saccharomyces cerevisiae coronin in the actin and microtubule cytoskeletons. *Curr Biol* **19**, 1281 – 1284.

Henning, S.W. and Cantrell, D.A. (1998). GTPases in antigen receptor signalling. *Curr Opin Immunol* **10**, 322 – 329.

Herzenberg, L.A. et al. (1986). The Ly-1 B cell lineage. *Immunol Rev* **93**, 81 – 102.

Hippenmeyer,S. et al. (2005). A developmental switch in the response of DRG neurons to ETS transcription factor signaling. *PLoS Biol* **3**, e159.

Hombach, J., Tsubata, T., Leclercq, L., Stappert, H. and Reth, M. (1990). Molecular components of the B-cell antigen receptor complex of the IgM class. *Nature* **343**, 760 – 762.

Hori, S., Nomura, T. and Sakaguchi, S. (2003). Control of regulatory T cell development by the transcription factor Foxp3. *Science* **299**, 1057 – 1061.

Hudrisier, D., Kessler, B., Valitutti, S., Horvath, C., Cerottini, J.C. and Luescher, I.F. (1998). The efficieny of antigen recognition by CD8+ CTL clones is determined by the frequency of serial TCR engagement. *J Immunol* **161**, 553 – 562.

Humphries, C.L., Balcer, H.L., D'Agostino, J.L., Winsor, B. Drubin, D.G., Barnes, G. et al. (2002). Direct regulation of Arp2/3 complex activity and function by the actin binding protein coronin. *J Cell Biol* **159**, 993 – 1004.

Iezzi, G., Scotet, E., Scheidegger, D. and Lanzavecchia, A. (1999). The interplay between the duration of TCR and cytokine signalling determines T cell polarization. *Eur J Immunol* **29**, 4092 – 4101.

Iizaka, M., Han, H.J., Akashi, H., Furukawa, Y., Nakajima, Y. et al. (2000). Isolation and chromosomal assignment of a novel human gene, CORO1C, homologous to coronin-like actin-binding proteins. *Cytogenet Cell Genet* **88**, 221 – 224.

Inaba, K., Metlay, J.P., Crowley, M.T. and Steinman, R.M. (1990). Dendritic cells pulsed with protein antigens in vitro can prime antigen-specific, MHC-restricted T cells in situ. *J Exp Med* **172**, 631 – 640.

Inaba, K., Turley, S., Iyoda, T., Yamaide, F., Shimoyama, S., Reis e Sousa, C., Germain, R.N., Mellman, I. and Steinman, R.M. (2000). The formation of immunogenic major histocompatibility complex class II-peptide ligands in lysosomal compartments of dendritic cells is regulated by inflammatory stimuli. *J Exp Med* **191**, 927 – 936.

Inaba, M., Kurasawa, K., Mamura, M., Kumano, K., Saito, Y. and Iwamoto, I. (1999). Primed T cells are more resistant to Fas-mediated activation-induced cell death than naive T cells. *J Immunol* **163**, 1315 – 1320.

Inoue, H., Nojima, H. and Okayama, H. (1990). High efficiency transformation of Escherichia coli with plasmids. *Gene* **96**, 23 – 28.

Irmler, M., Thome, M., Hahne, M., Schneider, P., Hofmann, K., Steiner, V. et al. (1997). Inhibition of death receptor signals by cellular FLIP. *Nature* **388**, 190 – 195.

Ishibashi, Y. and Arai, T. (1990). Effect of gamma-interferon on phagosome-lysosome fusion in Salmonella typhimurium-infected murine macrophages. *FEMS Microbiol Immunol* **2**, 75 – 82.

Itano, A.A., McSorley, S.J., Reinhardt, R.L., Ehst, B.D., Ingulli, E. et al. (2003). Distinct dendritic cell populations sequentially present antigen to CD4 T cells and stimulate different aspects of cell-mediated immunity. *Immunity* **19**, 47 – 57.

Itoh, S., Suzuki, K., Nishihata, J. Iwasa, M., Oku, T., Nakajin, S. Nauseef, W.M. and Toyoshima, S. (2002). The role of protein kinase C in the transient association of p57, a coronin family actin-binding protein, with phagosomes. *Biol Pharm Bull* **25**, 837 – 844.

Itoh, Y., Hemmer, B., Martin, R. and Germain, R.N. (1999). Serial TCR engagement and down-modulation by peptide:MHC molecule ligands: relationship to the quality of individual TCR signaling events. *J Immunol* **162**, 2073 – 2080.

Ivetic, A. and Ridley, A.J. (2004). Ezrin/radixin/moesin proteins and Rho GTPase signalling in leucocytes. *Immunology* **112**, 165 – 176.

Jaiswal, A.I. and Croft, M. (1997). CD40 ligand induction on T cell subsets by peptide-presenting B cells. *J Immunol* **159**, 2282 – 2291.

Jameson, S.C. (2002). Maintaining the norm: T-cell homeostasis. *Nat Rev Immunol* **2**, 547 – 556.

Janeway, C.A. (1989). Approaching the asymptote ? Evolution and revolution in immunology. *Cold Spring Harb Symp Quant Biol* **54** (Pt 1), 1 – 13.

Janeway, C.A., Travers, P., Walport, M. and Shlomchik, M.J. (2001). Immunobiology. The immune system in health and disease. 5th edition. Garland Publishing, New York.

Janeway, C.A. and Medzhitov, R. (2002). Innate immune recognition. *Annu Rev Immunol* **20**, 197 – 216.

Joyner, A.L. (1999). Gene Targeting. Second Edition. The Practical Approach Series, Oxford University Press, New York.

Jugloff, L.S. and Jongstra-Bilen, J. (1997). Cross-linking of the IgM receptor induces rapid translocation of IgM-associated Ig alpha, Lyn, and Syk tyrosine kinases to the membrane skeleton. *J Immunol* **159**, 1096 – 1106.

Jung, D. and Alt, F.W. (2004). Unraveling V(D)J recombination: insights into gene regulation. *Cell* **116**, 229 – 311.

Kaga, S., Ragg, S., Rogers, K.A. and Ochi, A. (1998). Stimulation of CD28 with B7-2 promotes focal adhesion-like cell contacts where Rho family small G proteins accumulate in T cells. *J Immunol* **160**, 24 – 27.

Kalia, V., Sarkar, S., Gourley, T.S., Rouse, B.T. and Ahmed, R. (2006). Differentiation of memory B and T cells. *Curr Opin Immunol* **18**, 255 – 264.

Karolchik, D., Baertsch, R., Diekhans, M., Furey, T.S., Hinrichs, A., Lu, Y.T., Roskin, K.M., Schwartz, M., Sugnet, C.W., Thomas, D.J., Weber, R.J., Haussler, D. and Kent, W.J. (2003). The UCSC Genome Browser Database. *Nucl. Acids Res* **31(1)**, 51-54.

Katsura, Y. (2002). Redefinition of lymphoid progenitors. *Nat Rev Immunol* **2**, 127 – 132.

Kelly, A.P., Monaco, J.J., Cho, S.G. and Trowsdale, J. (1991). A new human HLA class II-related locus, DM. *Nature* **353**, 571 – 573.

Kent, W.J., Sugnet, C. W., Furey, T. S., Roskin, K.M., Pringle, T. H., Zahler, A. M., and Haussler, D. (2002). The Human Genome Browser at UCSC. *Genome Res.* **12(6)**, 996-1006.

Kersh, E.N., Shaw, A.S. and Allen, P.M. (1998). Fidelity of T cell activation through multistep T cell receptor zeta phosphorylation. *Science* **281**, 572 – 575.

Khattri, R., Cox, T., Yasayko, S.A. and Ramsdell, F. (2003). An essential role for Scurfin in CD4+CD25+ T regulatory cells. *Nat Immunol* **4**, 337 – 342.

Khoruts, A. and Fraser, J.M. (2005). A causal link between lymphopenia and autoimmunity. *Immunol Lett* **98**, 23 – 31.

Kieper, W.C. and Jameson, S.C. (1999). Homeostatic expansion and phenotypic conversion of naive T cells in response to self peptide/MHC ligands. *Proc Natl Acad Sci USA* **96**, 13306 – 13311.

King, C., Ilic, A., Koelsch, K. and Savertnick, N. (2004). Homeostatic expansion of T cells during immune insufficiency generates autoimmunity. *Cell* **117**, 265 – 277.

Kirberg, J., Berns, A. and von Boehmer, H. (1997). Peripheral T cell survival requires continual ligation of the T cell receptor to major histocompatibility complex-encoded molecules. *J Exp Med* **186**, 1269 – 1275.

Korade-Mirnics, Z. and Corey, S.J. (2000). Src kinase-mediated signaling in leukocytes. J Leukoc Biol 68, 603 – 613.

Koretzky, G.A. and Myung, P.S. (2001). Positive and negative regulation of T-cell activation by adaptor proteins. *Nat Rev Immunol* **1**, 95 – 107.

Kropshofer, H., Arndt, S.O., Moldenhauer, G., Hammerling, G.J. and Vogt, A.B. (1997). HLA-DM acts as a molecular chaperone and rescues empty HLA-DR molecules at lysosomal pH. *Immunity* **6**, 293 – 302.

Krummel, M.F. and Davis, M.M. (2002). Dynamics of the immunological synapse: finding, establishing and solidifying a connection. *Curr Opin Immunol* **14**, 66 – 74.

Kundig, T.M., Shahinian, A., Kawai, K., Mittrucker, H.W., Sebzda, E., Bachmann, M.F., Mak, T.W. and Ohashi, P.S. (1996). Duration of TCR stimulation determines costimulatory requirement of T cells. *Immunity* **5**, 41 – 52.

Kung,C., and Thomas, M. L. (1999). Genomic organization and chromosomal localization of mouse coronin-1. *Mammalian Genome* **10**, 523-525.

Kupfer, A. and Singer, S.J. (1989). Cell biology of cytotoxic and helper T cell functions: immunofluorescence microscopic studies of single cells and cell couples. *Annu Rev Immunol* **7**, 309 – 337.

Kupfer, A., Mosmann, T.R. and Kupfer, H. (1991). Polarized expression of cytokines in cell conjugates of helper T-cells and splenic B cells. *Proc Natl Acad Sci USA* **88**, 775 – 779.

La Gruta, N.L., Driel, I.R. and Gleeson, P.A. (2000). Peripheral T cell expansion in lymphopenic mice results in a restricted T cell repertoire. *Eur J Immunol* **30**, 3380 – 3386.

Lakso, M., Sauer, B., Mosinger, B., Lee, E.J., Manning, R.W., Yu, S.H., Mulder, K.L. and Westphal, H. (1992). Targeted oncogene activation by site-specific recombination in transgenic mice*. Proc Natl Acad Sci USA* **89**, 6232 - 6236.

Lam, K.P., Kuhn, R. and Rajewsky, K. (1997). In vivo ablation of surface immunoglobulin on mature B cells by inducible gene targeting results in rapid cell death. *Cell* **90**, 1073 – 1083.

Lane, P., Traunecker, A., Hubele, S., Inui, S., Lanzavecchia, A. and Gray, D. (1992). Activated human T cells express a ligand for the human B-cell-associated antigen CD40 which participates in T cell-dependent activation of B lymphocytes. *Eur J Immunol* **22**, 2573 – 2578.

Lanzavecchia, A. (1987). Antigen uptake and accumulation in antigen-specific B cells. *Immunol Rev* **99**, 39 – 51.

Lanzavecchia, A. (1990). Receptor-mediated antigen-uptake and its effect on antigen presentation to class II restricted T-lymphocytes. *Annu Rev Immunol* **8**, 773 – 793.

Lanzavecchia, A., Reid, P.A. and Watts, C. (1992). Irreversible association of peptides with class II MHC molecules in living cells. *Nature* **357**, 249 – 252.

Lanzavecchia, A., Iezzi, G. and Viola, A. (1999). From TCR engagement to T cell activation: a kinetic view of T cell behavior. *Cell* **96**, 1 – 4.

Lanzavecchia, A. and Sallusto, F. (2000a). From synapses to immunological memory : the role of sustained T cell stimulation. *Curr Opin Immunol* **12**, 92 – 98.

Lanzavecchia, A. and Sallusto, F. (2000b). Dynamics of T lymphocyte responses: intermediates, effectors and memory cells. *Science* **290**, 92 – 97.

Lauber, K. Blumenthal, S.G., Waibel, M. and Wesselborg, S. (2004). Clearance of apoptotic cells: getting rid of the corpses. *Mol Cell* **14**, 277 – 287.

Leitenberg, D., Balamuth, F. and Bottomly, K. (2001). Changes in the T cell receptor macromolecular signaling complex and membrane microdomains during T cell development and activation. *Semin Immunol* **13**, 129 – 138.

Leptin, M. (1985). Monoclonal antibodies specific for murine IgM. II. Activation of B lymphocytes by monoclonal antibodies specific for the four constant domains of IgM. *Eur J Immunol* **15**, 131 – 137.

Letourneur, F. and Klausner, R.D. (1992). A novel di-leucine motif and a tyrosine-based motif independently mediate lysosomal targeting and endocytosis of CD3 chains. *Cell* **69**, 1143 – 1157.

Li, D. and Roberts, R. (2001). WD-repeat proteins: structure characteristics, biological function, and their involvement in human diseases. *Cell Mol Life Sci* **58**, 2085 – 2097.

Lin, J. and Weiss, A. (2001). Identification of the minimal tyrosine residues required for linker for activation of T cell function. *J Biol Chem* **276**, 29588 – 29595.

Lind, E.F., Prockop, S.E., Porritt, H.E. and Petrie, H.T. (2001). Mapping precursor movement through the postnatal thymus reveals specific microenvironments supporting defined stages of early lymphoid development. *J Exp Med* **194**, 127 – 134.

Liszweski, M.K., Farries, T.C., Lublin, D.M., Rooney, I.A. and Atkinson J.P. (1996). Control of the complement system. *Adv Immunol* **61**, 201 – 283.

Liu, Y.J. (1997). Sites of B lymphocyte selection, activation, and tolerance in spleen. *J Exp Med* **186**, 625 – 629.

Lotteau, V., Teyton, L., Peleraux, A., Nilsson, T., Karlsson, L., Schmid, S.L., Quaranta, V. and Peterson, P.A. (1990). Intracellular transport of class II MHC molecules directed by invariant chain. *Nature* **348**, 600 – 605.

Ma, A., Koka, R. and Burkett, P. (2006). Diverse functions of IL-2, IL-15, and IL-7 in lymphoid homeostasis. *Annu Rev Immunol* **24**, 657 – 679.

Machesky, L.M. et al. (1997). Mammalian actin-related protein 2/3 complex localizes to regions of lamellipodial protrusion and is composed of evolutionary conserved proteins. *Biochem J* **328**, 105 – 112.

Mackall, C.L., Hakim, F.T. and Gress, R.E. (1997). Restoration of T-cell homeostasis after T-cell depletion. *Semin Immunol* **9**, 339 – 346.

Mackay, I.R. and Rosen, F.S. (2000). T-cell function and migration: two sides of the same coin. *New Eng J Med* **343**, 1020 – 1034.

MacLennan, I.C.M., Gulbranson-Judge, A., Toellner, K.M., Casamayor-Palleja, M., Chan, E., Sze, D.M.Y., Luther, S.A. and Orbea, H.A. (1997). The changing preference of T and B cells for partners as T-dependent antibody responses develop. *Immunol Rev* **156**, 53 – 66.

Magnan, A., Di Bartolo, V., Mura, A.M., Boyer, C., Richelme, M., Lin, Y.L., Roure, A. et al. (2001). T cell development and T cell responses in mice with mutations affecting tyrosines 292 or 315 of the ZAP-70 protein tyrosine kinase. *J Exp Med* **194**, 491 – 505.

Malissen, M. et al. (1995). Altered T-cell development in mice with targeted mutation of the CD3-□gene. *EMBO J* **14**, 4641 – 4653.

Maniak, M., Rauchenberger, R., Albrecht, R., Murphy, J. and Gerisch, G. (1995). Coronin involved in phagocytosis: dynamics of particle-induced relocalization visualized by green fluorescent protein tag. *Cell* **83**, 915 – 924.

Marrack, P. and Kappler, J. (1997). Positive selection of thymocytes bearing □□ T cell receptors. *Curr Opin Immunol* **9**, 250 – 255.

Matloubian, M., Lo, C.G., Cinamon, G., Lesneski, M.J., Xu, Y., Brinkmann, V. et al. (2004). Lymphocyte egress from thymus and peripheral lymphoid organs is dependent on S1P receptor 1. *Nature* **427**, 355 – 360.

Meiri, K.F. (2004). Membrane/cytoskeleton communication. *Subcell Biochem* **37**, 247 – 282.

Melchers, F. and Rolink A.G. (1998). B-lymphocyte development and biology. In *Fundamental Immunology*. Edited by Paul, W.E.; Lippincott-Raven Publishers, Philadelphia.

Mempel, T.R., Henrickson, S.E. and von Andrian (2004). T-cell priming by dendritic cells in lymph nodes occurs in three distinct phases. *Nature* **427**, 154 – 159.

Millard, T.H., Sharp, S.J. and Machesky, L.M. (2004). Signalling to actin assembly via the WASP (Wiskott-Aldrich syndrome protein)-family proteins and the Arp2/3 complex. *Biochem J* **380**, 1 – 17.

Miller, J.F. and Osoba, D. (1967). Current concepts of the immunological function of the thymus. *Physiol Rev* **47**, 437 – 520.

Milne, C.D. and Paige, C.J. (2006). IL-7: a key regulator of B lymphopoiesis. *Sem Immunol* **18**, 20- 30.

Mond, J.J. et al. (1995a). T cell independent antigens. *Curr Opin Immunol* **7**, 349 – 354.

Mond, J.J., Lees, A. and Snapper, C.M.(1995b). T cell-independent antigens type 2. *Annu Rev Immunol* **13**, 655 – 692.

Monks, C.R., Freiberg, B.A., Kupfer, H., Sciaky, N. and Kupfer, A. (1998). Three-dimensional segregation of supramolecular activation clusters in T cells. *Nature* **395**, 82 – 86.

Montixi, C. Langlet, C., Bernard, A.M., Thimonier, J., Dubois, C., Wurbel, M.A., Chauvin, J.P., Pierres, M. and He, H.T. (1998). Engagement of T cell receptor triggers its recruitment to low-density detergent-insoluble membrane domains. *EMBO J* **17**, 5334 – 5348.

Morrissette, N.S., Gold, E.S., Guo, J., Hamerman, J.A., Ozinsky, A. et al. (1999). Isolation and characterization of monoclonal antibodies directed against novel components of macrophage phagosomes. *J Cell Sci* **112**, 4705 – 4713.

Muralikrishna, T., Begum, Z., Swamy, C.V. and Khar, A. (1998). Molecular cloning and characterization of a tumor rejection antigen from rat histiocytoma, AK-5. *DNA Cell Biol* **17**, 603 – 612.

Murali-Krishna, K. et al. (1999). Persistence of memory CD8 T cells in MHC class I-deficient mice. *Science* **286**, 1377 – 1381.

Nagata, S. (1997). Apoptosis by death factor. *Cell* **88**, 355 – 365.

Nakamura, T., Takeuchi, K., Muraoka, S., Takezoe, H., Takahashi, N. et al. (1999). A neurally enriched coronin-like protein, ClipinC, is a novel candidate for an actin cytoskeleton-cortical membrane-linking protein. *J Cell Biol* **274**, 13322 – 13327.

Nal, B. et al. (2004): Coronin-1 expression in T-lymphocytes: insights into protein function during T-cell development and activation. *Int Immunol* **16**, 231-240.

Neefjes, J.J., Momburg, F. and Hammerling, G.J. (1993). Selective and ATP-dependent translocation of peptides by the MHC-encoded transporter. *Science* **261**, 769 –771.

Neer, E.J., Schmidt, C.J., Nambudripad, R. and Smith, T.F. (1994). The ancient regulatory-protein family of WD-repeat proteins. *Nature* **371**, 297 – 300.

Niiro, H. and Clark, E.A. (2002). Regulation of B-cell fate by antigen-receptor signals. *Nat Rev Immunol* **2**, 945 – 956.

Nussenzweig, M.C., Shaw, A.C., Sinn, E., Danner, D.B., Holmes, K.L., Morse, H.C. and Leder, P. (1987). Allelic exclusion in transgenic mice that express the membrane from of immunoglobulin mu. *Science* **236**, 816 – 819.

Ochsenbein, A.F. et al. (1999). Control of early viral and bacterial distribution and disease by natural antibodies. *Science* **286**, 2156 – 2159.

Ochsenbein, A.F. and Zinkernagel, R.M. (2000). Natural antibodies and complement link innate and acquired immunity. *Immunol Today* **21**, 624 – 630.

O'Garra, A. and Arai, N. (2000). The molecular basis of T helper 1 and T helper 2 cell differentiation. *Trends Cell Biol* **10**, 542 – 550.

Okumura, M., Kung, C., Wong, S., Rodgers, M. and Thomas, M.L. (1998). Definition of family of coronin-related proteins conserved between humans and mice: close genetic linkage between coronin-2 and CD45-associated protein. *DNA Cell Biol* **17**, 779 – 787.

O'Rourke, L., Tooze, R. and Fearon, D.T. (1997). Co-receptors of B lymphocytes. *Curr Opin Immunol* **9**, 324 – 329.

Parente, J.A. Jr., Chen, X., Zhou, C., Petropoulos, A.C. and Chew, C.S. (1999). Isolation, cloning, and characterization of a new mammalian coronin family member, coroninse, which is regulated within the protein kinase C signaling pathway. *J Biol Chem* **274**, 3017 – 3025.

Parker, D.C. (1993). T cell-dependent B-cell activation. *Annu Rev Immunol* **11**, 331 – 340.

Paz, P.E., Wang, S., Clarke, H., Lu, X., Stokoe, D. and Abo, A. (2001). Mapping the Zap-70 phosphorylation sites on LAT (linker for activation of T cells) required for recruitment and activation of signalling proteins in T cells. *Biochem J* **356**, 461 – 471.

Pentcheva-Hoang, T., Egen, J.G., Wojnoonski, K. and Allison, J.P. (2004). B7-1 and B7-2 selectively recruit CTLA-4 and CD28 to the immunological synapse. *Immunity* **21**, 401 – 413.

Peschon, J.J., Morrisey, P.J., Grabstein, K.H., Ramsdell, F.J., Maraskovsky, E., Gliniak, B.C., Park, L.S., Ziegler, S.F. et al. (1994). Early lymphocyte expansion is severely impaired in interleukin 7 receptor-deficient mice. *J Exp Med* **180**, 1955 – 1960.

Pierce, S.K. (2002). Lipid rafts and B-cell activation. *Nat Rev Immunol* **2**, 96 – 105.

Pieters, J., Neefjes, J.J., Oorschot, V., Ploegh, H.L. and Geuze, H.J. (1991). Segregation of MHC class II molecules from MHC class I molecules in the Golgi complex for transport to lysosomal compartments. *Nature* **349**, 669 – 676.

Pieters, J., Bakke, O. and Dobberstein, B. (1993). The MHC class II-associated invariant chain contains two endosomal targeting signals within its cytoplasmic tail. *J Cell Sci* **106**, 831 – 846.

Porritt, H.E., Gordon, K. and Petrie, H.T. (2003). Kinetics of steady-state differentiation and mapping of intrathymic-signaling environments by stem cell transplantation in nonirradiated mice. *J Exp Med* **198**, 957 – 962.

Prockop, S.E. et al. (2002). Stromal cells provide the matrix for migration of early lymphoid progenitors through the thymic cortex. *J Immunol* **169**, 4354 – 4361.

Randolph, G.J. (2001). Dendritic cell migration to lymph nodes: cytokines, chemokines, and lipid mediators. *Semin Immunol* **13**, 267 – 274.

Rao, A., Luo, C. and Hogan, P.G. (1997). Transcription factors of the NFAT family: regulation and function. *Annu Rev Immunol* **15**, 707 – 747.
Rappleye, C.A., Paredez, A.R., Smoth, C.W., McDonald, K.L. and Aroian, R.V. (1999). The coronin-like protein POD-1 is required for anterior-posterior axis formation and cellular architecture in the nematode Caenorhabditis elegans. *Genes Dev* **13**, 2838 – 2851.

Rathmell, J.C. and Thompson, C.B. (1999). The central effectors of cell death in the immune system. *Annu Rev Immunol* **17**, 781 – 828.

Rathmell, J.C., Farkash, E.A., Gao, W. and Thompson, C.B. (2001). IL-7 enhances the survival and maintains the size of naive T cells. *J Immunol* **167**, 6869 – 6876.

Read, S., Mauze, S., Asseman, C., Bean, A., Coffman, R. and Powrie, F. (1998). CD38+CD45RblowCD4+ T cells: a population of T cells with immune regulatory activities in vitro. *Eur J Immunol* **28**, 3435 – 3447.

Refaeli, Y, Van Parijs, L., London, C.A., Tschopp, J. and Abbas, A.K. (1998). Biochemical mechanisms of IL-2-regulated Fas-mediated T cell apoptosis. *Immunity* **8**, 615 – 623.

Reichert, P., Reinhardt, R.L., Ingulli, E. and Jenkins, M.K. (2001). Cutting edge: in vivo identification of TCR redistribution and polarized IL-2 production by naive CD4 T cells. *J Immunol* **166**, 4278 – 4281.

Reth, M. (1989). Antigen receptor tail clue. *Nature* **338**, 383.

Roche, P.A. and Cresswell, P. (1990). Invariant chain association with HLA-DR molecules inhibits immunogenic peptide binding. *Nature* **345**, 615 – 618.

Rogers, J., Early, P., Carter, C., Calame, K., Bond, M., Hood, L. and Wall, R. (1980). Two mRNAs with different 3' ends encode membrane-bound and secreted forms of the immunoglobulin mu chain. *Cell* **20**, 303 – 312.

Rohagti, R., Ma, L., Miki, H., Lopez, M., Kirchhausen, T., Takenawa, T. and Kirschner, M.W. (1999). The interaction between N-WASP and the Arp2/3 complex links Cdc42-dependent signals to actin assembly. *Cell* **97**, 221 – 231.

Rolink, A.G., Winkler, T., Melchers, F. and Andersson, J. (2000). Precursor B-cell receptor-dependent B-cell proliferation and differentiation does not require the bone marrow or fetal liver environment. *J Exp Med* **191**, 23 – 32.

Rolink, A.G., Andersson, J. and Melchers, F. (2004). Molecular mechanisms guiding the late stages of B-cell development. *Immunol Rev* **197**, 41 – 50.

Rothenberg, M.E., Rogers, S.L., Vale, R.D., Jan, L.Y. and Jan, Y.N. (2003). Drosophila POD-1 crosslinks both actin and microtubules and controls the targeting of axons. *Neuron* **39**, 779 – 791.

Rudd, C.E. (1999). Adaptors and molecular scaffolds in immune cell signaling. *Cell* **96**, 5- 8.

Rybakin, V., Stumpf, M., Schulze, A., Majoul, I.V., Noegel, A.A. et al. (2004). Coronin 7, the mammalian POD-1 homologue, localizes to the Golgi apparatus. *FEBS Lett* **573**, 161 – 167.

Rybakin, V. and Clemen, C.S. (2005). Coronin proteins as multifunctional regulators of the cytoskeleton and membrane trafficking. *BioEssays* **27**, 625 – 632.

Ryser, J.E., Rungger-Brandle, C., Chaponnier, C., Gabbiani, G. and Vassalli, P (1982). The area of attachment of cytotoxic T lymphocytes to their target cells shows high motility and polarization of actin, but not myosin. *J Immunol* **128**, 1159 – 1162.

Saeterdal, I., Bjorheim, J., Lislerud, K., Gjertsen, M.K., Bukholm, I.K. et al. (2001). Frameshift-mutation-derived peptides as tumor-specific antigens in inherited and spontaneous colorectal cancer. *Proc Natl Acad Sci USA* **98**, 13255 – 13260.

Sakaguchi, S., Sakaguchi, N., Asano, M., Itoh, M. and Toda, M. (1995). Immunologic self-tolerance maintained by activated T cells expressing IL-2 receptor alpha-chains (CD25). Breakdown of a single mechanism of self-tolerance causes various autoimmune diseases. *J Immunol* **155**, 1151 – 1164.

Sakaguchi, S. (2004). Naturally arising CD4+ regulatory T cells for immunologic self-tolerance and negative control of immune responses. *Annu Rev Immunol* **22**, 531 – 562.

Sallusto, F. and Lanzavecchia, A. (1994). Efficient presentation of soluble antigen by cultured human dendritic cells is maintained by granulocyte/macrophage colony-stimulating factor plus interleukin 4 and downregulated by tumor necrosis factor alpha. *J Exp Med* **179**, 1109 – 1118.

Sallusto, F., Cella, M., Danieli, C. and Lanzavecchia, A. (1995). Dendritic cells use macropinocytosis and the mannose receptor to concentrate macromolecules in the major histocompatibility complex class II compartment: downregulation by cytokines and bacterial products. *J Exp Med* **182**, 389 – 400.

Samelson, L.E., Harford, J.B. and Klausner, R.D. (1985). Identification of the components of the murine T cell antigen receptor complex. *Cell* **43**, 223 – 231.

Sanford, L.P., Kallapur, S., Ornsby, I., and Doetschman, T. (2001). Influence of genetic background on knockout mouse phenotypes. *Methods Mol Biol* **158**, 217-25.

Schafer, D.A. (2002). Coupling actin dynamics and membrane dynamics during endocytosis. *Curr Opin Cell Biol* **14**, 76 – 81.

Schluns, K.S., Williams, K., Ma, A., Zheng, X.X. and Lefrancois, L. (2002). Cutting edge: requirement for IL-15 in the generation of primary and memory antigen-specific CD8 T cells. *J Immunol* **168**, 4827 – 4831.

Schulze, K.L., Broadie, K., Perin, M.S. and Bellen, H.J. (1995). Genetic and electrophysiological studies of Drosophila syntaxin-1A demonstrate its role in nonneuronal secretion and neurotransmission. *Cell* **80**, 311 – 320.

Seddon, B. and Zamoyska, R. (2002). TCR and IL-7 receptor signals can operate independently or synergize to promote lymphopenia-induced expansion of naive T cells. *J Immunol* **169**, 3752 – 3759.

Serrador, J.M., Nieto, M. and Sanchez-Madrid, F. (1999). Cytoskeletal rearrangements during migration and activation of T lymphocytes. *Trends Cell Biol* **9**, 228 – 233.

Shastri, N., Schwab, S. and Serwold, T. (2002). Producing nature's gene-chips: the generation of peptides for display by MHC class I molecules. *Annu Rev Immunol* **20**, 463 – 493.

Shevach, E.M. (2000). Regulatory T cells in autoimmunity. *Annu Rev Immunol* **18**, 423 – 449.

Silver, L.M. (1995). Mouse Genetics. Oxford University Press, New York.

Silverstein, S.C. (1995). Phagocytosis of microbes: insights and prospects. *Trends Cell Biol* **5**, 141 – 142.

Simons, K. and Ikonen, E. (1997). Functional rafts in cell membranes. *Nature* **387**, 569 – 572.

Smith, P.K., Krohn, R.I., Hermanson, G.T., Mallia, A.K., Gartner, F.H. et al. (1985). Measurement of protein using bicinchoninic acid. *Anal Biochem* **150**, 76 – 85.

Snapper, S.B. and Rosen, F.S. (1999). The Wiskott-Aldrich syndrome protein (WASP): roles in signaling and cytoskeletal organization. *Annu Rev Immunol* **17**, 905 – 929.

Sommers, C.L., Menon, R.K., Grinberg, A., Zhang, W., Samelson, L.E. and Love, P.E. (2001). Knock-in mutation of the distal four tyrosines of linker for activation of T cells blocks murine T cell development. *J Exp Med* **194**, 135 – 142.

Sondek, J., Bohm, A., Lambright, D.G., Hamm, H.E. and Sigler, P.B. (1996). Crystal structure of a G-protein beta gamma dimer at 2.1 A resolution. *Nature* **379**, 369 – 374.

Spies, T., Bresnahan, M., Bahram, S., Arnold, D., Blanck, G., Mellins, E., Pious, D. and DeMars, R. (1990). A gene in the human major histocompatibility complex class II region controlling the class I antigen presentation pathway. *Nature* **348**, 744- 747.

Spoerl, Z., Stumpf, M., Noegel, A.A., Hasse, A. (2002). Oligomerization, F-actin interaction, and membrane association of the ubiquitous mammalian coronin 3 are mediated by its carboxyl terminus. *J Biol Chem* **277**, 48858 – 48867.

Sprent, J. and Webb, S.R. (1995). Intrathymic and extrathymic clonal deletion of T cells. *Curr Opin Immunol* **7**, 196 – 205.

Sprent, J. and Surh, C.D. (2001). Generation and maintenance of memory T cells. *Curr Opin Immunol* **13**, 248 – 254.

Sprent, J. and Tough, D.F. (2001). T cell death and memory. *Science* **293**, 245 – 248.

Starr, T.K., Jameson, S.C. and Hogquist, K.A. (2003). Positive and negative selection of T-cells. *Annu Rev Immunol* **21**, 139 – 176.

Steimle, V., Siegrist C.A., Mottet, A., Lisowska-Grospierre, B. and Mach, B. (1994). Regulation of MHC class II expression by interferon-gamma mediated by the transactivator gene CIITA. *Science* **265**, 106 – 109.

Steinman, R.M., Pack, M. and Inaba, K. (1997). Dendritic cells in the T-cell areas of lymphoid organs. *Immunol Rev* **156**, 25 – 37.

Stinchcombe, J.C., Bossi, G., Booth, S. and Griffiths, G.M. (2001). The immunological synapse of CTL contains a secretory domain and membrane bridges. *Immunity* **15**, 751 – 761.

Stockinger, B. Kassiotis, G. and Bourgeois, C. (2004). Homeostasis and T cell regulation. *Curr Opin Immunol* **16**, 775 – 779.

Stowers, L., Yelon, D., Berg, L.J. and Chant, S. (1995). Regulation of the polarization of T cells toward antigen-presenting cells by Ras-related GTPase CDC42. *Proc Natl Acad Sci USA* **92**, 5027 – 5031.

Surh, C.D. and Sprent, J. (2000). Homeostatic T cell proliferation: how far can T cells be activated to self-ligands ? *J Exp Med* **192**, F9 – F14.

Suzuki, K., Nishihata, J., Arai, Y., Honma, N., Yamamoto, K. et al. (1995). Molecular cloning of a novel actin-binding protein, p57, with a WD repeat and a leucine zipper motif. *FEBS Lett* **364**, 283 – 288.

Swain, S.L., Hu, H. and Huston, G. (1999). Class II-independent generation of CD4 memory T cells from effectors. *Science* **286**, 1381 – 1383.

Takahashi, T., Kuniyasu, Y., Toda, M., Sakaguchi, N., Itoh, M. et al. (1998). Immunologic self-tolerance maintained by CD25+CD4+ naturally anergic and suppressive T cells: induction of autoimmune disease by breaking their anergic/suppressive state. *Int Immunol* **10**, 1969 – 1980.

Takeda, S., Rodewald, H.R., Arakawa, H., Bluethmann, H. and Shimizu, T. (1996). MHC class II molecules are not required for survival of newly generated CD4+ T cells, but affect their long-term life span. *Immunity* **5**, 217 – 228.

Tanchot, C., Lemmonnier, F.A., Peranau, B., Freitas, A.A. and Rocha, B. (1997). Differential requirements for survival and proliferation of CD8 naive and memory T cells. *Science* **276**, 2057 – 2062.

Taylor, P.R., Martinez-Pomares, L., Stacey, M., Lin, H.H., Brown, G.D. and Gordon, S. (2005). Macrophage receptors and immune recognition. *Annu Rev Immunol* **23**, 901 – 944.

Teyton, L., O'Sullivan, D., Dickson, P.W., Lotteau, V., Sette, A., Fink, P. and Peterson, P.A. (1990). Invariant chain distinguishes between the exogenous and endogenous antigen presentation pathways. *Nature* **348**, 39 – 44.

Thomas, K.R. and Capecchi, M.R. (1987). Site-directed mutagenesis by gene targeting in mouse embryo-derived stem cells. *Cell* **51(3)**, 503-12.

Thornton, A.M. and Shevach, E.M. (1998). CD4+CD25+ immunoregulatory T cells suppress polyclonal T cell activation in vitro by inhibiting interleukin 2 production. *J Exp Med* **188**, 287 – 296.

Timmerman, L.A., Clipstone, N.A., Ho, S.N., Northrop, J.P. and Crabtree, G.R. (1996). Rapid shuttling of NF-AT in discrimination of Ca2+ signals and immunosuppression. *Nature* **383**, 837 – 840.

Tomlinson, M.G., Lin, J. and Weiss, A. (2000). Lymphocytes with a complex: adapter proteins in antigen receptor signaling. *Immunol Today* **21**, 584 – 591.

Tonegawa, S. (1983). Somatic generation of antibody diversity. *Nature* **302**, 575 – 581.

Tonegawa, S. (1988). Somatic generation of immune diversity. *Biosci Rep* **8**, 3 – 26.

Trombetta, E.S. and Mellman, I. (2005). Cell biology of antigen processing in vitro and in vivo. *Annu Rev Immunol* **23**, 975 – 1028.

Tough, D.F. and Sprent, J. (1994). Turnover of naïve- and memory-phenotype T cells. *J Exp Med* **179**, 1127 – 1135.

Troy, A.E. and Shen, H. (2003). Cutting edge: homeostatic proliferation of peripheral T lymphocytes is regulated by clonal competition. *J Immunol* **170**, 672 – 676.

Tseng, S.Y., Liu, M. and Dustin, M.L. (2005). CD80 cytoplasmic domain controls localization of CD28, CTLA-4, and protein kinase C theta in the immunological synapse. *J Immunol* **175**, 7829 – 7836.

Tulp, A., Verwoerd, D. Dobberstein, B., Ploegh, H.L. and Pieters, J. (1994). Isolation and characterization of the intracellular MHC class II compartment. *Nature* **369**, 120 – 126.

Uetrecht, A.C. and Bear, J.E. (2006). Coronins: the return of the crown. Trends Cell Biol, electronic publication ahead of print.

Underhill, D.M. and Ozinsky, A. (2002). Phagocytosis of microbes: complexity in action. *Annu Rev Immunol* **20**, 825 – 852.

Valle, A., Zuber, C.E., Defrance, T., Djossou, O., De, R.M. and Banchereau, J. (1989). Activation of human B lymphocytes through CD40 andd interleukin 4. *Eur J Immunol* **19**, 1463 – 1467.

Valitutti, S., Muller, S., Cella, M., Padovan, E. and Lanzavecchia, A. (1995a). Serial triggering of many T-cell receptors by a few peptide-MHC complexes. *Nature* **375**, 148 – 151.

Valitutti, S., Dessing, M., Aktories, K., Gallati, H. and Lanzavecchia, A. (1995b). Sustained signaling leading to T cell activation results from prolonged T cell receptor occupancy. Role of T cell actin cytoskeleton.. *J Exp Med* **181**, 577 – 584.

Valitutti, S. and Lanzavecchia, A. (1997). Serial triggering of TCRs: a basis for the sensitivity and specificity of antigen recognition. *Immunol Today* **18**, 299.

Van den Merwe, P.A. (2002). Formation and function of the immunological synapse. *Curr Opin Immunol* **14**, 293 – 298.

Vella, A.T., Dow, S., Potter, T.A., Kappler, J. and Marrack, P. (1998). Cytokine-induced survival of activated T cells in vitro and in vivo. *Proc Natl Acad Sci USA* **95**, 3810 – 3815.

Vincente-Manzanares, M., Sancho, D., Yanez-Mo, M. and Sanchez-Madrid, F. (2002). The leukocyte cytoskeleton in cell migration and immune interactions. *Int Rev Cytol* **216**, 233 – 289.

Vivien, L., Benoist, C. and Mathis, D. (2001). T lymphocytes need IL-7 but not IL-4 or IL-6 to survive in vivo. *Int Immunol* **13**, 763 – 768.

Von Andrian, U.H. and Mempel, T.R. (2003). Homing and cellular traffic in lymph nodes. *Nat Rev Immunol* **3**, 867 – 878.

Von Boehmer, H., Aifantis, I., Azogui, O., Feinberg, J., Saint-Ruf, C., Zober, C., Garcia, C. and Buer, J. (1998). Crucial function of the pre-T-cell receptor (TCR) in TCR beta chain selection, TCR beta allelic exclusion and alpha beta versus gamma delta lineage commitment. *Immunol Rev* **165**, 111 – 119.

Von Freeden-Jeffry, U., Vieira, P., Lucian, L.A., McNeil, T., Burdach, S.E. and Murray, R. (1995). Lymphopenia in interleukin (IL)-7 gene-deleted mice identifies IL-7 as a nonredundant cytokine. *J Exp Med* **181**, 1519 – 1526.

Wallis, V.J., Leuchars, E., Chwalinski, S. and Davies, A.J. (1975). On the sparse seeding of bone marrow and thymus in radiation chimaeras. *Transplantation* **19**, 2 – 11.

Wang, R.F., Parkhurst, M.R., Kawakami, Y., Robbins, P.F. and Rosenberg, S.A. (1996). Utilization of an alternative open reading frame of a normal gene in generating a novel human cancer antigen. *J Exp Med* **183**, 1131 – 1140.

Ward, E.S. and Ghetie, V. (1995). The effector functions of immunoglobulins: implications for therapy. *Thera Immunol* **2**, 77 – 94.

Watts, C. (1997). Capture and processing of exogenous antigens for presentation on MHC molecules. *Annu Rev Immunol* **15**, 821 – 850.

Webb, Y., Hermida-Matsumoto, L. and Resh, M.D. (2000). Inhibition of protein palmitoylation, raft localization and T cell signaling by 2-bromopalmitate and polyunsaturated fatty acids. *J Biol Chem* **275**, 261 – 270.

Weiss, A., Shields, R., Newton, M., Manger, B. and Imboden, J. (1987). Ligand-receptor interactions required for commitment to the activation of the interleukin 2 gene. *J Immunol* **138**, 2169 – 2176.

Werlen, G., Hausmann, B., Naeher, D. and Palmer, E. (2003). Signaling life and death in the thymus: timing is everything. *Science* **299**, 1859 – 1863.

West, M.A., Lucocq, J.M. and Watts, C. (1994). Antigen processing and class II MHC peptide-loading compartments in human B-lymphoblastoid cells. *Nature* **369**, 147 – 151.

Wiltschke, C., Nemet, H., Holzinger, C., Gessl, A., Pernerstorfer, T., Forster, O., Boltz-Nitulescu, G. (1989). Murine recombinant GM-CSF-driven rat bone marrow cell differentiation and factors suppressing cell proliferation. *Immunobiology* **179**, 145 – 158.

Wu, M.N., Fergestad, T., Lloyd, T.E., He, Y., Broadie, K. et al. (1999). Syntaxin 1A interacts with multiple exocytic proteins to regulate neurotransmitter release in vivo. *Neuron* **23**, 593 – 605.

Wülfing, C., Sjaastad, M.D. and Davis, M.M. (1998). Visualizing the dynamics of T cell activation: intracellular adhesion molecule 1 migrates rapidly to the T cell/B cell interface and acts to sustain calcium levels. *Proc Natl Acad Sci USA* **95**, 6302 - 6307.

Xavier, R., Brennan, T., Li, Q., McCormack, C. and Seed, B. (1998). Membrane compartmentation is required for efficient T cell activation. *Immunity* **8**, 723 – 732.

Yan, M., Collins, R.F., Grinstein, S. and Trimble, W.S. (2005). Coronin-1 function is required for phagosome formation. *Mol Biol Cell* **16**, 3077 – 3087.

Yewdell, J.W., Schubert, U. and Bennink, J.R. (2001). At the crossroads of cell biology and immunology: DRiPs and other sources of peptide ligands for MHC class I molecules. *J Cell Sci* **114**, 845 – 851.

Zuniga-Pflücker, J.C. (2004). T-cell development made simple. *Nature Rev Immunol* **4(1)**, 67 – 72.

7 ABBREVIATIONS

A	Ampere
aa	Amino acid
AB	Antibody
AP	Alkaline phosphatase
APC	Allophycocyanin or antigen-presenting cells
APS	Ammonium persulfate
BCA	Bicinchoninic acid
BCR	B-cell receptor
BM	Bone marrow
BMM	Bone marrow-derived macrophages
bp	Base pair
BSA	Bovine serum albumine
CD	Cluster of differentiation
cDNA	complementary DNA
CLAAP	chymostatin, leupeptin, aprotinin, antipain, pepstatin
CLIP	Class II linked invariant chain peptide
conc.	Concentration
Coro	Coronin
cpm	Counts per minute
CR	Complement receptor
DC	Dendritic cell
dH_2O	Destilled water
ddH_2O	Double-destilled water
DMEM	Dulbecco's modified Eagle's medium
DMSO	Dimethylsulfoxide
DNA	Deoxyribonucleic acid
DNAse	Deoxyribonuclease
dNTP	Deoxynucleotidetriphosphate
DRiPs	Defective ribosomal products
DTT	Dithiothreitol
EBSS	Eagle's balanced buffered saline
ECL	Enhanced chemiluminescence
E.coli	Escherichia coli
EDTA	Ethylendiamine tetraacetate
EGFP	Enhanced green fluorescent protein
ER	Endoplasmic reticulum
ES cell	Embryonic stem cell
EtBr	Ethidium bromide
EtOH	Ethanol
FACS	Fluorescence assisted cell sorting
Fc	Immunoglobulin constant region
FcR	Fc receptor
FCS	Fetal calf (bovine) serum
Fd	Farad
FITC	Fluorescein isothiocyanate
FPLC	Fast performance liquid chromatography
g	gram
G418	Geneticin
GAPDH	Glyceraldehyde 3-phosphate dehydrogenase
GM-CSF	Granulocyte-macrophage colony-stimulating factor
GPI	Glycosylphosphatidyl inositol
GTPase	Guanosinetriphosphatase

hr	Hour
hrs	Hours
HBBS	Hank's balanced buffered saline
HEPES	Hydroxyethylpiperidine-ethanesulfonic acid
h.i.	Heat inactivated
HRP	Horseradish peroxidase
IFN	Interferon
Ig	Immunoglobulin
Ii	Invariant chain
IL	Interleukin
IMDM	Iscove's modified Dulbecco's medium
i.p.	Intra-peritoneal
ITAM	Immunoreceptor tyrosine-based activation motif
kb	Kilobases
kDa	Kilo Dalton
K.O.	Knock-out
l	Liter
LB	Luria-Bertani
LIF	Leukemia inhibiting factor
LPS	Lipopolysaccharide
M	mol/l
□	Micro
mAB	Monoclonal antibody
MACS	Magnet assisted cell sorting
MCS	Multiple cloning site
MEF	Mouse embryonic fibroblast
MEM	Minimal essential medium
MeOH	Methanol
MFI	Median fluorescence intensity
MHC	Major histocompatibility complex
MIIC	MHC class II compartment
min	Minute(s)
M_r	Molecular weight
mRNA	messenger RNA
MW	Molecular weight
MWCO	Molecular weight cut-off
n	Nano
NEB	New England Biolabs
neo	Neomycin
NFAT	Nuclear factor of activated T-cells
NF□B	Nuclear factor □B
NK cells	Natural killer cells
OD	Optical density
o/n	Overnight
PAGE	Polyacrylamide gel electrophoresis
PAMPs	Pathogen-associated molecular patterns
PBLs	Peripheral blood lymphocytes
PBS	Phosphate buffered saline
PBST	Phosphate buffered saline with Tween
PCR	Polymerase chain reaction
PE	Phycoerythrine
PFA	Paraformaldehyde
pH	Potentia hydrogenii
p.i.	post injection
PIPES	Piperazine-1,4-bis(2-ethanesulfonic)acid

PKC	Protein kinase C
PMA	Phorbol-12-myristate-13-acetate
pMHC	Peptide:MHC complex
PMSF	Phenylmethylsulfonylfluoride
PNS	Post nuclear supernatant
rad	Radiation absorbed dose
RNA	Ribonucleic acid
RNAi	RNA interference
rpm	Revolutions per minute
RPMI medium	Roswell Park Memorial Institute Medium
RT	Room temperature
SAP	Shrimp alkaline phosphatase
SB	Sample buffer
SD	Standard deviation
SDS	Sodium dodecylsulfate
sec	Second(s)
SH	Src homology
SMAC	Supramolecular activation cluster
SSC	Sodium chloride, sodium citrate
TACO	Tryptophan aspartate containing coat protein
TAP	Transporter associated with antigen processing
TBE	Tris-Borate-EDTA
TCA	Trichloroacetic acid
TCR	T-cell receptor
TE	Tris-EDTA
TEMED	N,N,N',N'-tetramethylenethylendiamine
TMCF	Transgenic Mouse Core Facility, University Basel
TNF	Tumor necrosis factor
Tris	Tris(hydroxymethyl)aminomethane
TX-100	Triton X-100
U	Unit
UV	Ultraviolet
V	Volt
v/v	Volume per volume
WASP	Wiskott-Aldrich syndrome protein
WD	Tryptophane-aspartate
w/o	Without
w/v	Weight per volume
WT	Wildtype
ZAP-70	□-chain associated protein-70

ACKNOWLEDGEMENTS

I want to thank Jean Pieters for supervising my Ph.D. thesis. In his lab I had the opportunity to work on an exciting project which taught me a lot. Thanks to his enthusiasm, and his visionary view of the potential of this project I had an exciting and very fruitful time. I think working together on the coronin-1 deficient mice we created a lot of very interesting new research projects.

I am very grateful to Antonius Rolink and Rod Ceredig for their invaluable help on the immunological side of this project. It was not only their generosity in sharing equipment and reagents but also their curiosity in the project itself which let us have a lot of interesting discussions. And last but not least, Rod made me becoming an immunologist and free thinker !

My thanks also go to Martin Spiess and Urs Jenal for being part of my thesis committee. I appreciated their critical and inspiring support over the last three years a lot.

Special thanks go to my present lab colleagues for the great time that we spent together doing science. Thank you very much for criticism, help and of course fun !

I also want to acknowledge my former lab mates John, Imke and Giorgio. They were there when I joined the lab, they got me started and continued to be there anytime there was something urgent to be discussed. Thank you a lot for your support !

Furthermore I want to express my gratitude to:

Daniela Finke, for her time, patience and excellent discussions about 'dying T-cells'. She allowed me to perform a couple of important experiments in her lab.

Silvia Arber, for introducing me to the adventure and pitfalls of making a knock-out.

The team of the transgenic mouse core facility at the Biozentrum, namely Daniela Nebenius-Oosthuizen and Annette Klewe-Nebenius, for their invaluable help in doing the extensive ES cell culture work and for making these beautiful chimaeras.

Toru Miyazaki, without him we wouldn't have got the first positive ES cell clone.

Ed Palmer and his team for sharing reagents and know-how for the work with T-cells.

Carmen Blum and Hans-Reimer Rodewald for doing all the histology work.

Stefan Dirnhofer and Andre Tichelli for doing histological analysis of paraffin sections and hematological analyses, respectively.

The team of the animal facility at the Biozentrum, especially Rene Zedi, for excellent animal husbandry.